CYANOGENESIS IN THE CYSTIC FIBROSIS PATHOGEN *PSEUDOMONAS AERUGINOSA*

Chandrika Goh Nair

Department of Life Sciences

Imperial College London

A thesis submitted for the degree of Doctor of Philosophy

April 2015

I dedicate this thesis to my parents, Ivy and Chandran,

for their love, guidance and relentless support.

DECLARATION

I declare that the contents of this thesis are my own work except where otherwise acknowledged.

The copyright of this thesis rests with the author and is made available under a Creative Commons Attribution Non-Commercial No Derivatives licence. Researchers are free to copy, distribute or transmit the thesis on the condition that they attribute it, that they do not use it for commercial purposes and that they do not alter, transform or build upon it. For any reuse or redistribution, researchers must make clear to others the licence terms of this work.

ABSTRACT

Lung disease is the most lethal manifestation of Cystic Fibrosis (CF). The bacterium *Pseudomonas aeruginosa* is a major pathogen of the CF lung, where it is able to persist for decades. *P. aeruginosa* is also one of only a few bacterial species capable of producing hydrogen cyanide (HCN). Since cyanide is detectable in the sputum of CF patients, and its presence is negatively correlated with lung function, it has been hypothesised that cyanogenesis in *P. aeruginosa* may increase virulence in humans. Here, the overall aims have been to explore the clinical relevance of cyanide production in the CF airway and to improve current understanding of the molecular microbiology of cyanogenesis.

Ciliary beat frequency (CBF) measurements were performed on nasal brushings and sino-nasal air-liquid interface (ALI) cultures obtained from healthy volunteers and CF patients. KCN decreased CBF in healthy nasal brushings (n=6) after 60 min (150μM: 47% fall, $p<0.0002$; 75μM: 32% fall, $P<0.0001$). Samples from CF patients (n=3) showed similar results (150μM: 55% fall, $P=0.0003$). CBF inhibition was not due to loss of cell viability and was reversible. The inhibitory mechanism was independent of ATP levels. KCN also significantly inhibited CBF in ALI cultures, albeit to a lesser extent. Additionally, CBF measurements on ALI cultures treated with culture supernatants from *P. aeruginosa* mutants implicated cyanide as a key cilio-inhibitory component.

In order to uncover novel determinants of cyanogenesis, a high throughput colourimetric cyanide screen was developed. Cyanogenesis values were obtained for 93% of mutants from a comprehensive non-redundant *P. aeruginosa* transposon library. Additionally, the validity of two severely impaired mutants, *PA2196* and *PA5339*, was confirmed by complementation.

Mapping the most severe cyanogenesis outliers onto the *P.aeruginosa* genome revealed previously unrelated regions of interest. In particular, overrepresentation of genes related to the motile-sessile switch and to the RoxRS system implicated a strong role for these in the regulation of cyanogenesis.

ACKNOWLEDGEMENTS

I would especially like to acknowledge and thank all those who volunteered their nose cells as 'healthy controls' for my research.

I also wish to extend my deepest gratitude to Dr Huw Williams and Prof Jane Davies for the opportunity to undertake this exciting project in their laboratories, and for providing such inspiring supervision throughout. I would like to strongly thank Amelia, Rishi and Ben for their experimental insights. I am also thankful to the other members of the HDW lab – Kathryn, Nandita, Rebecca and Katie, - for providing a stimulating and thoroughly enjoyable research environment to work in.

I am grateful to Luke and Helen for listening to my experimental woes, leading to the conceptualisation of CyQuant, and I would like to sincerely thank Volker for writing the script.

A special thanks goes to Luke and Nandita for being excellent lunch companions and fellow science conversationalists. I would also like to express my sincere gratitude towards friends and family for their sustained support.

I am also really grateful to Uncle Mo and Aunty Gill, for taking me in at a time when my rent came to an end, but the experiments didn't.

I would like to thank my parents, who have been a great source of strength and inspiration.

Finally, I am so grateful to Omar for helping me navigate the highs and lows of the write up – thank you!

CONTENTS

CHAPTER 1 INTRODUCTION 18

1.1 CYSTIC FIBROSIS 19

1.1.1 Overview 19

1.1.2 Predispostion to Infection 20

1.1.3 Pseudomonas aeruginosa is the Major Cystic Fibrosis Pathogen 22

1.2 *PSEUDOMONAS AERUGINOSA* 23

1.2.1 Overview 23

1.2.2 The Motile-Sessile Switch 24

1.2.3 The Mucoid Switch 26

1.2.4 Adaptation to Hypoxia in the CF Lung 27

1.3 CYANOGENESIS 31

1.3.1 Overview 31

1.3.2 HCN Synthesis 32

1.3.3 Quorum Sensing 33

1.3.4 Regulation of the hcnABC Operon 35

1.3.5 Gac/Rsm Pathway 35

1.3.6 Cyanogenesis Occurs in the CF Lung 36

1.4 THESIS OBJECTIVES 40

CHAPTER 2 MATERIALS AND METHODS 41

2.1 CILIA WORK 42

2.1.1 Human Airway Epithelium Collection 42

2.1.2 Air-Liquid Interface (ALI) Culture 42

2.1.3 Harvesting Bacterial Culture Supernatants 43

2.1.4 Measurement of Ciliary Beat Frequency 43

2.1.5 Viability Measurements 45

2.1.6 ATP Measurements 45

2.1.7 Statistical Analysis 45

2.2 MICROBIOLOGICAL WORK 45

2.2.1 Growth Media 45

2.2.2 Buffers and Solutions 46

2.2.3 Agarose Gels 46

2.2.4 Kits 46

2.2.5 Bacterial Strains 47

2.2.6 Oligonucleotides *48*
2.2.7 Growth of Cultures *49*
2.2.8 Determination of Optical Density *49*
2.2.9 Bacterial Transformation *49*
2.2.10 Pyocyanin Assay *50*
2.2.11 Cyanide Measurements Using an Ion-Selective Micro-Electrode *51*
2.2.12 PA14NR Replication and Sub-Library Production *52*
2.2.13 High Throughput Colourimetric Cyanide Screen *53*
2.2.14 Data Analysis in R *54*
2.2.15 Genomic Map Generation in CG View *54*

CHAPTER 3 INHIBITION OF CILIARY FUNCTION OF RESPIRATORY EPITHELIA BY CYANIDE CONCENTRATIONS FOUND IN THE *P. AERUGINOSA*-INFECTED AIRWAY 55

3.1 INTRODUCTION 56
3.1.1 Does Cyanogenesis Contribute to Virulence in CF Patients? *56*
3.2 AIMS 57
3.3 METHOD DEVELOPMENT 58
3.3.1 Optimisation of Ciliary Beat Frequency Measurements *58*
3.4 RESULTS 60
3.4.1 Cyanide Concentrations Found in CF Sputum Decrease Ciliary Beat Frequency in Human Nasal Brushings *60*
3.4.2 Combined effect of KCN and Pyocyanin on Ciliary Beat Frequency of Nasal Brushings .. *64*
3.4.3 Combined Effect of KCN and Pyocyanin on Ciliary Beat Frequency of Sino-nasal Air Liquid Interface Cultures *65*
3.4.4 Cyanide-Induced Decrease in Ciliary Beat Frequency is not Due to ATP Depletion *67*
3.4.5 Effect of P. aeruginosa Culture Supernatants on Ciliary Beat Frequency of Air-Liquid Interface Cultures *69*
3.5 DISCUSSION 71
3.5.1 Comparison with Sub-Lethal Cyanide Exposure on Cilia in Non-Human Models *71*
3.5.2 Possible Contribution of Cyanide to Cilio-Inhibition and Virulence in the Respiratory Tract *72*
3.5.3 What is the Cilio-Inhibitory Mechanism of Cyanide? *73*
3.5.4 Biological Detoxification of Cyanide *75*
3.5.5 Are CF Respiratory Epithelia More Susceptible to Cyanide and PYO? *76*
3.5.6 Possible Clinical Implications *77*

3.6 FUTURE WORK 79
CHAPTER 4 **IDENTIFICATION OF TWO NOVEL DETERMINANTS OF CYANOGENESIS IN *P. AERUGINOSA* 80**
4.1 INTRODUCTION 81
4.1.1 Can we Identify Novel Determinants of Cyanide Production? 81
4.2 AIMS 82
4.3 METHOD DEVELOPMENT 83
4.3.1 Development of a High-Throughput Colourimetric Cyanide Screen 83
4.4 RESULTS 85
4.4.1 Initial Screen 85
4.4.2 Identification of PA2196 by Visual Assessment 86
4.4.3 Identification of PA5339 by Visual Assessment 88
4.4.4 Re-Screen of a Mutant Sub-library to Confirm Cyanogenesis Defects Identified in the Initial Screen 90
4.4.5 Direct Cyanide Measurements on PA2196 and PA5339 92
4.4.6 Complementation Restores Cyanide Production of PA2196 and PA5339 94
4.4.7 PA2196 and PA5339 are not Defective in Pyocyanin Production 96
4.4.8 Effect of PA2196 Supernatant on Ciliary Beat Frequency of Air-Liquid Interface Cultures 96
4.5 DISCUSSION 98
4.5.1 Confirmation of dadA Cyanogenesis Defect 98
4.5.2 PA2196 is a Repressor of the TetR Family 98
4.5.3 What is the Role of PA2196 in Cyanogenesis? 101
4.5.4 PA5339 is a Putative Member of the yjgF Superfamily 102
4.5.5 What is the Role of PA5339 in Cyanogenesis? 102
4.6 FUTURE WORK 103
CHAPTER 5 QUANTITATIVE CYANIDE SCREEN OF THE PA14NR LIBRARY105
5.1 INTRODUCTION 106
5.1.1 Troubleshooting the Initial Screen 106
5.2 AIMS 108
5.3 METHOD DEVELOPMENT 109
5.3.1 Finding an Optimal Assay Window 109
5.3.2 Quantitative Digital Image Processing with CyQuant, a Purpose-Built Script 110
5.3.3 Quantitative Screen Workflow 113
5.4 RESULTS 114

5.4.1 Quantitative Screen of the PA14NR Library *114*
5.4.2 Clustering Analysis of Cyanide Screen data *116*
5.4.3 Re-Screen of Top 250 Underproducers and Top 150 Overproducers *120*
5.4.4 Distribution of Cyanogenesis Mutants on the PA14 Genome *122*
5.4.5 Involvement of the Motile-Sessile Switch *124*
5.4.6 Cyanogenesis of Flagella-Related Mutants *124*
5.4.7 Cyanogenesis of Type IV Pili-Related Mutants *128*
5.4.8 Cyanogenesis of Cup-related Mutants *133*
5.4.9 Cyanogenesis of Exopolysaccharide-Related Mutants *136*
5.4.10 Cyanogenesis of c-di-GMP regulators *140*
5.4.11 Involvement of the RoxSR system in the regulation of cyanogenesis *144*
5.4.12 Additional Regulators and Virulence Factors *147*
5.4.13 Cyanogenesis of Core Biofilm Genes *152*
5.5 DISCUSSION 153
5.5.1 Limitations of the Quantitative Screen *153*
5.5.2 Distinguishing Between 'No Cyanide' and 'Sustained Low Cyanogenesis' *155*
5.5.3 Screening Inconsistencies *155*
5.5.4 Cyanogenesis of P. aeruginosa Appendage-Related Mutants *157*
5.5.5 Concomitant Loss of Flagellum and Loss of Cyanogenesis *161*
5.5.6 Hypothesis: Cyanogenesis Plays a Role in Immune Evasion *162*
5.5.7 Hypothesis: The RoxSR System Regulates Cyanogenesis *163*
5.6 FUTURE WORK 169
CHAPTER 6 GENERAL DISCUSSION 170
6.1 SUMMARY OF THE FINDINGS PRESENTED IN THIS THESIS 171
6.2 RELEVANCE OF CYANOGENESIS TO HUMAN INFECTION AND DISEASE 172
REFERENCES 174
APPENDICES 194

LIST OF TABLES

TABLE 2-1 COMPOSITION OF BUFFERS AND SOLUTIONS USED IN THIS STUDY.. 46

TABLE 2-2 KITS USED IN THIS STUDY……..……..... 47

TABLE 2-3 STRAINS AND PLASMIDS…….....48

TABLE 2-4 PRIMERS USED IN THIS STUDY……..... 48

TABLE 3-1 BASELINE CBF OF AIR LIQUID INTERFACE CULTURES ORIGINATING FROM NON-CF AND CF VOLUNTEERS 65

TABLE 3-2 EFFECT OF KCN ON CBF IN OTHER MODELS OF THE AIRWAY..... 71

TABLE 3-3 SUMMARY TABLE - EFFECT OF KCN AND PYO ON NON-CF AND CF NASAL BRUSHINGS AND ALIS 77

TABLE 5-1 CLUSTERING OF KNOWN CYANOGENESIS MUTANTS BASED ON PARTITIONING AROUND MEDOIDS. 118

TABLE 5-2 CYANOGENESIS OF FLAGELLA-RELATED MUTANTS. 126

TABLE 5-3 CYANOGENESIS OF T4P REGULATORY MUTANTS. 128

TABLE 5-4 CYANOGENESIS OF T4PA-RELATED MUTANTS..... 130

TABLE 5-5 CYANOGENESIS OF T4PB-RELATED MUTANTS.. 131

TABLE 5-6 CYANOGENESIS OF T4PB-TAD MUTANTS.. 133

TABLE 5-7 CYANOGENESIS OF CUP FIMBRAE-RELATED MUTANTS. 135

TABLE 5-8 CYANOGENESIS OF EXOPOLYSACCHARIDE-RELATED MUTANTS. 138

TABLE 5-9 CYANOGENESIS OF C-DI-GMP RELATED MUTANTS. 143

TABLE 5-10 CYANOGENESIS OF MUTANTS RELATED TO THE ROXSR REGULON..... 146

TABLE 5-11 CYANOGENESIS OF ADDITIONAL MUTANTS RELATED TO THE MOTILE-SESSILE SWITCH. 149

TABLE 5-12 CYANOGENESIS OF ADDITIONAL SEVERE OUTLIERS IDENTIFIED IN BOTH SCREENS. 151

TABLE 5-13 CORE BIOFILM GENES THAT EXHIBIT A CYANOGENESIS DEFECT 152

TABLE 5-14 CYANOGENESIS UNDERPRODUCERS ALSO IDENTIFIED BY KAWAKAMI *ET AL.* 167

TABLE 5-15 CYANOGENESIS OF OVERPRODUCERS ALSO IDENTIFIED BY KAWAKAMI *ET AL.* 168

LIST OF FIGURES

FIGURE 1-1 LIFE EXPECTANCY OF CF SUFFERERS 20

FIGURE 1-2 LOW VOLUME HYPOTHESIS OF CYSTIC FIBROSIS PATHOGENESIS 21

FIGURE 1-3 PREVALENCE OF RESPIRATORY PATHOGENS, BY AGE 23

FIGURE 1-4 PROPOSED MOTILE-SESSILE SWITCH DURING LONG-TERM CF INFECTIONS. 25

FIGURE 1-5 LOSS OF MUCA FUNCTION HAS PLEIOTROPIC EFFECTS 27

FIGURE 1-6 PERSISTENCE OF *P. AERUGINOSA* WITHIN HYPOXIC MUCUS 28

FIGURE 1-7 BRANCHED RESPIRATORY CHAIN OF *PSEUDOMONAS AERUGINOSA*. 29

FIGURE 1-8 REGULATORY NETWORKS CONTROLLING *P. AERUGINOSA* TERMINAL OXIDASES. 30

FIGURE 1-9 CYANOGENESIS UNDER LABORATORY CONDITIONS. 32

FIGURE 1-10 PROPOSED HCN SYNTHESIS REACTION FROM GLYCINE. 33

FIGURE 1-11 HIERARCHICAL ARCHITECTURE OF THE QS SYSTEMS IN *P. AERUGINOSA*. 34

FIGURE 1-12 REGULATION OF *HCNA*BC TRANSCRIPTION. 35

FIGURE 1-13 REGULATION OF HCN PRODUCTION BY THE GAC/RSM SYSTEM 36

FIGURE 1-14 CYANIDE IS DETECTABLE IN THE SPUTUM OF *P. AERUGINOSA* INFECTED PATIENTS. 38

FIGURE 1-15 THE PRESENCE OF CYANIDE IS ASSOCIATED WITH DECREASED LUNG FUNCTION. 39

FIGURE 2-1 AIR LIQUID INTERFACE CULTURE PROTOCOL 43

FIGURE 3-1 OPTIMISATION OF CILIARY BEAT FREQUENCY MEASUREMENTS – REPLICATES. 58

FIGURE 3-2 OPTIMISATION OF CILIARY BEAT FREQUENCY MEASUREMENTS – TIMEFRAME. 59

FIGURE 3-3 PHYSIOLOGICALLY RELEVANT CONCENTRATIONS OF KCN DECREASE CILIARY BEAT FREQUENCY OF HUMAN NASAL BRUSHINGS IN A CONCENTRATION-DEPENDENT MANNER. 61

FIGURE 3-4 KCN DECREASE IN CBF ALSO OCCURS IN PAEDIATRIC CF NASAL BRUSHINGS.. 62

FIGURE 3-5 CBF DECREASE IS NOT DUE TO LOSS OF VIABILITY AND IS REVERSIBLE.. 63

FIGURE 3-6 COMBINED EFFECT OF KCN AND PYO ON CILIARY BEAT FREQUENCY OF HEALTHY NASAL BRUSHINGS.. 64

FIGURE 3-7 COMBINED EFFECT OF KCN AND PYO IN AIR-LIQUID INTERFACE CULTURES. 66

FIGURE 3-8 KCN-INDUCED DECREASE IN CILIARY BEAT FREQUENCY AFTER 60 MIN IS NOT DUE TO ATP DEPLETION.. 68

FIGURE 3-9 EFFECT OF CYANIDE AND PYO FROM P. AERUGINOSA CULTURE SUPERNATANTS ON CBF OF HEALTHY HUMAN *SINO-NASAL* AIR LIQUID INTERFACE CULTURES. 70

FIGURE 3-10 MODULATION OF CBF BY HOST AND PATHOGEN.. 74

FIGURE 4-1 ADAPTATION OF A QUALITATIVE CYANIDE DETECTION METHOD TO A 96-WELL SEMI-QUANTITATIVE ASSAY.. 83

FIGURE 4-2 CYANIDE SCREEN ASSAY PLATE SET UP.. 84

FIGURE 4-3 CONTROL PLATE.. 85

FIGURE 4-4 COVERAGE ISSUES DURING INITIAL SCREEN.. 86

FIGURE 4-5 CYANIDE DETECTION PAPERS FOR LIBRARY PLATE 06_04.. 87

FIGURE 4-6 CYANIDE DETECTION PAPERS FOR LIBRARY PLATE 06_02 89

FIGURE 4-7 *PA5340* MAY EXHIBIT SLIGHTLY IMPAIRED CYANOGENESIS. 90

FIGURE 4-8 CONFIRMATION OF CYANOGENESIS DEFECT IN MUTANTS IDENTIFIED BY THE INITIAL LIBRARY SCREEN.. 91

FIGURE 4-9 CYANOGENESIS MUTANTS GROUPED BY STRENGTH OF CYANIDE PRODUCTION INHIBITION. 92

FIGURE 4-10 DIRECT CYANIDE MEASUREMENT ON *PA2196*, *PA5339* AND *PA5340* 93

FIGURE 4-11 DIRECT CYANIDE MEASUREMENT ON *PA2196* AND *PA5339*.. 94

FIGURE 4-12 COMPLEMENTATION OF *PA2196* AND *PA5339* RESTORES CYANOGENIC ABILITY 95

FIGURE 4-13 *PA2196* AND *PA5339* PRODUCE WT LEVELS OF PYO.. 96

FIGURE 4-14 EFFECT OF *PA2196* SUPERNATANT ON CILIARY BEAT FREQUENCY OF HEALTHY AIR-LIQUID INTERFACE CULTURES. . 97

FIGURE 4-15 TETR-TETA REGULON.. 99

FIGURE 4-16 CIF-CIFR REGULON 99

FIGURE 4-17 GENE LOCUS OF PA2196, 154 BP DOWNSTREAM OF *HCNABC* OPERON 100

FIGURE 4-18 SURFACE REPRESENTATION OF PA2196. 100

FIGURE 4-19 GENE LOCUS OF PA5339, DOWNSTREAM OF *SPOT* 102

FIGURE 5-1 EDGE EFFECT ON CYANIDE DETECTION PAPER AS A RESULT OF WELL EVAPORATION DURING PREVIOUS SCREEN. 106

FIGURE 5-2 TROUBLE SHOOTING THE INITIAL SCREEN. 107

FIGURE 5-3 REDUCTION OF THE ASSAY WINDOW TO LIMIT WATER DAMAGE AND EDGE EFFECT..... 109

FIGURE 5-4 IMPROVED IMAGE QUALITY WITH REDUCED WATER DAMAGE AND REDUCED EDGE EFFECT. 110

FIGURE 5-5 ANALYSIS OF CYANIDE SCREEN DATA IN CYQUANT.. 112

FIGURE 5-6 MODIFIED CYANIDE SCREEN WORK FLOW TO ACHIEVE IMPROVED IMAGE QUALITY AND QUANTITATIVE DATA ANALYSIS..... 113

FIGURE 5-7 QUANTITATIVE SCREEN SUMMARY..... 115

FIGURE 5-8 SPREAD OF CYANOGENIC ABILITY IN THE PA14NR MUTANT LIBRARY.. 116

FIGURE 5-9 DETERMINATION OF NUMBER OF CLUSTERS TO LOOK FOR WITHIN THE CYANIDE SCREEN DATA..... 117

FIGURE 5-10 CLUSTERING OF CYANIDE SCREEN DATA INTO THREE GROUPS BASED OF GROWTH AND CYANIDE PRODUCTION.. 117

FIGURE 5-11 QUANTITATIVE CYANOGENESIS SCREEN DATA OF PREVIOUSLY IDENTIFIED MUTANTS.. 119

FIGURE 5-12 LAYOUT OF A SUB-LIBRARY PLATE FROM THE RE-SCREEN..... 120

FIGURE 5-13 HISTOGRAM OF CYANOGENIC ACTIVITY OF RESCREENED MUTANTS. 121

FIGURE 5-14 RE-SCREEN OF TOP 250 CYANIDE UNDERPRODUCERS AND TOP 150 CYANIDE OVERPRODUCERS..... 121

FIGURE 5-15 DISTRIBUTION OF THE TOP 150 UNDERPRODUCER GENES AROUND THE PA14 GENOME. 122

FIGURE 5-16 DISTRIBUTION OF THE TOP 50 OVERPRODUCER GENES AROUND THE PA14 GENOME. .. 123

FIGURE 5-17 THE MAJORITY OF MUTANTS WITH FLAGELLA-RELATED DEFECTS EXHIBIT ABERRANT CYANOGENESIS..... 125

FIGURE 5-18 CYANOGENESIS OF MUTANTS WITH T4P REGULATORY DEFECTS. 128

FIGURE 5-19 CYANOGENESIS OF MUTANTS WITH T4PA REGULATORY DEFECTS. 129

FIGURE 5-20 CYANOGENESIS OF T4PB-RELATED MUTANTS.. 131

FIGURE 5-21 CYANOGENESIS OF T4PB TAD -RELATED MUTANTS..... 132

FIGURE 5-22 CYANOGENESIS OF CUP FIMBRAE-RELATED MUTANTS.. 134

FIGURE 5-23 CYANOGENESIS OF EXOPOLYSACCHARIDE-RELATED MUTANTS. 137

FIGURE 5-24 MODEL OF KINB'S ROLE IN THE REGULATION OF VIRULENCE 140

FIGURE 5-25 CYANOGENESIS OF C-DI-GMP RELATED MUTANTS.. 142

FIGURE 5-26 CYANOGENESIS OF MUTANTS RELATED TO THE ROXSR REGULON. 145

FIGURE 5-27 CYANOGENESIS OF ADDITIONAL MUTANTS RELATED TO THE MOTILE-SESSILE SWITCH.. 148

FIGURE 5-28 CYANOGENESIS OF ADDITIONAL SEVERE OUTLIERS IDENTIFIED IN BOTH SCREENS. 150

FIGURE 5-29 PROPOSED CHANGES TO THE SCREEN METHODOLOGY IN ORDER TO BETTER CLASSIFY CYANOGENESIS MUTANTS.. 154

FIGURE 5-30 INTERCONSISTENCY OF *WSPR, WSPF, WSPE* AND *WSPB* CYANOGENESIS PHENOTYPES.. 156

FIGURE 5-31 *P. AERUGINOSA* APPENDAGES ARE EMPLOYED AT DIFFERENT STAGES OF BIOFILM FORMATION. 157

FIGURE 5-32 COMPONENTS OF THE BACTERIAL FLAGELLUM 158

FIGURE 5-33 COMPONENTS OF TYPE IV PILI. 159

FIGURE 5-34 MODEL: CONCOMITANT LOSS OF FLAGELLA AND DOWNREGULATION OF CYANOGENESIS MAY PLAY A ROLE IN LUNG INFECTIONS.. 161

FIGURE 5-35 MODEL: THE ROLE OF THE ROXSR SYSTEM MAY BE TO ENSURE THAT CYANOGENESIS ONLY OCCURS WHEN *P. AERUGINOSA* IS ABLE TO PROTECT ITSELF FROM POTENTIAL DELETERIOUS EFFECTS.. 164

FIGURE 5-36 PQS GENES, WHICH ARE UPREGULATED BY ROXSR DURING ENTRY INTO STATIONARY PHASE, MAY PLAY A POSITIVE REGULATORY ROLE IN CYANOGENESIS. 166

FIGURE 5-37 CYANOGENESIS UNDERPRODUCERS ALSO IDENTIFIED BY KAWAKAMI *ET AL.* (2010) ... 167

FIGURE 5-38 CYANOGENESIS OVERPRODUCERS ALSO IDENTIFIED BY KAWAKAMI *ET AL.* (2010) 168

FIGURE 6-1 HYPOTHETICAL MODEL OF THE ROLE OF CYANOGENESIS IN *P. AERUGINOSA* CHRONIC LUNG INFECTIONS..... 173

LIST OF ABBREVIATIONS AND ACRONYMS

°C	Degrees Celsius
AHL	N-acylhomoserine lactone
ALI	Air liquid interface culture
ATP	Adenosine triphosphate
BCC	Burkholderia cenocepacia complex
BLAST	Basic Local Alignment Search Tool
cAMP	Cyclic adenosine monophsophate
CBF	Ciliary beat frequency
C-di-GMP	Cyclic di-guanosine monophosphate
CF	Cystic fibrosis
CFTR	Cystic fibrosis transmembrane conductance regulator
COPD	Chronic Obstructive Pulmonary Disease
Cup	Chaperon usher pathway
dH2O	Distilled water
DNA	Deoxyribonucleic acid
g	Unit of force equal to force exerted by gravity
g	Gram(s)
GTP	Guanosine triphosphate
Gm	Gentamicin
ISE	Ion-Selective Electrode
LB	Luria Bertani
m	Metre(s)
M	Molar
MCC	Muco-ciliary clearance
MIC	Minimum inhibitory concentration

mRNA	Memory RNA
OD	Optical density
ORF	Open reading frame
PBS	Phosphate buffered saline
PCR	Polymerase chain reaction
QS	Quorum sensing
RBS	Ribosome binding site
RNA	Ribonucleic acid
rpm	Revolutions per minute
SE	Standard error
T4P	Type IV pili
UTP	Uridine triphosphate
V	Volt
vol	Volume (s)

PUBLICATION AND PRESENTATION OF THIS WORK

Journal Article

Nair, C., Shoemark, A., Chan, M., Ollosson, S., Dixon M, Hogg, C., Alton, E.W., Davies, J.C. & Williams, H.D. (2014) Cyanide levels found in infected cystic fibrosis sputum inhibit airway ciliary function. *The European respiratory journal*. doi:10.1183/09031936.00097014.

Book Chapter

Nair, C.G., Ryall, B. & Williams, H.D. (2014) Cyanide measurements in bacterial culture and sputum. *Methods in molecular biology* (Clifton, N.J.). 1149325–336. doi:10.1007/978-1-4939-0473-0_27.

Conference Presentations

Nair, C., Shoemark, A., Donovan, S., Hogg, C., Alton, E.W., Davies, J.C. & Williams, H.D. (2012) The toxic *P. aeruginosa* exoproducts cyanide and pyocyaning inhibit ciliary function of human respiratory epithelia *via* different mechanisms. *Pediatric Pulmonology* 47: 329-329.

Nair, C.G., Shoemark, A., Donovan, S., Hogg, C., Alton, E.W., Williams, H.D. & Davies, J.C. (2011) Poison in the Lung – Cyanide, at concentrations found in the sputum of *Pseudomonas aeruginosa*-infected CF patients inhibits the beating of human respiratory cilia in vitro. *Pediatric Pulmonology* 46: 319-319.

Chapter 1
INTRODUCTION

1.1 Cystic Fibrosis

1.1.1 Overview

Cystic Fibrosis (CF) is one of the most common life-shortening genetic diseases in the UK, where it affects over 9000 individuals and has an incidence of 1 in 2500 Caucasian live births (Collins, 1992). Globally, there are an estimated 100 000 sufferers. The mode of inheritance of CF is monogenic and autosomal recessive, with an estimated carrier frequency of 1 in 25 among Europeans (UK Cystic Fibrosis Trust, 2012). CF arises from mutations in CFTR, a gene located on the long arm of chromosome 7, which encodes the Cystic Fibrosis Transmembrane conductance Regulator (CFTR), a 160 kDa ion channel (Riordan *et al.*, 1989; Cheng *et al.*, 1990; Bear *et al.*, 1992). Over 1900 different CFTR mutations have been characterised, the most common being deletion of phenylalanine-508, Phe508del (Kartner *et al.*, 1992; Bobadilla *et al.*, 2002). Phe508del is present on at least one allele in 90% of patients (Boyle & De Boeck, 2013).

Since its first pathologic description in 1938, advances in our understanding and treatment of CF have extended the life expectancy of patients (Figure 1-1). The median age of death for CF sufferers in the UK in 2012 was 28 years. However, the CF registry predicts that the median survival for its current cohort will be closer to 43.5 years (CF Registry Annual Data Report, 2012).

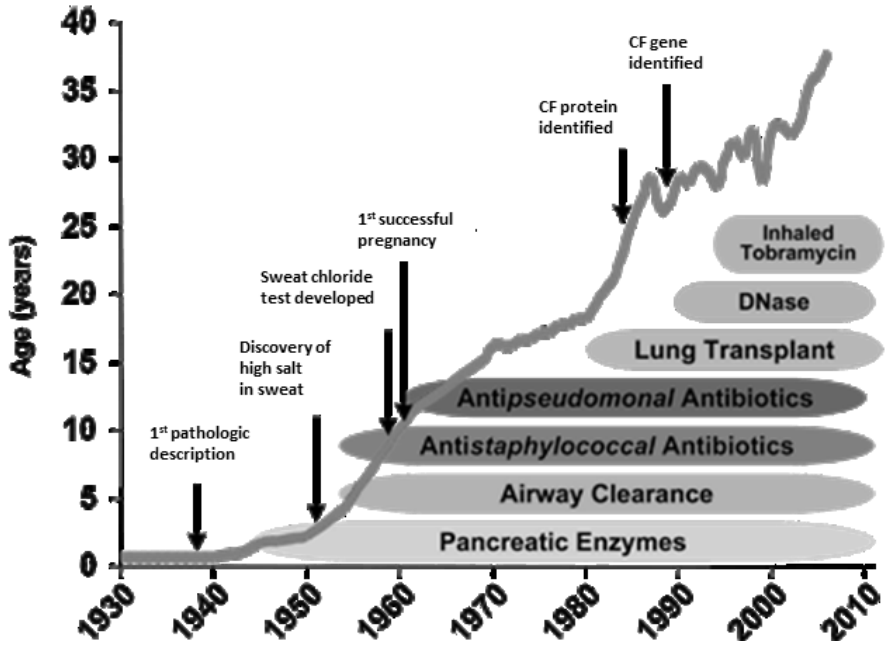


Figure 1-1 Life Expectancy of CF Sufferers (CF Foundation Annual Data Report, 2005).

CFTR is a chloride ion channel belonging to the ATP-binding cassette (ABC) transporter C class superfamily, that regulates epithelial salt and fluid transport. CFTR is expressed in many tissues, including apical membranes in the lung, intestine, pancreas, reproductive tract, and sweat gland (Riordan *et al.*, 1989). Loss of CFTR function results in the accumulation of viscous mucus in the bronchi of the lungs, loss of pancreatic exocrine function and elevated chloride levels in sweat. Originally recognised in infants with pancreatic insufficiency, who often succumbed to malnutrition and lung infections, CF is nowadays described as a mucosal immune-deficiency syndrome (Cohen & Prince, 2012). The CFTR defect renders the airways of CF sufferers prone to chronic bacterial colonization, and aggressive, often prophylactic, antibiotic regimens can successfully eradicate early infections. However, progressive deterioration of pulmonary function and subsequent adaptation of pathogens to the CF lung environment is usually inevitable, such that many sufferers require the continuous use of antibiotics, nutritional supplements, airway clearance therapies and frequent hospitalizations.

1.1.2 Predispostion to Infection

A number of hypotheses have been postulated to explain the propensity for infection in the CF lung (Pilewski & Frizzell, 1999; Reddy & Quinton, 2005; Boucher, 2007; Quinton, 2008; Tate *et al.*, 2002; Wine, 2001). Recently, evidence from human, murine and porcine CF models have suggested that the CFTR defect may compromise innate immunity prior to infection in several important ways, summarised as follows.

Firstly, dysregulation of ion transport in CFTR mutants is thought to create salty, low-volume, dehydrated mucus which may impair the clearance of inhaled pathogens. Failure of reabsorption of chloride (Cl^-) by CFTR leads to the retention of sodium (Na^+) in the sweat, in order to balance ionic charge (Figure 1-2). For example, dysregulation of Na^+ reabsorption from skin provides the basis for the chloride sweat test used to aid the diagnosis of CF (Rock *et al.*, 2014). The 'low volume' dehydrated mucus hypothesis is supported by the finding that epithelial sodium channel (ENaC)-overexpressing mice, which are thought to mimic CF ion transport pathophysiology, develop CF-like lung disease (Zhou *et al.*, 2011). In practice, studies investigating muco-ciliary clearance (MCC) in CF patients suggest that the severity of the clearance defect is highly variable, ranging from severely impaired to normal (Rutland & Cole, 1981; Regnis, Robinson, Bailey, *et al.*, 1994; Robinson & Bye, 2002; McShane, Davies, Wodehouse, *et al.*, 2004). The current paradigm is that young CF patients exhibit reduced but measurable muco-ciliary clearance rates, supporting the existence of a mechanism that regulates PCL height in the absence of fully functional CFTR. This mechanism is currently understood to be shear-induced ATP release (Tarran *et al.*, 2005). This ATP signalling system is vulnerable to viral insults. Tarran *et al.*, (2005) showed that PCL depletion in CF cells could be triggered *via* up-regulation of extracellular ATPase activity, by a viral pathogen, respiratory syncitial virus (RSV). This finding could help to explain the heterogeneity of MCC observed in CF patients, and provides a link between viral infections and disease exacerbations.

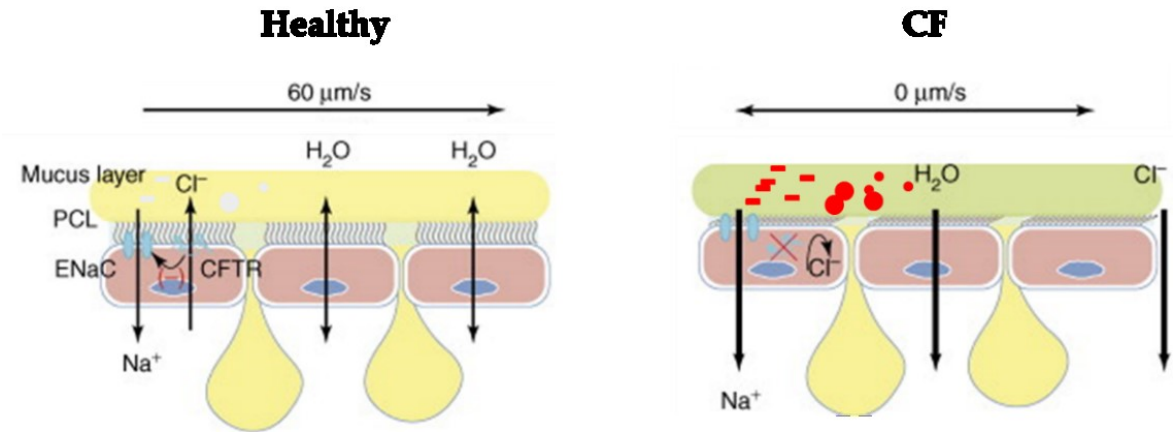


Figure 1-2 Low Volume Hypothesis of Cystic Fibrosis Pathogenesis. Airway surface liquid (ASL) comprises top mucus and bottom periciliary layers (PCL). The mucus layer is a gel composed of high molecular weight mucins that entrap inhaled particles, while the bottom PCL is a low viscosity, aqueous gel, in which cilia beat in a coordinated fashion to move the mucus and thus expel pathogens from the body. This process is known as muco-ciliary clearance (MCC). In the normal lung, PCL is generally the height of fully extended cilia. In the CF lung, however, depletion of the ASL and dehydration may cause it to collapse, such that viscous mucus invades the PCL and obstructs ciliary beating, thus preventing effective MCC.

A second hypothesis implicates the role of bicarbonate (HCO_3^-) in mucus homeostasis. Impaired airway epithelial HCO_3^- secretion due to the CFTR defect may cause a drop in the pH of the airway surface liquid (ASL). Lowering ASL pH has the effect of reducing the efficiency of salt-sensitive antimicrobials, such as defensins, and impairs phagocytosis (Hayes *et al.*, 2011). Conversely, increasing ASL pH in new-born CF pigs has been shown to rescue bacterial killing (Pezzulo, Tang, Hoegger, *et al.*, 2012).

An additional consequence of reduced ASL pH is mucus plugging, since mucin viscosity is pH dependent (Berkebile & McCray, 2014). Increased mucin viscosity is thought to impact MCC, by obstructing the airways. It may also impair the ability of antimicrobials to combat infection. For example, neutrophil and epithelial cell-derived cathelicidin, LL-37, can become sequestered by binding to viscous mucus and thus be prevented from coming into contact with its pathogenic targets. In CF mice, the addition of HCO_3^- was shown to reduce viscosity and restore normal ASL properties (Gustafsson *et al.*, 2012).

Is ASL pH lower in CF patients? While they did observe increased mucus viscosity, Jayaraman *et al.*, (2001) did not find a difference in pH when they compared the gland fluids of CF and normal airways obtained at the time of lung transplantation. Similarly, a later study by McShane *et al.*, (2003) did not find a pH difference between ASL pH of CF and non-cystic fibrosis patients. These findings contradict an important role of CFTR in regulating airway surface pH in humans. However, in a recent small pilot study, Abou *et al.*, (2014) reported that reduced nasal liquid pH could be observed in neonates with CF (pH 5.2 ± 0.3 for CF vs pH 6.4 ± 0.2 for non-CF), but not in CF children and adults. It is therefore possible that a CFTR-dependent pH defect may indeed occur in babies with CF, but that, as they age, ASL pH is observed to increase due to secondary disease manifestations.

1.1.3 *Pseudomonas aeruginosa* is the Major Cystic Fibrosis Pathogen

Lung disease is currently the most lethal manifestation of CF, such that chronic lung infections account for >90% of all CF deaths (Donaldson & Boucher, 2003; Fodor *et al.*, 2012). While CF pulmonary infections are initially poly-microbial in nature, by adulthood 80% of CF patients suffer predominantly from chronic *Pseudomonas aeruginosa* infections (Cystic Fibrosis Foundation, 2010; Williams & Davies, 2012; Davies *et al.*, 2003) (Figure 1-3). Once a switch to a chronic lifestyle has occurred, and despite aggressive antibiotic therapy, individual *P. aeruginosa* strains are able to outcompete other pathogenic species and to persist within the CF lung for decades (Markussen *et al.*, 2014; Hall *et al.*, 2014). Recently, it has become apparent that the CF lung microbiome also includes hard to culture

obligate anaerobes, most commonly *Prevotella* species (Mahenthiralingam, 2014). However, the full contribution of CF anaerobes to disease remains to be elucidated.

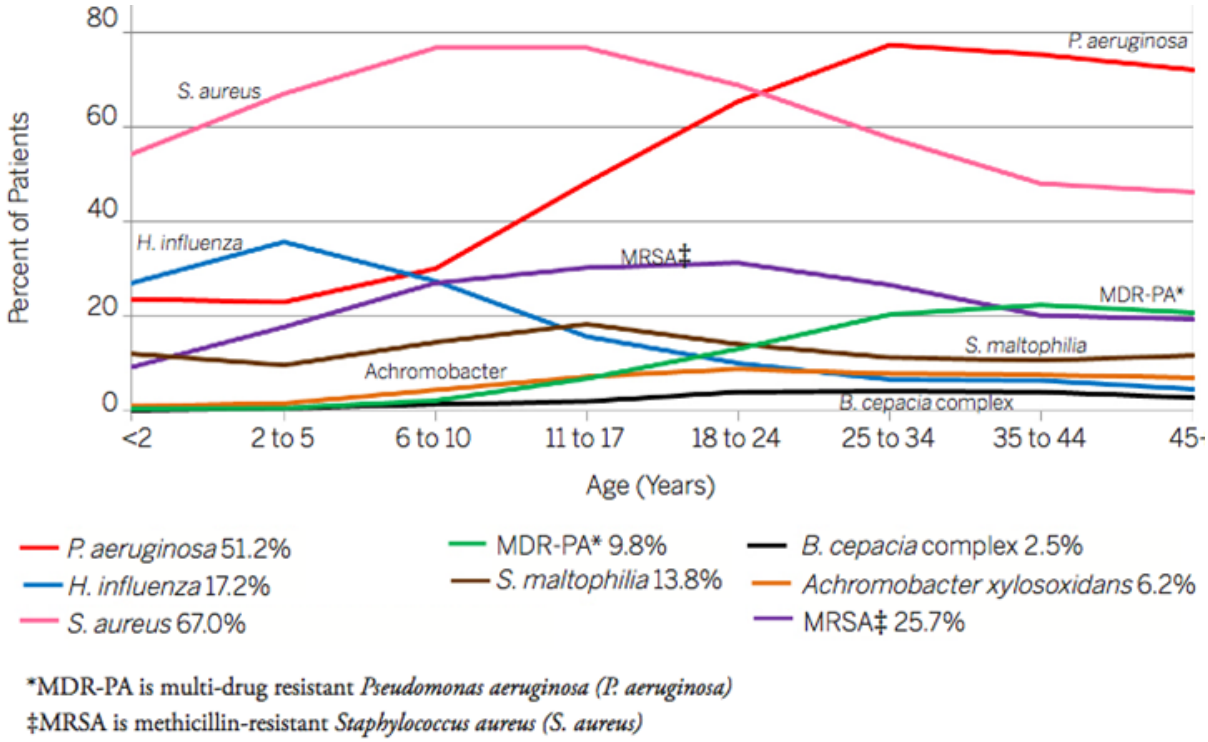


Figure 1-3 Prevalence of respiratory pathogens, by age. (CF Foundation patient registry, 2010)
P. aeruginosa outcompetes other pathogens over time. While early infections are usually polymicrobial in nature, by adulthood 80% of adult CF patients suffer predominantly from chronic *P. aeruginosa* infections.

1.2 *Pseudomonas aeruginosa*

1.2.1 Overview

P. aeruginosa is an aerobic, Gram-negative, rod-shaped bacterium comprising a genome of 6.3 million base pairs (Mbp) and 5,270 predicted open reading frames (ORFs) (PAO1 strain; Stover *et al.*, 2000). This large genome size, as well as a plethora of transcriptional regulators, representing 9% of *P. aeruginosa* ORFs, may help to explain this organism's substantial ecological versatility (Juhas *et al.*, 2005; Balasubramanian *et al.*, 2012).

P. aeruginosa is a ubiquitous saprophyte in soil, marshes and marine habitats (Hardalo & Edberg, 1997). Due to its high metabolic diversity, *P. aeruginosa* is also a coloniser of non-living surfaces, such as urinary catheters, where it aggregates into biofilms. Biofilms are structured bacterial

communities that exhibit improved resistance to external stresses, such as antibiotics and predation (Yan *et al.*, 2014).

In addition, *P. aeruginosa* is capable of switching from a free-living state to a pathogenic lifestyle. This is because certain *P. aeruginosa* isolates, such as the lab strain PA14, possess an extensive virulence gene repertoire enabling them to infect a broad range of hosts, including the model organisms *Arabidopsis thaliana, Caenorhabditis elegans, Drosophila melanogaster* and *Dictyostelium discoideum* (Baldini *et al.*, 2014; He *et al.*, 2004). *P. aeruginosa* virulence factors previously shown to exacerbate infections include exotoxin-A, the redox active pigment pyocyanin (PYO), pili, alginate, extracellular proteases and biofilm formation (Pessi, Williams, Hindle, *et al.*, 2001; Britigan, Railsback & Cox, 1999; Hamood, Griswold & Colmer, 1996; Brint & Ohman, 1995). PYO is a blue-green pigment which gives *P. aeruginosa* its characteristic colouring. It is also a potent virulence factor, which causes oxidative damage to host cells and impairs phagocytosis (Bianchi *et al.*, 2008). It has been speculated that the reason why *P. aeruginosa* evolved so many proficient virulence mechanisms may have been to counter eukaryotic predation, for instance by environmental phagocytes (Abd *et al.*, 2008; Lelong *et al.*, 2011; Lima *et al.*, 2011).

In humans, *P. aeruginosa* is an opportunist, rarely causing infections in healthy individuals. However, it is of clinical significance as a leading cause of nosocomial infections, such as infections of burn wounds and of the urinary tract (Chim *et al.*, 2007; Bitsori, Maraki *et al.*, 2012). In addition, *P. aeruginosa* also causes severe disease in the immunocompromised, and in patients with lung disease, including those suffering from CF. Once established, chronic *P. aeruginosa* infections of the CF lung can be virtually impossible to eradicate (Hart & Winstanley, 2002; Hall *et al.*, 2014)). Infective strains persist for decades, during which time niche-specific microevolution takes place (Mowat *et al.*, 2011). As a result, within patient isolate diversity is extremely high. Common adaptations observed in chronic clinical isolates include altered virulence, hypermutability and increased resistance to antimicrobials (Hogardt & Heesemann, 2010; Behrends *et al.*, 2010; Zlosnik *et al.*, 2014; Huse *et al.*, 2010).

1.2.2 The Motile-Sessile Switch

P. aeruginosa depends on numerous signalling systems to sense, respond and adapt to changing environments (Mikkelsen *et al.*, 2011). These pathways are broadly responsible for determining population behaviour, such as switching from a planktonic to a sessile lifestyle or transitioning between acute and chronic modes of virulence (Figure 1-4).

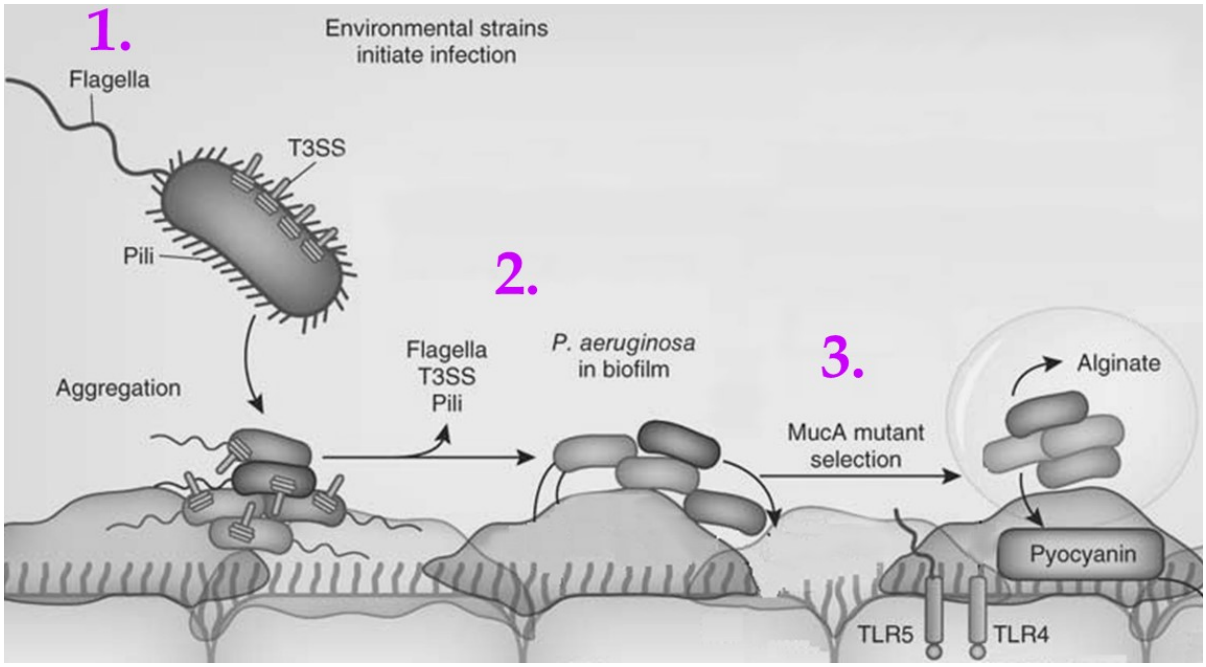


Figure 1-4 Proposed motile-sessile switch during long-term CF infections (Adapted from Cohen & Prince, 2013). 1. *P. aeruginosa* appendages are required for initial attachment and aggregation of environmental strains. 2. Following aggregation, bacteria lose their flagella and pili, switching from a motile to a sessile biofilm lifestyle. A simultaneous switch from acute to chronic virulence occurs, involving the loss of Type III Secretion. 3. A common adaptation selected for within the CF lung environment is the *mucA* mutation, which, among other phenotypes, causes overproduction of the exopolysaccharide alginate. Mucoid switch variants can be said to be highly adapted to a sessile lifestyle. They also benefit from enhanced protection against antimicrobials and are less cytotoxic than environmental strains. For example, they exhibit deregulation of the virulence factor PYO. PYO contributes to lung deterioration *via* oxidative damage and by promoting destructive host inflammatory responses.

Early CF clinical strains recovered from acute infections are often indistinguishable from environmental isolates. They display normal motility and produce cytotoxic levels of virulence factors. In contrast, later chronic isolates are typically highly adapted to long-term biofilm survival. They are typically non-motile and relatively non-cytotoxic (Mahenthiralingam *et al.*, 1994). Mutations inactivating flagellar function are very commonly recovered from chronically infected patients (Garrett *et al.*, 1999). In a way, these chronically-adapted strains could be considered to have the sessile mode semi-permanently switched 'on'. This has led some to speculate that the same regulatory systems that modulate the motile-sessile switch may also play a role in timing the acute-to-chronic lifestyle transition, which is a salient feature of long term CF infections (Tümmler *et al.*, 2014) .

1.2.3 The Mucoid Switch

The mucoid switch is a major event in the course of chronic *P. aeruginosa* infection and is often a determinant of worsened prognosis for patients (Martin *et al.*, 1993; Flynn & Ohman, 1988). Mucoidy results from loss of regulation of the alternate sigma factor, AlgU, which in wildtype strains is sequestered by the anti-sigma factor, MucA, as well as the negative regulator, MucB.

Loss of function mutations in *mucA* are the principal vehicle of constitutive AlgU activation in CF clinical isolates. The most commonly observed *mucA* mutation is *mucA22*, which causes a C-terminal truncation, resulting in 2 to 6-fold higher levels of alginate production (Mathee *et al.*, 1999; Mathee *et al.*, 1997). (Figure 1-5). The resultant increase in exopolysaccharide is thought to constitute an important virulence factor in itself, as this added protectant layer confers *P. aeruginosa* biofilms with increased resistance to external stresses, including killing by antimicrobials and effectors of the immune system (Wood & Ohman, 2012; Lee *et al.*, 2011; Høiby *et al.*, 2011).

Interestingly, MucA loss of function also has a much larger pleiotropic effect. In a longitudinal study of clinical isolates, to identify early adaptive developments, Rau *et al.*, 2010 observed that as infection progressed, an initially non-mucoid wildtype colonising strain rapidly converted to five clonal mucoid lineages, each possessing a different *mucA* sequence. The authors went on to perform a microarray analysis on the most dominant of these lineages. This lineage exhibited 668 gene expression changes compared to wildtype. Among these changes, the up-regulation of the transcriptional regulators AlgR, AlgB and AlgZ were hypothesised by the authors to have wide ranging effects. These regulators are known to modulate, among other processes, osmotic stress tolerance, virulence and flagellar motility (Ryall *et al.*, 2014; Behrends *et al.*, 2010) .

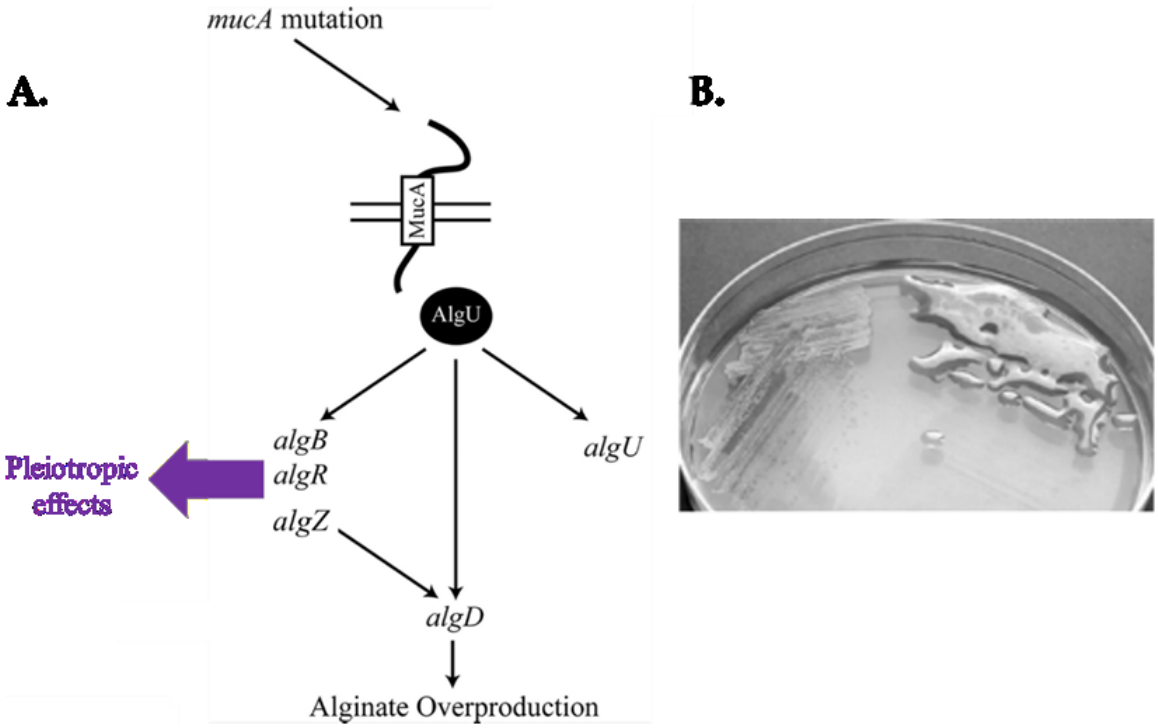


Figure 1-5 Loss of MucA function has pleiotropic effects (photo from Jain & Ohman, 2005). A. In the absence of functional MucA, the sigma factor AlgU is constitutively activated and promotes expression of the transcriptional activators AlgB, AlgR and AlgZ, which are themselves responsible for regulating a number of target genes. These genes are thought to alter virulence, inhibit flagellar motility and affect osomotic stress tolerance. Additionally, constitutive AlgU activity results in overexpression of AlgD, leading to alginate overproduction. B. Mucoid *P. aeruginosa* strains overproduce alginate. This gives them a distinctive pearlescent appearance and confers increased resistance to external stressors.

What is the virulence strategy of mucoid strains? Ryall *et al.*, (2014) found that increased availability of AlgU in mucoid strains subtly altered the regulation of virulence factor production. During early stationary phase, in comparison to WT, *mucA22* strains were found to be deficient in PYO, elastase and cyanide production. However, during late stationary phase, unlike the wildtype, these mucoid strains maintained and sustained low levels of virulence production, such that cyanide was still detectable in *mucA* cultures after 30 hours. This suggests that the mucoid switch, a common adaptation seen in clinical isolates, may be associated with a shift towards 'leaky', that is, low but sustained, virulence factor production.

1.2.4 Adaptation to Hypoxia in the CF Lung

The diverse modes of energy metabolism available to *P. aeruginosa* contribute to its ubiquity and its propensity to adapt to nutritionally challenging environmental niches, including within infected hosts.

P. aeruginosa utilises a wide range of carbon sources to derive precursor metabolites, reducing power, and the energy required to generate ATP and the proton motive force (ΔP) (Williams *et al.*, 2007). At least 17 respiratory dehydrogenases are predicted to feed electrons into the quinone pool (Williams *et al.*, 2007). *P. aeruginosa* also benefits from a highly branched respiratory chain, terminated by multiple terminal oxidases and denitrifying enzymes (Arai, 2011).

This remarkable versatility gives *P. aeruginosa* an edge over other microbial species in the oxygen-limited environments that exist within the CF lung (Schobert & Tielen, 2010; Tielen *et al.*, 2011) (Figure 1-6). Even under microaerobic and anaerobic conditions, spherical *P. aeruginosa* macro-colonies grow to exceed 100 µm in diameter (Worlitzsch *et al.*, 2002).

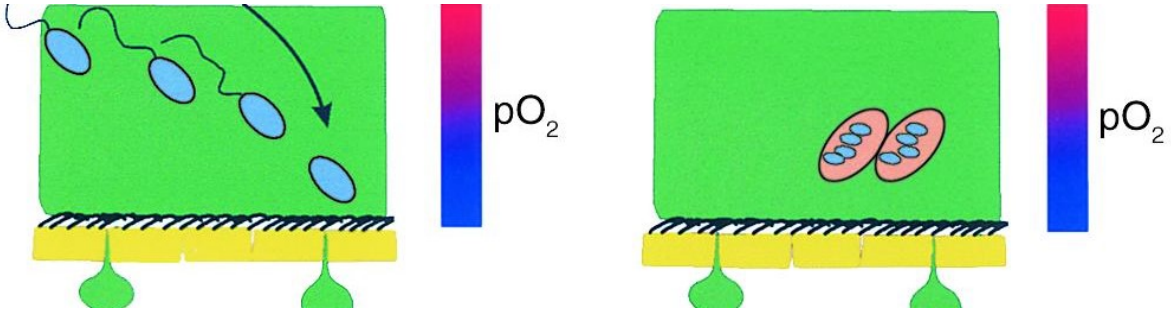


Figure 1-6 Persistence of *P. aeruginosa* within hypoxic mucus (Worlitzsch *et al.*, 2002). As it invades the thick viscous CF mucus, *P. aeruginosa* encounters, and successfully adapts to, steep hypoxic gradients.

The five terminal oxidases of *P. aeruginosa* consist of three Cytochrome C Oxidases, Cbb3-1, Cbb3-2 and Aa3, and two Quinol Oxidases, Bo3 (Cyo) and the Cyanide Insensitive Oxidase (CIO) (Figure 1-7). In addition, multiple nitrogen oxides permit growth under anaerobic conditions in the presence of nitrate or nitrite (Zumft, 1997).

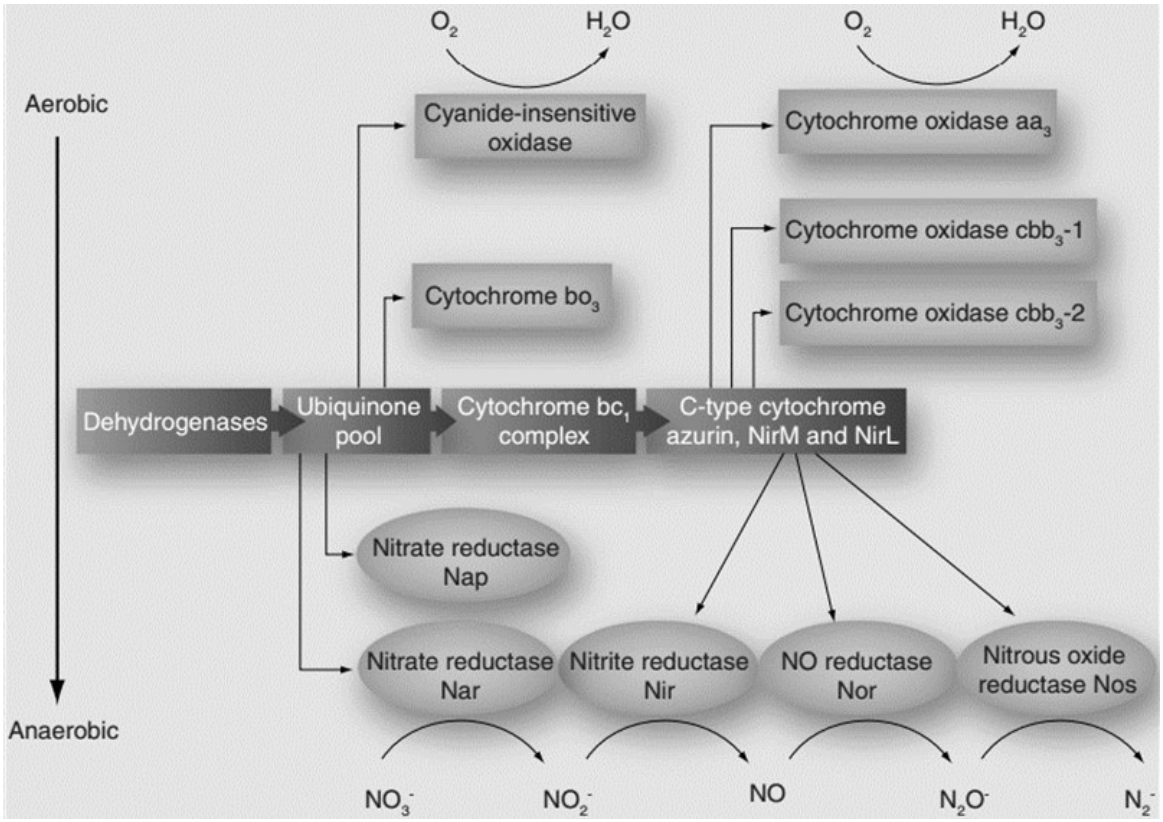


Figure 1-7 Branched respiratory chain of *Pseudomonas aeruginosa* (Zumft, 1997). *P. aeruginosa* has at its disposal a variety of electron donors and acceptors to generate energy. These various terminal oxidases all possess specific affinities for oxygen (O_2), specific proton translocation efficiencies and different sensitivities to respiratory toxins, such as cyanide. Unusually, Aa3, which in other bacteria plays a major role in aerobic respiration, is only expressed under nutrient stress conditions in *P. aeruginosa*. In the case of the quinol oxidases, Cyo is expressed under iron starvation and in the presence of nitric oxide, while the CIO is induced by copper starvation and the presence of cyanide (Kawakami *et al.*, 2010). Despite its high affinity for O_2, Cbb3-1 appears to be the dominant oxidase under normal aerobic conditions and during exponential growth of *P. aeruginosa* (Comolli & Donohue, 2004). Cbb3-2, in contrast, is upregulated under low O_2 tensions by the Anaerobic global Regulator, ANR.

The regulation of terminal oxidases in *P. aeruginosa* is summarised in Figure 1-8.

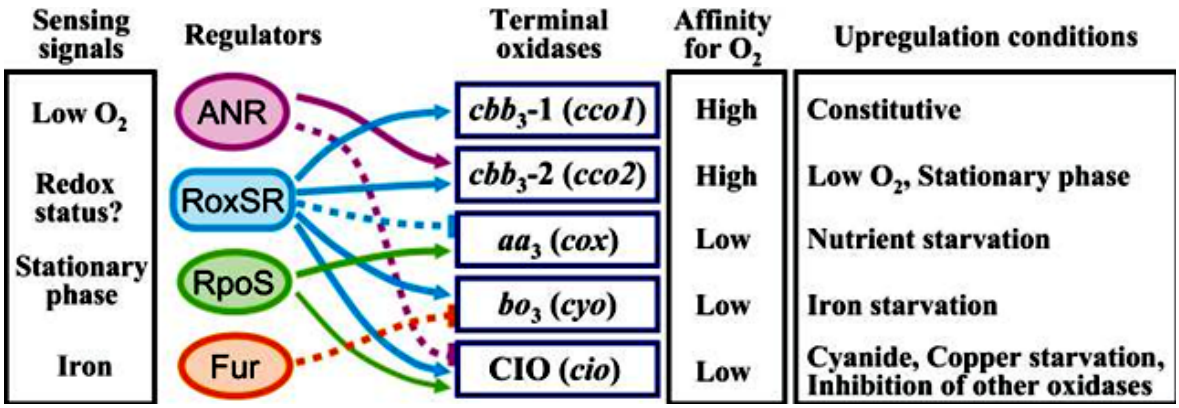


Figure 1-8 Regulatory networks controlling *P. aeruginosa* terminal oxidases (Arai, 2011). Expression of Aa3 under nutrient starvation is promoted by the stationary phase sigma factor, RpoS. Aa3 is repressed by the redox-sensitive regulator RoxSR. Cyo is expressed under iron starvation and is regulated by the ferric uptake regulator, Fur. The CIO is induced by copper starvation and by the presence of cyanide, and is oppositely regulated by ANR and RoxSR. Cbb3-1 is the dominant oxidase under normal aerobic conditions and during exponential growth, and is regulated by RoxSR. RoxSR also upregulates Cbb3-2. Cbb3-2 is upregulated under low O_2 tensions by ANR.

ANR is thought to prevent the overexpression of the CIO in relation to other oxidases, and to promote cyanide production under microaerophilic conditions. However, since cyanide upregulates *cio* expression, ANR repression of the CIO is relieved under microaerophilic conditions.

RoxSR is a redox-responsive two-component transcriptional regulator, consisting of the membrane-bound sensor kinase RoxS and its response regulator RoxR. RoxSR works to positively regulate the expression of the CIO *via* a mechanism that is thought to involve Cbb3-1, but not Cbb3-2 (Comolli and Donohue, 2004). It has been hypothesised that the flow of electrons through Cbb3-1 may be the signal recognised by RoxS (Arai, 2011).

The current paradigm is that Cbb3-1 plays a major role in aerobic growth irrespective of [O_2] and that Cbb3-2 provide compensatory or supplementary activity under oxygen-depleted conditions. A *cco1 cco2* double mutant, lacking Cbb3-1 and Cbb3-2, is unable to grow under microaerobic conditions (2% O2) (Alvarez-Ortega & Harwood, 2007). Under microaerobiosis, ANR promotes cyanogenesis. The poor growth of the *cco1 cco2* double mutant may therefore be suggestive of increased cyanide sensitivity.

Why is Cbb3-1 the dominant oxidase in *P. aeruginosa*? It could be that high affinity oxidases take prominence in *P. aeruginosa* because this organism has adapted to thrive in microaerobic ecological niches, such as its own highly structured biofilms and mucoid communities. It has been suggested that Cbb3-1 may provide benefits beyond oxygen reduction, such as enhanced sensing and faster responsivity to changes in redox homeostasis, possibly *via* RoxSR (Jo *et al.*, 2014).

1.3 Cyanogenesis

1.3.1 Overview

Interestingly, *P. aeruginosa* is one of only a few bacterial species capable of producing hydrogen cyanide (HCN) (Castric, 1983, 1975; Williams *et al.*, 2007). Other cyanogenic bacteria include *Pseudomonas fluorescens, Pseudomonas entomophila, Chromobacterium violaceum* and *Burkholderia cepacia* (Laville *et al.*, 1998; Ryall *et al.*, 2008; Ryall *et al.*, 2009; Campbell *et al.*, 2001; Blumer & Haas, 2000; Knowles & Bunch, 1986). *P. fluorescens* and *P. entomophila* are of agricultural relevance, respectively in the biocontrol of soil-borne pathogens, and as a potential insecticide. Cyanide-production by *C. violaceum* is currently being utilised in the process of commercial gold extraction. Intriguingly, *B. cepacia*, like *P. aeruginosa*, is a CF pathogen capable of synthesising cyanide. This raises the question of whether cyanide could be an important factor in the survival and virulence of these pathogens during chronic infection of the CF lung (Anderson *et al.*, 2010; Lenney and Gilchrist, 2011).

At lethal concentrations, cyanide is a potent inhibitor of biological processes. Its toxicity is attributed to its high affinity for metal ions, such as ferric iron (Fe^{3+}) in haem groups and metallo-enzymes, including Cytochrome C Oxidase, the terminal component of the electron transport chain of most aerobic organisms (Blumer & Haas, 2000). Known symptoms of cyanide poisoning in humans range from nausea and vomiting to loss of consciousness and death. A blood cyanide concentration of 25-100 μM is considered fatal (Bhattacharya & Vijayaraghavan, 2002; Pettersen & Cohen, 1993; Way *et al.*, 1988). At these levels, cyanide inhibits Cytochrome C Oxidase, preventing intracellular oxygen utilization and leading to metabolic acidosis.

1.3.2 HCN Synthesis

In liquid culture, optimal cyanogenesis by *P. aeruginosa* ranges from 300-500 μM HCN and is achieved at 34-37 °C, under microaerophilic conditions (5% O_2) and during entry into stationary phase (OD 0.8-1) (Pessi & Haas, 2001; Zlosnik & Williams, 2004; Nair *et al.*, 2014) (Figure 1-9).

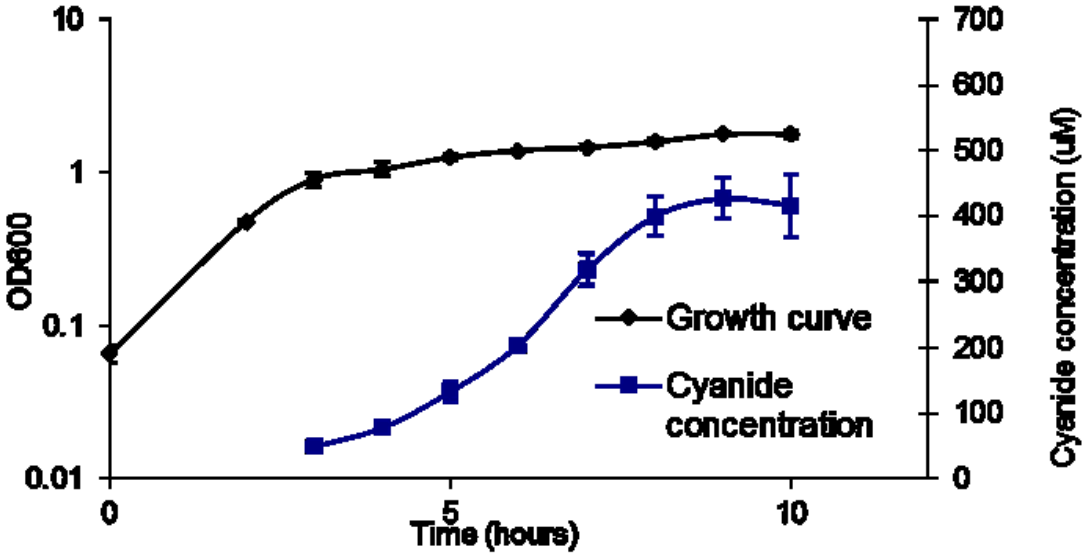


Figure 1-9 Cyanogenesis under laboratory conditions. When grown in rich LB medium, *P. aeruginosa* lab strain PAO1 starts to produce detectable cyanide during entry into stationary phase. Under optimal conditions, concentrations of up to 400 μm can be detected.

Concentrations of 300-500 μM HCN are capable of inhibiting most forms of aerobic respiration, however *P. aeruginosa* protects itself from the toxic effects of its own HCN production. This is understood to be achieved in part by encoding the CIO and *via* the conversion of cyanide to thiocyanate by a cyanide sulfurtransferase, rhodanese (Zlosnik *et al.*, 2006; Cipollone *et al.*, 2007). Zlosnik *et al.* (2006) observed a delay in *C.elegans* killing kinetics of *cioAB* mutants and a 2 to 4 fold reduction in minimum inhibitory concentration (MIC) compared to wildtype during stationary phase. However, the *cioAB* mutants were able to produce equivalent levels of cyanide to wild type in stationary phase. Cippolone *et al.* (2007) reported that a rhodanese mutant, *rdhA*, was outcompeted by WT *P. aeruginosa* under cyanogenic conditions, supporting a partial role for rhodanese in detoxification.

A proposed mechanism for *P. aeruginosa* HCN generation is the oxidative decarboxylation of glycine to form HCN and CO_2, *via* an immino acetic acid intermediate (Wissing, 1975) (Figure 1-10).

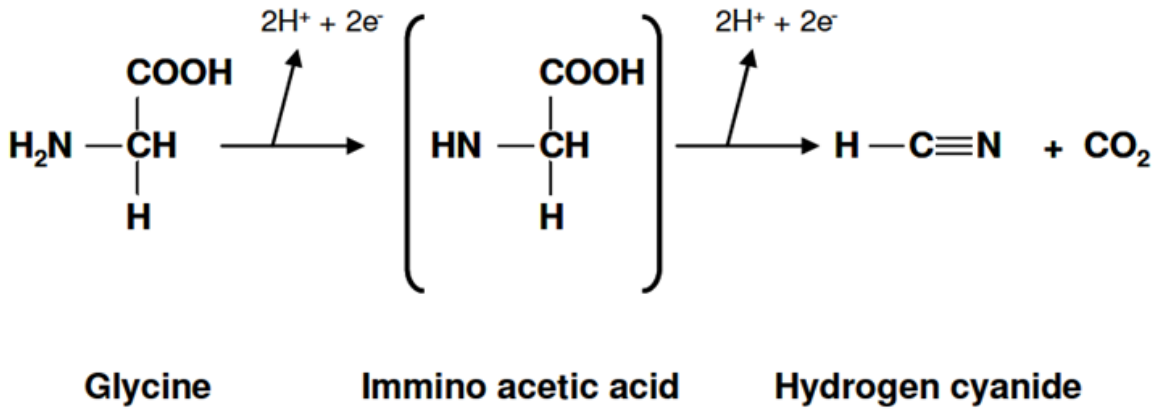


Figure 1-10 Proposed HCN Synthesis Reaction from Glycine (Wissing, 1975).

The HCN synthesis reaction generates four electrons, and it was previously hypothesised that these may be transferred to the CIO. However, this was disproved when Zlosnik *et al.* (2006) demonstrated that *cioAB* mutants were capable of producing WT levels of cyanide. The electron sink for HCN synthesis in *P. aeruginosa* therefore remains unknown.

Cyanogenesis is catalysed by a cell membrane-associated flavoprotein, the HCN synthase enzyme, encoded by the *hcnABC* operon. Each of the HCN synthase subunits shows orthology with known enzymes: To formate dehydrogenases for HcnA, and to amino acid oxidases for HcnB and HcnC (Laville *et al.*, 1998). Both *hcnB* and *hcnC* encode two predicted transmembrane segments, and it has been hypothesised that the topology of HCN synthase may lead to cyanide being released into the periplasm rather than the cytoplasm, thus reducing its toxic effects on the cell (Blumer & Haas, 2000). It has also been hypothesised that HCN synthase may constitute a respiration-linked amino acid dehydrogenase which happens to also make cyanide (Williams *et al.*, 2007).

1.3.3 Quorum Sensing

Previous research investigating cyanogenesis regulation in *P. aeruginosa* suggests that it is highly complex. Cyanide is one of many virulence factors under the control of Quorum Sensing (QS). QS is a cell-to-cell communication system which allows coordinated gene expression in response to cell-population density fluctuations. In line with its overall versatility, *P. aeruginosa* possesses three different QS systems, which exist in a cross-talking hierarchy: The Las system, the Rhl system and the *Pseudomonas* Quinolone Signal (PQS) system (Diggle, Cornelis, Williams, *et al.*, 2006; Diggle, Winzer, Lazdunski, *et al.*, 2002) (Figure 1-11). In addition, PqsE is thought to activate an unknown subset of virulence factors independently of the QS regulator, PqsR (Farrow *et al.*, 2008).

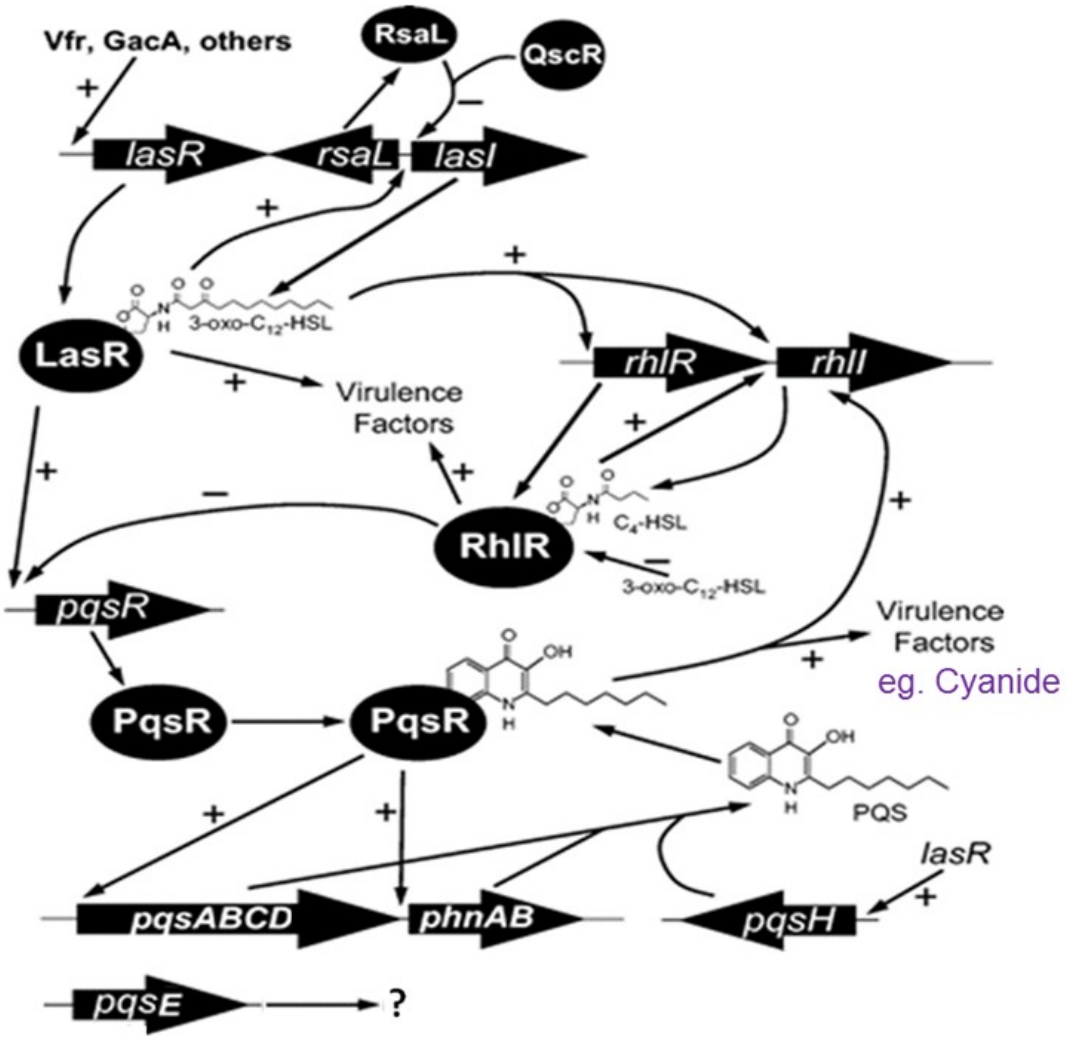


Figure 1-11 Hierarchical Architecture of the QS Systems in *P. aeruginosa* (Adapted from Missouri Western State iGEM, 2008). LasR and RhlR belong to the LuxR family of transcriptional regulators and bind to N-(3oxododecanoylhomoserine lactone (3-oxo-C12-HSL) and N-butanoylhomoserine lactone (C4-HSL), respectively. These lactones are signalling molecules produced by LasI and RhlI. As the HSLs promote their own synthesis, the QS systems are subject to positive feedback, or autoinduction. Autoinduction above a certain threshold results in the enhanced expression of target genes, many of these virulence factors. In the AHL-dependant QS hierarchy, the Las system comes above the Rhl system because both *rhlR* and *rhlI* are regulated by LasR/12-oxo-C12-AHL. The Las system also positively regulates the PQS system, while the Rhl system negatively affects PQS production. The PQS system functions through 2-heptyl-3-hydroxy-4-quinolone to promote virulence and upregulate the Rhl system. PqsE is thought to activate an unknown subset of virulence factors independently of PqsR.

1.3.4 Regulation of the *hcnABC* Operon

The *hcnABC* promoter contains three distinct start sites and maximal transcription of the cyanide biosynthetic operon is currently understood to require the concerted action of the QS networks, the low oxygen dependent regulator, ANR, as well as the alginate regulator, AlgR (Cody *et al.*, 2009; Pessi & Haas, 2001) (Figure 1-12).

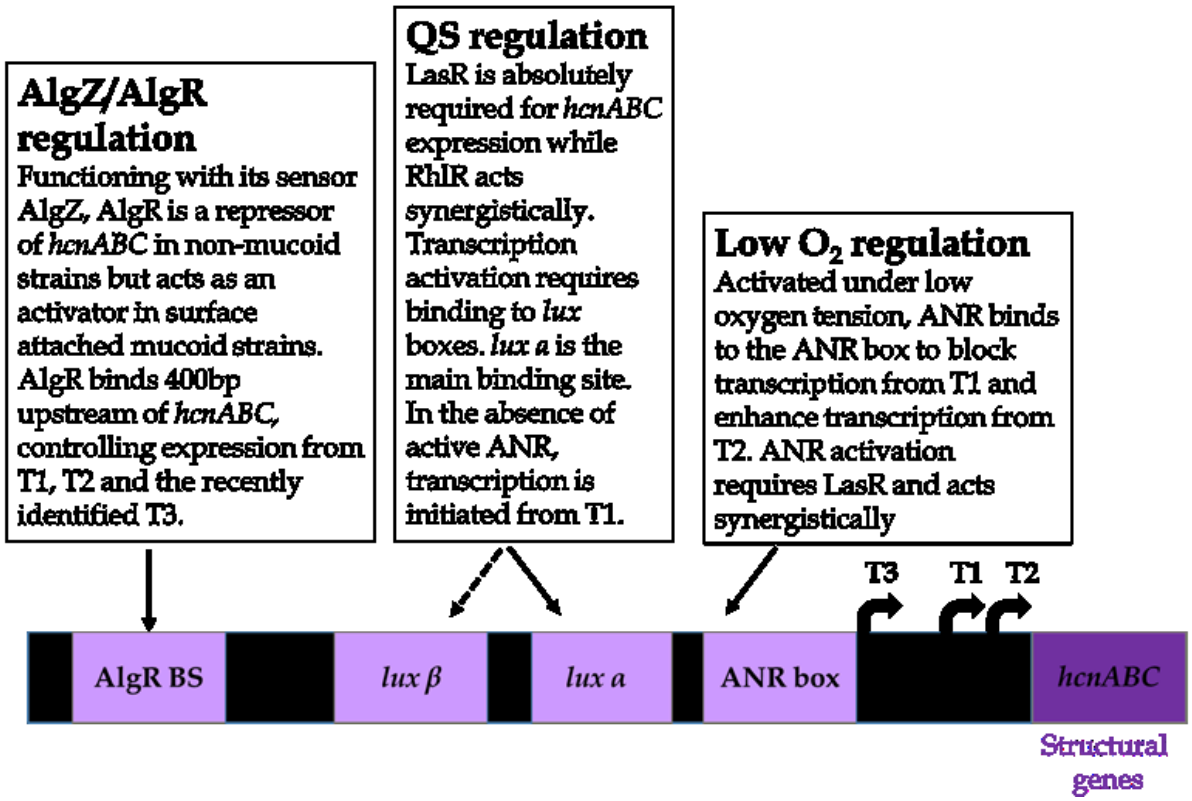


Figure 1-12 Regulation of *hcnA*BC transcription. Transcription can be driven from three start sites T1, T2 and T3. Transcript output from T3 is greater than that of T1 and T2.While LasR is absolutely required for transcription, RhlR and ANR act synergistically. Interestingly, AlgR is thought to act as a repressor of cyanogenesis in non-mucoid strains but promotes expression of *hcnABC* in surface-attached mucoid strains.

1.3.5 Gac/Rsm Pathway

Cyanogenesis is also under the control of the Gac/Rsm pathway. The Gac/Rsm system is a conserved two-component signal transduction pathway, initiated by the sensor kinase GacS and its corresponding response regulator GacA. Activation of GacA promotes the transcription of the small RNAs (sRNAs) *rsmXYZ*, which relieve the repression exerted by RsmAE on genes related to biofilm formation and virulence. In this way, activation of GacA is thought to help determine whether *P. aeruginosa* adopts a sessile or biofilm lifestyle (Coggan & Wolfgang, 2012). The Gac/Rsm system regulates cyanogenesis

indirectly at the transcriptional level *via* QS, and directly at the post-transcriptional level, by relieving the repression of RsmA at the *hcnABC* ribosome-binding site (RBS) (Pessi & Haas, 2001; Bordi *et al.*, 2010) (Figure 1-13).

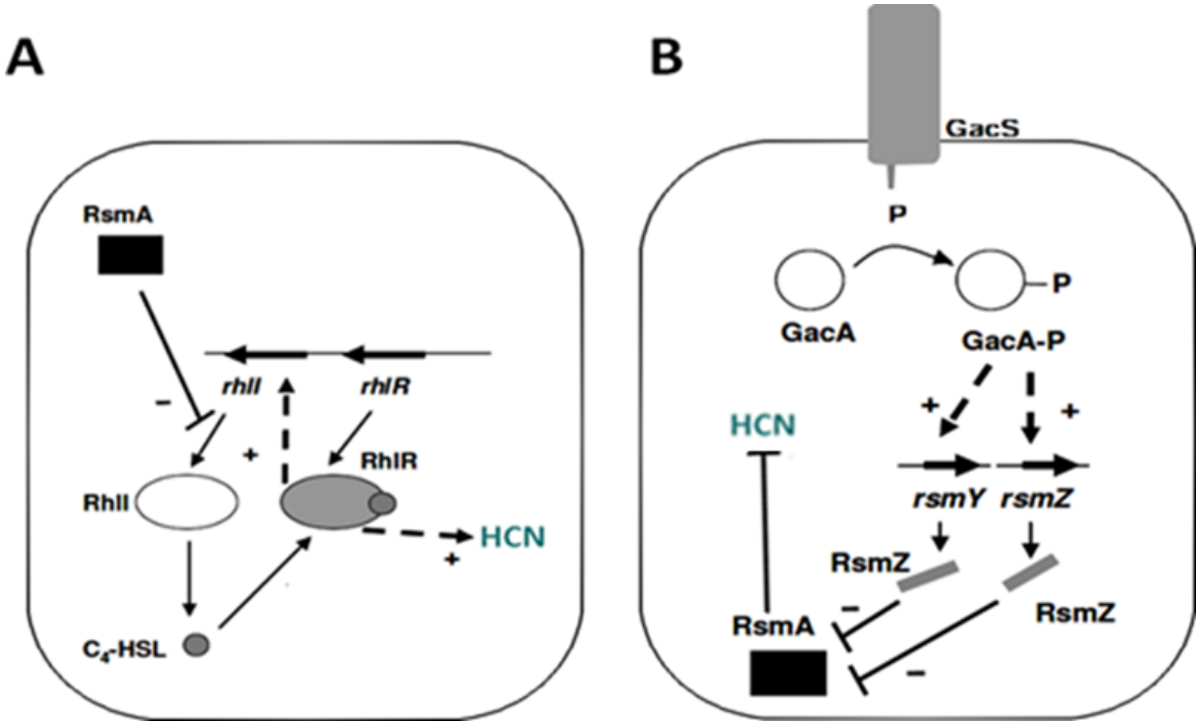


Figure 1-13 Regulation of HCN production by the Gac/Rsm system (A) In the absence of GacA-P activity, RsmA indirectly represses HCN production by negatively regulating RhlR synthesis. It also represses *hcnABC* transcription directly (not shown). (B) When the GacS/GacA system becomes activated, GacA-P acts to sequester RsmA, thus relieving its repression of the Rhl system and HCN production.

1.3.6 Cyanogenesis Occurs in the CF Lung

A role for cyanide production in environmental and pathogenic strains has yet to be elucidated, and it is hoped that uncovering further details regarding how and when *P. aeruginosa* deploys this known respiratory inhibitor may shed some light on its significance. The current picture of cyanogenesis regulation in *P. aeruginosa* is complex, apparently requiring the coordination of strict environmental conditions, for instance high bacterial cell density and low oxygen levels. However, as per the findings of Ryall *et al.*, (2012), in mucoid isolates, which are frequently recovered from chronically infected CF patients, there appears to be an abrogation of this tight regulation (Ryall *et al.*, 2014).

Conditions for cyanogenesis are satisfied in the CF lung: CF sputum frequently contains $>10^9$ cells per mL, and microaerobic niches are available due to hypoxic gradients created by the thick mucus layer (Worlitzsch *et al.*, 2002). In accordance with this, HCN has been detected in the sputa of CF patients suffering from *P. aeruginosa* infections at a mean level of 72 ± 6.6 μM (maximum 130 μM) (Ryall *et al.*, 2008) (Figure 1-14). Cyanide levels were shown to be independent of bacterial load, suggesting that HCN production is strain specific. This was subsequently confirmed by Gilchrist *et al.*, (2011) who compared 96 clinical isolates and observed varying degrees of HCN production between the strains. Sanderson *et al.*, (2008) have also reported the presence of cyanide in the lungs of patients, at concentrations ranging from 0.37–2.81 μg/mL, which is equivalent to 14-104 μM. Following its discovery in the lung, there has been a growing interest in the use of cyanide as a volatile marker for the diagnosis of *P. aeruginosa* infection in children who cannot expectorate sputum (Stutz *et al.*, 2011; Enderby *et al.*, 2009).

Since 25-100 μM blood cyanide concentrations are considered fatal, it has been suggested that the levels found in sputa may fall within the toxic range for aerobic respiration (Baud, 2007). Interestingly, Ryall *et al.* (2008) found that the presence of HCN in sputum negatively correlated with lung function, with mean predicted forced expiratory volume (FEV1%) of 26.8%±3.8% for patients with HCN in their sputum versus 46.0±6.7% for those without (Figure 1-15).

This result raises the question of whether HCN concentrations present in sputum affect lung function and contribute to long-term damage during *P. aeruginosa* infection.

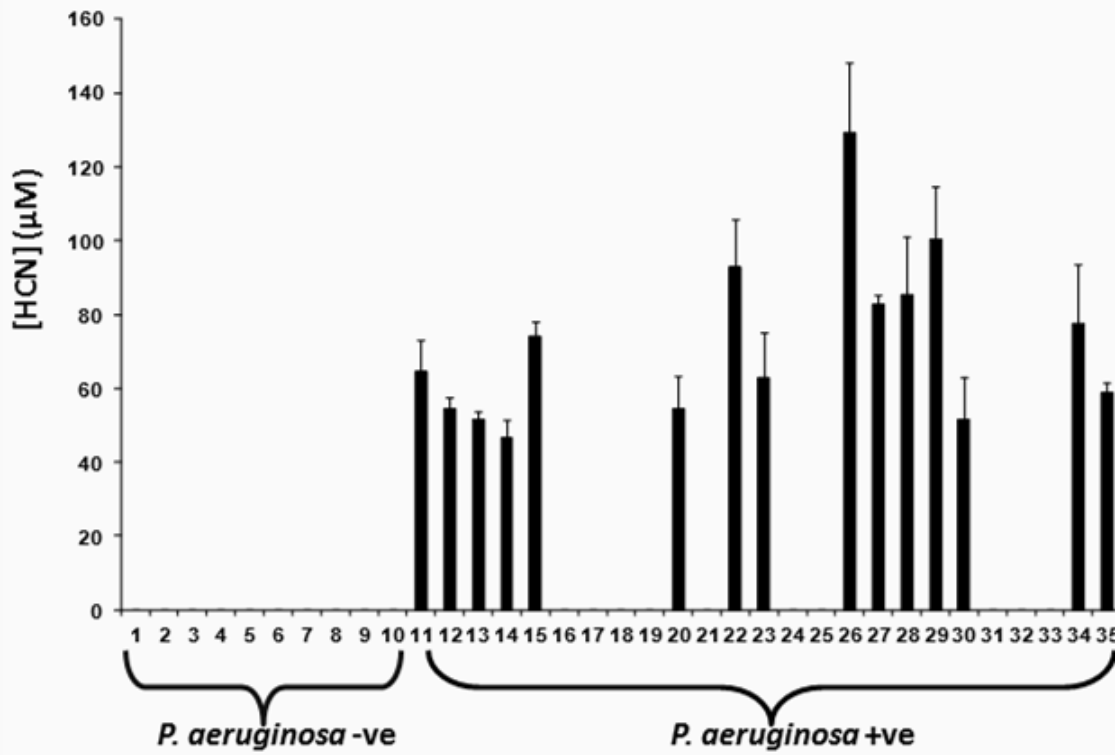


Figure 1-14 Cyanide is detectable in the sputum of *P. aeruginosa* infected patients (Ryall *et al.*, 2008). Up to 150 μM HCN was measured in sputum of CF patients using a cyanide ion-selective micro-electrode (mean [HCN] = 72 μM). Cyanide was absent from the sputum of patients without *P. aeruginosa* infection.

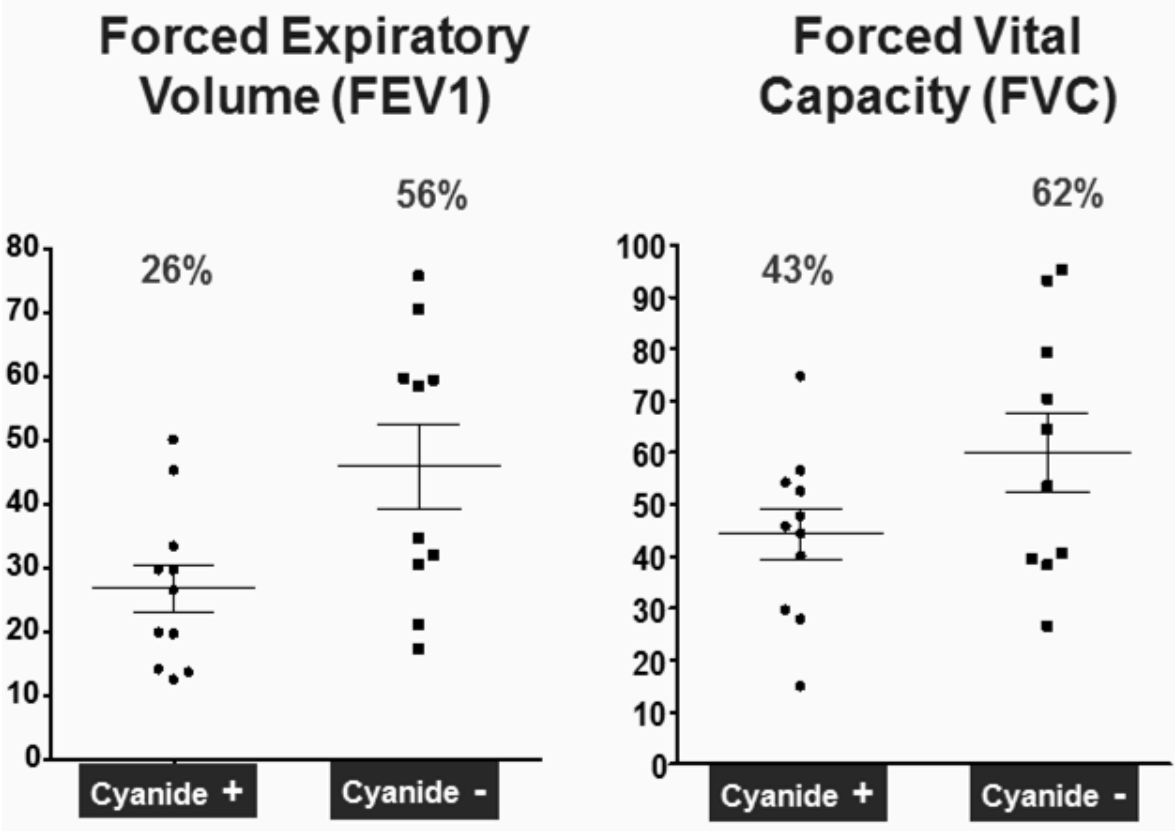


Figure 1-15 The presence of cyanide is associated with decreased lung function (Ryall *et al.*, 2008).

1.4 Thesis Objectives

This thesis aims to address two key issues: Firstly, the significance of *P. aeruginosa* cyanogenesis in the context of CF infections and secondly, the complex mechanisms by which *P. aeruginosa* is able to fine-tune the production of this virulence factor.

The experiments presented in Chapter 3 employ two models of the human airway, nasal brushings and sino-nasal air liquid interface cultures, to investigate the effect on ciliary function of cyanide concentrations found in *P. aeruginosa*-infected sputum. This chapter aims to address the following question:

> *Do physiologically-relevant cyanide concentrations have a direct effect on lung function in vitro?*

The work described in Chapter 4 utilises a colourimetric screening approach to identify novel determinants of cyanide production from a comprehensive library of *P. aeruginosa* transposon insertion mutants. This chapter aims to answer the following question:

> *Using a simple screening approach, can we identify novel regulators of cyanide production?*

In Chapter 5, the aim is to refine the screening methodology from Chapter 4 in order to improve coverage and to obtain quantitative cyanogenesis values. This chapter aims to answer the following question:

> *Using the data obtained from a quantitative cyanide screen, can we gain further insights into the role and regulation of P. aeruginosa cyanogenesis?*

Chapter 2
MATERIALS AND METHODS

2.1 Cilia Work

2.1.1 Human Airway Epithelium Collection

Strips of healthy human nasal epithelium were obtained from the inferior turbinate of volunteers using a cytology brush. CF samples were obtained from children undergoing clinically-indicated bronchoscopy under general anaesthesia or from adults attending outpatient clinics. Brushings were dispersed by agitation into a universal tube containing 3 mL medium 199 with Earle's salts and HEPES buffer (40 mM, pH 7.4) (Invitrogen). Samples were stored at 4 °C and used within 24 hours of collection. The sample collection was approved by Hounslow and Hillingdon Research Ethics Committee under project 07/H0709/73. All subjects (or parents of children) provided informed consent.

2.1.2 Air-Liquid Interface (ALI) Culture

ALI cultures (ALIs) were kindly provided by Dr Amelia Shoemark at the Royal Brompton Hospital. Nasal brushings were cultured using a protocol adapted from a previously described method (Fulcher *et al.*, 2005). The culture of ALIs used in this study is summarised in Figure 2-1.

Basal cells from a nasal brushing were selected for, using specific selective growth media, Bronchial Epithelial Cell Growth Medium (Lonza, USA). The population of basal cells were split into flasks and expanded in number. Once there were sufficient cells, these were seeded into transwells and re-differentiated into ciliated epithelium. This new ciliated epithelium did not contain any ciliated cells from the original sample and had been grown in sterile conditions.

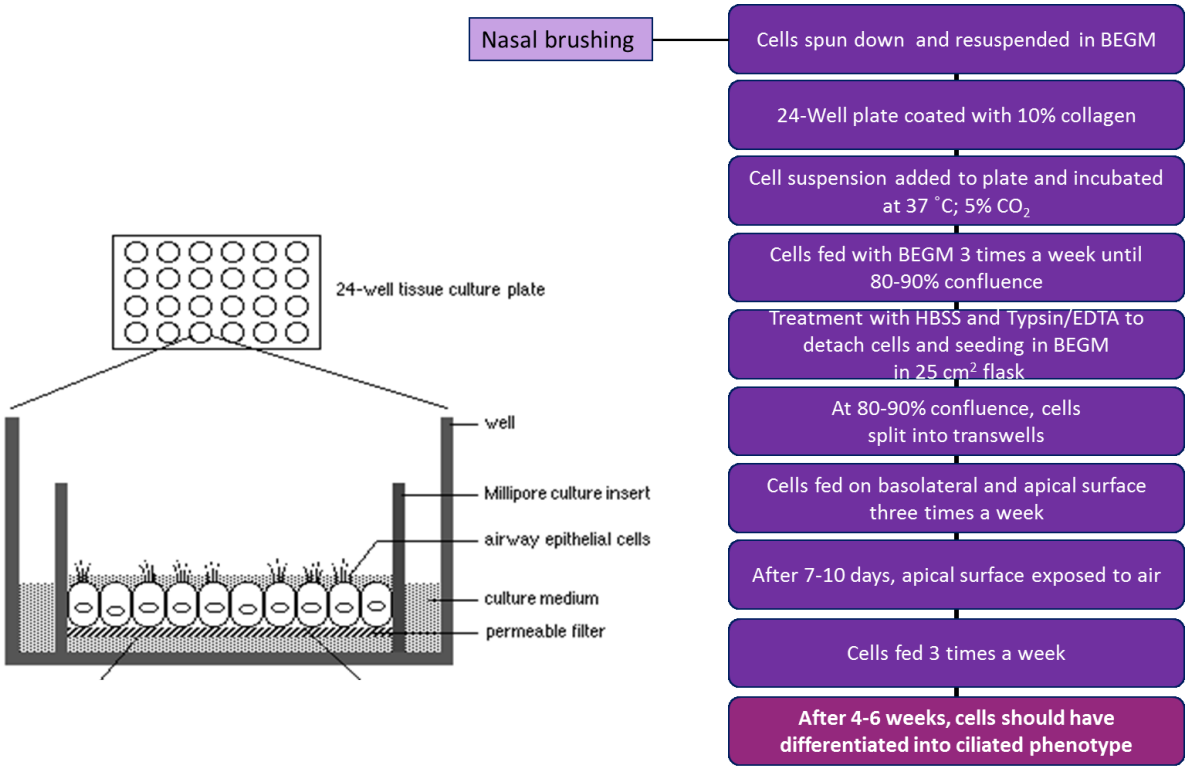


Figure 2-1 Air Liquid Interface Culture Protocol utilised by Dr Shoemark.

The nasal brushings were obtained from patients with CF or from patients being investigated for Primary Ciliary Dyskinesia, but with normal results of investigations, who did not have a muco-ciliary clearance defect and are referred to as non-CF controls. Experiments were conducted on the ALIs 2-6 weeks after cilia were first observed.

2.1.3 Harvesting Bacterial Culture Supernatants

The *P. aeruginosa* strain PA14 and isogenic Δ*hcnA* and Δ*phzS* mutants were cultured in Luria Bertani Broth (LB) (10 g/L peptone, 5 g/L NaCl, 5 g/L yeast extract). Cultures were grown aerobically at 37 °C in 50 mL of culture medium in a 250 mL Erlenmeyer flask with shaking at 200 rpm. Overnight cultures were adjusted to an OD^{600} of 1 with LB and culture supernatants harvested by sedimenting the bacterial cells by centrifugation at 4000 x g for 15 min. The supernatant fraction was then removed and filter sterilised using a 0.2 µm pore (Pall Life Sciences).

2.1.4 Measurement of Ciliary Beat Frequency

CBF measurement set up:

Ciliary beat frequency was measured using light microscopy and high-speed video recordings using a 40x magnification objective of an Axio observer D1 inverted microscope (Zeiss), a DC60 warm stage

(Linkam Scientific Instruments) and a high speed video camera (Troubleshooter, Fastcam imaging). All reagents were pre-heated to 37 °C.

CBF calculation:

Camlink (Fastec) software was used to record a 5s video of ciliated epithelium. This video was then analysed at a slower playback speed by the experimenter and the number of frames that elapsed in the time taken to count 10 ciliary beats, each consisting of a power and a recovery stroke, was recorded in an Excel spreadsheet.

CBF was then calculated as follows: CBF = Frame record rate / (frame count/beats count)

Blinding:

Treatment assignment was blinded to the experimenter prior to CBF measurements. 30 mL Sterilin universal tubes containing substances to be tested were labelled A, B, C, and D, by another researcher. The identity of the treatments was revealed at the end of the experiment.

CBF of nasal brushings:

Following treatment with KCN, PYO, KCl or 40 mM HEPES buffer, 150 µl aliquots of nasal epithelium were pipetted onto a CoverWell (Electron Microscopy Sciences) and mounted onto a slide for analysis. Only undisrupted ciliated strips, consisting of >3 cells, were studied.

Nasal brushing CBF measurement replication:

At each time point in the study, CBF was calculated as the mean value of six distinct ciliated strips.

Reversibility:

In order to assess reversibility of CBF inhibition, nasal strips were washed twice in PBS by centrifugation at 1500 x g for 10 min and re-suspended in pre-warmed phosphate buffered saline (PBS, Sigma). CBF was measured before washing and at 30 min and 90 min after washing.

CBF of ALIs:

For CBF measurements of ALI cultures, one ALI insert was used per experimental condition tested. Each insert was washed twice with 200 µL warm PBS to remove mucus and other debris, then placed in a fresh 12-well culture plate for CBF analysis. 150 µL of pre-warmed PBS was added apically and

baseline CBF was measured for 15 min. PBS was then replaced with 150 µL of pre-warmed KCN (75 µM), PYO (75 µM), KCN/PYO (75 µM) or HEPES (40mM). For bacterial culture supernatant experiments, PBS was removed and replaced with 150 µL of *P. aeruginosa* culture supernatant.

CBF was calculated as the mean value of measurements made on 6 different areas from the ALI culture. The same six areas were used at each subsequent time point. Comparison experiments were performed on inserts from the same individual grown at the same time. Replicates of experiments were made on ALI cultures from different individuals.

2.1.5 Viability Measurements

Cell viability was determined using trypan blue staining (Strober, 2001). Following treatment, 50 µL aliquots of nasal brushings were incubated for 60 min at 37°C. 50 µL trypan blue was then added and cells were disaggregated by gentle pipetting. Cell viability was assessed by direct cell counting of the number of stained and unstained cells in a haemocytometer.

2.1.6 ATP Measurements

Following 1 hr treatment with HEPES, KCN or PYO, cellular ATP content was measured using the CellTiter Glo (Promega) luminescent cell viability assay according to the manufacturer's instructions.

2.1.7 Statistical Analysis

Data are expressed as mean (±SEM). Results were submitted to analysis of variance (ANOVA) followed post-hoc by the Tukey test using GraphPad Prism (GraphPad software Inc). Due to variation in baseline CBF between ALI cultures originating from the same patient, data from ALI experiments are expressed as percentage of baseline. The null hypothesis was rejected at $p<0.05$.

2.2 Microbiological Work

2.2.1 Growth Media

All media was made up in dH20 and sterilised by autoclaving. Where necessary, antibiotics were added to the media after autoclaving.

The media used were Luria Bertani Broth (LB) (10 g/L peptone, 5 g/L NaCl, 5 g/L yeast extract) and LB agar (10 g/L peptone, 5 g/L NaCl, 5 g/L yeast extract, 15 g/L agar) supplemented with antibiotics where appropriate.

2.2.2 Buffers and Solutions

Table 2-1 shows the composition of buffers and solutions used in this study. All solutions were made up in dH2O and were sterilised by autoclaving where necessary.

0.5 M KCN stock solution	0.5 M KCN (Fluka) made up in 2 g/L KOH (Sigma)
Pseudomonas transformation buffer	10 mM MOPS (Sigma), pH 7, 10 mM RbCl (Sigma) and 100 mM MgCl2 (Sigma)
Cyanide detection solution	5 mg/ mL copper ethylacetoacetate (Alfa Aesar) and 5 mg/mL tetrabase 4,4'-methylenebis dissolved in chloroform (Sigma)
TAE buffer	0.04 M Tris-acetate (Sigma) and 0.001 M EDTA (Sigma)

Table 2-1 Composition of solutions and buffers.

2.2.3 Agarose Gels

DNA gels were made using biotechnology grade Agarose I™ (Amresco) and TAE buffer. Generally, 0.1 % w/v agarose gels were used except for gDNA gels, which were 0.07 % w/v agarose. SYBR® Safe DNA gel stain (Invitrogen) was added to gels after melting and gels were run in TAE.

DNA samples were re-suspended in Promega Blue / Orange Loading Dye (Promega). The gel was run at 80 V in 1x TAE until the dye front (bromophenol blue) of the marker reached the bottom of the gel. Gels were visualised under blue light.

2.2.4 Kits

Table 2-2 lists commercially available kits used in this study.

Kit	Use
QIAprep® Spin Miniprep Kit **(Qiagen)**	Purification of plasmid DNA
QIAquick® PCR Purification Kit **(Qiagen)**	Gel extraction of DNA
Rapid DNA ligation Kit **(Thermo Scientific)**	Ligation of genes into vectors
TOPO TA Cloning Kit **(Life Technologies)**	Vector used for easy ligation and sequencing
Pfu DNA polymerase Kit **(Thermo Scientific)**	DNA amplification

Table 2-2 Kits used in this study.

2.2.5 Bacterial Strains

To provide a source of bacteria for all experimental work, strains were streaked for single colonies on Luria Bertani (LB) agar plates containing appropriate antibiotics, initially grown up overnight at 37°C and then stored at 4°C. Long term storage of strains was in glycerol stocks stored at -80°C. Plasmids were maintained in *E. coli* HB101.

Table 2-3 lists strains and plasmids used in this study.

Plasmids/Strains	*Description*	*Source*
P. aeruginosa		
PA14	Wild-type, clinical isolate, CF lung	M. Ausubel (Rahme *et al.*, 1995)
PA14NR library	5850 transposon insertion mutants of non-essential PA14 genes. Mariner-based transposon, MAR2xT7 (~1 kb)	M. Ausubel
pUCP18::PA2196	pUCP18 with cloned fragment of PA2196 from PA14	This study
pUCP18::5339	pUCP18 with cloned fragment of PA5339 from PA14	This study
E. coli		
pUCP18	*E. coli – Pseudomonas* shuttle vector AmpR / CbR	*(*Schweizer*,* 1991*)*

Table 2-2 Bacterial Strains and Plasmids

2.2.6 Oligonucleotides

Table 2 4 lists primers used for PCR reactions in this study. Oligonucleotides were synthesised by Beckman Coulter Genomics.

Primer	**Direction**	**Sequence**
PA2196GNFW	Forward	5’-GGATCCATGAAACCCAGCTACGACGAC-3’
PA2196GNBW	Reverse	5’-AAGCTTTCAGATTTCCAGCAGGCTGC-3’
PA5339GNFW	Forward	5’-GGATCCATGACCAAGACCGTTATCCAC-3’
PA5339GNBW	Reverse	5’-AAGCTTTTATTCGAGGACGACGATGG-3’

Table 2-3 Primers used in this study.

2.2.7 Growth of Cultures

Overnight starter cultures were produced by inoculating 5 ml of LB (plus appropriate antibiotics) in a sterile 20 ml plastic screw top tube (Sterilin) with a single colony from an LBA plate. The cultures were grown overnight at 37°C in an orbital shaker set at 200 rpm.

During the day, cultures were grown by aseptically inoculating 50 mL of LB (plus appropriate antibiotics) in a sterile 250 mL conical flask with 1 mL of overnight starter culture. Strains were aerobically at 37 °C with shaking at 200 rpm in identical conical flasks unless otherwise indicated.

2.2.8 Determination of Optical Density

Optical density (OD) was measured at 600 nm (OD^{600}) on a spectrophotometer using aseptically collected 1 ml samples in 1.5 ml disposable plastic cuvettes (Plastibrand). Where necessary, culture samples were diluted so that OD^{600} readings were below 0.4 to ensure linearity. For cultures grown in 96-well plates, OD was measured using a plate reader (Tecan).

2.2.9 Bacterial Transformation

Preparation of chemically competent *E. coli*:

To provide a starter culture, 50 ml of LB broth in a 250 ml conical flask was inoculated with a single colony from a stock plate using a flamed wire loop. The flask was incubated overnight at 37°C in an orbital shaker at 200 rpm, 8 ml of the culture was aseptically added to 400 ml of fresh LB broth in a 1 litre conical flask, which was incubated (37°C, 200 rpm) until the culture had an OD^{600} reading of 0.5 – 1.0. The culture was split into eight equal aliquots in 50 ml tubes (Falcon) and spun at 3000 g for 10 min at 4°C in a centrifuge to pellet cells. After discarding the supernatant, pellets were re-suspended in 200 mL cold 0.01 $MgCl_2$ (Sigma) in four 50 mL tubes (Falcon) and incubated on ice for 20 min. The cells were then pelleted as before and re-suspended in 100 ml of cold 0.1 M $CaCl_2$ (Sigma) in two 50 ml Falcon tubes and incubated on ice for a further 20 minutes. The cells were pelleted again and re-suspended in 5 ml of cold 0.1 M $CaCl_2$ (Sigma) + 14 % glycerol (Sigma) and split into in 50 µl aliquots in chilled 1.5 ml tubes (Eppendorf) before being immediately frozen at -80°C.

Preparation of chemically competent *P. aeruginosa*:

Cultures were grown in 50 ml LB broth in 250 ml conical flasks incubated in an orbital shaker at 200 rpm and 37°C, until the culture had an OD^{600} reading of 0.4 – 0.5. The culture was transferred to two 50 ml tubes (Falcon) and spun at 3000 g for 10 minutes at

4°C in a centrifuge to pellet cells. Each pellet was re-suspended in 25 ml of ice cold *Pseudomonas* transformation buffer and incubated on ice for 20 min. Cells were re-suspended in 2.5 mL ice cold *Pseudomonas* transformation buffer and divided into 0.2 mL aliquots in 1.5 mL tubes (Eppendorf). These were used immediately for transformation.

Heat shock transformation of chemically competent bacterial cells:

Chemically competent cells were defrosted on ice. The contents of ligation reaction/plasmid DNA were added in the following amounts: 0 µl (negative control), 2 µl and 10 µl and mixed with the tip of a P20 Gilson pipette. Tubes were incubated on ice for 45 minutes and heat shocked for 1 minute at 42°C in a heat block before being returned to ice for a further 2 minutes. 1 ml of fresh LB was added to each tube and they were incubated for 1 hour at 37°C in an orbital shaker at 200 rpm. 100 µl was then plated onto appropriate selective LB-agar plates and incubated at 37°C.

2.2.10 Pyocyanin Assay

Cultures were grown in 50 ml LB broth in 250 ml conical flasks incubated in an orbital shaker at 200 rpm and 37°C. Cultures were grown to 2 hours post stationary phase initiation, growth being followed by determining the OD^{600} of the culture media every hour. After determination of the final OD^{600} reading, 20 ml of culture media was centrifuged at 6000 g for 20 minutes. The supernatant was transferred to a 50 ml screw top polypropylene tube (Falcon) and 3 ml of chloroform (Sigma) was added. The tube was shaken to extract the PYO into the chloroform layer, which was then transferred to a fresh 50 ml tube containing 1 ml of

0.2 M HCl. The tube was shaken to extract the PYO to the HCl layer, which was then carefully removed using a P1000 Gilson pipette and the absorbance at 520 nm (A520) was measured using a spectrophotometer. The A520 reading was then normalised by dividing by the final OD^{600} reading, the resulting values were used to compare PYO production between strains.

2.2.11 Cyanide Measurements Using an Ion-Selective Micro-Electrode

A cyanide ion-selective micro-electrode (Lazar Research Laboratories, L.A., CA, USA) connected to a Eutech Cyber scan pH510 pH meter set to read in mV was used for measuring cyanide. The electrode was used according to the manufacturer's instructions.

Precautions:

A 0.5 M KCN stock solution was made up weekly and used to make standard solutions for calibration. The following precautions were taken for storing and handling the KCN powder and the 0.5 M KCN stock solution:

1. The KCN powder (250 g) was kept in a locked cupboard.

2. Gloves and a dust mask were worn when handling KCN powder.

3. KCN powder was added directly to 1 ml of 2 g/l KOH in a 20 ml Sterilin tube.

Highly toxic HCN gas is released from KCN on contact with acid, dissolving the KCN in alkali ensured against this.

4. A single amount of KCN of approximately the correct weight to make 5 ml of 0.5 M KCN solution was added to the 1 ml KOH, further KOH was then added to make a 0.5 M KCN solution.

5. Gloves were worn when handling the 0.5 M KCN stock and the tube was clearly labelled as toxic.

Calibration:

In order to determine cyanide concentration in μM, a calibration curve was produced on each day the electrode was used. Calibration was carried out in the same media in which subsequent measurements were made. Standard solutions of cyanide of concentrations over the likely range of measurement (50 μM-1000 μM) were set up in the appropriate solution using a 0.5 M KCN stock solution with 1 % (v/v) 10 M NaOH (ionic strength adjustment buffer) added. After conditioning in 1000 μM KCN for 10 minutes, the electrode was placed in the lowest concentration standard for 10 minutes. Measurements were made for each standard starting with the lowest concentration and working up. The log of cyanide concentration (μM) was then plotted against the meter readings (mV) and a linear trend line with equation generated in Microsoft Excel (the relationship between the electrical potential and cyanide concentration is logarithmic), only equations with an R^2 value > 0.95 were used. The equation was used to convert sample mV readings into the log of the cyanide concentration value, which was converted into the cyanide concentration by calculating the inverse log.

Measurement of cyanide in liquid culture:

1 ml samples of culture were harvested and placed in 1.5 ml assay tubes (Eppendorf). The tube was centrifuged at 7000 g in an bench top centrifuge (Eppendorf 5415) for 8 minutes to pellet cells. 0.8 ml of supernatant was removed and placed in a new tube with 8 µl of 10 M NaOH. Measurements were performed on cultures two hours after stationary phase initiation (6 hours post inoculation).

2.2.12 PA14NR Replication and Sub-Library Production

The PA14NR library is a non-redundant, single transposon-insertion mutant library of 5850 PA14 mutants corresponding to 4596 predicted genes (Liberati *et al.*, 2006). The library was supplied as 64 96-well micro-titre plates to be stored at -80°C. LB supplemented with 15 µg/mL gentamicin (LB-gen) was used to select for insertion of the MAR2xT7 transposon. The PA14NR library was constructed by the Ausubel group in Boston using the following approach. Transposon insertion mutants were generated in wild-type *P. aeruginosa* strain PA14 using a transposon-site hybridization (TraSH) compatible mariner-based transposon, MAR2xT7, carried on a suicide vector and propagated by a pir+ *E. coli* strain. MAR2xT7 insertions into the PA14 genome were obtained *via* 10 separate tripartite mating events and were selected using plates with 15 µg/mL gentamicin and 1 µg/mL Irgasan. Near saturation of the PA14 genome was achieved. Putative transposon insertion mutants were then robotically picked into 250 µl of LB containing 15 µg/mL gentamicin in 96-well micro-titer plates. T7 promoters placed at both ends of MAR2xT7 allowed each MAR2xT7 mutant to be uniquely identified *via* PCR-amplification of the genomic sequence adjacent to the transposon. Sequences obtained from 24,089 of these mutants were mapped to 20,530 unique loci within the PA14 genomic sequence, with an average of 4.3 transposon insertions mapped to each gene. Insertions were isolated in 75% of the predicted PA14 genes. The protocol that follows was optimised from the library instruction manual provided by the authors to minimise well-to-well contamination, an issue highlighted in several of their communications. Library work was carried out in a Class II Safety Cabinet to provide a sterile environment, and with dry ice to minimise thawing of the library plates.

Inoculation of culture blocks:

600 µL LB-gen were dispensed into the wells of 2 mL Deep 96-well Polypropylene Titerblocks (USA Scientific). These were then covered with sterile non-breathable aluminium seals (Greiner Bio-One) and quick spun at 1000 rpm and at room temperature for 2 s. PA14NR plates were taken out from

storage at -80°C, kept on dry ice where possible, and quick spinned at 1500 rpm at 4°C for approximately 5 s immediately before use. Care was taken when removing the seals from library plates not to dislodge any remaining culture. Sterile tips on a 12-channel pipette were used to inoculate corresponding wells in the culture block with frozen material from the library plates. The library plates were then re-sealed with sterile non-breathable aluminium seals and stored at -80°C. For the production of sub-libraries, a sterile tip was used to pierce the area of the seal directly above an individual well of interest, following which the entire seal was removed and replaced. Following inoculation, culture blocks were sealed with a breathable membrane (Breathe-Easy, Sigma-Aldrich) and incubated with shaking at 37 °C and 200 rpm for 20 hours.

Replicate production:

OD^{600} of 100 µL samples taken from each well of the culture block was measured and variation in growth was recorded. So as to minimise contamination, sterile LB-glycerol was then added to each well to a final concentration of 15% w/v. 40 µL from each well were dispensed into corresponding wells of sterile 96-well micro-titre plates (Greiner Bio-One) containing 160 µL 15% LB-glycerol w/v. The resulting replicate or sub-library plates were sealed with a sterile aluminium seal and stored at -80°C.

2.2.13 High Throughput Colourimetric Cyanide Screen

A qualitative method for the detection of cyanogenic bacteria was first described by (Castric & Castric, 1983). An adaptation of this method to a 96-well format for the quantitative measurement of HCN production in plants was later described by Takos *et al.* (2010), and advice from these authors has allowed the optimisation of the following protocol for the semi-quantitative detection of cyanogenesis mutants in the PA14NR library.

Feigl-Anger cyanide detection paper:

3MM paper (Whatmann) was cut into 8x12 cm rectangles and wetted with 2 mL cyanide detection solution, consisting of 2.5 mg/mL copper(II) ethylacetoacetate and 2.5 mg/mL 4,4'-methylenebis-(N,N-dimethylaniline) dissolved in chloroform (Feigl and Anger, 1966).

Detection mechanism: HCN gas in contact with cyanide detection paper reacts with copper (I) ions producing CuCN, following which tetrabase is oxidised by Cu(II) ions to form a blue stain.

Original Screening protocol:

Culture blocks were inoculated with desired strains and incubated at 37 °C and 200 rpm for 24 hours, until OD^{600} 0.6-1.5 was reached in the majority of wells. LB-glycerol was then added to

the culture blocks to a final concentration of 15% glycerol w/v so as to increase viscosity and prevent contamination during the transfer of material, and 10 µL from each well was used to inoculate 180 µL LB-gen in the corresponding wells of a sterile 96-well micro-titre plate (1:20 dilution). A sheet of cyanide detection paper was placed directly on top of the wells of the 96-well plate. In order to obtain discrete spots, cyanide detection sheets were secured onto the plate by means of a Breathe-Easy membrane. A plate roller was used to press the membrane down and assure a secure and uniform fit. The 96-well plates were then incubated, without shaking, at 37 °C for 20 hours. OD^{600} measurements were recorded for each well. The cyanide detection paper above each plate was collected and scanned at 300 dpi and saved as a PDF document using the scan-to-email feature of a Hewlett Packard Colour LaserJet printer.

Optimised screening protocol:

In order to overcome image quality issues caused by condensation and evaporation, changes were made to the incubation times. Once inoculated, assay plates were incubated statically at 35 ˚C with the lids on for 10 hours. This was followed by a 10 hour lidless static incubation at 37 ˚C hours.

2.2.14 Data Analysis in R

Clustering based on distance was conducted using the partitioning around medoids (PAM) in the free statistical package R (http://www.r-project.org/). The optimal number of clusters for PAM was chosen using the average cluster stability.

2.2.15 Genomic Map Generation in CG View

Genes identified through screening were mapped onto the PA14 genome using the free software CG View (http://wishart.biology.ualberta.ca/cgview/). Maps were generated with assistance from the Imperial Bioinformatics Support Service.

Chapter 3
INHIBITION OF CILIARY FUNCTION OF RESPIRATORY EPITHELIA BY CYANIDE CONCENTRATIONS FOUND IN THE INFECTED AIRWAY

3.1 Introduction

To date, there have been relatively few investigations into *P. aeruginosa* cyanogenesis from a medical standpoint, and a pathophysiological role, if any, during CF lung infections, has yet to be elucidated (Anderson *et al.*, 2010).

HCN has a boiling point of 25.6-26.6 ˚C, and is therefore released as a gas in many of the biological contexts where it is produced by *P. aeruginosa*. HCN also partially ionises in water, and therefore sputum, to give the cyanide anion, CN^- For the purposes of this chapter, both HCN and CN^- will henceforth be referred to as 'cyanide'.

3.1.1 Does Cyanogenesis Contribute to Virulence in CF Patients?

The work presented in this chapter follows on from previous research in our lab, which demonstrated that sub-lethal levels of cyanide could be detected in the sputa of CF patients infected with *P. aeruginosa*. Ryall *et al.* (2008) found that cyanide accumulated in *P. aeruginosa*-infected sputum at mean concentrations of between 32-72 μM (max 150 μM). Additionally, the presence of cyanide negatively correlated with lung function, with mean predicted forced expiratory volume (FEV1%) of 26.8%+3.8% for patients with cyanide in their sputum versus 46.0%±6.7%. for those without ($P<0.05$). This chapter explores the possible mechanisms for this association, focussing on the effect of physiologically relevant concentrations of cyanide on human respiratory epithelial cell function. We hypothesise that cyanogenesis by *P. aeruginosa* constitutes a virulence factor contributing to the decrease in lung function observed in CF patients with detectable sputum cyanide.

3.2 Aims

- To characterise the effect of physiologically relevant concentrations of cyanide on human respiratory ciliary beat frequency (CBF) in two models of the human airway: Nasal brushings and *sino-nasal* air liquid interface cultures (ALIs).

- To investigate the interplay between cyanide and another simultaneously secreted ciliostatic *P. aeruginosa* exoproduct, PYO.

- To evaluate the relative importance of different components of *P. aeruginosa* supernatant on respiratory CBF using wildtype, cyanide-deficient and PYO-deficient strains.

3.3 Method Development

3.3.1 Optimisation of Ciliary Beat Frequency Measurements

The CBF measurement method used in this study was adapted from a diagnostic procedure for Primary Ciliary Dyskinesia (PCD) routinely carried out at the Royal Brompton Hospital (RBH): Briefly, a nasal brushing is obtained from a patient suspected of having PCD and ciliary function is assessed by observing ciliary beating in 10 separate healthy strips from a single sample using light microscopy and high-speed video imaging. Prior to any experiments, and in order to increase the suitability of this method for quantitative studies, timeframe, number of replicates, experimental design and controls were optimised.

A replicate number was determined empirically by plotting out cumulative mean CBF data from 26 patients. A mean derived from n=6 only differed from a mean derived from n=10 by 0.062 Hz, and this difference was not significant ($p>0.05$) (Figure 3-1). It was therefore decided that in subsequent experiments each time point would be derived from the mean of 6 technical replicates.

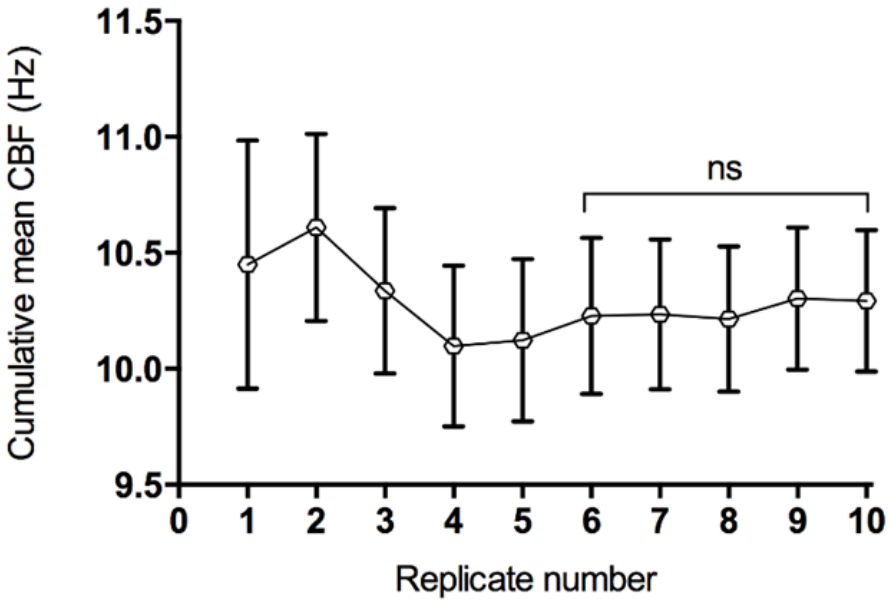


Figure 3-1 Optimisation of ciliary beat frequency measurements – number of replicates. Cumulative mean CBF data from 26 patients. n=6 technical replicates provides an accurate estimate of CBF (mean difference of 0.062 Hz for n=6 vs n=10, $P>0.05$). Error bars are S.E. of technical replicates.

A timeframe of 30-90 min has been employed in previous studies on the effect of toxic compounds on CBF (Smith, 1996; Winters *et al.*, 2007). A preliminary test of the effect of 150 μM and 75 μM KCN, at 37 ˚C, confirmed that a marked effect on CBF could be observed within this timeframe (Figure 3-2).

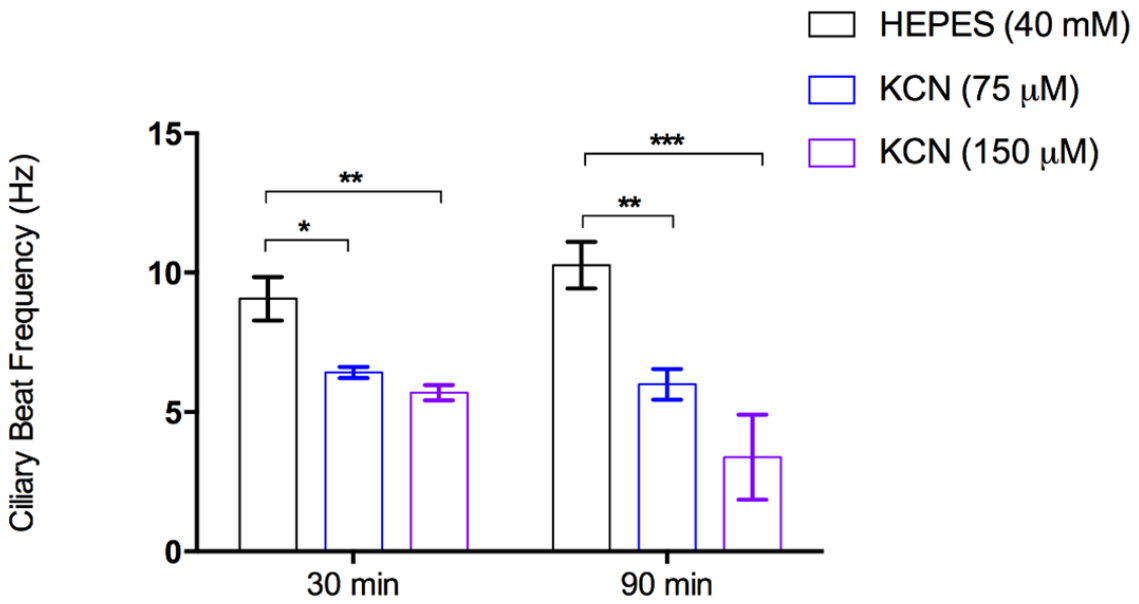


Figure 3-2 Optimisation of ciliary beat frequency measurements – timeframe. Effect of KCN on CBF after 30 and 90 min. Error bars are S.E of 6 technical replicates. 75 µM KCN; 30 min; 29% decrease P<0.05; 75 µM KCN; 60 min; 37% decrease P<0.001; 150 µM KCN; 30 min; 37% decrease P<0.001; 150 µM KCN; 60 min; 60% decrease P<0.0001. Stars represent statistical comparisons (One way ANOVA with a post-hoc Tukey's test) ∗ : P < 0.05, ∗∗ : P < 0.001; ∗∗∗ : P < 0.0001.

3.4 Results

3.4.1 Cyanide Concentrations Found in CF Sputum Decrease Ciliary Beat Frequency in Human Nasal Brushings

To test the effect of sub-lethal concentrations of cyanide on epithelial cell function, CBF was monitored in human nasal brushings obtained from healthy volunteers (n=6; age range: 21-50) following exposure to physiologically relevant levels of KCN (150 μM and 75 μM; Figure 3-3). Both HEPES and KCl have been used as controls in studies on cyanide toxicity (Kupriyanov *et al.*, 1996; Kruse *et al.*, 2008;). When compared with HEPES and KCl controls, 150 μM KCN caused a marked decrease in CBF (baseline CBF: 12.3 Hz ± 2.8; 150 μM KCN; 46% decrease compared to KCL control after 60 min $P<0.0001$; Figure 3-3A). This effect was apparent within the first 15 min (29% decrease $P<0.05$) and was maximal by 30 min.

The inhibitory effect of KCN on CBF was found to be concentration-dependent, with 75 μM causing a lesser but still significant decrease in a separate experiment (n=6; age range: 21-34; baseline CBF: 14.3 Hz ± 1.9; 75 μM KCN; 60 min; 32% decrease $P<0.00001$; Figure 3-3 B). As was seen with 150 μM KCN, the inhibitory effect of cyanide appeared to plateau by 30 min.

A decrease in CBF following treatment with 150 μM KCN was also observed in nasal brushings obtained from paediatric CF patients. As expected from the literature, once removed from the CF lung environment where the ASL is depleted, CF nasal brushings exhibited normal baseline CBF values (n=3; baseline CBF: 13.8 Hz ± 3.2; age range: 2-16). Addition of 150 μM KCN resulted in a 55% decrease compared to the KCl control after 60 min ($P<0.01$; Figure 3-4).

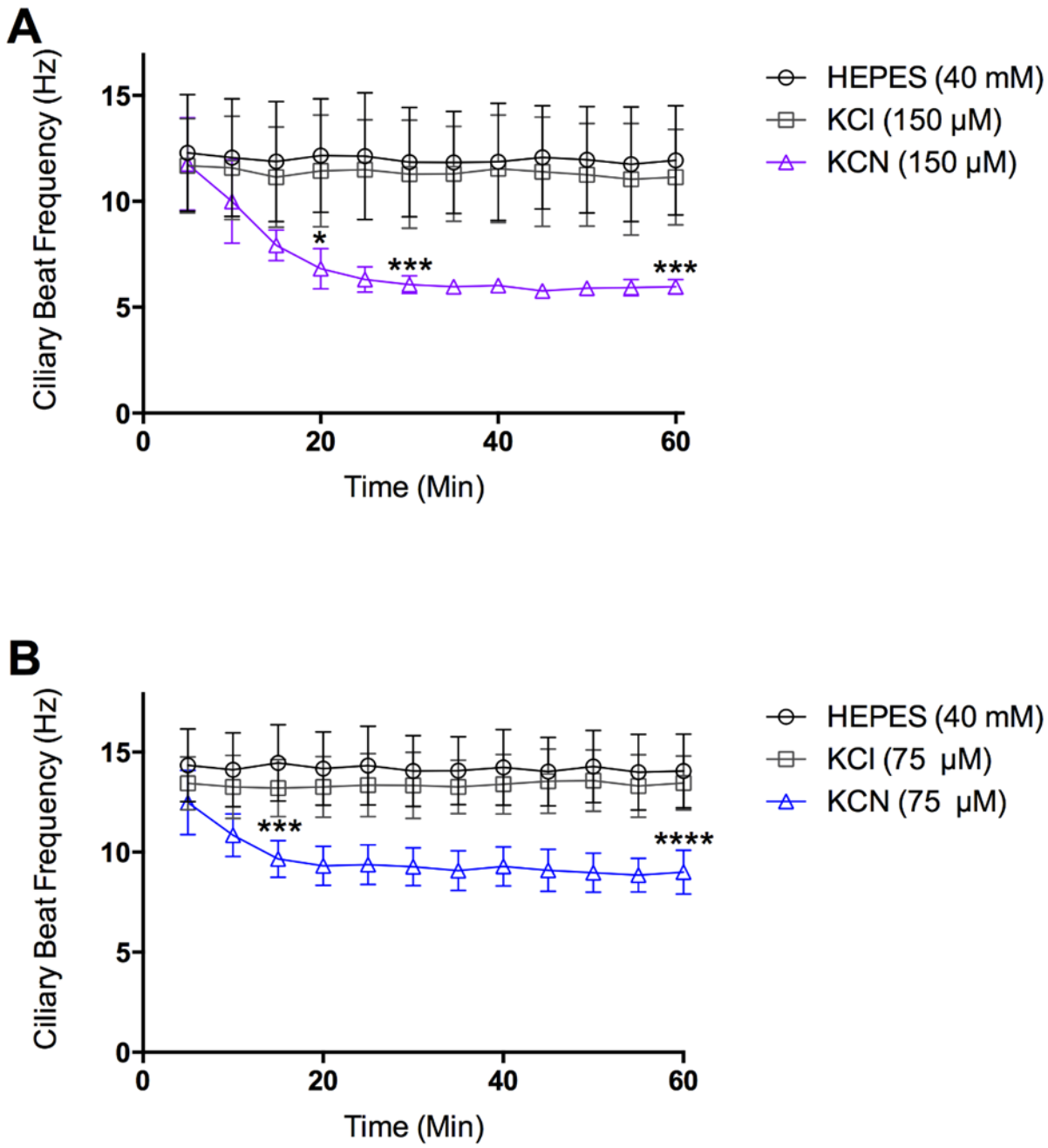


Figure 3-3 Physiologically relevant concentrations of KCN decrease ciliary beat frequency of human nasal brushings in a concentration-dependent manner. Error bars are S.E. of biological replicates. (A) Healthy volunteers, n=6; 150 µM KCN, 46% fall after 60 min P<0.0001. (B) Healthy volunteers, n=6; 75 µM KCN, 32% fall after 60 min, P<0.00001. Stars represent statistical comparisons by one-way ANOVA; * : P < 0.05, ** : P < 0.001; *** : P < 0.0001; **** : P < 0.00001.

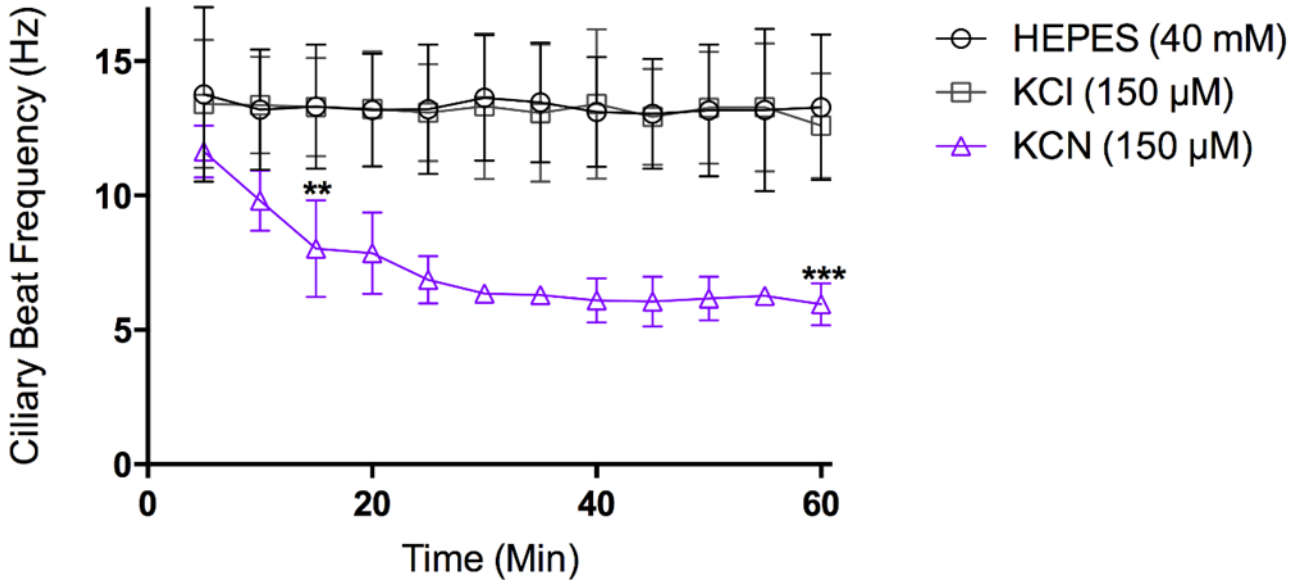


Figure 3-4 KCN decrease in CBF also occurs in paediatric CF nasal brushings. Error bars are S.E. of biological replicates. n=3; 150 µM KCN; 60 min; 55% decrease P<0.001. Stars represent statistical comparisons (One way ANOVA with a post-hoc Tukey's test) ∗ : P < 0.05, ∗∗ : P < 0.001; ∗∗∗ : P < 0.0001.

Next, the cilio-inhibitory mechanism of KCN was further characterised. The fall in CBF was not due to a loss of cell viability as assessed by trypan blue staining (ns compared to KCl P>0.05; Figure 3 5A). In further support of this, cyanide-mediated inhibition of CBF was found to be reversible (Figure 3 5B). Following maximal inhibition of CBF with 150 µM KCN after 30 min, CBF recovered to baseline levels when cyanide was removed by washing (n=6; 150 µM KCN; 30 min; 6.5 Hz 54% decrease P<0.0001; post-washing 60 min 13.8Hz ns P>0.05), and CBF was still normal after 120 min (post-washing 120 min 13.85 Hz ns p>0.05).

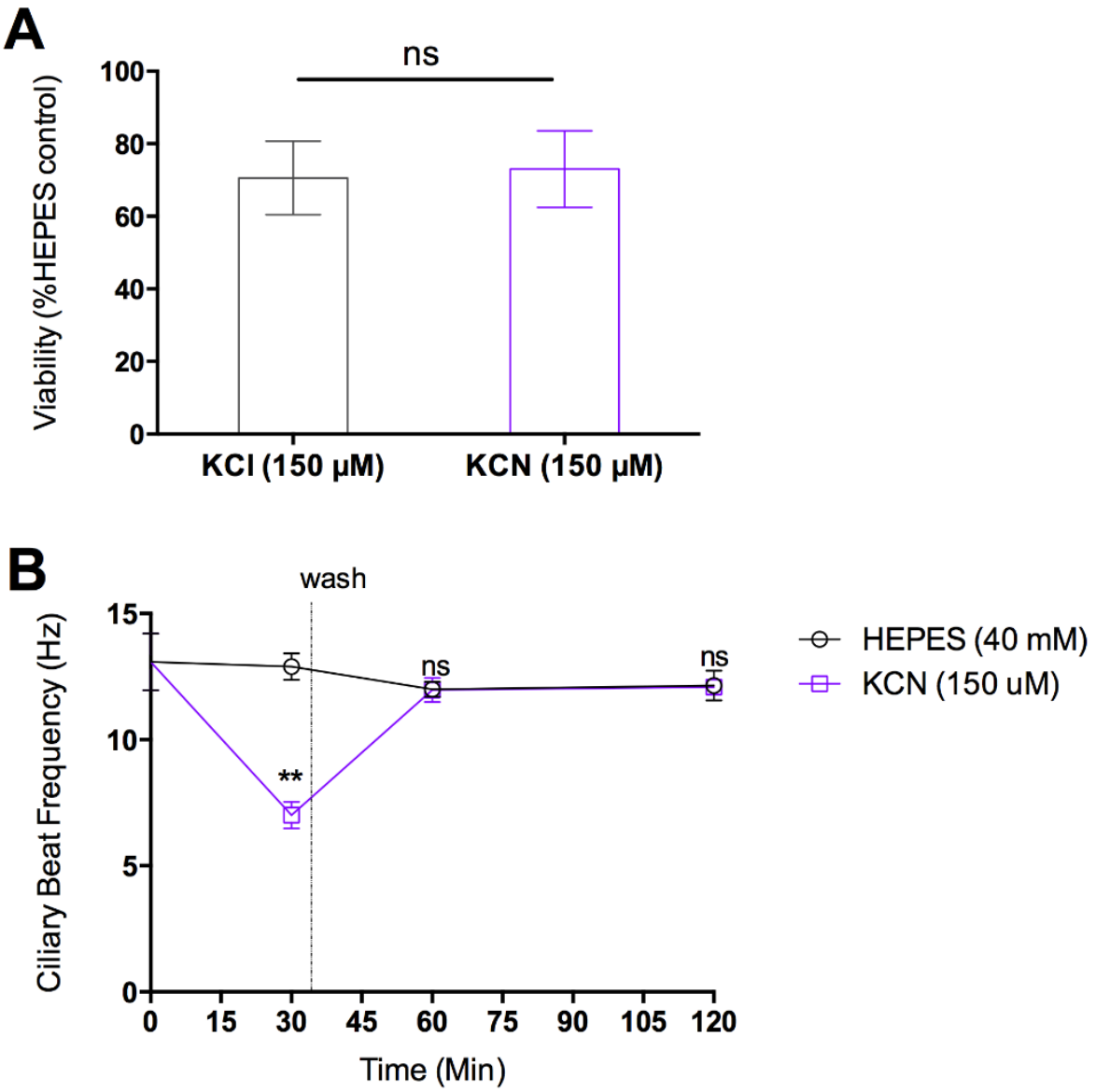


Figure 3-5 CBF decrease is not due to loss of viability and is reversible. Error bars are S.E. of biological replicates. (A) No difference in viability compared to KCl control after 60 min (n=6; P>0.05) (B) Recovery to baseline CBF after removal of KCN by washing (150 µM KCN; 30 min; 6.5 Hz; 54% decrease, P<0.001; 60 min; 13.8 Hz; P> 0.05; 120 min 13.85 Hz; P> 0.05). Stars represent statistical comparisons (One way ANOVA with a post-hoc Tukey's test) ∗ : P < 0.05, ∗∗ : P < 0.001; ∗∗∗ : P < 0.0001.

3.4.2 Combined effect of KCN and Pyocyanin on Ciliary Beat Frequency of Nasal Brushings

Like cyanide, the *P. aeruginosa* virulence factor PYO is detectable in sputum at concentrations of 75-100 µM and has previously been shown to slow CBF (Wilson *et al.*, 1988) . To evaluate the implications of the presence of both PYO and cyanide in the lung, their combined effect on CBF was studied. Nasal brushings from healthy volunteers were exposed to physiologically relevant concentrations of KCN, PYO or KCN+PYO for 60 min (n=3; age range: 24-30; baseline CBF: 13.04 ± 1.2; Figure 3-6). In accordance with Wilson *et al.* (1988), 75 µM PYO significantly decreased CBF (75 µM PYO; 60 min; 27% decrease P<0.0001), but this effect was less marked than with physiologically relevant concentrations of cyanide. Treatment with 75 µM KCN caused a 36% decrease after 60 min compared to the KCL control (P<0.0001). Interestingly, combined treatment with KCN+PYO caused a significantly greater decrease in CBF than treatment with PYO alone (75 µM KCN+PYO; 60 min; 51% decrease compared to HEPES control P<0.0001; 27% decrease compared with PYO alone; P<0.001).

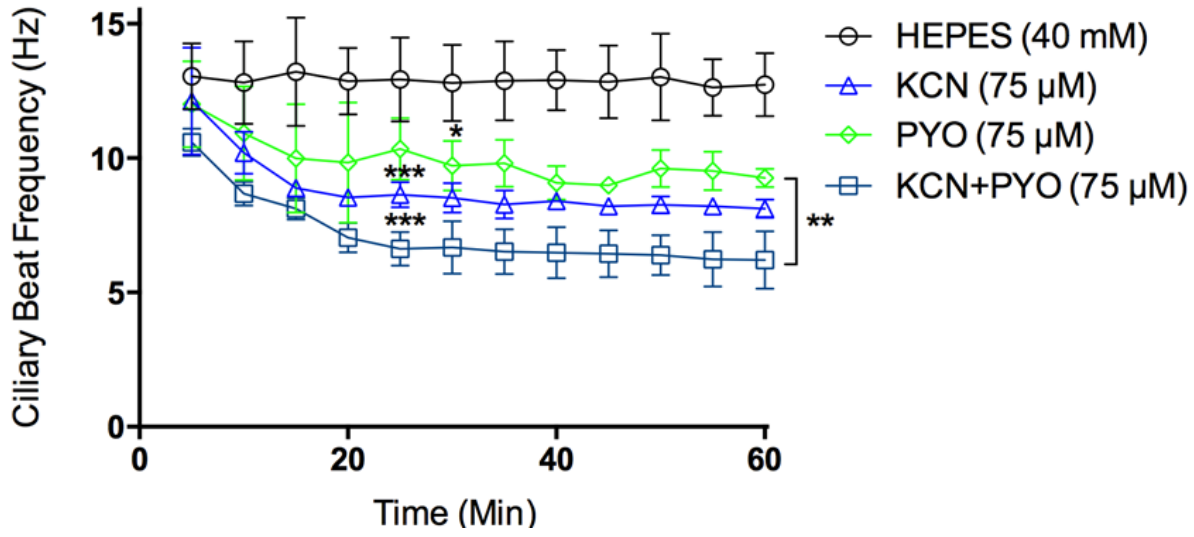


Figure 3-6 Combined effect of KCN and PYO on ciliary beat frequency of healthy nasal brushings. Error bars are S.E. of biological replicates. Healthy volunteers n=3; Baseline CBF 12.7 Hz; 75 µM PYO; 60 min; 27% decrease P<0.001; 75 µM KCN; 60 min; 42% decrease P<0.0001; 75 µM PYO+KCN; 60 min; 51% decrease P<0.01. Stars represent statistical comparisons (One way ANOVA with a post-hoc Tukey's test) ∗ : P < 0.05, ∗∗ : P < 0.001; ∗∗∗ : P < 0.0001.

3.4.3 Combined Effect of KCN and Pyocyanin on Ciliary Beat Frequency of *Sino-nasal* Air Liquid Interface Cultures

In the lung environment, toxic exoproducts secreted by *P. aeruginosa* typically come into contact with the apical surface of epithelial tissue. For this reason, respiratory ALIs provide a more relevant topographical model of the airway than nasal brushings in suspension. However, they are difficult and time consuming to grow and therefore were not available for all the experiments in this chapter. Once the nasal brushing data were available, it was considered important to explore these findings in the ALI model. ALI cultures consist of mucus-producing, ciliated monolayers and these have been shown to accurately represent the in vivo airway epithelial transcriptome.

ALI cultures were cultured from 4 non-CF and 3 CF patients. For each patient, 4 ALI cultures were grown in separate wells on the same 24-well plate and one well was used per treatment. Each of the 4 cultures originating from the same patient had its own baseline CBF, and these varied substantially (Table 3-1). For this reason, data on the effect of KCN and PYO on CBF in the ALI model are expressed as percentage baseline CBF of individual cultures.

Non-CF Sample #	**1**	**2**	**3**	**4**
	7.89 Hz ± 2.68	8.31 Hz ± 2.68	7.99 Hz ± 1.84	8.05 Hz ± 2.56
CF Sample #	**1**	**2**	**3**	
	10.18 Hz ± 2.37	9.59 Hz ± 2.47	8.96 Hz ± 1.79	

Table 3-1 Baseline CBF of Air Liquid Interface cultures originating from non-CF and CF volunteers (n=4 ALIs from healthy volunteers; n=3 ALIs from CF patients). Variation in starting CBF of ALIs from the same patient is indicated as ± SD. Due to the intra-patient variation in baseline CBF, ALI CBF data in subsequent experiments is expressed as percentage baseline.

CBF of ALIs cultured from healthy airway epithelium was measured following treatment with KCN, PYO or KCN+PYO (n=4; Figure 3-7A). After 60 min, the compounds tested significantly inhibited CBF but to a lesser extent than was observed in the nasal brushing model. 75 μM KCN caused a 13% decrease in CBF ($P<0.0001$), while 75 μM PYO caused a 5% decrease ($P<0.05$). Combined treatment with 75 μM PYO+KCN resulted in an 18% decrease in CBF after 60 min ($P<0.0001$). This decrease

was significantly greater than that observed following treatment with PYO alone (P<0.001), but was not significantly greater than that seen following treatment with KCN alone (ns; P>0.05).

These observations were also confirmed in ALIs cultured from CF patients (n=3; 75 µM KCN; 60 min; 20% decrease P<0.0001; 75 µM PYO; 60 min; 10% decrease P<0.001; 75 µM PYO+ 75 µM KCN; 60 min; 22% decrease P<0.0005, n=3, Figure 3-7B). Interestingly, KCN and PYO appear to have a greater effect in CF ALIs compared to non-CF ALIs (75 µM KCN; 60 min; 13% decrease in non-CF vs 20% decrease in CF ALIs; 75 µM PYO; 60 min; 5% decrease in non-CF vs 10% decrease in CF ALIs).

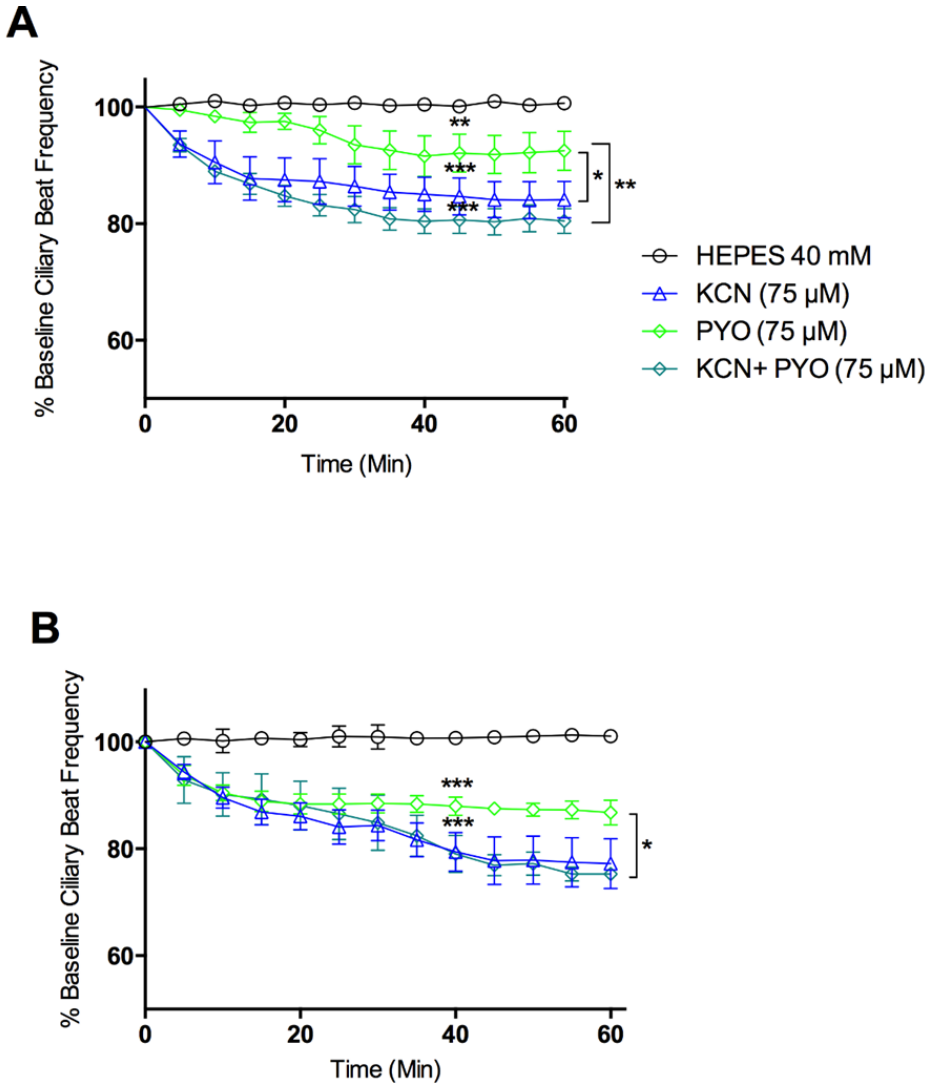


Figure 3-7 Combined effect of KCN and PYO in air-liquid interface cultures. Error bars are S.E. of biological replicates. (A) Non-CF controls n=4; 75 µM KCN; 60 min; 13% decrease P<0.0001; 75 µM PYO; 60 min; 5% decrease P<0.05; 75 µM PYO+KCN; 60 min; 18% decrease P<0.0001; (B) CF patients n=3; 75 µM KCN; 60 min; 20% decrease P<0.0001; 75 µM PYO; 60 min; 10% decrease P<0.001; 75 µM PYO+KCN; 60 min; 22% decrease P<0.0001. Stars represent statistical comparisons (One way ANOVA with a post-hoc Tukey's test) ∗ : P < 0.05, ∗∗ : P < 0.001; ∗∗∗ : P < 0.0001.

3.4.4 Cyanide-Induced Decrease in Ciliary Beat Frequency is not Due to ATP Depletion

Given that cyanide is a mitochondrial cytochrome c oxidase inhibitor at lethal concentrations, a logical next step was to determine whether the mechanism of CBF reduction by sub-lethal levels of KCN was *via* depletion of ATP levels. ATP measurements were first optimised in the immortalised normal bronchial epithelial cell line 16-HBE.

ATP levels of 16-HBE cells were measured after 60 min exposure to HEPES, KCN, PYO or KCN+PYO (Figure 3-8A). Concordant with previous findings, PYO caused a marked decrease in ATP levels compared to the HEPES control (75 μM PYO; 60 min; 48% fall $P<0.0001$; 150 μM PYO; 60 min; 60% fall $P<0.0001$, n=6) (Kanthakumar *et al.*, 1993). However, KCN had no effect on ATP levels at either concentration. Combined treatment with 75 μM KCN+75 μM PYO did not cause a significantly greater decrease in ATP levels than treatment with PYO alone (ns; $P>0.05$). In contrast, combined treatment with 150 μM KCN+PYO did cause a significantly greater decrease in CBF than PYO alone.

Since 16-HBE cells are not fully differentiated and lack cilia, ATP measurements were repeated in the human nasal brushing model (n=5; Figure 3-8B). Similar findings were seen for PYO (75 μM PYO; 60 min; 70% decrease in ATP $P<0.0001$, n=5), while 75 μM KCN had no significant effect. In order to maximise the number of live cells in each well, and is was a closer match to the mean cyanide levels detectable in patient sputum, only 75 μM KCN was tested with the nasal brushings.

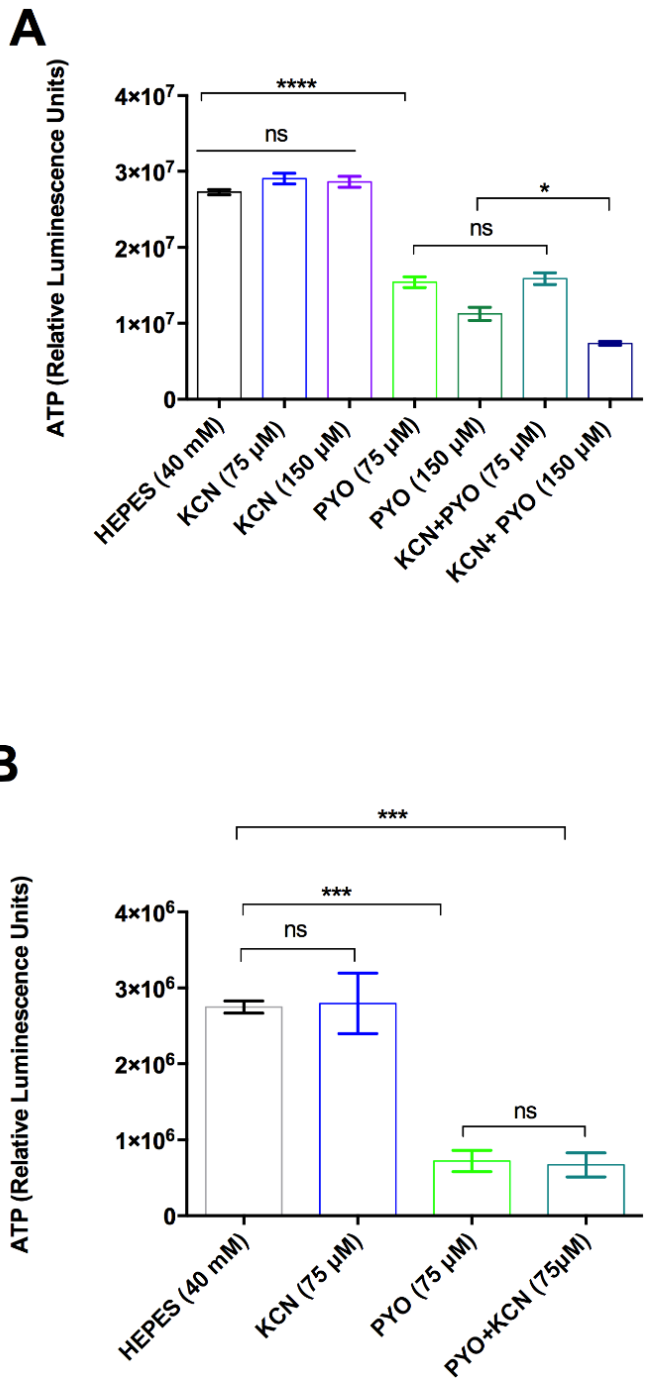


Figure 3-8 KCN-induced decrease in ciliary beat frequency after 60 min is not due to ATP depletion. (A) 16-HBE cells n=6. Error bars are S.E. of technical replicates. 75 µM PYO; 60 min; 48% decrease P<0.0001; 150 µM PYO; 60 min; 60% decrease P<0.0001); 150 µM KCN; 60 min; no effect P>0.05; 75 µM KCN; 60 min; no effect P>0.05 (B) Nasal brushings from healthy volunteers n=5; Error bars are S.E. of biological replicates. 75 µM PYO; 60 min; 70% decrease P<0.001; 75 µM KCN; 60 min; no effect (P>0.05). Stars represent statistical comparisons (One way ANOVA with a post-hoc Tukey's test) ∗ : P < 0.05, ∗∗ : P < 0.001; ∗∗∗ : P < 0.0001.

3.4.5 Effect of *P. aeruginosa* Culture Supernatants on Ciliary Beat Frequency of Air-Liquid Interface Cultures

The production of HCN and PYO is co-ordinately regulated by QS in *P. aeruginosa*, and both components accumulate extra-cellularly in the culture environment. The effect on CBF of supernatant fractions from cultures of a *P. aeruginosa* wildtype strain (PA14), a cyanide-deficient mutant (*hcnA*) and a PYO-deficient mutant (i) was tested (Figure 3-9). Under the growth conditions used the culture supernatants of PA14 and *phzS* strains produced 73 μM and 75 μM cyanide in solution respectively, whereas no detectable cyanide was present in the *hcnA* strain (Figure 3 9A; cyanide electrode detection limit: 50 μM). Under these conditions, PA14 and *hcnA* produced 59 and 61 μM PYO, while the *phzS* produced no PYO (Figure 3 9B). The culture supernatant from PA14 caused a significant decrease in CBF after 60 min (23% decrease $P<0.001$; Figure 3 9C). Minimal statistically insignificant levels of inhibition were observed with the culture supernatant from the cyanide-deficient mutant *hcnA* (ns $P>0.05$), whereas supernatant from the PYO-deficient *phzS* strain inhibited CBF at levels similar to wildtype (19% decrease $P<0.001$).

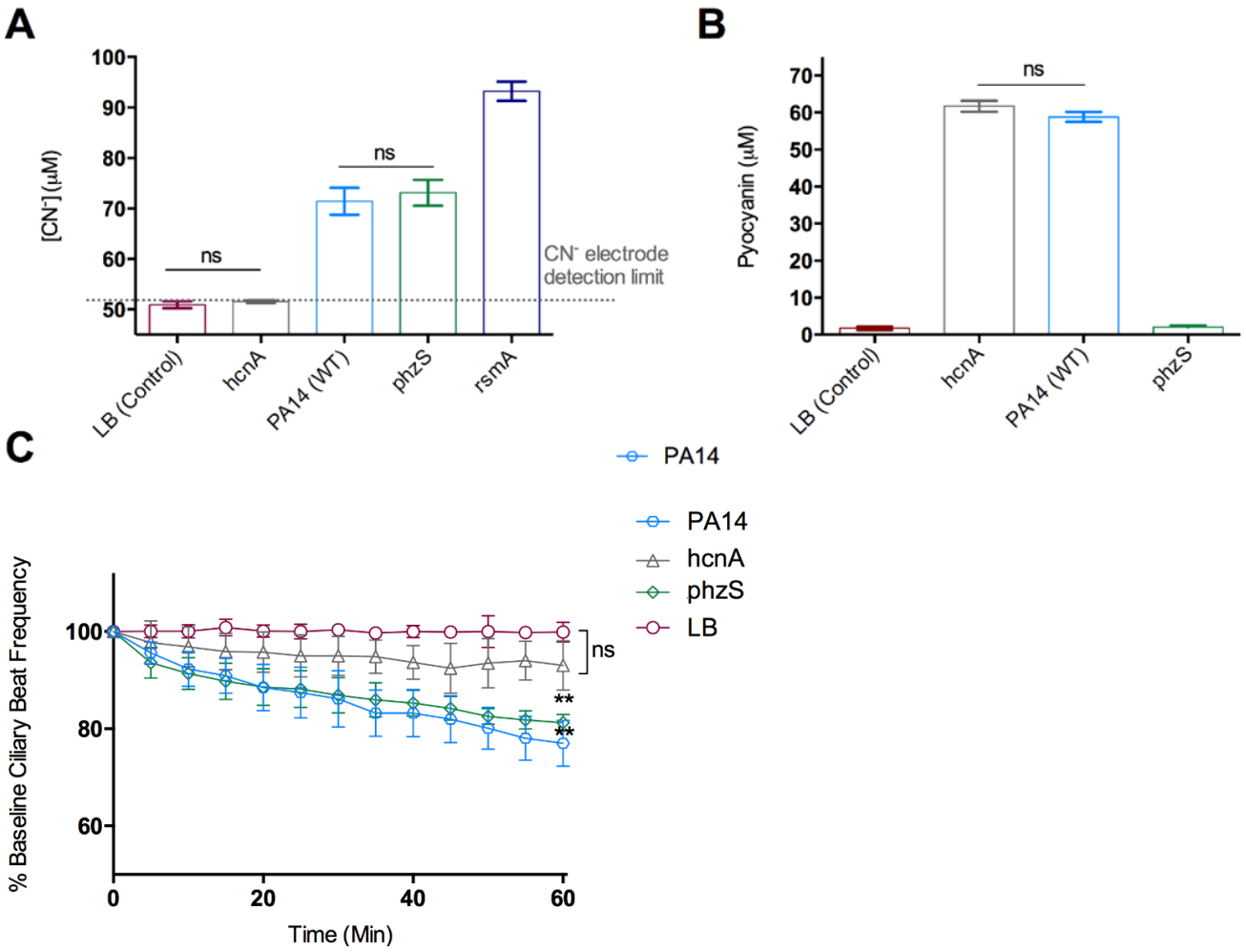


Figure 3-9 Effect of cyanide and PYO from *P. aeruginosa* culture supernatants on CBF of healthy human *sino-nasal* air liquid interface cultures. n=3; Error bars are S.E. of biological replicates. (A) Cyanide production of *P. aeruginosa* strains after 16 hours. PA14 (WT) and *phzS* did not differ significantly in cyanide production (ns p>0.05). *hcnA* did not produce detectable levels of cyanide above the electrode detection limit. rsmA was included as a positive control as it is a known cyanide overproducer (93 µM CN- p<0.0001). (B) PYO production of P. aeruginosa strains after 16 hours. PA14 (WT) and *hcnA* did not differ significantly in cyanide production (ns p>0.05). *rsmA* was included as a positive control as it is a known cyanide overproducer. (C) *hcnA* exhibited attenuated virulence and did not cause a significant fall in CBF compared to LB control (ns; P>0.05). *phzS* caused inhibition of CBF comparable to that of PA14 (ns; P>0.05). Stars represent statistical comparisons (One way ANOVA with a post-hoc Tukey's test) ∗ : P < 0.05, ∗∗ : P < 0.001; ∗∗∗ : P < 0.0001.

3.5 Discussion

This chapter aimed to determine whether patho-physiologically relevant concentrations of cyanide could directly affect airway epithelial cells. We hypothesised that *P. aeruginosa* cyanogenesis may contribute to reduced lung function. Specifically, ciliary beating was measured, as it is a clinically important feature of muco-ciliary clearance. CBF measurements following treatment with cyanide in two human models of the airway, nasal brushings and ALIs, indicated that cyanide concentrations similar to those detected in sputum of *P. aeruginosa*-infected patients could be sufficient to significantly inhibit ciliary beating of epithelial cells *in vitro*.

3.5.1 Comparison with Sub-Lethal Cyanide Exposure on Cilia in Non-Human Models

Under the conditions tested, patho-physiologically relevant concentrations of cyanide (75-100 μM) inhibit CBF of non-CF and CF human nasal brushings in a dose-dependent and reversible manner. Cyanide was also found to inhibit CBF, albeit to a lesser extent, in ALIs, a more realistic model of the intact airway.

Much of the literature on sub-lethal cyanide toxicity to cilia comes from studies on the effect of cigarette smoke condensate (CSC) on CBF, with models ranging from freshwater mussel gills to hamster oviducts (Table 3-2).

Model	Cyanide source	[CN^-]	Effect	Reference
Freshwater mussel	HCN	CSC (8 puffs)	55% inhibition by CSC. Marked reduction in inhibition when HCN removed by filtration.	(Walker & Kiefer, 1966)
Chicken trachea	HCN	CSC (8-80 puffs)	Rapid recovery of CBF when HCN removed by filtration.	(Battista & Kensler, 1970)
Hamster oviduct	KCN (KCl control)	50 μM and 100 μM	25% inhibition (50 μM) 70% inhibition (100 μM) Full recovery when KCN removed by washing.	(Talbot *et al.*, 1998)

Table 3-2 Effect of KCN on CBF in other models of the airway.

The kinetics of inhibition reported in this chapter are broadly concordant with previous observations that sub-lethal cyanide levels cause a concentration-dependent and reversible decrease in CBF.

3.5.2 Possible Contribution of Cyanide to Cilio-Inhibition and Virulence in the Respiratory Tract

The data presented here suggests that cyanide could play a role in inhibition of CBF *in vitro*, a conclusion supported by experiments using supernatants from *P. aeruginosa* cultures. In the ALI model, culture supernatants from a PYO-deficient mutant, *phzS* were able to inhibit CBF to a similar extent as the wild type, PA14, while low levels of inhibition were observed with a cyanide deficient mutant, *hcnA*. This is a contrast to the previous finding that 75 μM significantly inhibits CBF of nasal brushings, and suggests that PYO may act differently in other models.

A previous study on *P. aeruginosa* supernatant cilio-inhibitory components implicated a number of secreted factors. Hingley *et al.*, (1986) , investigated heat-stable and chloroform-extractable material from 24 hr and 48 hr *P. aeruginosa* culture supernatatants and found that, of these, PYO and rhamnolipids had the strongest inhibitory effect on the cilia of rabbit tracheal explants. After 60 min exposure rhamnolipid (2800 μg/mL) irreversibly demembranated cilia, removed some of the outer dynein arms and resulted in complete stasis. Purified PYO (~240 μM) caused a 40% decrease in CBF that was not associated with cilia ultrastructure damage and could be reversed with ATP.

Kanthakumar *et al.*, (1993) further characterised the cilio-inhibitory mechanism of PYO. A decrease in CBF in human nasal brushings following 60 min treatment with PYO was associated with a significant fall in intracellular cyclic AMP (cAMP) (90% decrease) and ATP (66% decrease). ATP provides the pool for cAMP, which is required by protein kinase A (PKA) to phosphorylate the outer dynein arms and stimulate maximal CBF (Salathe, 2007). In addition, in frog esophagus epithelium, ATP has been shown to interact with protein kinase C to induce Ca2+ waves that enhance CBF (Levin *et al.*, 1997).

The carbohydrate-binding lectins LecA and LecB are also part of *P. aeruginosa*'s cilio-inhibitory arsenal. LecA and LecB bind the glycocalyx of airway cells, allowing the pathogen to attach itself more efficiently. Additionally, LecA and LecB are thought to immobilise ciliary beat and thus prevent clearance by the muco-ciliary escalator (Adam *et al.*, 1997). Inhibition of CBF in human nasal explants

by 1 μM LecA only takes effect after 1 hour and results in severe inhibition of CBF by 5 hours (82% decrease) (Mewe *et al.*, 2005).

It is becoming increasingly apparent that both host and pathogen are engaged in a battle to respectively enhance or inhibit muco-ciliary clearance. There is growing evidence to support a chemosensory role for motile cilia (Shah *et al.*, 2009). Bacterial AHLs, which play a role in QS, are sensed by bitter taste receptors expressed and localised on the cilia of airway epithelia. Binding of *P. aeruginosa* AHL to the bitter taste receptor T2R38 upregulates Ca^{2+} and NO production, resulting in increased ciliary beat frequency and enhanced clearance of the pathogen. The importance of this mechanism was supported by the finding that polymorphisms in T2R38 could underlie increased susceptibility to upper airway infections (Lee *et al.*, 2012) .

The data presented in this chapter suggest a cilio-inhibitory effect of cyanide, at concentrations detected in CF suptum. Along with other cilio-inhibitory compounds, cyanide could help *P. aeruginosa* counter host muco-ciliary clearance defences and allow it to establish a foothold early on in infection.

Cyanide demonstrably accumulates in the sputum of *P. aeruginosa* infected patients (Ryall *et al.*, 2008; Sanderson *et al.*; 2008). However, it is possible that previous studies investigating the effect of *P. aeruginosa* supernatants on CBF may not have picked up on an effect of cyanide due to experimental artefacts, for example heat treatment of supernatants leading to evaporation or growth conditions unsuitable for cyanogenesis. Indeed, as cyanide-production in wildtype strains is regulated by quorum, growth to OD600 <0.8 would result in little to no recoverable cyanide. In addition, growth for longer than 18 hours would also yield little to no cyanide from the culture supernatant of WT strains. This is because under standard liquid growth conditions, WT cyanide production peaks between 8-10 hours, and there is no detectable cyanide in the culture after 20 hours (Ryall *et al.*, 2014).

3.5.3 What is the Cilio-Inhibitory Mechanism of Cyanide?

A striking result in this chapter was the lack of effect on ATP levels of 75 μM KCN, both in 16-HBE cells and human nasal brushings (Figure 3-8.). 75 μM PYO, in contrast, caused a 48% decrease in ATP levels of nasal brushings after 60 min. This finding was concordant with previous studies that showed that PYO reversibly reduces CBF *via* depletion of ATP and of cAMP, which is required by protein kinase A (PKA) to stimulate maximal ciliary beating (Wilson *et al.*, 1987; Kanthakumar *et al.*, 1993; Levin *et al.*, 1997).

The data from the ATP experiments suggest that cyanide inhibits CBF in a different, ATP-independent manner. Due to the rapid, transient and reversible nature of the inhibition observed, the target of cyanide inhibition is hypothesised to be a secondary messenger. A currently accepted model of CBF regulation puts forward the idea that cilia beat at a basal level, a 'slow mode' (~7 Hz), which requires additional stimulation by secondary messengers to induce a switch to a maximal 'fast mode' (~ 9.5Hz) (Salathe & Bookman, 1999; Lansley & Sanderson, 1999; Salathe, 2007). In addition to the concerted action of Ca^{2+}, cAMP, cGMP, ATP, NO and HCO^{3-}, CBF is directly regulated by PKA, protein kinase G (PKG), protein kinase C (PKC), pH, temperature and shear stress (A diagrammatic representation has been put together in Figure 3-10).

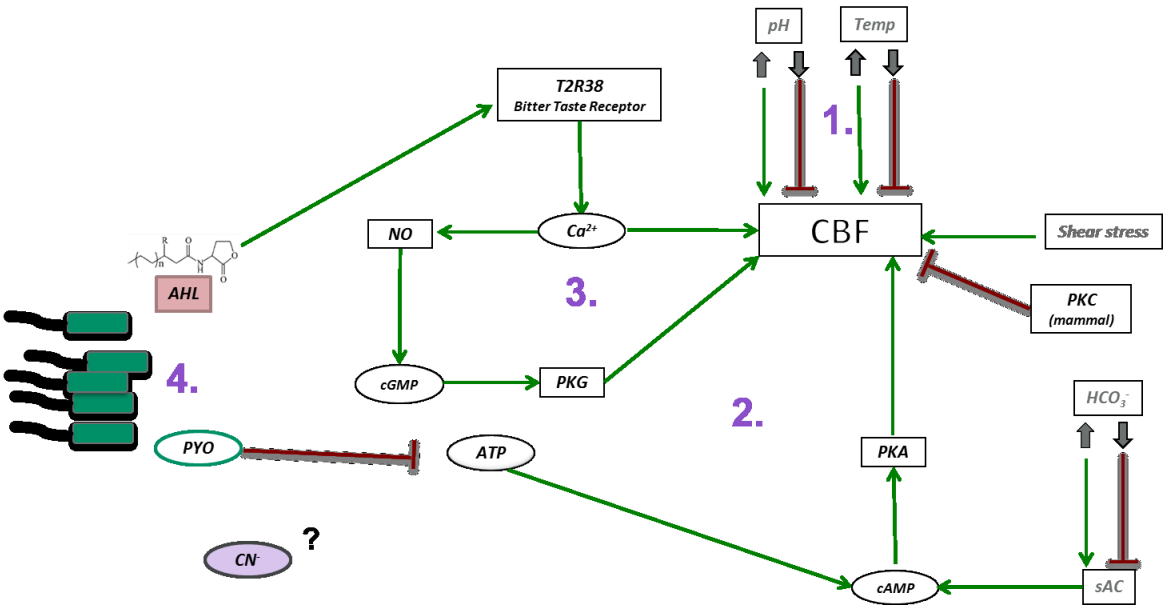


Figure 3-10 Modulation of CBF by host and pathogen. (1) CBF is regulated directly by pH, temperature and shear stress. (2) In addition, protein kinases phosphorylate the dynein arms to switch ciliary beating from a 'slow mode' to a 'fast mode'. PKA and PKG require cyclic nucleotides cAMP and cGMP respectively. The role of PKC is stimulatory in frog cilia, but inhibitory in mammalian cilia. (3) The role of Ca^{2+} is controversial. Ca^{2+} is a positive regulator of CBF *via* cross-talk with other pathways, such as NO/cGMP/PKG. Ca^{2+} is also thought to have a direct, transient, but as yet uncharacterised effect on cilia *via* intra-ciliary concentrations. (4) Cilia are chemosensory and have evolved mechanisms to detect and clear pathogens from the airway. High levels of bacteria are detected *via* bitter-taste receptors that sense QS molecules, and this triggers upregulation. As a counter measure, *P. aeruginosa* secretes cilio-inhibitory compounds such as PYO. PYO decreases ATP and cAMP levels, thus preventing phosphorylation of dynein arms by PKA. This prevents stimulation of maximal CBF

and may help *P. aeruginosa* establish a foothold. Our results suggest that *P. aeruginosa* cyanogenesis may similarly affect maximal CBF *in vitro*, but *via* a different mechanism.

While it is possible that cyanide may be affecting any of the ATP-independent pathways, [Ca^{2+}] perturbation as a mechanism of CBF inhibition is a plausible hypothesis. Ca^{2+} is involved in the crosstalk with other stimulatory pathways, for instance, Ca^{2+} upregulates nitric oxide (NO) and cGMP, which is then needed by PKG to phosphorylate the dynein arms of cilia to stimulate maximal CBF (Salathe, 2007). In addition, Ca^{2+} is implicated in direct regulation of CBF *via* intra-ciliary Ca^{2+} spikes (Andrade *et al.*, 2005).

The role of Ca^{2+} in regulating CBF remains somewhat controversial, however it is currently thought that CBF is not regulated by absolute [Ca^{2+}] but by differential changes in [Ca^{2+}]. Modelling work by (Kotov *et al.*, 2011) suggests that intraciliary [Ca^{2+}] concentrations are maintained several orders of magnitude higher than intracellular [Ca^{2+}] concentrations. Transport of Ca^{2+} between the cilia and the cell body occurs *via* channels and can be disrupted by membrane depolarization. For example, TRPV4 is a calcium channel expressed in cilia, which has been shown to provide Ca^{2+} entry and modulate upregulation of CBF (Liedtke & Heller, 2007; Lorenzo *et al.*, 2008).

Johnson *et al.* (1987) have reported that 100 μM KCN is capable of rapidly disrupting Ca^{2+} homeostasis in PC12 neuronal cells, causing accumulation of cytosolic Ca^{2+} from the extracellular compartment *via* Ca^{2+} channels. If sub-lethal [CN^-] were to similarly perturb [Ca^{2+}] concentrations in respiratory ciliated epithelia, this could result in the type of transient and rapid inhibition observed in this chapter. Ca^{2+} is present in both DMEM and PBS media that were used for CBF measurements, so CBF may have been stimulated from the start of these experiments, with the cilia beating in 'fast mode'. It could then be hypothesized that cyanide at the concentrations applied disrupted Ca^{2+} homeostasis and caused ciliary beating to switch to a 'slow mode'.

3.5.4 Biological Detoxification of Cyanide

Cyanide, at concentrations detectable in the *P. aeruginosa*-infected airway, and within the short time frame tested, does not appear to decrease airway cell viability. A possible explanation for this is that mitochondria possess a rhodanese and a mercaptopyruvate sulfurtransferase (MTS) capable of detoxifying cyanide (Nagahara & Nishino, 1996). These convert cyanide to thiocyanate, (SCN^-). Additionally, cyanide may be detoxified by hydrogen peroxide (H_2O_2) to form cyanate, CNO^-. H_2O_2

plays an important role in mucosal surface host defence, and Dual oxidase 2 (Duox2) has been reported to be the main source of H_2O_2 in the airway (Geiszt *et al.*, 2003; Donkó *et al.*, 2005). Duox2 is a component of a lung defence system called the lactoperoxidase system, which produces the antimicrobial compound hypothiocyanite ($OSCN^-$) *via* the oxidation of SCN^- by H_2O_2 (Pruitt & Tenovuo, 1982). It is thought that the lactoperoxidase system may be defective in Cystic Fibrosis patients due to impaired SCN^- transport or malnutrition (Minarowski *et al.*, 2008). A study by Lorentzen *et al.*, (2011) reported that a higher [SCN^-] was correlated with better lung function in human CF patients. The same study found that the CFTR defect only slightly reduced SCN^- content in the tracheobronchial ASL of pigs, while [SCN^-] varied considerably among human CF patients, regardless of CFTR mutation status.

3.5.5 Are CF Respiratory Epithelia More Susceptible to Cyanide and PYO?

In CF, the cilia are thought to be normal (Rutland *et al.*, 1983; Rutland & Cole, 1981). Accordingly, nasal brushings and ALIs from CF patients studied in this chapter had normal basal CBF values. The data from experiments in nasal brushings and the ALIs, suggest that CF samples might be more sensitive to sub-lethal [CN^-] and [PYO] than non–CF samples. Table 3-3 provides a summary of previous results on the effect of cyanide and PYO on non-CF and CF samples in the nasal brushings and ALI models.

	Non-CF	CF
Nasal brushings **150 µM KCN, 60 min**	Baseline CBF: 14.3±1.9 n=6 **46% decrease**	Baseline CBF: 13.8±3.2 n=3 **55% decrease**
ALIs **75 µM KCN, 60 min**	Baseline CBF: 8.06±0.8 n=4 **13% decrease**	Baseline CBF: 9.58±0.6 n=3 **20% decrease**
ALIs 7 **75 µM PYO, 60 min**	Baseline CBF: 8.06±0.8 n=4 **5% decrease**	Baseline CBF: 9.58±0.6 n=3 **10% decrease**

Table 3-3 Summary table - Effect of KCN and PYO on non-CF and CF nasal brushings and ALIs

The effect seen in CF ALIs was close to double that observed in non-CF ALIs. However, due to the small sample size, replication of these findings will be of key importance to substantiate this finding.

If this observation is confirmed through further experimentation, one possible explanation for increased severity in CF vs non-CF epithelium could be that the mitochondria of CF patients are reported to suffer from several defects. It has been suggested that CF mitochondria are depolarized, consume more oxygen and have increased Ca^{2+} uptake (Feigal & Shapiro, 1986; von Ruecker, Bertele & Harms, 1984; Antigny, Girardin, Raveau, *et al.*, 2009). These findings led Shapiro (1989) to hypothesise that these defects would render CF mitochondria more susceptible to inhibitors of the electron transport chain.

3.5.6 Possible Clinical Implications

The conclusions of this chapter are based on in vitro observations and are therefore preliminary. Further studies in vivo will be required to test whether cilio-inhibition by cyanide occurs in CF patients. If this were the case, reversing cilio- inhibition could be of great benefit. A study in isolated sheep trachea reported a 56% increase in MCC when CBF was increased by 16% (Seybold *et al.*, 1990). Abnormal

MCC is thought to be key in the development of lung disease in CF, yet past MCC clinical studies have not consistently demonstrated a CF-related defect. Instead, reduction in MCC may require a secondary insult, such as viral infection. There may therefore be no primary MCC defect in CF, rather a gradual decrease with increased lung disease severity. The largest study to date reported that CF patients had MCC approximately 50% that of the normal rate (Robinson & Bye, 2002).

P. aeruginosa is an important pathogen of other lung diseases including acute exacerbations of Chronic Obstructive Pulmonary Disease (COPD) and in non-cystic fibrosis bronchiectasis. It is entirely plausible that cyanide production could affect CBF and MCC in these disease contexts. Indeed cyanide has been detected in sputum of non-CF bronchiectasis patients infected with *P. aeruginosa* (Ryall *et al.*, 2008).

At present, there are several therapeutics that have been developed to improve MCC including mannitol, amiloride, and hypertonic saline, which aim to rehydrate the airway, and uridine triphosphate (UTP), which may also impact CBF. The reversibility of the cilio-inhibition reported in this chapter suggests that diluting out the cyanide with these therapies may help to reduce its effect (Figure 3-5 B.). A more promising strategy could be to detoxify cyanide directly, for example through complex formation with hydroxycobalamin (a vitamin B12 precursor), which is already being employed to counter cyanide toxicity in smokers and victims of fires (Cottrell *et al.*, 1978; Broderick *et al.*, 2006).

3.6 Future Work

In order to better understand the implications of the presence of cyanide in the CF lung, the time frame of CBF measurements could be extended. Nasal brushings can be kept for 24 hours, during which time we have observed that basal CBF is not affected. Additionally, commercially available ALIs such as Epithelix MucilAir cultures (SARL, Geneva) may be suitable, as these claim to be functional for over a year. Another improvement could be to automate CBF measurements. Switching to an automated set-up with dedicated software, as described in other studies, could provide increased technical replication, reduce experimental bias, and would allow for longer experiments (Smith *et al.*, 2012).

The effect of bacterial supernatants on CBF could be explored in future experiments. For example, *hcnA* culture supernatant contains all *P. aeruginosa* secreted cilio-toxic components, except cyanide. The effect of *hcnA* culture supernatant, spiked with varying [KCN] could be tested. Following treatment with WT supernatant or spiked *hcnA* supernatant, the effect on CBF of adding therapeutics, such as the cyanide chelator hydroxycobalamin, could also be investigated.

In order to elucidate the cilio-inhibitory mechanism, the hypothesis that cyanide is affecting Ca^{2+} homeostasis could be tested using simultaneous CBF measurements and Ca^{2+} measurements following treatment with known [KCN], or with *hcnA* supernatant spiked with varying [KCN].

An interesting trend observed in this chapter was a hypothesised difference between non-CF and CF samples. In order to investigate this, it would be advantageous to test at a larger sample size to confirm whether there is increased susceptibility of CF epithelium to cyanide and PYO. Additionally, ATP measurements should be carried out on CF samples, as was previously done with healthy samples, to test whether cyanide is having a differential effect.

Chapter 4
IDENTIFICATION OF TWO NOVEL DETERMINANTS OF CYANOGENESIS IN *P. AERUGINOSA*

4.1 Introduction

4.1.1 Can we Identify Novel Determinants of Cyanide Production?

Many gene regulators in *P. aeruginosa* have yet to be characterised, including at least 64 putative two-component systems (Rodrigue *et al.*, 2000). This chapter tests the hypothesis that screening an ordered, nonredundant library of *P. aeruginosa* mutants can uncover novel genetic or metabolic factors affecting cyanogenesis.

The library contains a set of 5850 mutants of non-essential genes in the pathogenic lab strain PA14. In each mutant strain, a gene of interest has been disrupted by the insertion of a mariner-based transposon, MAR2xT7 (~1 kb in length).

For the purposes of this chapter, transposon mutants from the PA14NR library will be referred to by the specific gene that has been interrupted by a transposon insertion:

Eg. *hcnA:: MAR2xT7* will be referred to as *hcnA*

4.2 Aims

- To develop a high-throughput assay to screen an existing library of 5850 *P. aeruginosa* transposon-knockouts for cyanogenesis mutants.
- To identify novel determinants of cyanide production through visual analysis.
- To confirm identified cyanogenesis defects through direct cyanide measurements and complementation studies.

4.3 Method Development

4.3.1 Development of a High-Throughput Colourimetric Cyanide Screen

A primary aim of this chapter was to identify novel determinants of cyanogenesis within a comprehensive library of 5850 *P. aeruginosa* mutants. The library was purchased as frozen glycerol stocks arranged in a 96-well format. A preliminary step was to adapt an existing qualitative method for the detection of cyanogenic bacteria, first described by Castric and Castric (1983), to a high-throughput 96-well assay suitable for screening the library (Figure 4-1).

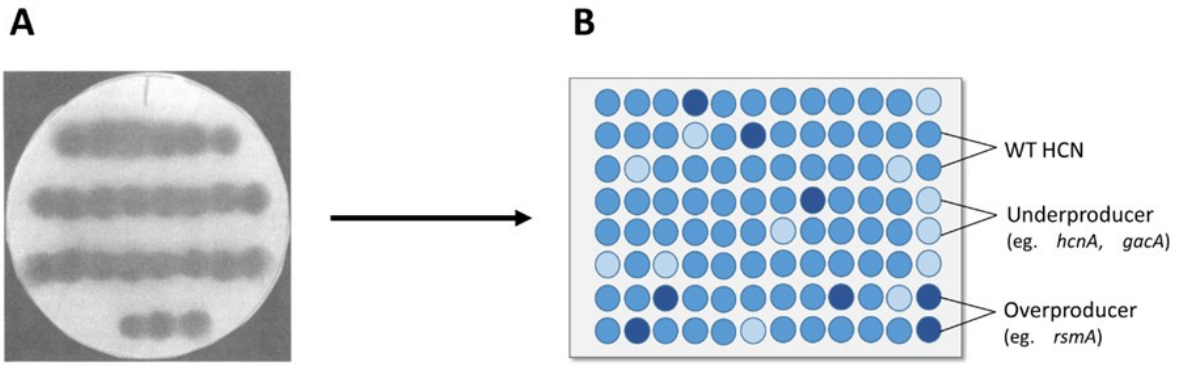


Figure 4-1 **Adaptation of a qualitative cyanide detection method to a 96-well semi-quantitative assay.** (A) In the original Castric and Castric (1983) method, cyanide detection paper, which is impregnated with copper ethylacetoacetate and tetrabase, is placed over colonies of *P. aeruginosa* on a peptone-agar plate, growing at 35 ˚C for 18 hours. HCN gas reacts with copper (I) ion producing CuCN. Following this, tetrabase is oxidized by Cu (II) ion to form a blue stain. Castric and Castric utilize the presence of a stain above individual colonies as an indicator of cyanogenic ability (Yes/No output). (B) For this study, an adaptation of the previous method was developed, where cyanide detection paper is placed over a 96-well plate containing *P. aeruginosa* library mutants grown in liquid culture at 37 ˚C for 24 hours. In conjunction with OD600 values for each well, spot intensities are used to discriminate visually between normal 'wildtype' (WT) cyanide production, cyanide underproduction and cyanide overproduction. Additionally, spot intensity above uncharacterised mutants is compared to that of known cyanogenesis mutants, such as the underproducers, *hcnA* and *gacA*, or an overproducer, *rsmA*, in order to give a semi-quantitative estimation of the cyanide defect.

A key step in improving the quality of spots generated by the assay was finding a suitable way of weighing down the detection papers. This was to prevent HCN from leaking into adjacent wells, which was found to result in undetectable, faint or diffuse spots. Following attempts with several other methods, the use of breathable films was found to be the most suitable solution, yielding reproducible

results (Figure 4-2). Plates were incubated without their lids so as to minimise condensation, which interferes with the cyanide detection reaction.

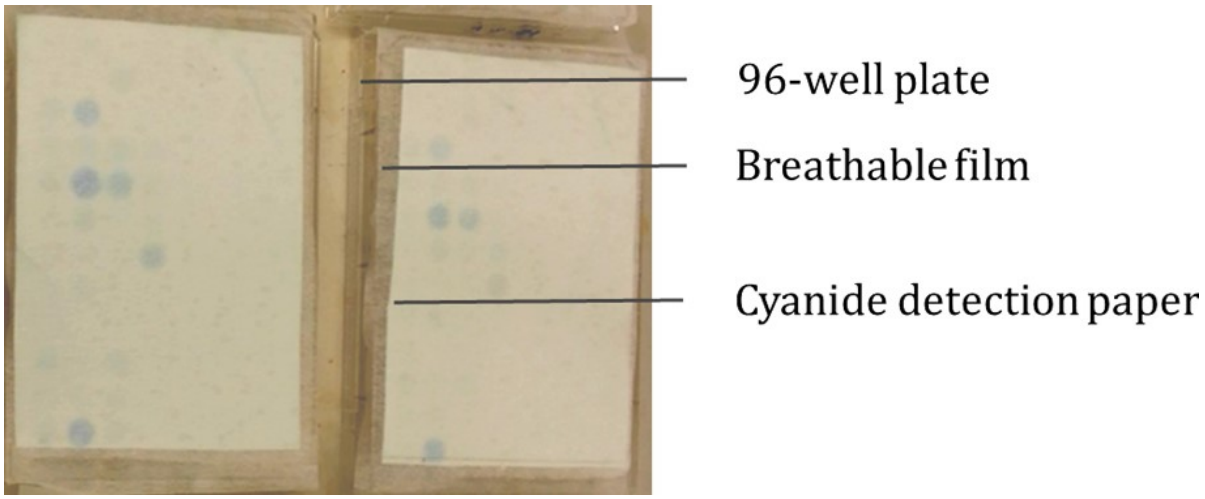


Figure 4-2 Cyanide screen assay plate set up. Breathable seals were used to weigh down cyanide detection papers on 96-well assay plates containing *P. aeruginosa* cultures, grown without a lid, statically at 37 ˚C. Two biological replicates are shown.

Optimal inoculum OD^{600} values, culture volumes and incubation times were determined experimentally using a 'control plate', a sub-library designed to include positive and negative controls of cyanogenesis. The mutants present on the control plate included the wildtype library background strain PA14 (WT cyanogenesis), the cyanide biosynthetic gene *hcnA* (no cyanide), the global regulator *gacA* (heavily impaired cyanogenesis) and the post-translational regulator *rsmA* (cyanide overproducer). When tested in biological triplicate, these control strains were observed to yield expected phenotypes (Figure 4-3).

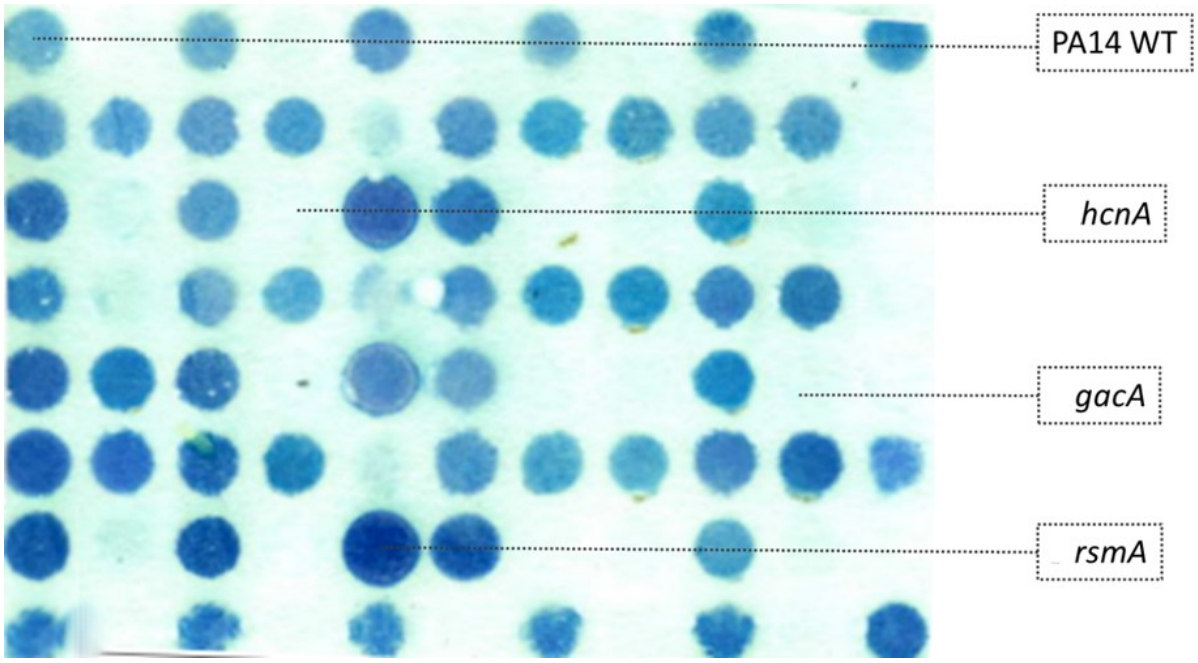


Figure 4-3 Control plate. n=3 biological replicates (representative image shown). Strains with expected cyanogenesis phenotypes were included as controls: PA14 (WT cyanide), *hcnA* (no cyanide), *gacA* (heavily impaired cyanogenesis) and *rsmA* (cyanide overproduction).

Since the control plate gave expected results, it was decided that the optimised assay methodology should be employed to screen the remainder of the library strains.

The library was screened in batches of 8-12 plates. The control plate was assayed alongside each batch, firstly as an internal control of the assay quality, and secondly as a visual aid in the assessment of cyanide production ability, by way of comparison of novel mutants with known cyanogenesis controls.

4.4 Results

4.4.1 Initial Screen

Employing the conditions determined above, the entire library was screened in triplicate for novel cyanogenesis mutants. Cyanide detection papers from each plate were then subjected to visual analysis as follows. Spots for each mutant were compared to those of the other mutants on the same library plate, as well as to those of known cyanogenesis mutants on the control plate.

Unfortunately, the coverage of the screen was estimated to be only 40-50%, due to poor growth in some of mutants (OD600<0.7 after 24 hours) or damage to the cyanide detection papers due to condensation and evaporation (Figure 4-4).

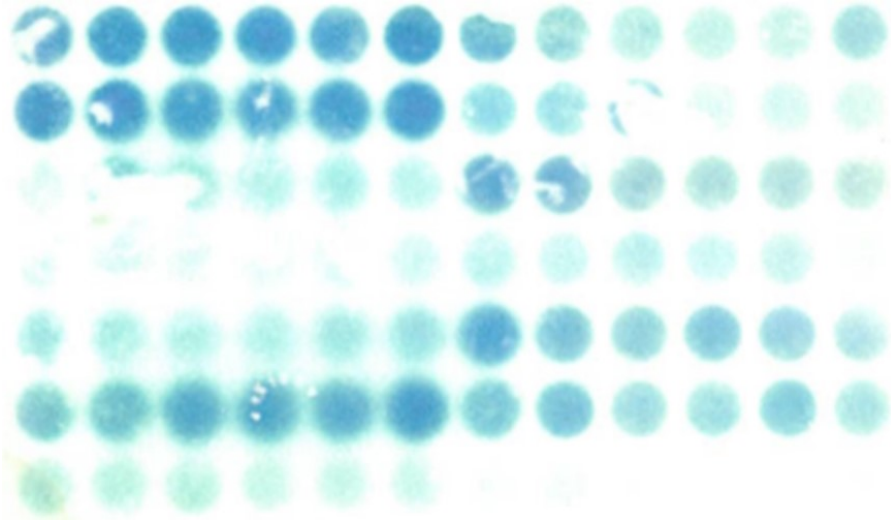


Figure 4-4 Coverage issues during initial screen. (Representative image). Strains to be tested for cyanogenesis were incubated with cyanide detection paper for 24 hours at 37 ˚C. Assay papers suffered from water damage, as a result of the humid environment of the incubator. In addition, well evaporation resulted in fainter spots for mutants located in the edge wells. Arrows indicate examples of water damage and of fainter spots caused by an 'edge effect'.

Despite the limited coverage of the initial screen, it was nevertheless possible to identify novel cyanide production mutants by visual assessment. Only mutants that had grown to an OD^{600} > 0.7-1 and exhibited a pronounced defect in cyanogenesis in all three replicates were selected for further analysis. These included two novel genes, *PA5339* and *PA2196*, for which roles in cyanide production or regulation had not been previously assigned.

4.4.2 Identification of *PA2196* by Visual Assessment

Figure 4-5 provides a representative analysis of library plate 06_04, which contained the novel cyanogenesis mutant *PA2196*.

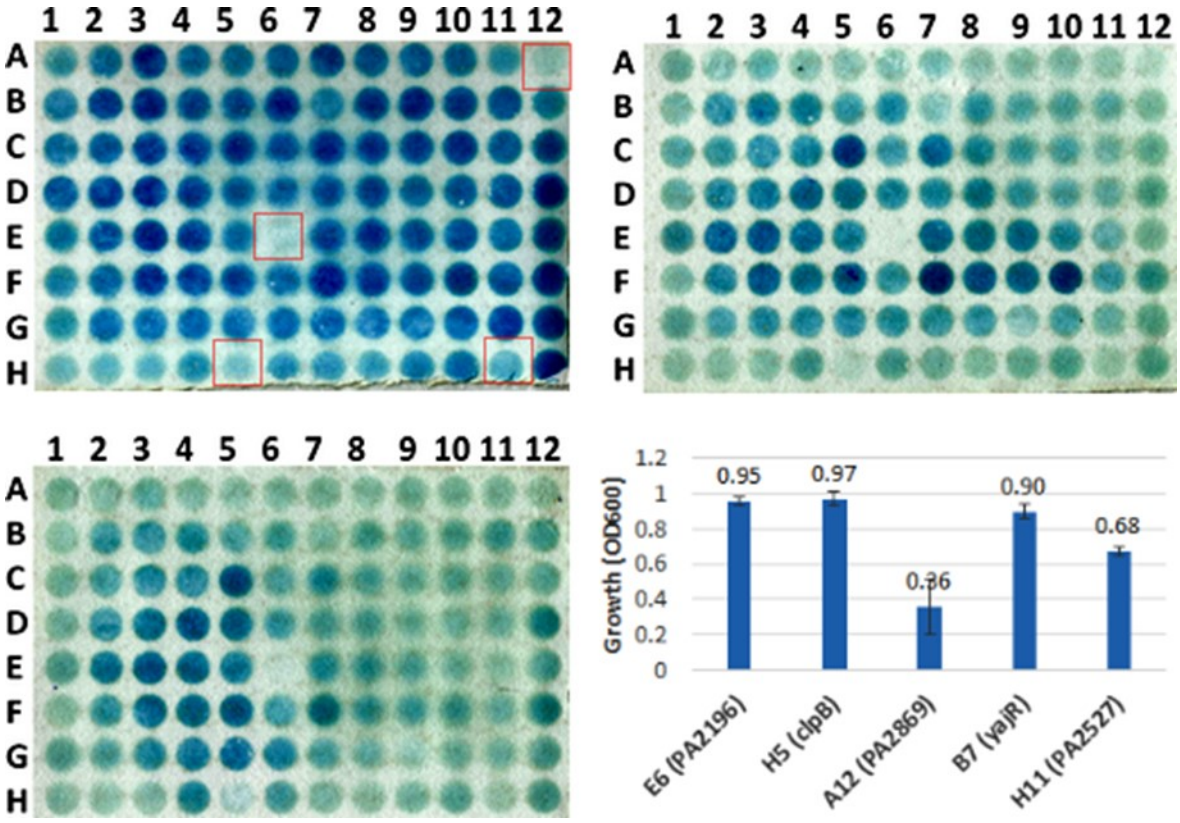


Figure 4-5 Cyanide detection papers for library plate 06_04. n=3; error bars are S.E of biological replicates. Wells E6, H5, A12 and H11 produced fainter spots than were visible above other wells. A graph of well growth (n=3, ± SEM) indicates that faint spots above A12, and above H11, were due to a growth defect (OD^{600}<0.7). Mutants in H5 and B7, *clpB* and *yajR* respectively, did not produce wildtype spots in spite of reaching a high OD^{600} (impaired cyanogenesis). More strikingly, the mutant in well E6 exhibited the most pronounced cyanogenic defect on the plate (heavily impaired cyanogenesis/no cyanide). *PA2196* encodes a putative regulator with a TetR family signature located 154 bp downstream of the *hcnABC* biosynthetic operon.

The faint spots above the mutants in wells A12 and H11 could be attributed to poor growth. In contrast, the mutant in well H5, defective in a chaperone protein, and the mutant in B7, lacking a major facilitator superfamily (MFS) transporter, grew to suitable OD600 values of 0.97 and 0.9 respectively. These produced visibly fainter spots than other mutants on the plate (impaired cyanogenesis). Of particular interest, however, was the very pronounced cyanogenesis defect above well E6 (heavily impaired cyanogenesis/no cyanide). This mutant, *PA2196*, grew to an OD600 of 0.95, yet produced no visually discernible cyanide. Due to the severity of the cyanogenesis defect, and because of its gene location, 154 bp downstream of the cyanide synthase biosynthetic operon, *PA2196* was selected for further study.

4.4.3 Identification of *PA5339* by Visual Assessment

Figure 4-6 provides a representative analysis of the assay papers for library plate '06_02', which contained the novel cyanogenesis mutant *PA5339*. This plate contained two mutants that produced fainter spots than wild type but which were omitted from further analysis due to a growth defect (PII in A4, *cbrA* in A7), one mutant with an expected cyanogenesis defect (*rhlI* in C2) and one novel cyanogenesis mutant (*PA5339* in F12; heavily impaired cyanogenesis).

According to the *Pseudomonas* genome database (Winsor *et al.*, 2011), *PA5339* is predicted to form an operon with another gene, *PA5340*. Subsequent reassessment by visual analysis of the cyanide detection paper from the plate containing *PA5340* suggested that this mutant also may also exhibit a slight cyanogenesis defect, despite growing to an OD600 of 0.97 (Figure 4-7).

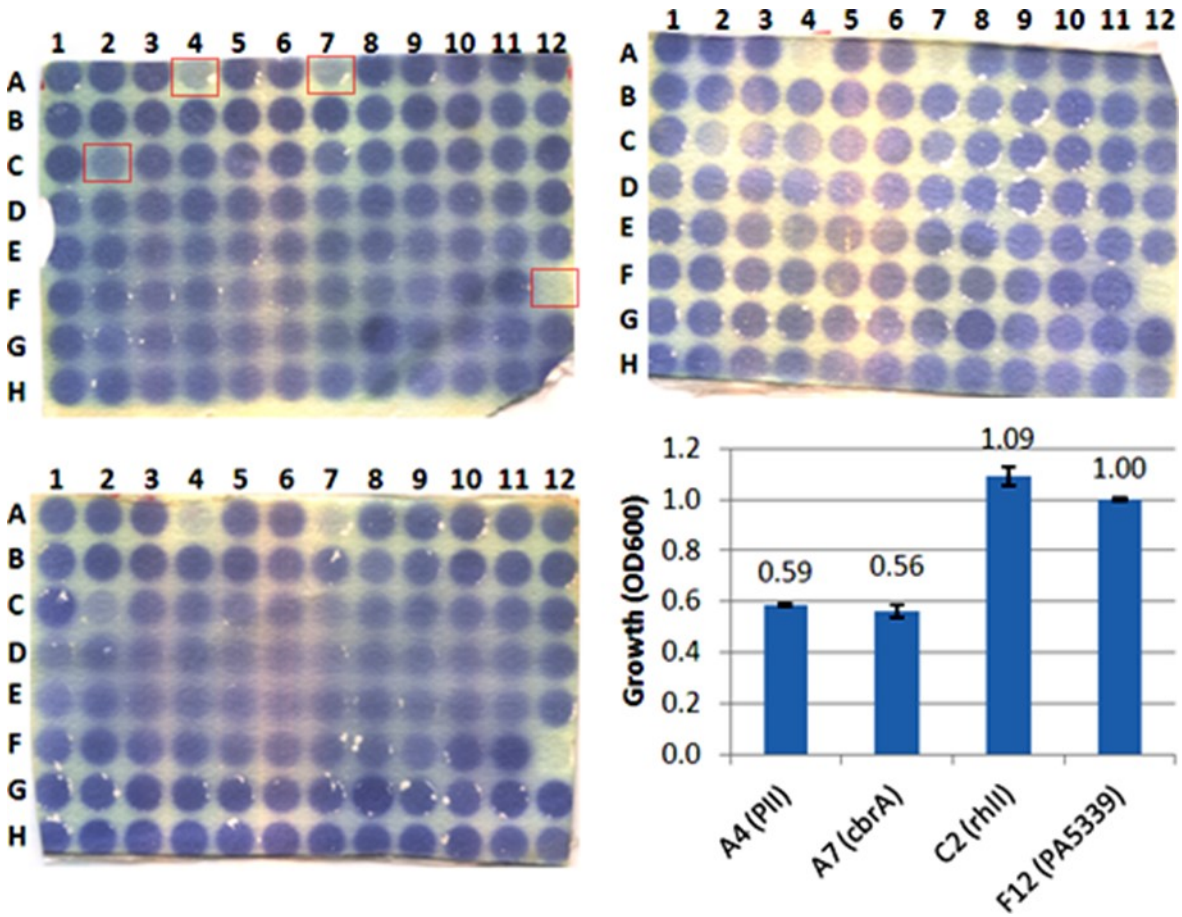


Figure 4-6 Cyanide detection papers for library plate '06_02'. n=3. Error bars are S.E of biological replicates. Wells A4, A7, C2 and F12 produced fainter spots than average, when compared visually with the rest of the plate. A graph of well growth (OD600, n=3, ± SEM) indicates that faint spots above A4 (PII, a nitrogen regulatory protein), and above A7 (*cbrA*, a two component sensor), were due to a growth defect (OD600 <0.7). The mutant in C2 grew to an OD600 >1, which discounts a growth defect. Impaired cyanogenesis is an expected phenotype as this mutant lacks RhlI, which catalyses the synthesis of the autoinducer in the Rhl QS system and is therefore a positive regulator of HCN production. The cyanogenesis mutant in F12 (*PA5339*) also grew to an OD>0.9-1 but displayed heavily impaired cyanogenesis. *PA5339* is a conserved hypothetical protein with putative endoribonuclease activity.

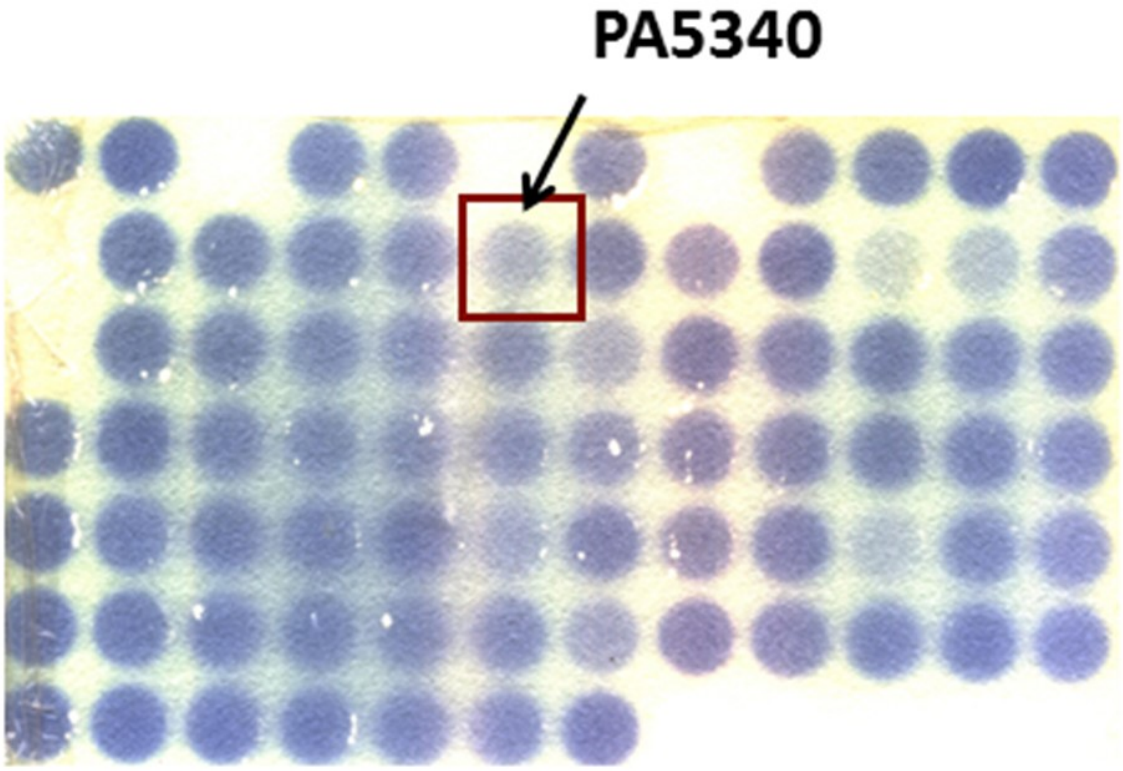


Figure 4-7 *PA5340* may exhibit slightly impaired cyanogenesis.

4.4.4 Re-Screen of a Mutant Sub-library to Confirm Cyanogenesis Defects Identified in the Initial Screen

In addition to *PA2196* and *PA5339*, 10 other genes were identified by visual analysis in the initial screen. These mutants were subsequently re-screened to confirm a cyanogenesis defect: a sub-library containing 6 technical replicates of each strain was constructed and screened with six biological replicates, yielding 36 spots per mutant. Three representative spots for each are presented in Figure 4-8. All mutants grew to an OD^{600} >1. The sub-library contained the following cyanogenesis controls: PA14 (WT cyanide), *hcnA* (no cyanide) and *gacS* (heavily impaired cyanogenesis).

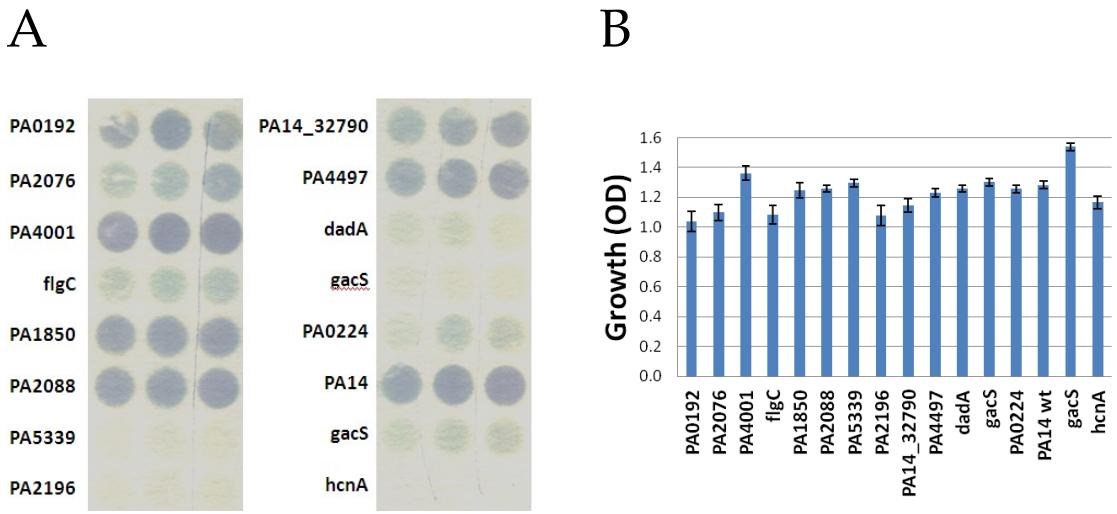
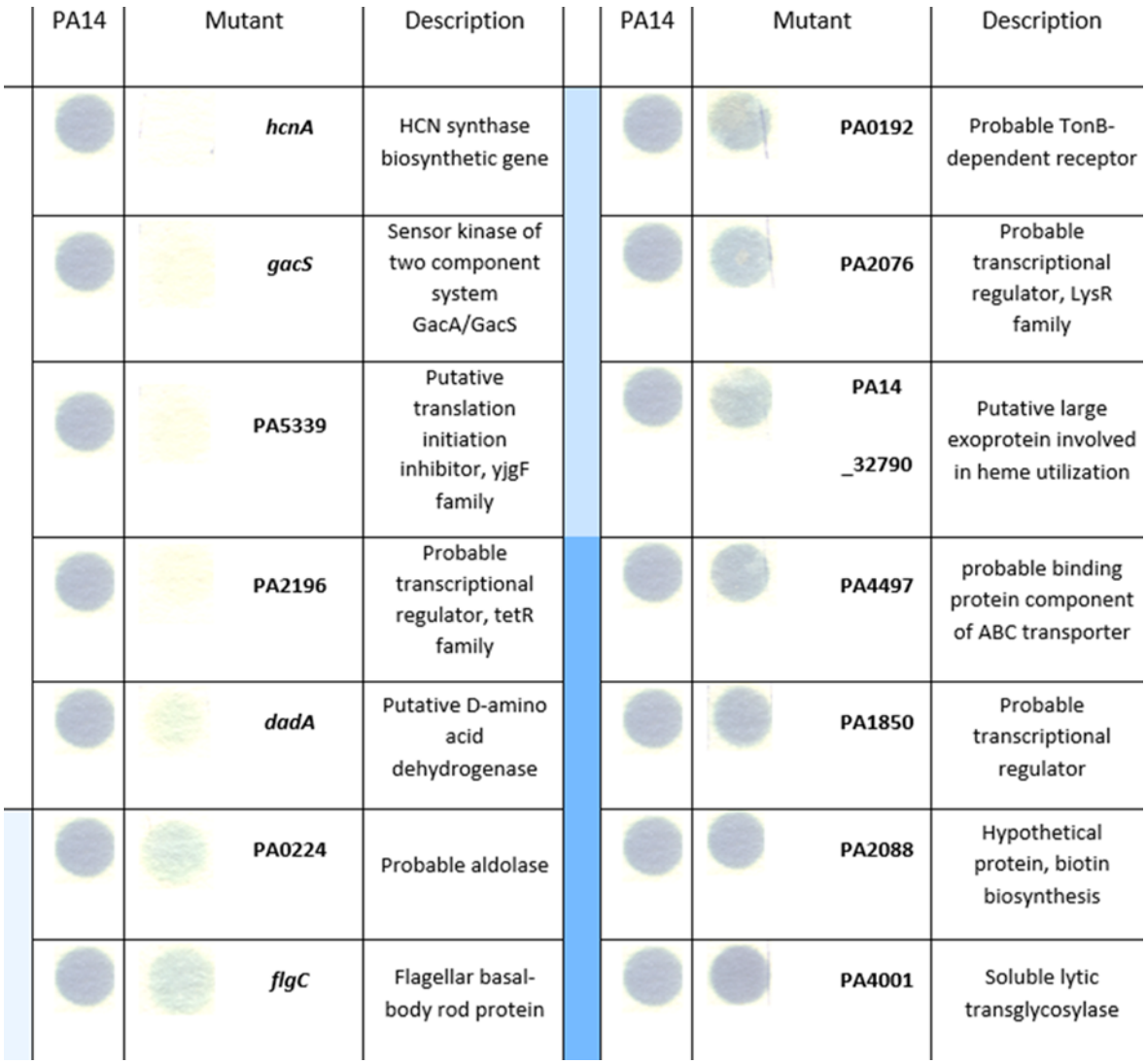


Figure 4-8 Confirmation of cyanogenesis defect in mutants identified by the initial library screen. n=6 error bars are S.E of biological replicates. A. Mutants previously identified by a preliminary screen of the PA14NR library were subsequently retested to confirm a cyanogenesis defect. Distinctly fainter spots than PA14 (WT HCN production) were observed above the wells of most, but not all mutants. B. None of the mutants possessed a growth defect, as all grew to an OD600 >0.9-1.

Figure 4-9 provides a summary of this visual analysis, where the mutants are presented alongside PA14 for comparison, and ordered based on the severity of cyanogenesis defect. 8 out of the 12 mutants tested exhibited a reproducible cyanogenesis defect. The other 4 mutants produced spots of wildtype intensity and were therefore discounted as false positives of the initial screen.



PA14	Mutant	Description	PA14	Mutant	Description
	hcnA	HCN synthase biosynthetic gene		**PA0192**	Probable TonB-dependent receptor
	gacS	Sensor kinase of two component system GacA/GacS		**PA2076**	Probable transcriptional regulator, LysR family
	PA5339	Putative translation initiation inhibitor, yjgF family		**PA14 _32790**	Putative large exoprotein involved in heme utilization
	PA2196	Probable transcriptional regulator, tetR family		**PA4497**	probable binding protein component of ABC transporter
	dadA	Putative D-amino acid dehydrogenase		**PA1850**	Probable transcriptional regulator
	PA0224	Probable aldolase		**PA2088**	Hypothetical protein, biotin biosynthesis
	flgC	Flagellar basal-body rod protein		**PA4001**	Soluble lytic transglycosylase

Figure 4-9 Cyanogenesis mutants grouped by strength of cyanide production inhibition. 8/12 mutants exhibited a reproducible cyanogenesis defect.

4.4.5 Direct Cyanide Measurements on *PA2196* and *PA5339*

Cyanide measurements were performed using an Ion-Selective Electrode (ISE) on *PA2196* and *PA5339* following growth for 6 and 7 hours (Figure 4-10). *PA5340* was also included in these measurements, as it is predicted to form an operon with *PA5339*. The ISE measurements confirm a pronounced cyanogenesis defect in *PA2196* and *PA5339* (ns compared to hcnA control, $p>0.05$). PA340 also exhibited a slight cyanogenesis defect ($p<0.05$).

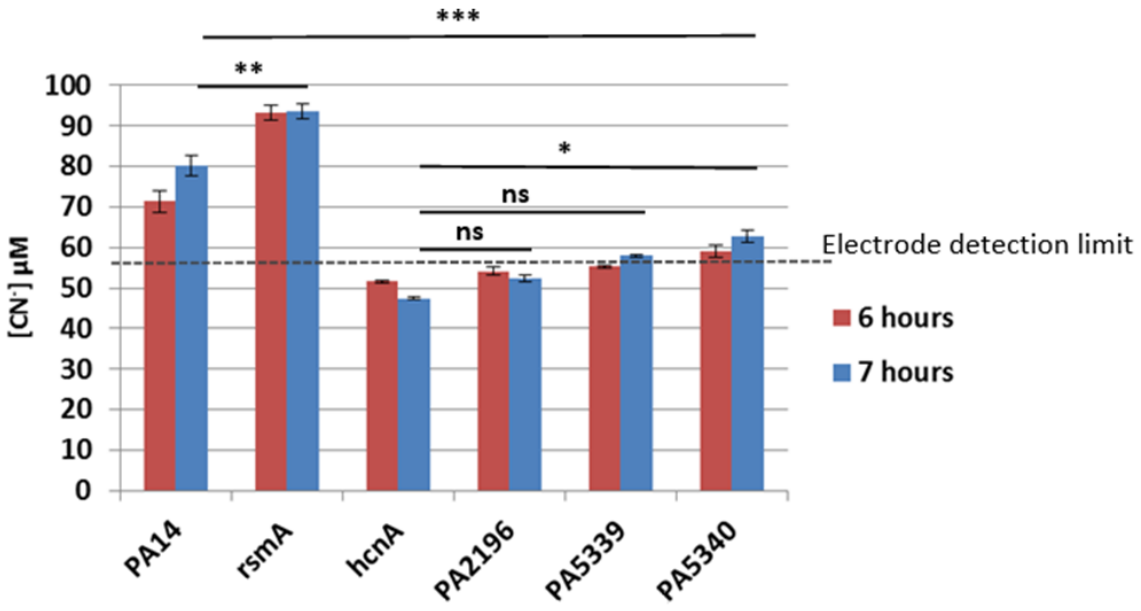


Figure 4-10 Direct cyanide measurement on *PA2196*, *PA5339* and *PA5340*. n=3 error bars are S.E of biological replicates. Cyanide ISE measurements were performed after 6 and 7 hours on 50 mL cultures grown at 37 ˚C and 225 rpm. Negative control *hcnA* produced no cyanide (below detection limit), while the known overproducer rsmA produced significantly more cyanide than PA14 (*rsmA* 93.2 µM; PA14 71.4 µM; P<0.001) *PA2196* and *PA5339* produced no cyanide (ns compared to *hcnA* control; P>0.05). *PA5340* produced significantly more cyanide than the *hcnA* control (5340 62.7 µM; P<0.05), and significantly less than the WT control (*PA5340* 62.7 µM; PA14 71.4 µM; P>0.0001). Stars represent statistical comparisons (One way ANOVA with a post-hoc Tukey's test) ∗ : $P < 0.05$, ∗∗ : $P < 0.001$; ∗∗∗ : $P < 0.0001$.

Cyanide ISE measurements were repeated on *PA2196* and *PA5339* using a newer electrode with greater sensitivity (Figure 4-11).

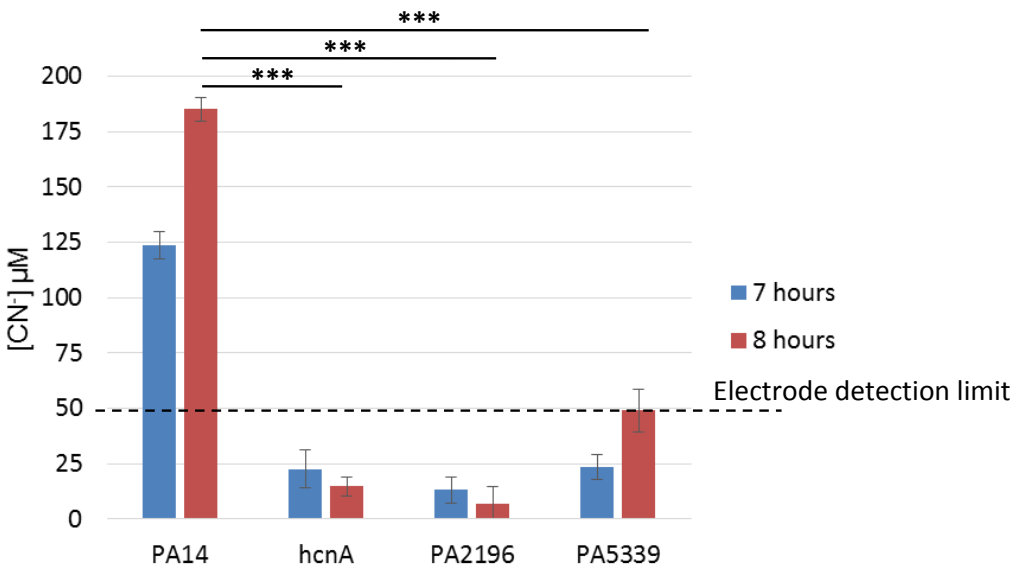


Figure 4-11 Direct cyanide measurement on *PA2196* and *PA5339*. n=3 error bars are S.E of biological replicates. Cyanide ISE measurements were performed after 7 and 8 hours on 50 mL cultures grown at 37 ˚C and 225 rpm. Negative control *hcnA* produced no cyanide (below detection limit). *PA2196* did not produce detectable cyanide (below detection limit). Cyanide production by *PA5339* was below the level of detection at 7 hours but just in range of detection at 8 hours. Stars represent statistical comparisons (One way ANOVA with a post-hoc Tukey's test) ∗ : $P < 0.05$, ∗∗ : $P < 0.001$; ∗∗∗ : $P < 0.0001$.

Again, direct cyanide measurements demonstrated a cyanogenesis defect in both mutants. However, while *PA2196* did not produce detectable cyanide after either 7 or 8 hours, *PA5339* was observed to produce small amounts of cyanide after 8 hours, which may have been just within the range of detection.

In parallel to the ion-selective cyanide measurements, a cyanogenesis defect in *PA5339* was also confirmed by a colleague, Dr Rishi Parbary, through direct CN^- measurement using selected-ion flow-tube mass spectrometry (SIFT-MS) at St Mary's Hospital London (see Appendices).

4.4.6 Complementation Restores Cyanide Production of *PA2196* and *PA5339*

The PA14NR mutant library was constructed by transposon mutagenesis, and it is possible that these transposon insertions could have had polar effects on downstream genes (Liberati *et al.*, 2006). For this reason, it was necessary to confirm that the genes identified through screening did indeed play individual roles in cyanogenesis.

Complementation of *PA2196* and *PA5339* was performed using pUCP18, a high copy *E. coli-Pseudomonas* shuttle vector. The *PA2196* and *PA5339* genes were amplified by PCR and cloned into pUCP18 under the control of a constitutive *lac*- promoter. The resulting recombinant plasmids were transformed into *PA2196* and *PA5339* PA14NR transposon mutants. Next, the cyanide spot assay was performed on the mutants to investigate whether cyanogenic ability could be restored (Figure 4-12).

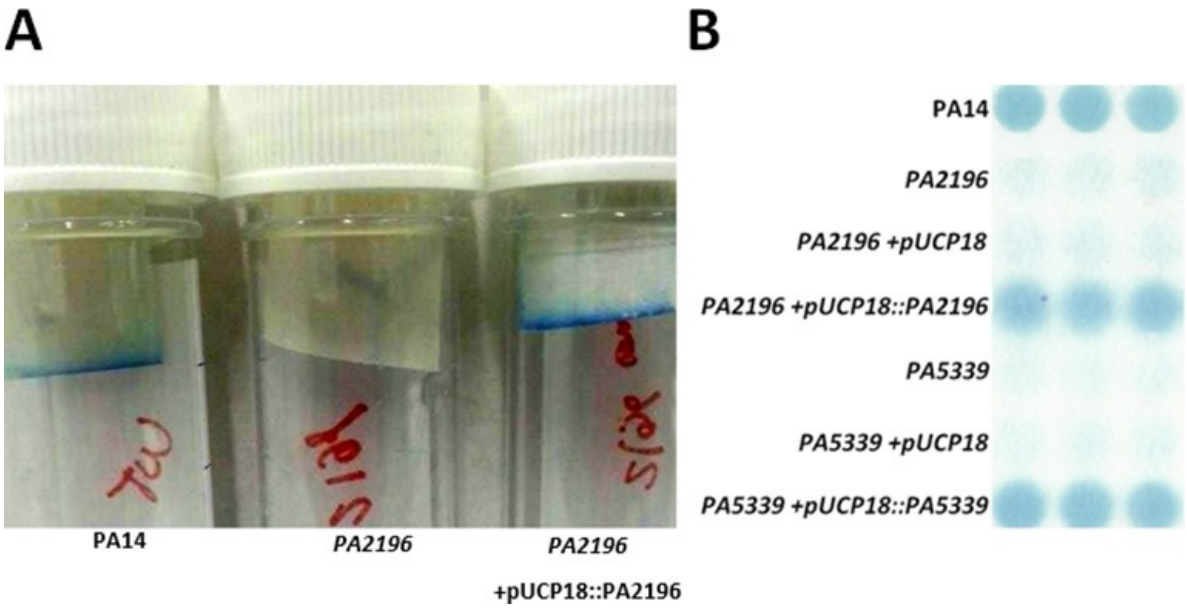


Figure 4-12 Complementation of *PA2196* and *PA5339* restores cyanogenic ability. A. HCN detection paper was added to *PA2196* cultures transformed with pUCP18::*PA2196*. Within 30 min, the paper in the tube containing *PA2196* +pUCP18::*PA2196* turned blue, indicative of restored cyanogenic ability similar to that of PA14 WT. No colour change was observed with untransformed *PA2196*. B. Spot assay (n=8 biological replicates) *PA2196* and *PA5339* were transformed with either empty pUCP18 vector or complementation constructs. *PA2196* and *PA5339* mutants transformed with empty vectors retained a highly impaired cyanogenesis phenotype. In contrast, cyanogenesis was restored in *PA2196* and *PA5339* mutants transformed with recombinant complementing vectors, as evidenced by the presence of blue spots of wildtype-like intensity.

As complementation with the gene products provided by the recombinant plasmids was sufficient to restore cyanogenesis to the strains, this provided a proof of principle that these genes do contribute to normal cyanide production in *P. aeruginosa*, and shows that the screen can be used to identify true mutants of cyanogenesis.

4.4.7 *PA2196* and *PA5339* are not Defective in Pyocyanin Production

PYO production, like cyanide production, is under the control of QS. As such, a mutant affecting QS regulation could be hypothesised to affect both cyanide and PYO production. PYO measurements were performed on *PA2196* and *PA5339* following growth for 24 hours (Figure 4-13). A negative control, a mutant of a QS regulator *rhlR*, produced little to no PYO. In contrast, *PA2196* and *PA5339* produced 77.4 µM and 74.6 µM respectively, which was not significantly different from PA14 PYO production (70.1 µM; ns P>0.05).

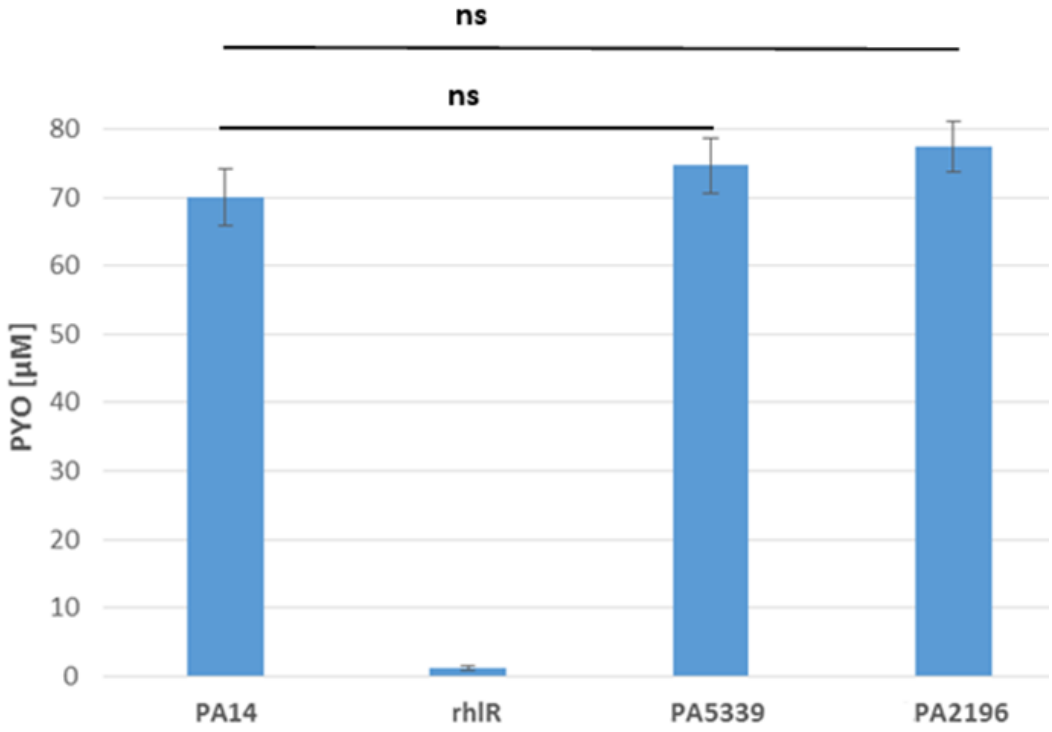


Figure 4-13 *PA2196* and *PA5339* produce WT levels of PYO. Unlike the QS mutant *rhlR*, *PA2196* and *PA5339* are not defective in PYO production (ns compared to PA14; P>0.05).

4.4.8 Effect of *PA2196* Supernatant on Ciliary Beat Frequency of Air-Liquid Interface Cultures

In order to test the virulence of *PA2196*, the effect on CBF of supernatant fractions from cultures of PA14 (WT cyanide), *hcnA* (no cyanide), *PA2196* +pUCP18 (highly impaired cyanogenesis) and *PA2196* +pUCP18::*PA2196* (restored cyanogenesis) was tested (Figure 4-14).

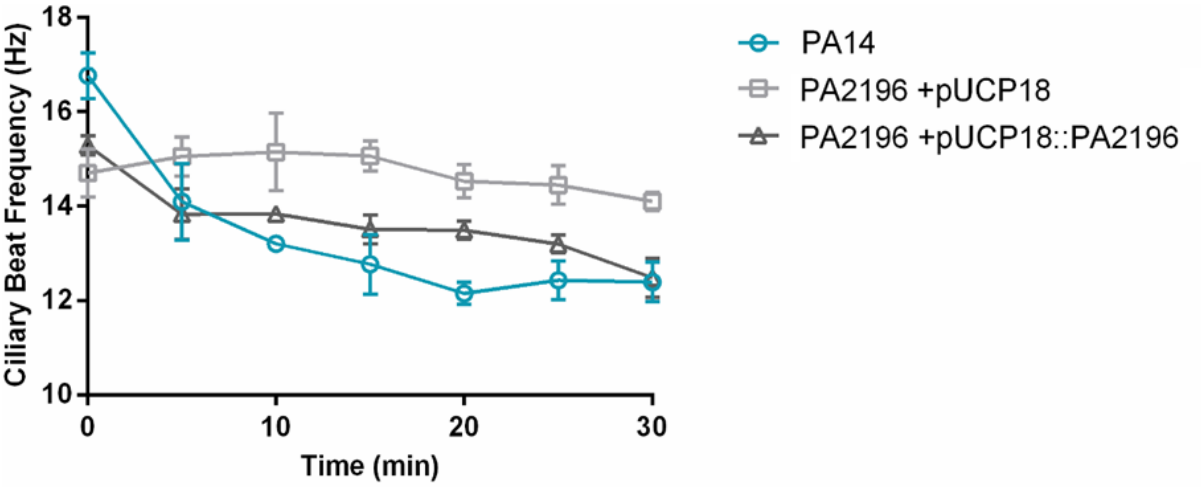


Figure 4-14 Effect of *PA2196* supernatant on ciliary beat frequency of healthy air-liquid interface cultures. n=1 Error bars are S.D of 6 technical replicates. *PA2196* +pUCP18 caused a slight fall in CBF after 30 min (7.7%). Supernatant from PA14 caused a 24.4% fall in CBF over the same time period. *PA2196* +pUCP18::*PA2196* caused a 18.4% fall in CBF, suggesting that complementation with the *PA2196* gene product partially restored virulence.

4.5 Discussion

This chapter tested the hypothesis that there existed unknown regulators of cyanogenesis, and that these could be identified by interrogating the *P. aeruginosa* genome using a colourimetric assay. An adapted method made suitable for high throughput screening led to the discovery of two novel determinants of cyanogenesis by visual assessment. The validity of these two genes, *PA2196* and *PA5339*, both of which were found to be highly impaired in cyanogenesis under our screening conditions, was confirmed by complementation: The *PA2196* and *PA5339* gene products supplied *via* recombinant plasmids were sufficient to restore cyanogenic ability to the mutant strains.

The screen was not comprehensive. Due to poor growth (OD<0.6 after 24 h), an estimated 20% of the mutants in the library were discounted from consideration. In addition, damage to the assay papers resulting from condensation during the incubation step meant that up to a further 30% of mutants could not be screened. Additionally, since the identification of cyanogenesis mutants relied on a visual assessment, only mutants that exhibited marked defects in all three replicates were chosen for further assessment. It is therefore likely that the number of mutants recovered from this initial screen represents a considerable underestimate.

4.5.1 Confirmation of *dadA* Cyanogenesis Defect

The screen identified several genes exhibiting marked cyanogenic defects, including *dadA*.

A role for *dadA* in impaired cyanogenesis had been reported by Hagins *et al.*, (2009) , in the *P. aeruginosa* clinical strain FRD1. *dadA* encodes a putative D-amino acid dehydrogenase involved in glycine metabolism. As glycine is the precursor to cyanide in *P. aeruginosa*, mutants lacking *dadA* lose some of their cyanogenic ability. Cyanide production can be increased by the addition of glycine to the growth medium.

As it exhibits a previously reported defect in cyanide-production, in our study *dadA* can be considered a cyanogenesis control that was successfully identified and, as such, represents a marker for quality control.

4.5.2 *PA2196* is a Repressor of the TetR Family

This work describes the first link between *PA2196* and a cyanogenesis defect. *PA2196* is predicted to encode a 21.7 kDa cytoplasmic repressor of the TetR family. Regulators of the TetR family are homodimeric DNA-binding proteins with varied roles, for example the regulation of transporters and

pumps involved in antibiotic resistance or tolerance to toxic compounds (Ramos *et al.*, 2005; Yu *et al.*, 2010).

The regulation of tetracycline resistance in *P. aeruginosa* by TetR is the archetypal example. Briefly, repression exerted by TetR on *tetA* gene expression is relieved in the presence of its ligand tetracycline, the compound which TetA acts to efflux from the cell (Figure 4-15). This ensures that *tetA* genes are only active when they are needed, that is, in the presence of tetracycline.

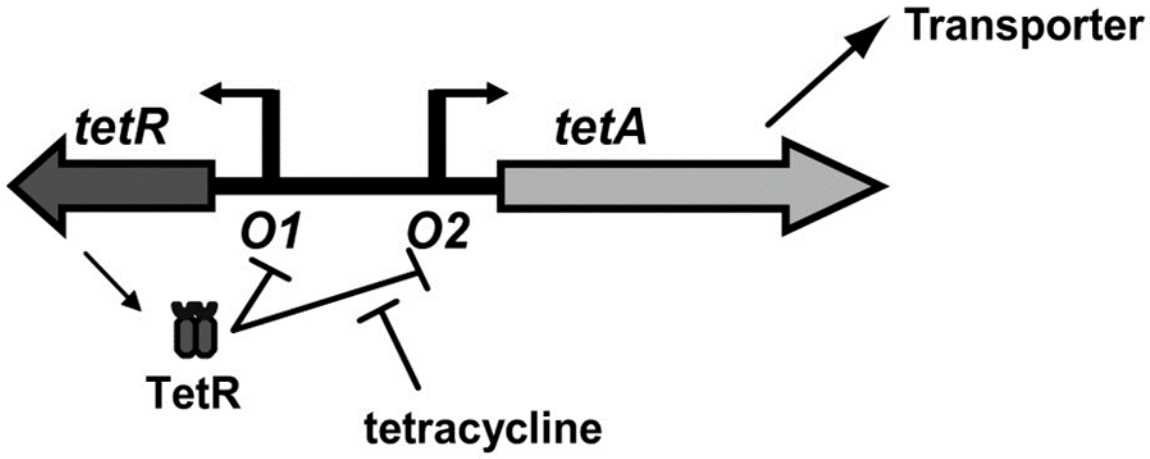


Figure 4-15 tetR-tetA regulon. (Yu *et al.*, 2010). In the absence of tetracycline, TetR represses tetA expression by binding to upstream operator DNA. This repression is relieved in the presence of tetracycline, which binds to TetR and creates an inactive complex. tetA is then free to mediate efflux of tetracycline from the cell.

TetR regulators have also been implicated in virulence. For example, *P. aeruginosa* has been shown to modulate CFTR expression *via* the regulation of the toxin, CFTR Inhibitory Factor (Cif), by a TetR family regulator, cifR (MacEachran *et al.*, 2008) (Figure 4-16).

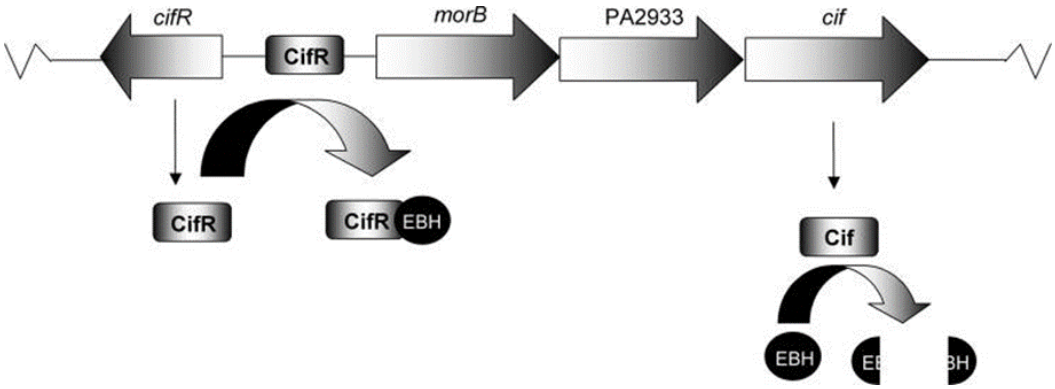


Figure 4-16 Cif-CifR regulon (MacEachran *et al.* 2008). In the absence of epoxide epibromohydrin (EBH), CifR represses cif gene expression by binding to the operator DNA adjacent to the cif genes.

Binding of EBH causes dissociation of CifR, leading to increased cif gene expression and degradation of EBH. Degradation of EBH results in reduced apical membrane expression of CFTR in epithelial cells. The mechanism by which this occurs is unknown, though it has been hypothesised that EBH may play a role in epithelial cell signalling.

TetR regulators are commonly found adjacent to the genes they regulate, typically binding to upstream or intergenic regions to act as repressors. It is therefore of considerable interest that *PA2196* is located 154 bp downstream of the HCN synthase operon, *hcnABC* (Figure 4-17).



Figure 4-17 Gene locus of *PA2196*, 154 bp downstream of *hcnABC* operon. (*Pseudomonas* genome database, Winsor *et al.*, 2011)

A crystal structure was resolved for *PA2196*, revealing that it possesses many of the features expected of a TetR regulator (Kim *et al.* 2013; Kang & Choe, 2011). The N-terminal α helices form a DNA-binding domain with a helix-turn-helix motif that recognises palindromic DNA. The C-terminal domains are thought to contain a ligand binding pocket (523 Å) with two entrances. The nature of the ligand is not yet known but it is predicted to be hydrophobic and negatively charged.

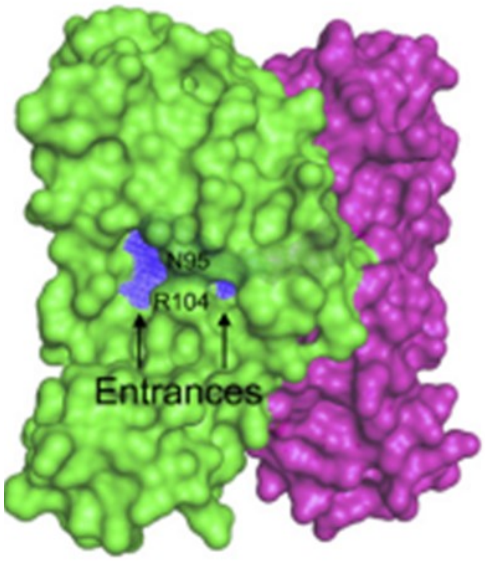


Figure 4-18 Surface representation of *PA2196*. (Kang & Choe, 2011) Based on the resolved crystal structure, there are two predicted entrances to a ligand-binding pocket near residues N95 and R104. The ligand is predicted to be negatively charged and hydrophobic.

Kang & Choe (2011) also reported that *PA2196* is likely to regulate its own expression by binding to a 25bp semi-palindromic sequence upstream of itself (5′-GTTTCTAGACGACTGGTCTAATTCA-3′). Two dimers of *PA2196* are predicted to form a complex with this operator DNA.

4.5.3 What is the Role of PA2196 in Cyanogenesis?

No cyanide production was observed in the *PA2196* mutant, neither in the colourimetric assay nor by direct CN- measurements using an ISE. The role of *PA2196* in cyanide-production was later confirmed through a complementation study: *PA2196* gene product supplied by a recombinant plasmid was sufficient to restore cyanogenesis in the *PA2196* mutant.

Interestingly, when compared to PA14 in a ciliary beat frequency ALI model (Figure 2-14; n=1), supernatant from the *PA2196* mutant exhibited significantly attenuated virulence. This may come as no surprise since, based on the results in Section 1.3.7. (p. 781), a mutant deficient in cyanide production is expected to exhibit reduced cilio-inhibition.

PA2196 was not attenuated in PYO production. As PYO production is QS-controlled, this implies that *PA2196* is not a modulator of these networks. Instead, the data suggests that *PA2196* is more directly involved in cyanogenesis. For example, *PA2196* may directly or indirectly regulate expression of the hcnABC operon. Since the semi-palindromic DNA sequence reported by Kang *et al.* is not present upstream of the hcnABC genes, it is likely that this regulation is indirect. *PA2196* may exert control over the transcription of other genes which themselves regulate hcnABC expression.

Due to its nature as a TetR family regulator, and inferred from the presence of an upstream palindromic DNA binding site, it can hypothesised that *PA2196* binds to and represses itself in the absence of a ligand. In the presence of this ligand, predicted to be hydrophobic and negatively-charged, *PA2196* repression is relieved and the switch results in altered cyanogenic output.

A possible hypothesis is that *PA2196* regulation plays a role in virulence, or in sensing and detoxifying a toxic compound, perhaps cyanide itself. For example, *PA2196* may modulate the timely production of cyanide as part of a successful infection strategy, or it may give *P. aeruginosa* a competitive edge over other microbes, in a form of biological warfare (Trejo-Hernández *et al.*, 2014).

4.5.4 PA5339 is a Putative Member of the yjgF Superfamily

This work describes the first link between *PA5339* and a cyanogenesis defect. PA5339 is a 13.6 kDa cytoplasmic protein of unknown function. Based on sequence homology, *PA5339* is predicted to be an endoribonuclease of the liver perchloric acid-soluble protein (L-PSP) superfamily, belonging to a widely distributed family of homotrimeric yjgF proteins. yjgF proteins are conserved in all domains of life, and in bacteria, these have been shown to play a role in the transport or transformation of small molecules, including antibiotics (Dietrich *et al.*, 2008). In *E. coli*, the translational inhibitor TdcF is a YjgF member involved in sensing and detoxifying the toxic metabolite 2-ketobutyrate, an intermediate in the biosynthetic pathway of L-isoleucine (Burman *et al.*, 2007).

PA5339 is located downstream of *spoT*, which mediates the stringent response to diverse stresses. Additionally, *PA5339* is predicted to be in an operon with the adjacent gene, *PA5340*, a 26.1 kDa protein with a putative lipid cleavage site (Figure 4-19).

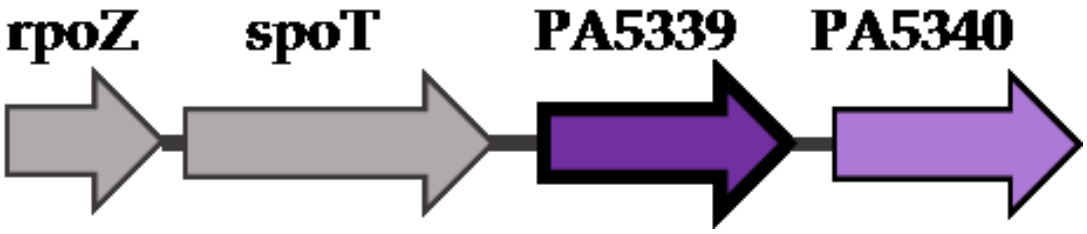


Figure 4-19 Gene locus of PA5339, downstream of *spoT*. (*Pseudomonas* genome database, Winsor *et al.* 2011). *PA5339* has been computationally predicted to form an operon with *PA5340*.

4.5.5 What is the Role of PA5339 in Cyanogenesis?

Based on computational predictions, PA5339 may function as a translation initiation repressor *via* mRNA degradation. Alternatively, it may play a role in purine degradation, since a Basic Local Alignment Search Tool (BLAST) analysis indicates it shares 43% protein identity with *Escherischia coli* RutC, which detoxifies a toxic by-product of this pathway. A protein-BLAST search of *PA5340* against all bacterial genomes revealed orthologs in other *Pseudomonas* spp. but did not uncover any putative conserved domains.

At present, there is insufficient data to provide a functional link between PA5339 and cyanogenesis in *P. aeruginosa*. However, combined data from the colourimetric screen, direct cyanide measurements and complementation experiments suggest that interrupting *PA5339* severely impairs cyanogenic

output. As *PA5339* does not suffer from a PYO production defect, it can be hypothesised that it is not a regulator of QS.

Interestingly, a study by Massier *et al.*, (2012) identified *PA5339* as a gene upregulated after treatment with sub-lethal pulsed light treatment, implicating a role in adaptation to external stress. In another study, both *PA5339* and *PA5340* were identified as two of only 40 "core biofilm genes" that were observed to be upregulated >1.4 fold in three different microarray data sets, comparing planktonic and biofilm stationary-phase gene expression (Patell *et al.*, 2010). It can therefore be hypothesised that *PA5339* and *PA5340* may be involved in *P. aeruginosa* adaptation to external changes, for instance in the switch from a motile to sessile biofilm lifestyle at the onset of chronic infection.

4.6 Future Work

In summary, the initial screening method was successful in uncovering novel genes with striking cyanogenic defects. However, due to coverage issues and limitations in the analysis approach, this screen was unable to provide a complete picture of cyanide production in *P. aeruginosa*. Steps were therefore taken in parallel to improve output quality and to make the data analysis more quantitative, in Chapter 5.

With regards to *PA2196* and *PA5339*, while their role in cyanogenesis was confirmed *via* complementation experiments described in this chapter, further work will be required to elucidate the details of their contributions. For example, the effect of *PA2196* and *PA5339* mutations on *hcnABC* transcription and translation could be tested by transforming *PA2196* and *PA5339* strains with lacZ transcriptional and translational fusions. Alternatively, in order to obtain a detailed picture of transcriptional regulation, RNA-seq could be performed on RNA extracted from *PA2196* and *PA5339*, preferably from clean deletion mutants. Different growth conditions, such as exponential, early stationary and late stationary should be investigated.

In addition, the cyanide-sensitivity of *PA2196* and *PA5339* could be tested to see if they are involved in cyanide detoxification or tolerance. MIC measurements with varying [KCN] would be useful to reveal increased sensitivity to cyanide of mutants compared to WT.

The effect of *PA2196* and *PA5339* mutations on QS could be investigated by assaying multiple QS-regulated factors such as elastase and alkaline protease. Alternatively, levels of QS molecules could be measured directly, for example by GC-MS or using a bio-reporter strain.

The hypothesis that *PA2196* responds to cyanide or cyanide-related pathways could be tested as follows. PA2196 protein could be purified and DNA gel shift assays performed with its upstream palindromic box, in the presence or absence of cyanide, or its detoxification products, such as thiocyanate.

In a preliminary experiment (n=1) using supernatant from the *PA2196,* the mutant exhibited reduced virulence compared to WT. Complementation by the *PA2196* product supplied on a plasmid was observed to restore virulence. Additional replicates should be tested to verify this effect. In addition, these experiment should also be carried out with the *PA5339* mutant.

Chapter 5
QUANTITATIVE CYANIDE SCREEN OF THE PA14NR LIBRARY

5.1 Introduction

The semi-quantitative screen in the previous chapter demonstrated a potential for uncovering novel regulators of cyanogenesis within the PA14NR library. In this chapter, we hypothesise that further improvements to the screening protocol and a targeted quantitative approach to data analysis may help to identify many additional determinants of cyanogenic output in *P. aeruginosa*, thus providing a more elaborate understanding of cyanide production in this organism.

5.1.1 Troubleshooting the Initial Screen

In the previous screen, a 24 h incubation step of the cyanide detection paper in a 37˚C incubator led to image defects, due to condensation. In addition, evaporation was responsible for fainter spots for mutants located in the edge wells (Figure 5-1). In order to resolve these issues, incubation times of the assay plates, without their lids, and in contact with the cyanide detection paper, needed to be kept to a minimum. Therefore, an optimal assay window had to be determined.

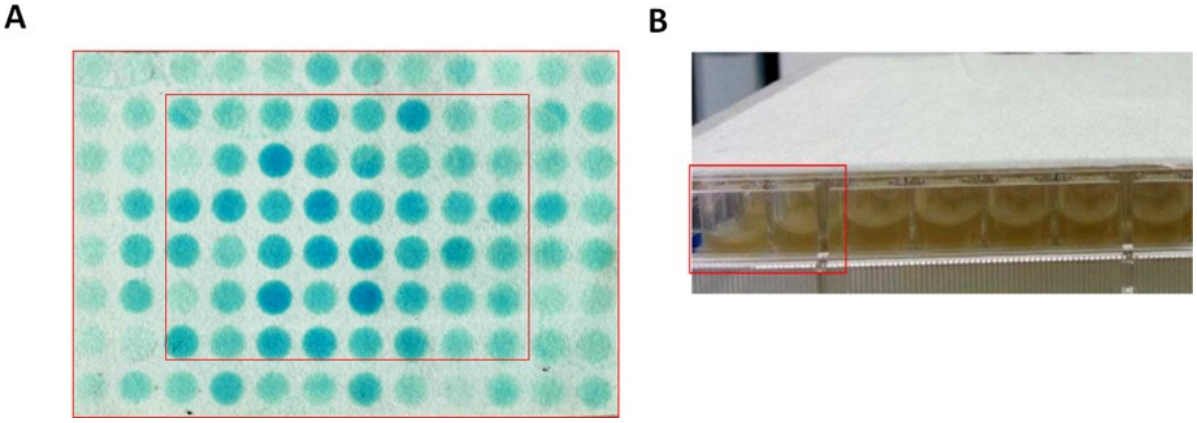


Figure 5-1 Edge effect on cyanide detection paper as a result of well evaporation during previous screen. A) Spots corresponding to the edge wells (outer red border) appear on average fainter than those corresponding to the inside wells (inner red box). B) This is because long incubation times (24 hr) at 37 ˚C, without a lid, result in greater evaporation from the edge wells (red border) compared to inner wells. This means that mutants in the edge wells exhibit fainter spots than would be representative of their cyanogenic ability.

An additional drawback of the previous screen was the analysis method: Cyanide-deficient mutants were identified by visual assessment and through comparison with known controls on a separate control plate. This was only semi-quantitative, time-intensive and subject to human error. It was therefore decided that digital image processing of scanned cyanide detection papers would be employed to speed up the data analysis step and to generate more accurate and quantitative cyanogenesis values.

Figure 5-2 summarises the key issues identified in the semi-quantitative screen methodology. These needed to be optimised in order to achieve the spot quality and quantitative data analysis presented in this chapter.

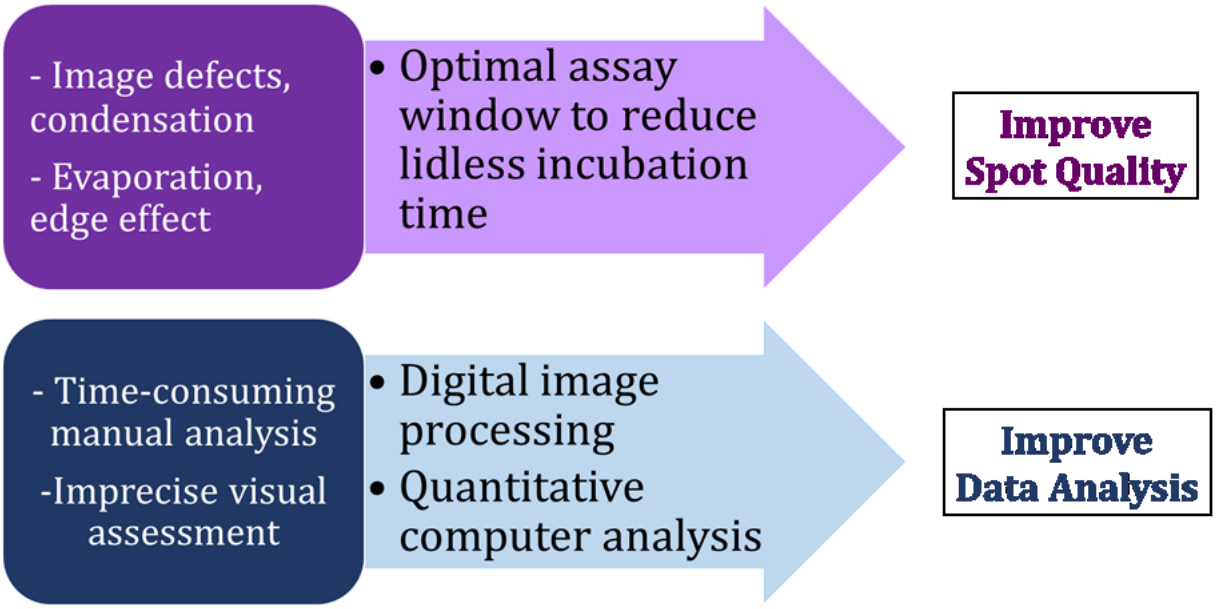


Figure 5-2 Trouble shooting the initial screen. Problems identified during the previous screen relating to spot quality (purple) and data analysis (blue) are presented alongside potential solutions to be addressed in this chapter.

5.2 Aims

- To improve image quality of cyanide detection papers obtained from screen
- To optimise digital image processing and generate quantative cyanogenesis data
- To rescreen the entire PA14NR library with the optimised protocol
- To identify additional mutants with altered cyanogenic output in order to expand our understanding of the determinants that control cyanide production in *P. aeruginosa*

5.3 Method Development

5.3.1 Finding an Optimal Assay Window

In order to resolve issues of condensation and well-evaporation, the amount of time the assay plates were incubated without their lids, and were in contact with cyanide detection paper, needed to be reduced.

Monitoring growth in 96-well plates indicated that mutants achieve an OD^{600} of ~0.2 after 10 hours, when grown statically at 35˚C with the lid on (data not shown). An assumption was made that no cyanide would be produced during this time, since cyanide production in PA14 WT occurs during entry into stationary phase, at an OD^{600} 0.8-1. The screening protocol was therefore amended to include an additional 10 hour incubation step, at 35˚C with the lid on, followed by a 10 hour lidless incubation at 37˚C, with the cyanide detection paper (Figure 5-3).

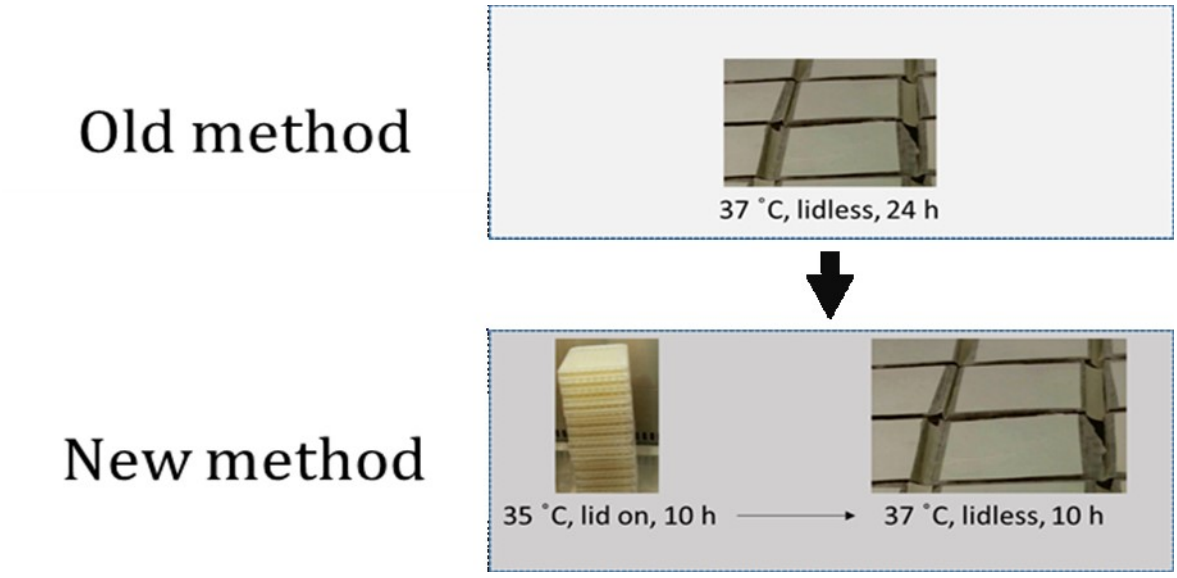


Figure 5-3 Reduction of the assay window to limit water damage and edge effect.

The reduced lidless incubation window at 37˚C minimised edge effects and greatly improved image quality (Figure 5-4).

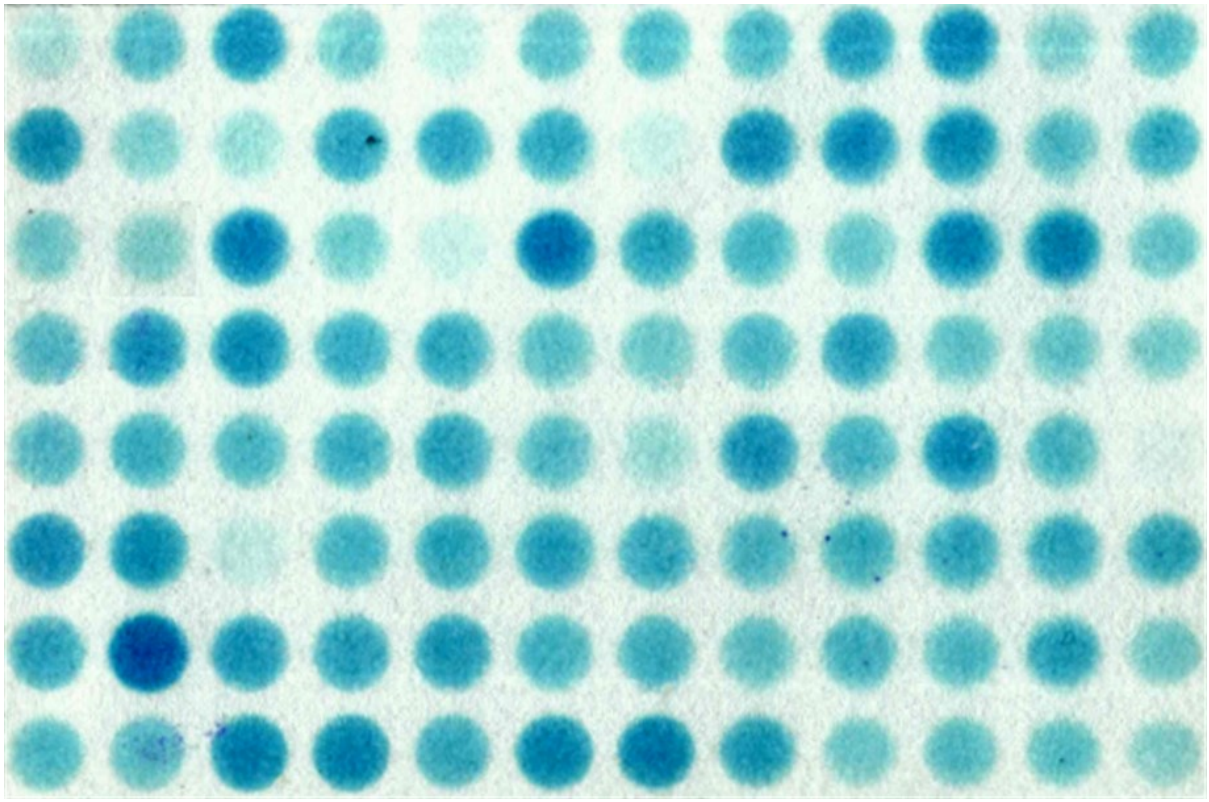


Figure 5-4 Improved image quality with reduced water damage and reduced edge effect.

5.3.2 Quantitative Digital Image Processing with CyQuant, a Purpose-Built Script

Modifications to the screening protocol detailed above greatly improved image quality, coverage and accuracy, allowing more thorough analysis of the library than was possible in the previous screen.

In accordance with conclusions from the previous chapter, manual analysis was deemed too time intensive and lacking quantification.

Instead, a digital image processing approach was undertaken. With the assistance of Luke Tweedy, a colleague from the Systems Biology department, steps were taken to develop a plug-in to analyse scanned cyanide detection papers in a free image-analysis software, ImageJ. The principle behind the ImageJ plug-in was that it could recognise the template of a 96-well plate and measure mean colour intensities from 96 circular 'zones' corresponding to the locations of blue spots on a scanned cyanide detection paper. Pixel intensity values could then be extracted for each spot into an Excel spreadsheet and be divided by corresponding OD^{600} values to give a quantitative 'cyanogenesis' for each mutant. Using this plug-in, cyanide overproducers, such as *rsmA*, produced higher values than WT (~300 vs ~100 pixel intensity values), while cyanide underproducers, such as *gacA* and *hcnA*, produced smaller values (~30 pixel intensity).

The plugin provided a proof of principle that digital image processing could be used to make the screen quantitative. However, its use was time intensive, since each image had to be processed individually and the cyanogenesis value calculations had to be performed separately and manually in Excel.

For this reason, data generated from the improved screening methodology was instead analysed using a purpose-built script, CyQuant, written by our collaborator in the Faculty of Medicine, Dr Volker Behrends.

CyQuant is a MATLAB graphical interface specifically designed to analyse colourimetric cyanide screen data in triplicate. It simultaneously measures spot pixel intensity values of scanned cyanide detection papers, calculates cyanogenesis values using OD^{600} data, and provides instant graphical visualisations of outliers.

CyQuant was designed to take growth and cyanide production kinetics into account: Mutants that did not grow to an $OD^{600}<0.3$ were discounted from analysis. Additionally, cyanogenesis values for each mutant plate were normalised to a WT plate, containing PA14 WT in every well, in order to account for the effect of well location on spot intensity.

Figure 5-5 shows the CyQuant graphical interface and summarises how it is used to analyse cyanide screen data.

z

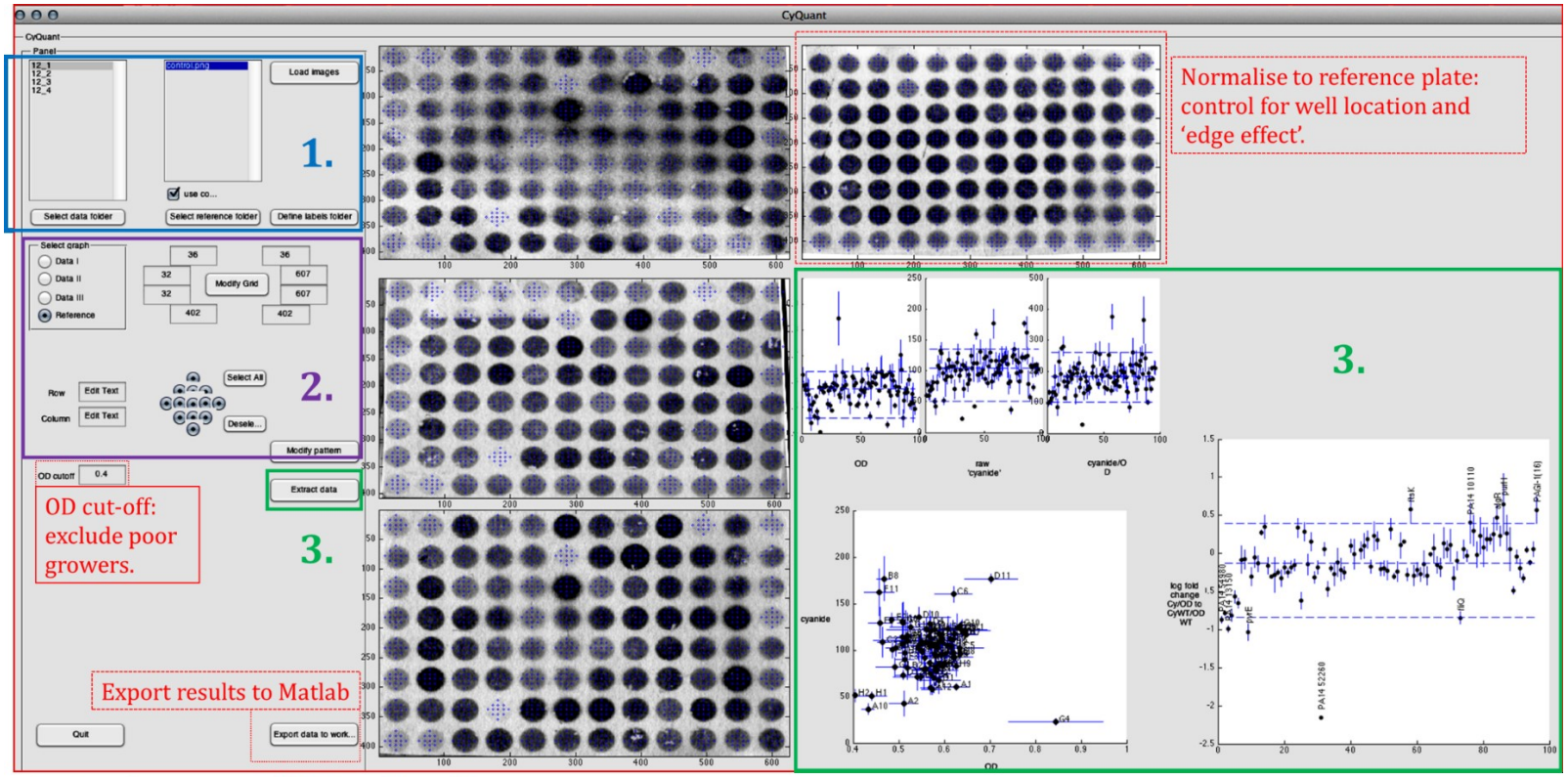


Figure 5-5 Analysis of cyanide screen data in CyQuant. CyQuant simultaneously measures spot intensities of scanned cyanide detection papers, calculates cyanogenesis values using OD600 data and provides instant graphical visualisations of outliers.

5.3.3 Quantitative Screen Workflow

Figure 5-6 illustrates the improved cyanide screen protocol.

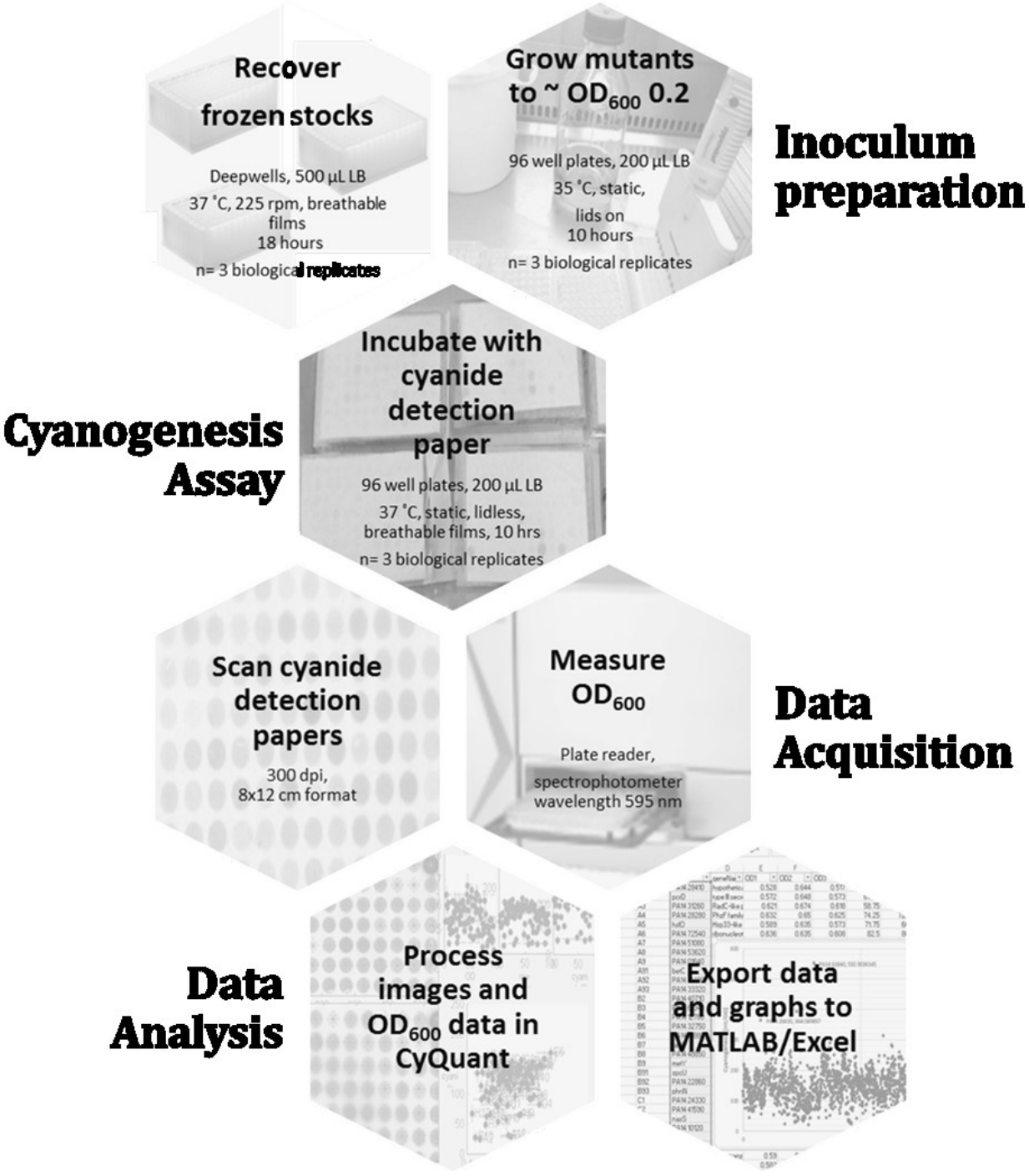


Figure 5-6 Modified cyanide screen work flow to achieve improved image quality and quantitative data analysis.

5.4 Results

5.4.1 Quantitative Screen of the PA14NR Library

Using the improved methodology described above, the PA14NR library was screened in its entirety, and in biological triplicate, to identify novel cyanogenesis mutants. In comparison to the previous, semi-quantitative screen, coverage with the new method was greatly improved. Cyanogenesis values were obtained for 5448/5850 mutants, representing 93% coverage. The minimum, average and maximum pixel intensity values values calculated in CyQuant were 15, 172 and 550.

Due to the existing format of the PA14NR library, it was not possible to compare mutants to a WT assayed on the same plate. Instead, mutant cyanogenesis values were normalised to the plate median. Figure 5-7 summarises the overall results of the screen. The majority of mutants cluster near the median cyanogenesis value for each plate. However, several mutants produced cyanogenesis values several log2 transformed fold change (log2 FC) different from the median, indicating a wide spread in cyanogenic ability within the library (Figure 5-9).

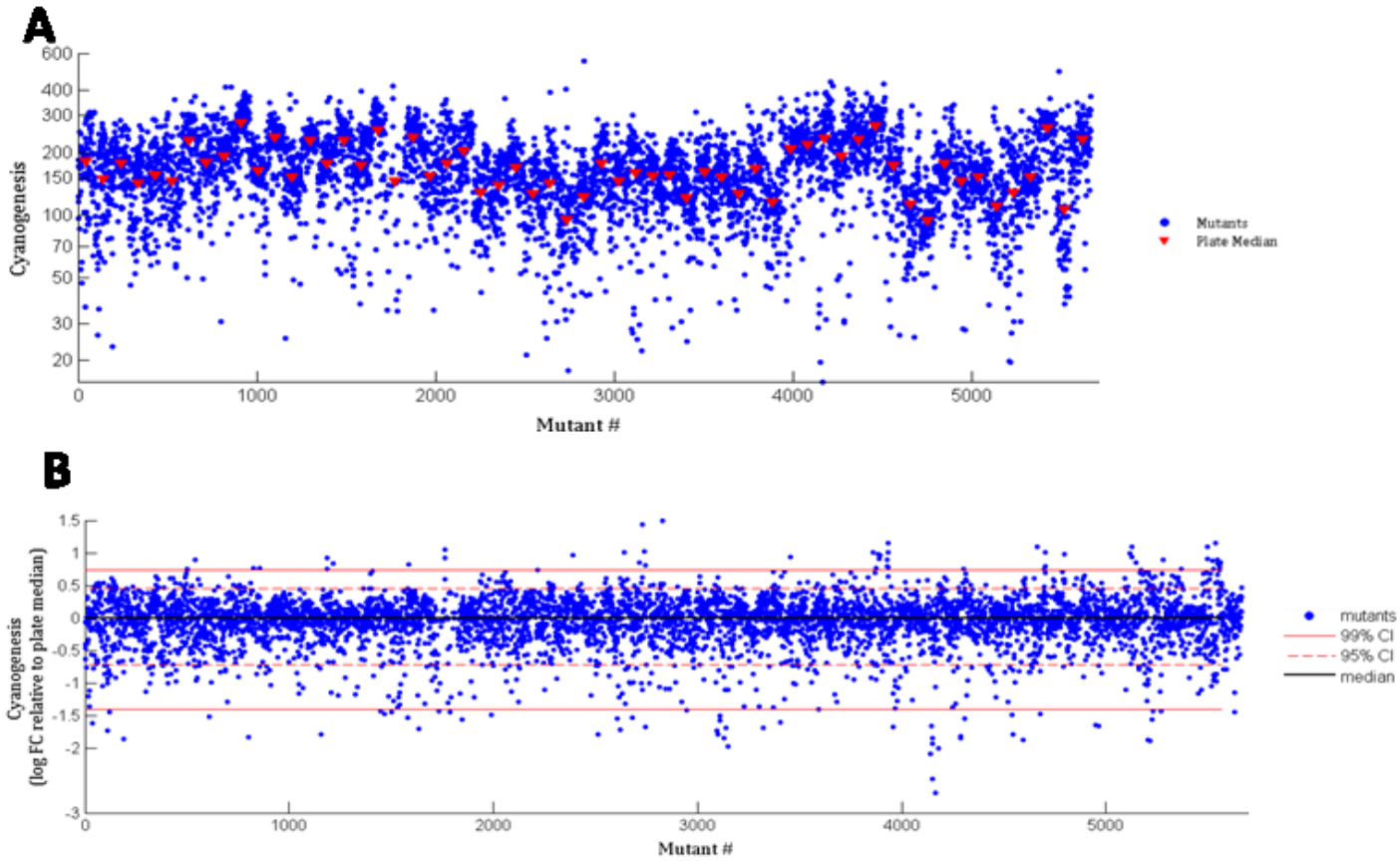


Figure 5-7 Quantitative screen summary. Scatterplot of cyanogenesis values calculated in CyQuant. Mutants on the same plate are shown grouped together (mutants 1-96 on plate 1, mutants 97-193 on plate 2 etc.). Red triangles represent plate median values. B. Scatterplot of log2 transformed fold-change cyanogenesis compared to plate median (black line). Dashed red lines = 95% confidence interval limit. Solid red lines = 99% confidence interval limit.

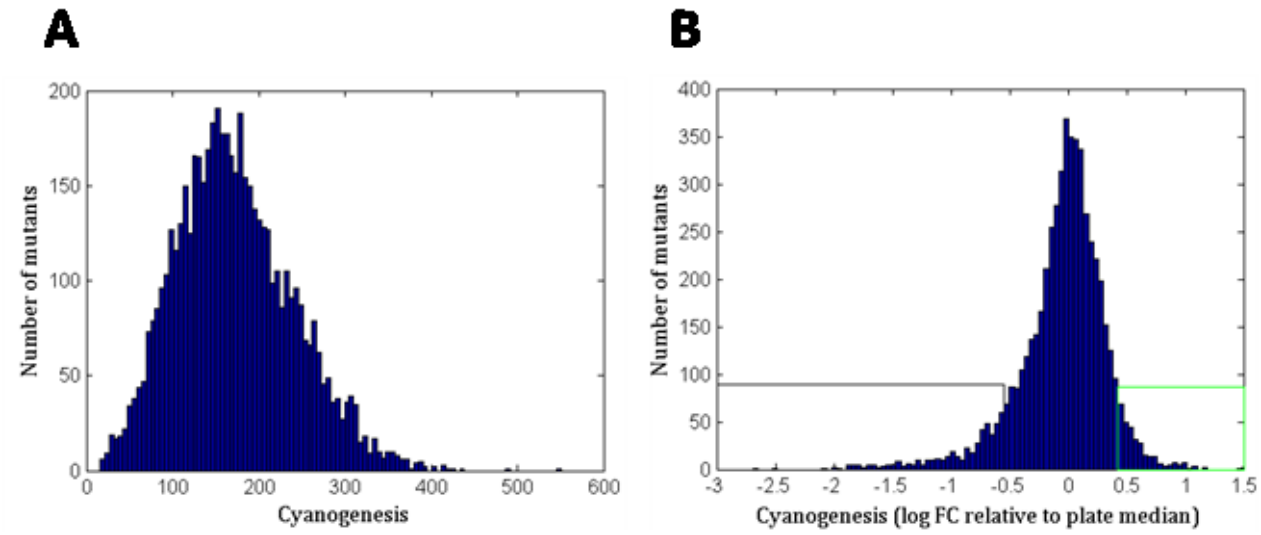


Figure 5-8 Spread of cyanogenic ability in the PA14NR mutant library. A. Histogram of cyanogenesis values calculated in CyQuant. B. Log2 transformed fold-change values of mutants, relative to plate median. 95% confidence intervals are displayed in black (underproducers) and green (overproducers) boxes.

5.4.2 Clustering Analysis of Cyanide Screen data

Next, we wanted to test if outliers, that is, mutants exhibiting altered cyanide production kinetics, could be identified computationally. Due to the large size of the dataset, means clustering was elected as a simple, unsupervised approach. This method had been employed previously to analyse mutant screen data (Musken *et al.*, 2010). A k-medoids clustering algorithm, "partitioning around medoids" (pam), was chosen over the standard k-means methods, as it is considered more robust to noise and outliers.

OD600 values and spot intensity data was analysed in the statistical software, R. Firstly, the appropriate number of clusters, k, to look for within the cyanide screen dataset was determined by performing a plot of 'within groups sum of squares' by 'number of clusters extracted'. A bend in the plot indicated the appropriate number of clusters was 3 (Figure 5-9).

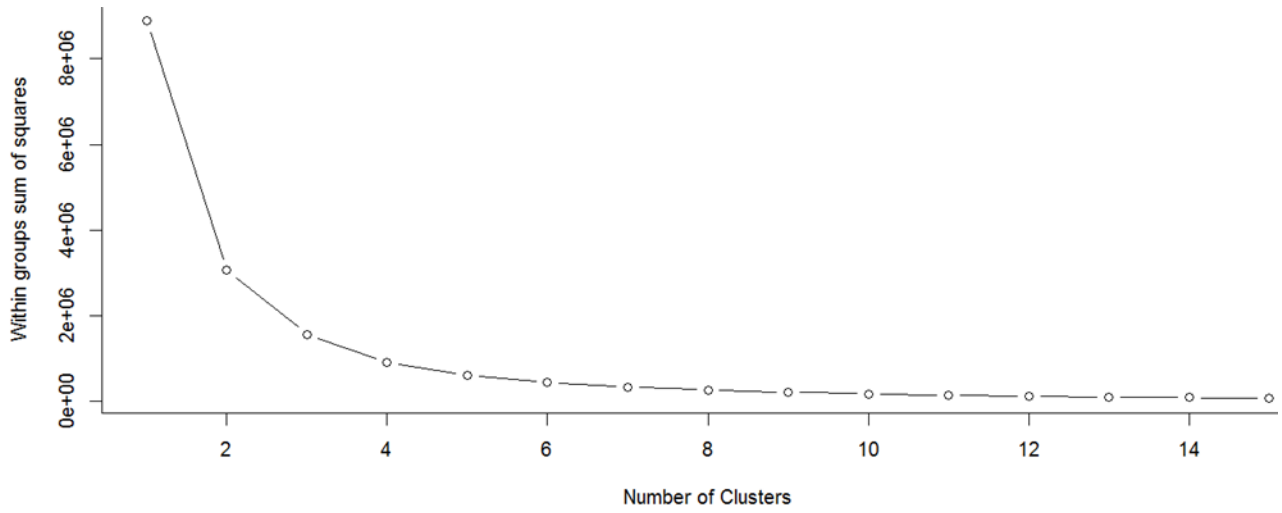


Figure 5-9 Determination of number of clusters to look for within the cyanide screen data. There was a distinct drop in within groups sum of squares when moving from 1 to 3 clusters. After three clusters, this decrease dropped off, suggesting that a 3-cluster solution was a good fit to the data.

Employing k=3, clustering analysis was carried out. The results of the analysis indicated that mutants could be successfully classified into three clusters based on cyanide production kinetics (Figure 5-10).

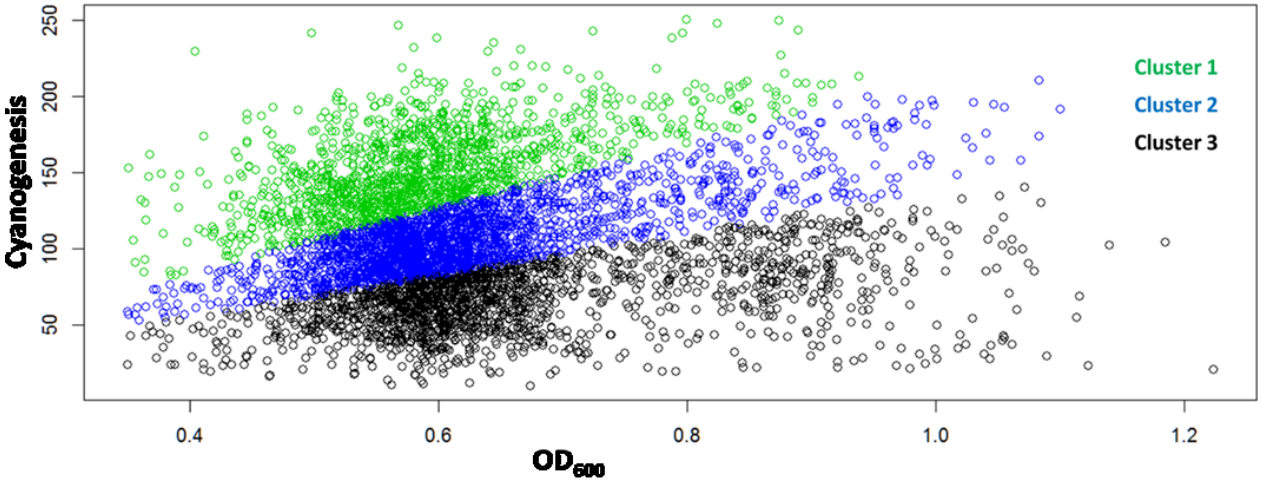


Figure 5-10 Clustering of cyanide screen data into three groups based of growth and cyanide production. Mutants in Cluster 2 (blue) represent normal cyanide production kinetics. In contrast, mutants in Cluster 1 (green) exhibit a higher cyanogenesis/OD^{600} ratio and can be considered overproducers. Conversely, mutants in Cluster 3 (black) may be considered underproducers as they exhibit low cyanogenesis/OD^{600} ratios.

Each cluster contained a centre, or medoid. Cluster 1 consisted of 1411 mutants clustered around a medoid with an OD^{600} 0.58 and a cyanogenesis value of 253 (putative overproducers). Cluster 2 consisted of 2243 mutants, centred around a medoid with an OD^{600} 0.58 and a cyanogenesis value of

171 (normal). Cluster 3 consisted of 1780 mutants centred around a medoid with and OD^{600} 0.66 and a cyanogenesis value of 105 (putative underproducers).

In order to assess the validity of the clustering approach, we looked at how known cyanogenesis controls had clustered (Table 5-1). The majority of mutants, such as biosynthetic genes and QS regulators, clustered as expected. Corresponding cyanogenesis data (Log2 transformed fold-change relative to plate median) for these mutants is shown in Figure 5-11.

The large size of the outlier groups identified suggests that cyanide production is a complex process that can be affected by a range of factors. Due to the large number of putative outliers identified by the clustering method, instead of rescreening all the outliers, we decided to rank underproducing and overproducing mutants by severity of cyanogenesis defect, and to rescreen the 400 most severe outliers (top 250 underproducers and top 150 overproducers) to validate their cyanogenesis phenotypes.

Table 5-1 Clustering of known cyanogenesis mutants based on partitioning around medoids.

Cluster 1= Overproducer Cluster 2= WT Cluster 3= Underproducer

	Gene	Description	Cluster	OD_{600}	Cyanogenesis
Identified in previous screen	*PA2196*	TetR regulator	**3**	0.6	46.7
	PA5339	Translation inhibitor	**3**	0.63	51.8
	PA5340	In an operon with PA5339	**2**	0.64	131
	dadA	d-amino acid dehydrogenase	**3**	0.5	32.7
	flgC	Flagellar basal-body rod protein	**2**	0.56	106.9
	PA0224	Probable aldolase	**3**	0.6	33.9
	PA0192	Small molecule transporter	**3**	0.68	87.33
Synthesis	*hcnA*	HCN biosynthetic gene	**3**	0.58	13.75
	hcnB	HCN biosynthetic gene	**2**	0.56	115.91
	hcnC	HCN biosynthetic gene	**3**	0.59	73
Gene regulation	*gacA*	Global virulence response regulator	**3**	0.59	68.75
	gacS	Global virulence sensor kinase	**3**	0.68	25.42
	rhlR	QS regulator	**3**	0.79	20.1
	rhlI	QS signal	**2**	0.6	126.5
	lasI	QS signal	**3**	0.46	40.1
	Anr	Anaerobic global regulator	**3**	0.52	60.58
	algZ	Alginate and motility regulator	**2**	0.9	105.3
	algR	Alginate biosynthesis regulator	**1**	0.7	183

**hcnB* is mislabelled or contamintated in the library **lasR* is not present in the library **rsmA* did not grow to an OD_{600}>0.4 in the whole library screen but was included in the re-screen (Section 5.4.3)

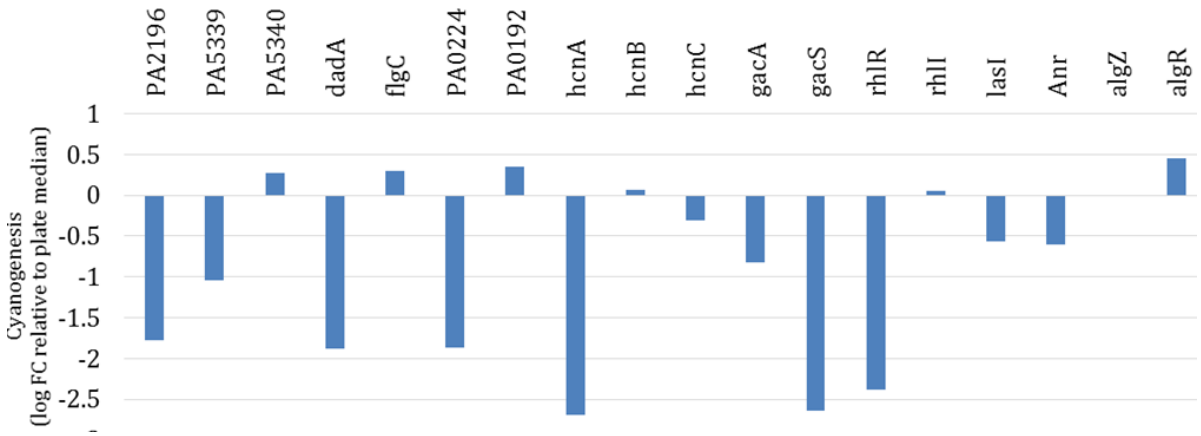


Figure 5-11 Quantitative cyanogenesis screen data of previously identified mutants. Bar plot of Log2 transformed fold-change cyanogenesis relative to plate median. Dashed red line = 95% confidence interval.

5.4.3 Re-Screen of Top 250 Underproducers and Top 150 Overproducers

In order to obtain severity rankings, mutants were ordered by log2 FC relative to the plate median. Following this, a sub-library of the 250 most severe cyanogenesis underproducers and the 150 most pronounced overproducers was created and re-screened in biological triplicate.

Each sub-library plate was designed to contain WT, *gacA* (underproducer) and *rsmA* (overproducer) controls, and only the inner wells (rows B-G; columns 2-11) were inoculated, in order to minimise an edge effect (Figure 5-12).

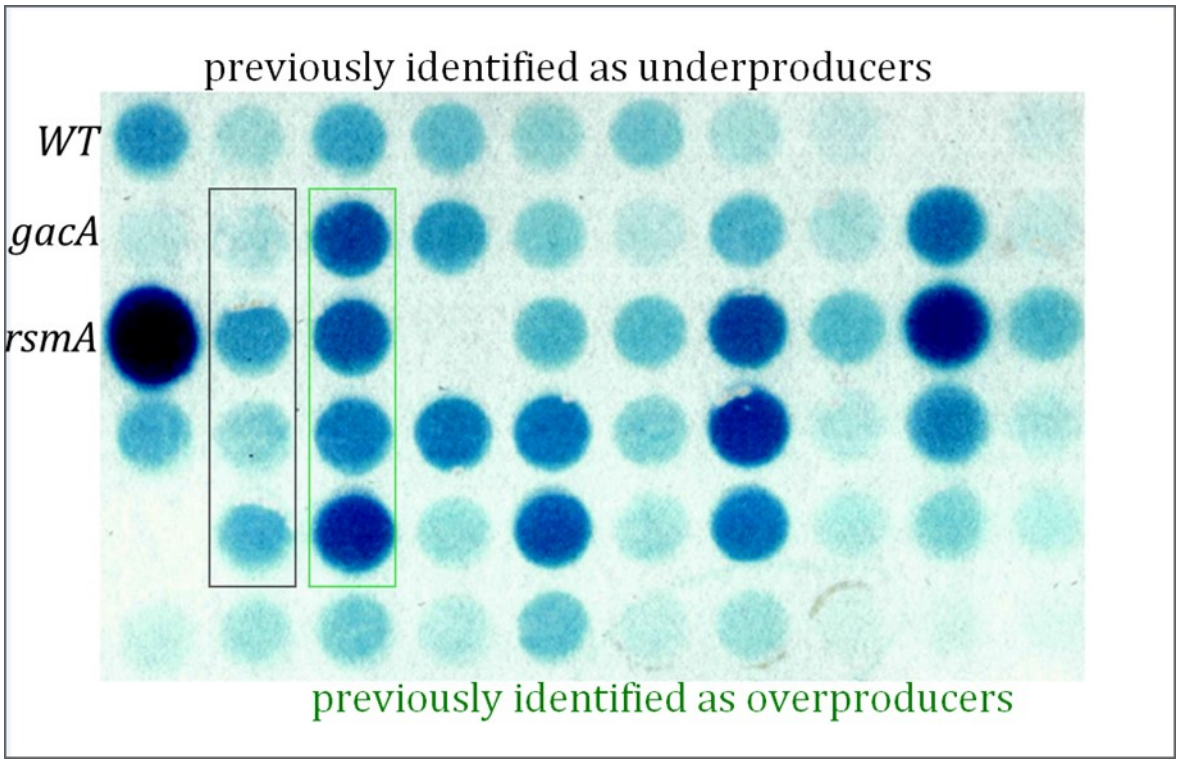


Figure 5-12 Layout of a sub-library plate from the re-screen. Each sub-library plate contains alternating columns of underproducer and overproducer mutants identified in the first screen, as well as PA14 (WT), gacA (underproducer) and rsmA (overproducer) controls. Only the inner wells (rows B-G; columns 2-11) are inoculated, in order to minimise an edge effect.

The results of the re-screen are summarised in Figure 5-13. As expected, and in contrast to the histogram from the whole library screen, most of the mutants rescreened either produced small or large cyanogenesis values. Nevertheless, ~100 mutants produced cyanogenesis values in the 'normal' range, which suggests that some of those identified in the previous screen, ranked based on log2 FC relative to their respective plate medians, may have been false positives.

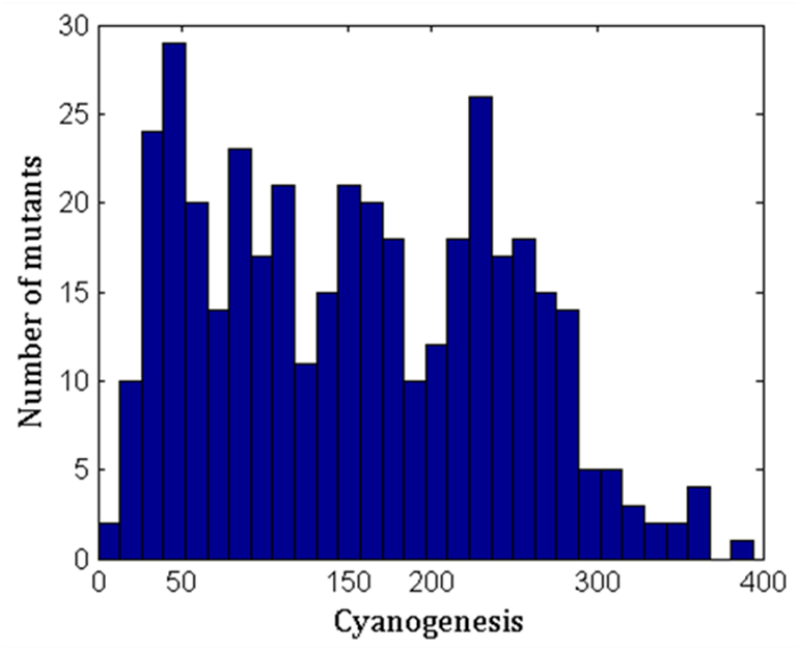


Figure 5-13 Histogram of cyanogenic activity of rescreened mutants.

Figure 5-14 shows the spread of cyanogenic activity within each sub-library plate. The *rsmA* mutant (green triangles) behaved more consistently across the plates than either *gacA* (black triangles) or WT (blue triangles).

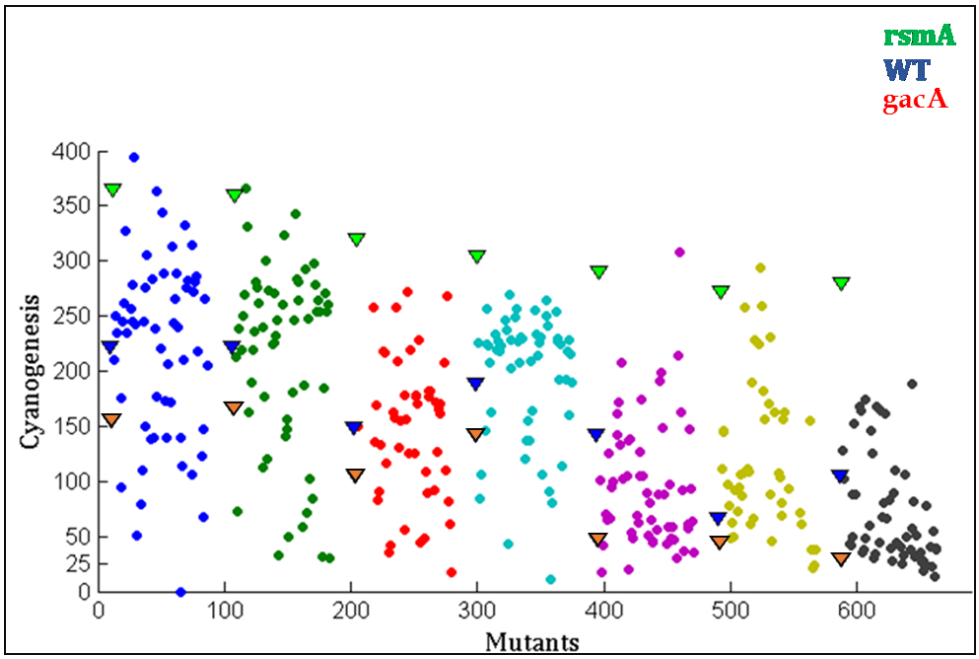


Figure 5-14 Re-screen of top 250 cyanide underproducers and top 150 cyanide overproducers. n= 3 biological replicates. Scatterplot of cyanogenesis values of sub-library plates. *rsmA*, PA14 WT and *gacA* controls on each plate are shown as green, blue and orange triangles respectively.

5.4.4 Distribution of Cyanogenesis Mutants on the PA14 Genome

Re-screened mutants were ranked by severity of cyanogenesis defect based on log2 FC relative to WT and the top 150 underproducers and top 50 overproducers were mapped onto the PA14 genome (Figure 5-15 and Figure 5-16).

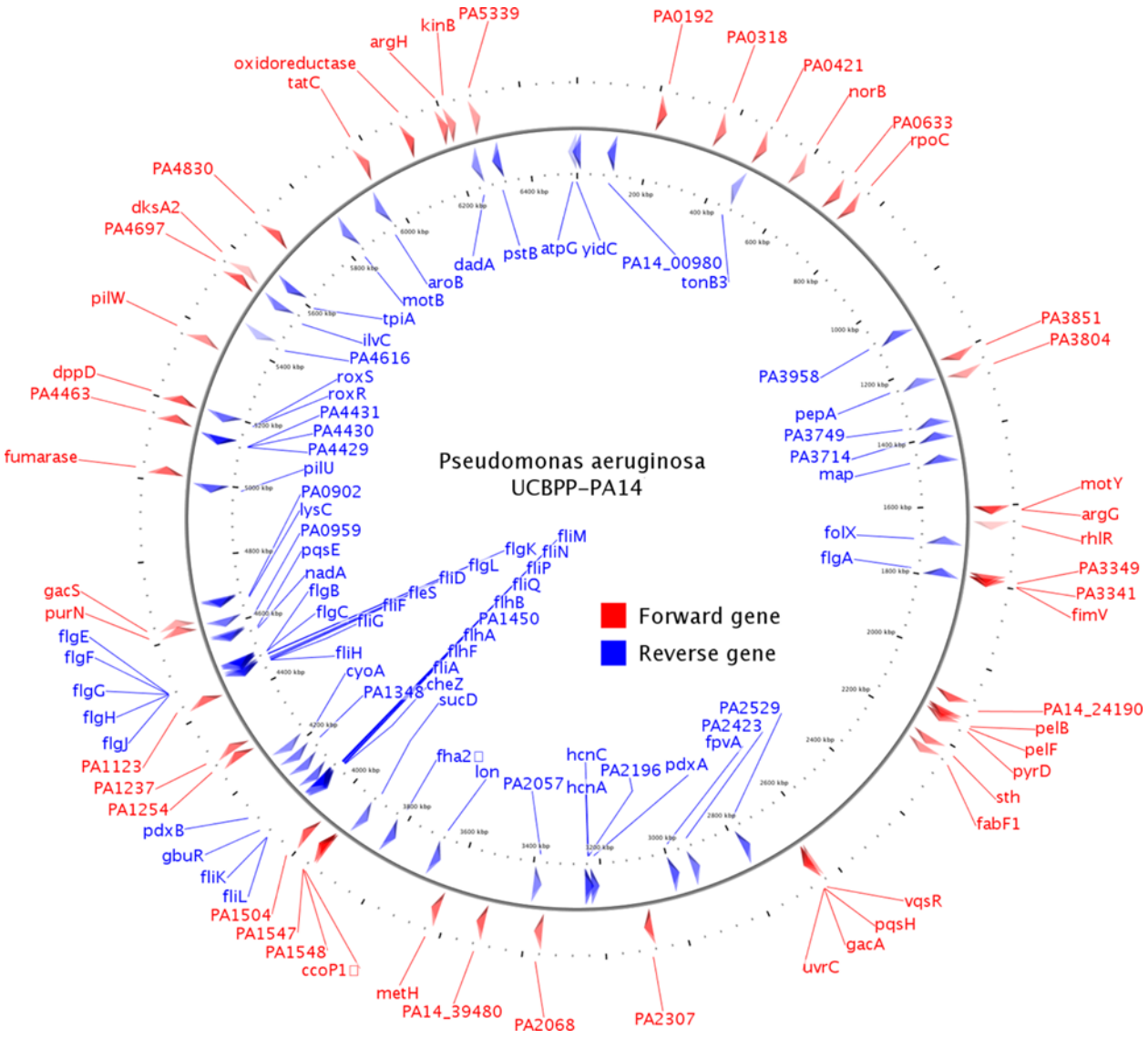


Figure 5-15 Distribution of the top 150 underproducer genes around the PA14 genome. Intensity of the shading of the arrows indicates relative severity of the cyanogenic defect. Mutants were validated by rescreening. Red= Forward gene; Blue = Reverse gene

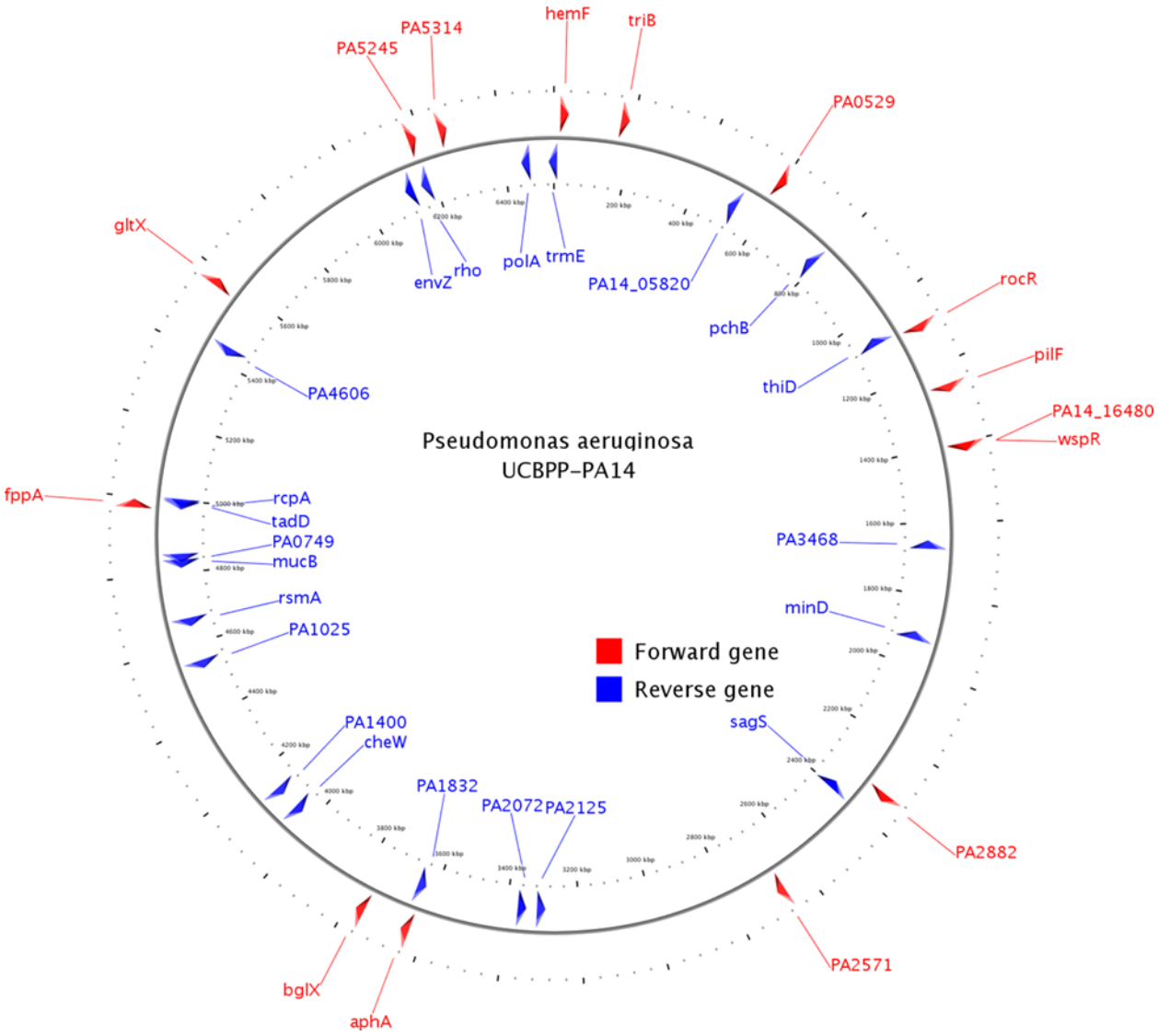


Figure 5-16 Distribution of the top 50 overproducer genes around the PA14 genome. Intensity of the shading of the arrows indicates relative severity of the cyanogenic defect. Mutants were validated by rescreening. Red= Forward gene; Blue = Reverse gene

Rather than definitive answers, the data from our cyanide screen provides a preliminary basis for hypothesis generation. A list of these mutants can also be found in the Appendices.

The genomic maps reveal clustering of sets of genes. In the following sections, groupings of genes that lend themselves to testable hypotheses will be considered. In addition, the identification of novel regulators and virulence factors with no previous connection to cyanide production will be reported.

5.4.5 Involvement of the Motile-Sessile Switch

A striking result to emerge from the quantitative screen, as illustrated by the genomic maps of the most severe outliers, was the high proportion of genes and regulons involved in motility or attachment. These included mutants affected in flagellar biosynthesis, function and regulation, as well as mutants defective in Type IV pili (T4P) and chaperon usher (Cup) fimbrae. There was also an over representation of mutants defective in exopolysaccharide production, mucoidy, and other genes associated with a *P. aeruginosa* lifestyle switch from free swimming single cells to structured multicellular communities.

For this reason, it was decided to investigate the cyanogenesis of genes, operons and regulons related to motile-sessile switch in more detail. The following sections present cyanide screen data of operons related to flagella, T4P, cup fimbrae, secreted exopolysaccharides (*pel*, *psl* and *alg*), as well as cyclic di-guanosine monophosphate (c-di-GMP) modulating, biofilm-related pathways.

5.4.6 Cyanogenesis of Flagella-Related Mutants

In the whole library screen, the majority of structural, regulatory and chemosensory flagella-related mutants exhibited a cyanogenesis defect relative to their respective plate medians (Figure 5-17). Table 5-2 shows cyanogenesis data from both the whole library screen and the rescreen. In the rescreen, mutants were assayed alongside a WT on the same plate. Using log2 FC relative to plate WT as a measure of cyanogenic ability, several of the flagella-related mutants, *flgC, flgE, flgF, fliC, fliJ, fliM, flhB* and *fleN*, which exhibited a normal cyanogenic phenotype in the first screen, were found to be underproducers in the rescreen. One exception was the σ28 sigma factor *fliA*, which gave an underproducer phenotype in the whole library screen, but possessed a normal phenotype in the rescreen.

Overall, these results suggest that interference with flagellar function at either the level of transcriptional regulation (*fleQ, fleS, fleR*), biosynthesis (*flgBCDE, flgFGHIJ, fliK, fliMNOPQ, flhB, flhA, flhF, fleN, flgA*), mechanical rotation (*motAB*) or chemotaxis (*cheYZ, cheAB, cheW, cheRV*), results in some of the most severe deregulation of cyanogenesis observed in our screen.

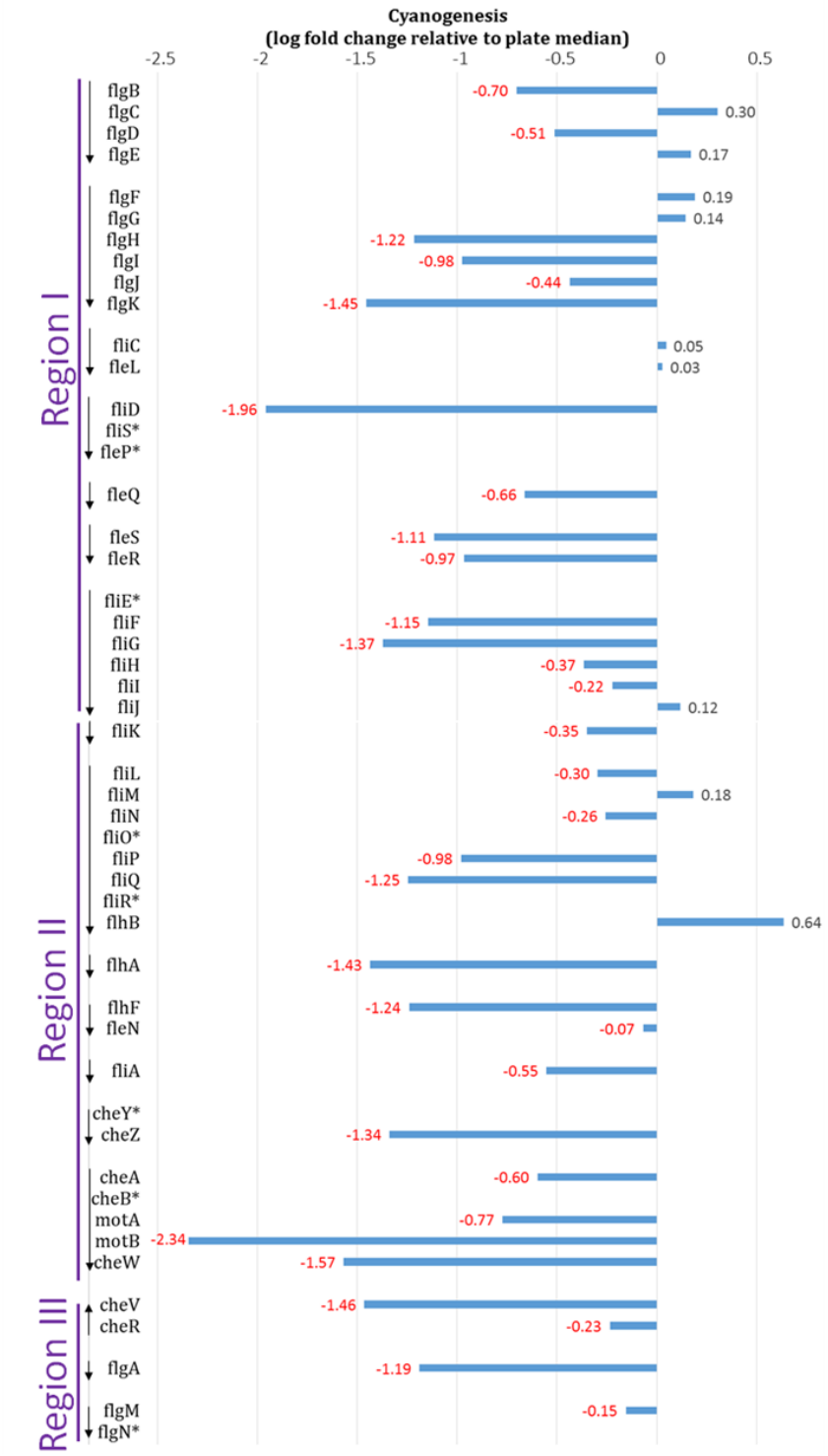


Figure 5-17 The majority of mutants with flagella-related defects exhibit aberrant cyanogenesis. (n=3 biological replicates) Bar plot of cyanogenesis from whole library screen (log2 transformed fold-change relative to plate median). Flagella-related mutants are organised by operon. * = mutant not in library. Dashed red line = 95% confidence interval.

	Gene	Description	Cyanogenesis (log fc)		
				Screen1	Screen 2
Region I	*flgB*	Basal body rod		-0.70	-1.09
	flgC	Basal body rod		0.30	-1.57
	flgD	Hook cap scaffold		-0.51	-1.58
	flgE	Hook	0.17		-1.93
	flgF	Basal body rod	0.19		-2.55
	flgG	Basal body rod	0.14		-2.24
	flgH	Rod, L-ring		-1.22	-1.47
	flgI	Rod, P-ring		-0.98	n/a
	flgJ	Scaffold protein		-0.44	-2.01
	flgK	Hook-filament joint		-1.45	-0.96
	fliC	Flagellin	0.05		-1.75
	fleL	Filament length control	0.03		n/a
	fliD	Cap, mucin adhesion		-1.96	-0.67
	fliS	Filament elongation	n/a		n/a
	fleP	Type IV pili length	n/a		n/a
	fleQ	c-di-GMP responsive transcriptional activator, major flagellar gene regulator, represses *pel* genes		-0.66	-0.75
	fleS	HK flagellar synthesis, mucin adhesion		-1.1	-0.53
	fleR	RR, flagellar synthesis mucin adhesion		-0.97	-2.1
	fliE	Basal body component, MS ring/rod adapter	n/a		n/a
	fliF	Basal body MS ring, mounting plate for motor/switch		-1.15	-0.58
	fliG	Motor/switch, rotor component		-1.37	-2.55
	fliH	Negative regulator of fliI		-0.37	-0.22
	fliI	ATPase		-0.22	-1.51
	fliJ	Chaperone, hook protein export	0.12		-2

Table 5-2 Cyanogenesis of flagella-related mutants. Genes are organised by operon.

		fliK	Hook length control		-0.35	n/a
Region 2		*fliL*	Unknown		-0.30	n/a
		fliM	Motor/switch	0.18		-2.06
		fliN	Motor/switch	-0.26		-1.88
		fliO	Flagellar export	n/a		n/a
		fliP	Flagellar export		-0.98	-2.27
		fliQ	Flagellar export		-1.25	-1.78
		fliR	Flagellar export	n/a		n/a
		flhB	Flagellar export	**0.64**		-2.1
		flhA	Flagellar export		-1.43	-0.2
		flhF	Polar flagellar site determination		-1.24	-1.74
		fleN	Flagellar number regulation		-0.07	-0.66
		fliA	σ28 sigma factor		-0.55	-0.01
		cheY	Switch regulator	n/a		n/a
		cheZ	cheY phosphatase		-1.34	-1.3
		cheA	cheY and cheB kinase		-0.60	n/a
		cheB	Chemoreceptor methyltransferase	n/a		n/a
		motA	Motor rotation		-0.77	-0.88
		motB	Motor rotation		-2.34	-0.51
		cheW	Positive regulator of cheA		-1.57	n/a
Region 3		*cheV*	**Chemotaxis regulator**		**-1.46**	**n/a**
		cheR	Chemoreceptor methyltransferase		-0.23	n/a
		flgA	P-ring assembly		-1.19	-1.26
		flgM	σ28 sigma factor		-0.15	n/a
		flgN	Initiation of filament assembly	n/a		n/a

Table 5-2 (continued) Cyanogenesis of flagella-related mutants. Genes are organised by operon.

5.4.7 Cyanogenesis of Type IV Pili-Related Mutants

Next, we investigated the cyanogenic ability of mutants defective in the three systems of T4P encoded by *P. aerginosa*: T4Pa, T4Pb and Tad pili.

A preliminary look at the cyanogenesis data of the regulatory genes, *pilZ* and *pilS*, which are essential for T4P biogenenesis, implicated a possible link between cyanogenesis and T4P biology (Figure 5-18, Table 5-3). *pilZ* and *pilS* suffered from cyanogenesis defects of -0.95 and -0.38 log2 FC relative to the plate median, respectively. Surprisingly, the *pilR* mutant present in the library, which is expected to lack T4P, did not give an outlier phenotype.

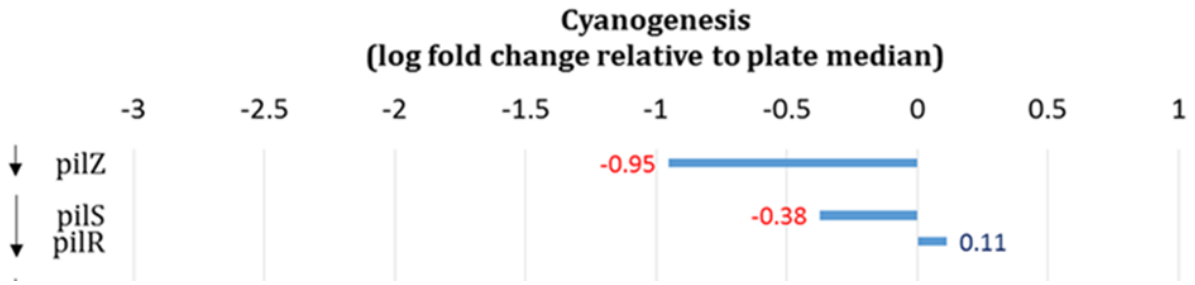


Figure 5-18 Cyanogenesis of mutants with T4P regulatory defects. (n=3 biological replicates) Bar plot of cyanogenesis from whole library screen (log2 transformed fold-change relative to plate median). Flagella-related mutants are organised by operon. Dashed red line = 95% confidence interval.

	Gene	Description	Cyanogenesis (log fc)	
			Screen 1	Screen2
T4P regulation	*pilZ*	T4P control protein, c-di-GMP regulated	-0.95	n/a
	pilS	HK localised to cellular poles, complex regulation of T4P, modulates pilA expression	-0.37	n/a
	pilR	RR, upregulates pilA, even in the absence of pilS	0.11	n/a

Table 5-3 Cyanogenesis of T4P regulatory mutants. Genes are organised by operon

The results for T4Pa-related mutants, which are involved in both twitching motility and adherence to surfaces, were less clear cut than those of the flagella-related mutants (Figure 5-19). While there was a general trend towards a cyanogenesis defect, with 15/25 mutants exhibiting lower cyanogenesis values relative to the plate median, several mutants, specifically *fimU, pilC, pilQ, pilS, pilM* and *pilK*, seemed

unaffected, while *pilC,* a platform protein which interacts with ATPases, and the chemotaxis-related gene, *pilG*, gave cyanide overproducer phenotypes: 0.43 and 0.86 log2 FC relative to the plate median, respectively.

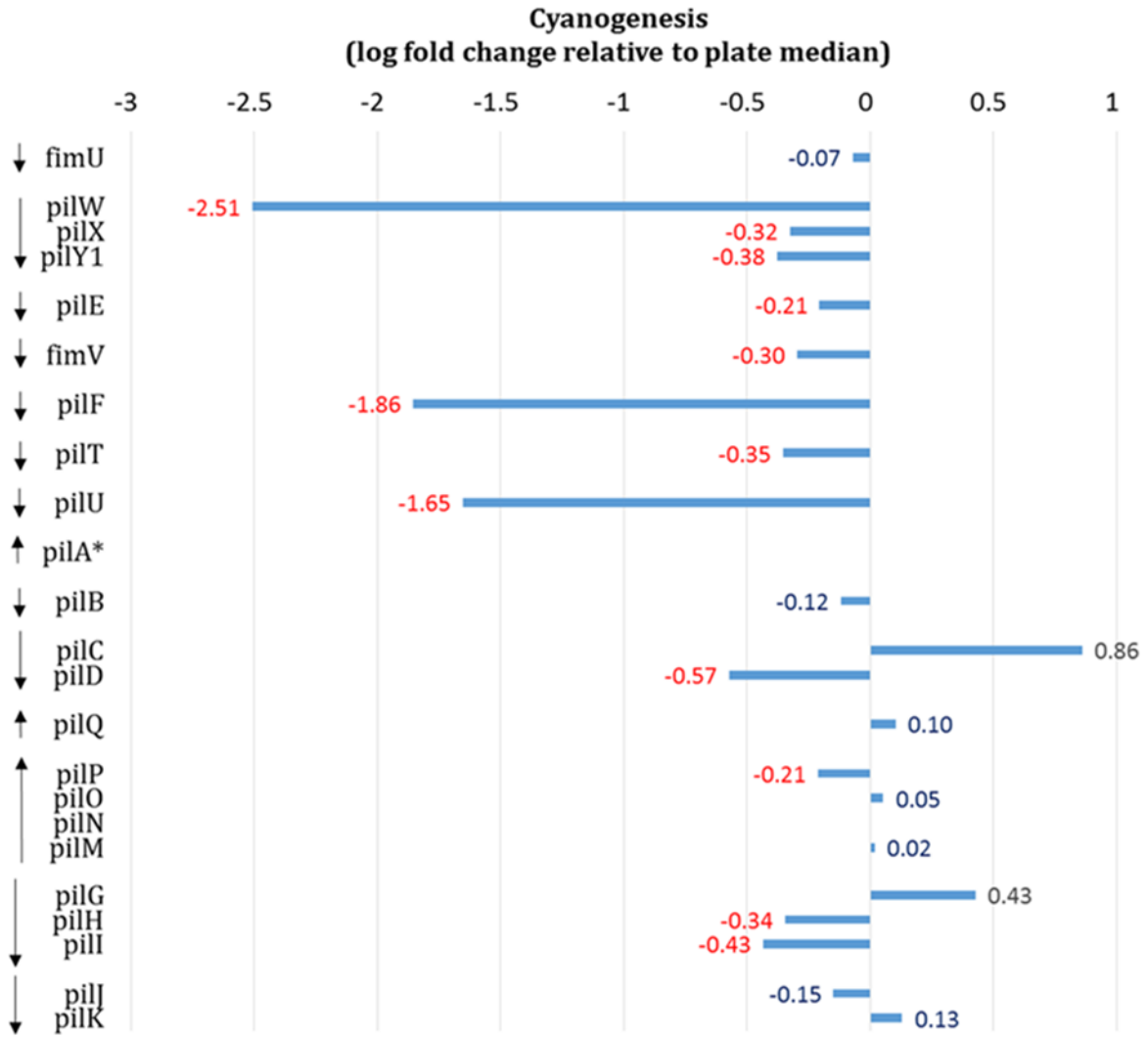


Figure 5-19 Cyanogenesis of mutants with T4Pa regulatory defects. (n=3 biological replicates) Bar plot of cyanogenesis from whole library screen (log2 transformed fold-change relative to plate median). Mutants are organised by operon. * = mutant not in library. Dashed red line = 95% confidence interval.

	Gene	Description	Cyanogenesis (log fc)		
			Screen 1		Screen2
T4Pa structure and function	*fimU*	Minor pilin		- 0.07	n/a
	pilW	Minor pilin, promoter of pilus assembly		-2.5	-2.8
	pilX	Minor pilin		-0.32	n/a
	pilY1	Pilus biogenesis and other functions, c-di-GMP regulated	-0.38		n/a
	pilE	Minor pilin	-0.2		n/a
	fimV	Promotes assembly of secretin	-0.30		-1.39
	pilF	Secretin pilotin, pilQ localisation and oligomerisation		-1.86	-2.24
	pilT	Retraction ATPase		-0.35	n/a
	pilU	Retraction ATPase , pilT paralogue		-1.65	-1.59
	pilA	Major pilin		n/a	n/a
	pilB	Retraction ATPase, energy for assembly and retraction	-0.12		n/a
	pilC	Platform protein, interacts with ATPases	**0.86**		n/a
	pilD	Prepilin peptidase, cleaves T4a and T4b prepilins		-0.57	n/a
	pilQ	Secretin multimerization, channel for pilus assembly	0.1		n/a
	pilP	Type 4a pilus alignment subcomplex	-0.21		n/a
	pilO	Type 4a pilus alignment subcomplex	0.05		n/a
	pilN	Type 4a pilus alignment subcomplex		n/a	n/a
	pilM	Type 4a pilus alignment subcomplex		0.02	n/a
	pilG	cheY-like regulator, regulated by ANR		**0.43**	n/a
	pilH	cheY-like regulator	-0.35		n/a
	pilI	cheW homolog		-0.43	n/a
	pilJ	Methyl accepting chemotaxic protein		-0.15	n/a
	pilK	cheR homolog	0.12		n/a

Table 5-4 Cyanogenesis of T4Pa-related mutants. Genes are organised by operon.

As was observed with the T4Pa mutants, a trend was not immediately apparent with the T4Pb-related mutants, which are not typically involved in motility. The type 4b secretin *pilN2* and the type II secretion

system protein *pilR2* had cyanogenesis values of -0.51 log2 FC and -0.72 log2 FC relative to the plate median.

In contrast, *pilV2*, a minor pilin involved inter-strain transfer, and *pilM2*, a protein of unknown function in the same operon as *pilV2*, were overproducers with cyanogenesis values 0.59 log2 FC and 0.55 log2 FC, respectively. All other T4Pb related genes exhibited normal cyanogenesis phenotypes (Figure 5-20; Table 5-5).

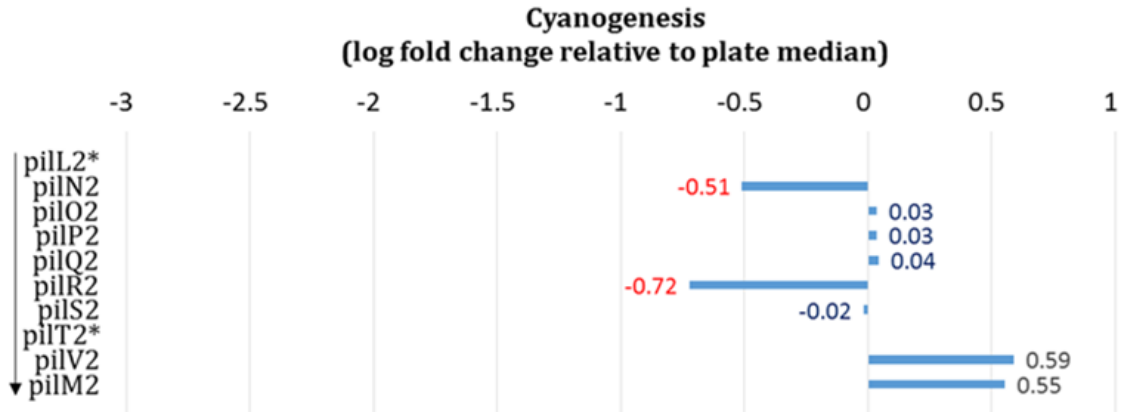


Figure 5-20 Cyanogenesis of T4Pb-related mutants. Bar plot of cyanogenesis from initial screen (log2 transformed fold-change relative to plate median). Mutants are organised by operon. * = mutant not in library. Dashed red line = 95% confidence interval.

	Gene	Description	Cyanogenesis (log fc)		
				Screen 1	Screen 2
T4Pb structure and function	*pilL2*	Motor/switch, rotor component, lipoprotein		n/a	n/a
	pilN2	Type 4b secretin		-0.51	n/a
	pilO2	Type 4b accessory protein		0.03	n/a
	pilP2	Type 4b pilus assembly protein	0.03		n/a
	pilQ2	Type 4b ATPase		0.04	n/a
	pilR2	Type 4b type II secretion system protein		-0.72	n/a
	pilS2	Type 4b major pilin, required for interstrain transfer	-0.02		n/a
	pilT2	Type 4b ATPase	n/a		n/a
	pilV2	Type 4b minor pilin, required for interstrain genetic transfer	**0.59**		n/a
	pilM2	Inner membrane protein, unknown function		**0.55**	n/a

Table 5-5 Cyanogenesis of T4Pb-related mutants. Genes are organised by operon.

Interestingly, in the case of Tad pili, which are involved in tight adhesion, the regulators *pprB*, and *pprA*, as well as the prepilin, *fppA*, had strong overproducer phenotypes, with cyanogenesis values of 0.7, 0.46 and 0.89 log2 FC relative to the plate median (Figure 5-21; Table 5-6). Other mutants with less severe but still overproducing phenotypes were the ATPase TadA, TadG and the minor pilin TadF. In addition, during the rescreen, the secretin *rcpA* and the pilotin TadD, exhibited strong overproducer phenotypes, of 0.55 and 0.59 log2 FC relative to the plate wildtype, respectively. Overall, the high proportion of overproducers and the absence of strong underproducers among mutants of this type of pilus was in contrast to the results seen in the other T4P systems, suggesting, at least preliminarily, a differential effect of T4Pb Tad pili mutation on cyanogenesis compared to other T4P expressed by *P. aeruginosa*.

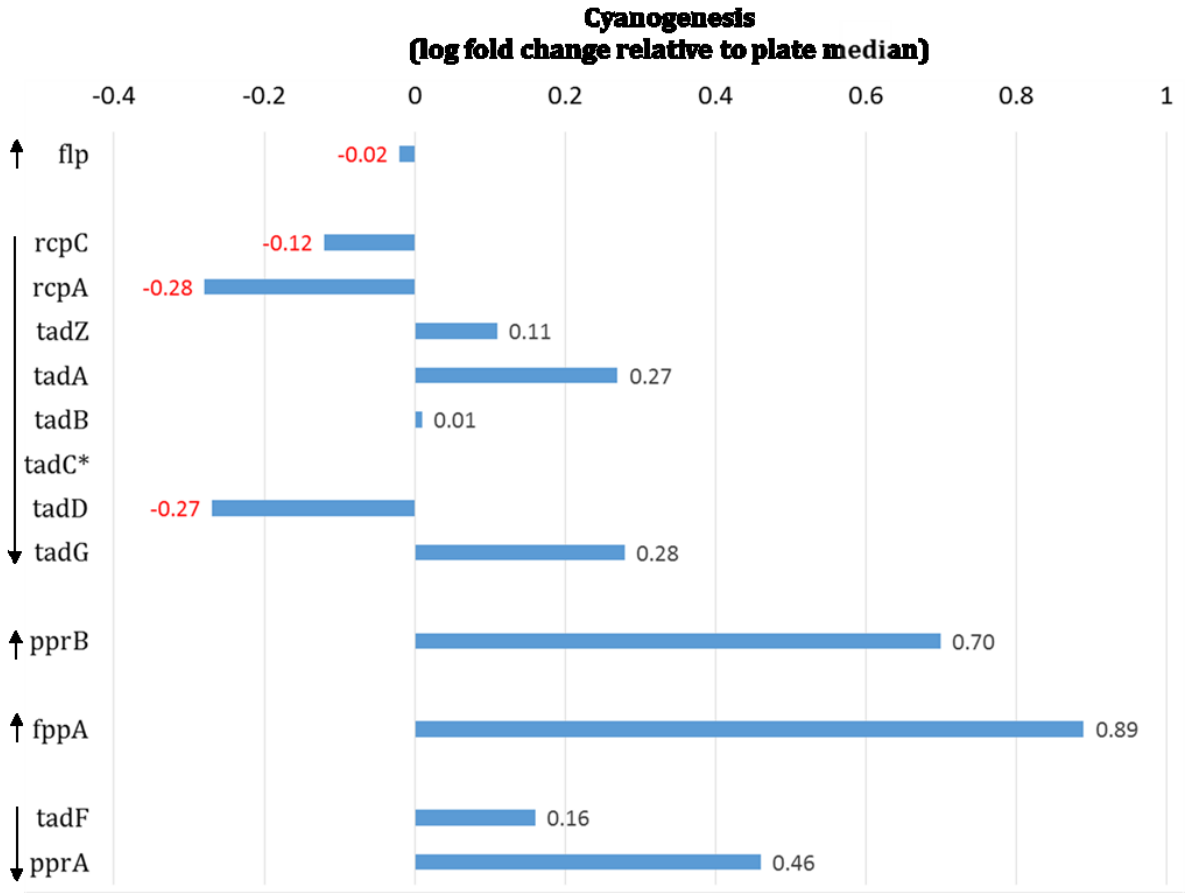


Figure 5-21 Cyanogenesis of T4Pb Tad -related mutants. Bar plot of cyanogenesis from whole library screen (log2 transformed fold-change relative to plate median). Mutants are organised by operon. * = mutant not in library. Dashed red line = 95% confidence interval.

	Gene	Description	Cyanogenesis (log fc)	
			Screen 1	Screen2
T4Pb *Tad* structure and function	*Flp*	Pilin	-0.02	n/a
	rcpC	Unknown, no homolog	-0.12	n/a
	rcpA	Secretin	-0.28	**0.55**
	TadZ	Unknown, no homolog	0.11	n/a
	TadA	ATPase	**0.27**	n/a
	TadB	Platform protein, pilC like	0.01	n/a
	TadC	Platform protein, pilC like	n/a	n/a
	TadD	Pilotin	-0.27	**0.59**
	TadG	Unknown, no homolog	**0.28**	n/a
	pprB	RR, concerted *Tad* gene and *cupE* gene regulation	**0.7**	n/a
	fppA	Prepilin peptidase	**0.89**	**0.83**
	TadF	Minor pilin	**0.16**	n/a
	pprA	HK, concerted *Tad* gene and *cupE* gene regulation	**0.46**	n/a

Table 5-6 Cyanogenesis of T4Pb-Tad mutants. Genes are organised by operon.

5.4.8 Cyanogenesis of Cup-related Mutants

In addition to the flagellum and T4P, *P. aeruginosa* also possesses extracellular appendages known as Cup pili, organised into the CupA, CupB, CupC, CupD, and CupE pathways. While little is known about the role of these specialised pili, current evidence points towards a role in biofilm formation and organisation. Among the Cup genes, the following genes were cyanide underproducers based on log2 FC relative to their plate median: usher protein *cupA3*, -0.59 log2 FC, the adhesin *cupB5*, -0.29 log2 FC, the usher protein, *cupC3*, -0.55 log2 FC, the pilin *cupD1*, -2.06 log2 FC, and the fimbrial-like subunit *cupE1*, -0.57 log2 FC. In contrast, the chaperone *cupB2* had an overproducer phenotype, with a cyanogenesis value 0.76 log2 FC relative to the plate median (Figure 5-22). These results do not implicate a role for specific Cup fimbrial pathways in cyanogenesis. However, the presence of severe outliers does suggests a certain level of involvement.

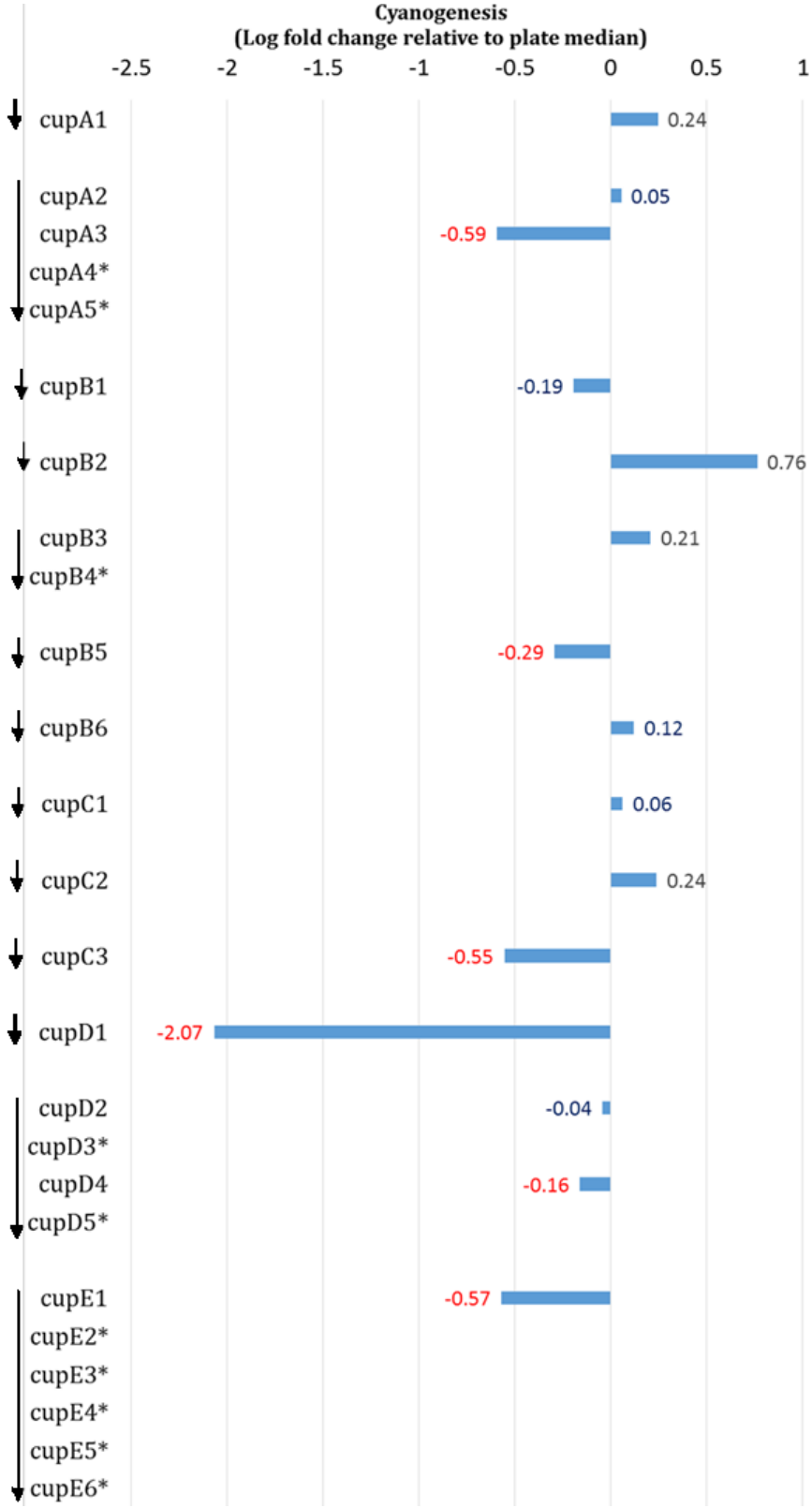


Figure 5-22 Cyanogenesis of Cup fimbrae-related mutants. Bar plot of cyanogenesis from whole library screen (log2 transformed fold-change relative to plate median). Mutants are organised by operon. * = mutant not in library. Dashed red line = 95% confidence interval.

	Gene	Description	Cyanogenesis (log fc)	
			Screen 1	Screen2
cupA	*cupA1*	Pilin	0.24	n/a
	cupA2	Pilus assembly chaperone	0.05	n/a
	cupA3	Usher protein	-0.59	n/a
	cupA4	Adhesion	n/a	n/a
	cupA5	Pilus assembly chaperone	n/a	n/a
cupB	*cupB1*	Pilin, pilC like	-0.19	n/a
	cupB2	Pilus assembly chaperone	**0.76**	n/a
	cupB3	Usher protein	0.2	n/a
	cupB4	Pilus assembly chaperone	n/a	n/a
	cupB5	Adhesin, TspA-like	-0.29	n/a
	cupB6	Adhesin	0.12	n/a
cupC	*cupC1*	Pilin	0.06	n/a
	cupC2	Pilus assembly chaperone	0.24	n/a
	cupC3	Usher protein	-0.55	n/a
cupD	*cupD1*	Pilin	-2.06	n/a
	cupD2	Pilus assembly chaperone	-0.04	n/a
	cupD3	Adhesion	n/a	n/a
	cupD4	Pilus assembly chaperone	-0.16	n/a
	cupD5	Pilus assembly chaperone	n/a	n/a
cupE	*cupE1*	Fimbrial-like	-0.57	n/a
	cupE2	Fimbrial-like	n/a	n/a
	cupE3	Fimbrial-like	n/a	n/a
	cupE4	Assembly chaperone	n/a	n/a
	cupE5	Usher protein	n/a	n/a
	cupE6	Adhesion-like protein	n/a	n/a

Table 5-7 Cyanogenesis of Cup fimbrae-related mutants. Genes are organised by operon.

5.4.9 Cyanogenesis of Exopolysaccharide-Related Mutants

P. aeruginosa encodes at least three exopolysaccharides involved in different aspects of biofilm formation: Pel, Psl and alginate. Current understanding of *P. aeruginosa*'s attachment strategy suggests that Pel and Psl are involved in the early acute stages of biofilm formation, while alginate can be considered a 'stress response' exopolysaccharide necessary for chronic infection biofilms (Schurr, 2013). PA14 contains a partial deletion of three genes in the *psl* locus, and is therefore incapable of synthesising this polysaccharide (Colvin *et al.*, 2011; Colvin *et al.*, 2012).

As expected, no pronounced cyanide underproduction was observed in genes of the partial *psl* operon encoded by PA14. Nevertheless, the biosynthetic mutants *pslE* and *pslJ* appear to be strong cyanide overproducers. In contrast, transposon insertion into the Pel genes resulted in impaired cyanogenesis: 5/5 of the Pel mutants present in the library were defective (Figure 5-23; Table 5-8).

Genes involved in the mucoid switch, including the alginate biosynthesis operon, provided less easily interpretable results. The majority of alginate biosynthetic genes did not give an obvious phenotype. However, loss of the phosphomannose isomerase, *algA*, did result in a cyanogenesis defect, -0.51 log2 FC. In addition, the alginate o-acetyltransferase mutant, *algI*, was also defective, with a cyanogenesis value of -0.66 log2 FC. In contrast, loss of the glucose 6-dehydrogenase, *algD*, resulted in slight cyanide overproduction, 0.26 log2 FC compared to the plate median.

Loss of a positive regulator of mucoidy, *algW*, should promote a non-mucoid phenotype. *algW* exhibited a cyanide overproduction phenotype, 0.43 log2 FC. An *algU* mutant is expected to be hyper motile, non-mucoid, and severely defective in biofilm formation (Bazir *et al.*, 2010). Based on the results of the whole library screen, *algU* was a cyanide overproducer: 1 log2 FC.

mucD and *mucB*, which are both defective in mucoidy repression, are expected to possess slightly mucoid phenotypes. These mutants were not underproducers. Instead, they produced more cyanide than WT: 1.45 and 0.75 log2 fold change, respectively. This is consistent with a previous finding by Carterson *et al.*, (2004) , who reported that a mucoid *mucB* PAO1 mutant produced 3-fold more cyanide than wildtype.

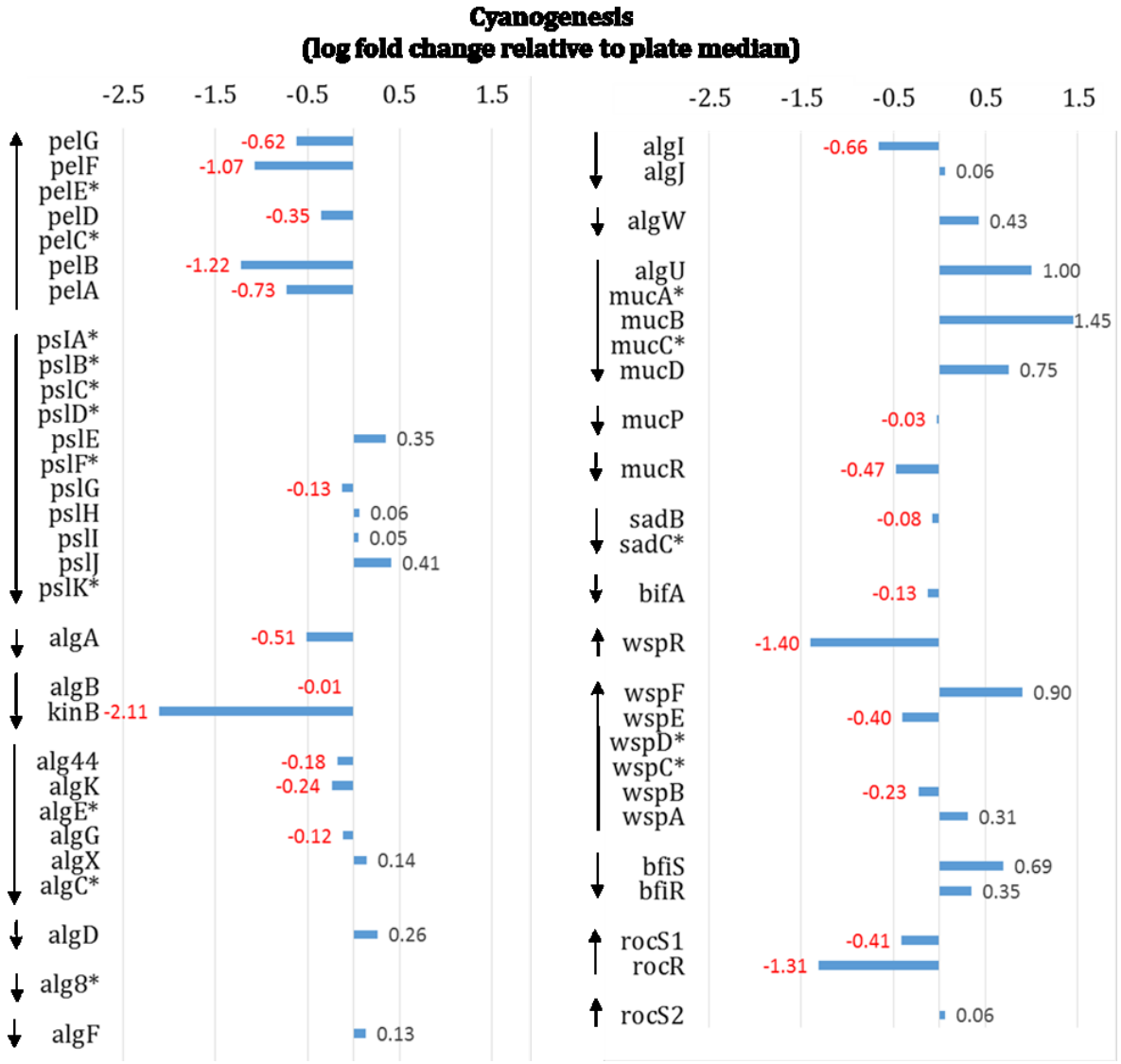


Figure 5-23 Cyanogenesis of exopolysaccharide-related mutants. Bar plot of cyanogenesis from whole library screen (log2 transformed fold-change relative to plate median). Mutants are organised by operon. * = mutant not in library. Dashed red line = 95% confidence interval.

	Gene	Description	Cyanogenesis (log fc)		
			Screen 1		Screen2
Pel genes	*pelG*	Transmembrane protein		-0.62	n/a
	pelF	Glycosyltransferase		-1.07	-1.65
	pelE	Sucrose synthase		n/a	n/a
	pelD	Transmembrane protein, c-di-GMP receptor	-0.35		n/a
	pelC	Glycosyltransferase	n/a		n/a
	pelB	Outer membrane protein	-1.22		-0.51
	pelA	Oligogalacturonide lyase		-0.73	n/a
Psl genes	*pslE*	Exopolysaccharide synthesis		**0.35**	n/a
	pslF	Glycosyltransferase		n/a	n/a
	pslG	Beta-xyloxidase		-0.13	n/a
	pslH	Glycosyltransferase	0.06		n/a
	pslI	Glycosyltransferase	0.05		n/a
	pslJ	Exopolysaccharide synthesis		**0.41**	n/a
	pslK	Exopolysaccharide synthesis	n/a		n/a
Alginate genes/Mucoid switch	*algA*	Phosphomannose isomerase	-0.51		n/a
	algB	RR, negatively controls Alginate through AlgW, mucA proteolysis		-0.01	n/a
	kinB	HK, negatively controls Alginate through AlgW, mucA proteolysis		-2.11	-1.64
	alg44	Alginate polymersization, c-di-GMP receptor		-0.18	n/a
	algK	Alginate biosynthesis precursor		-0.24	n/a
	algE	Alginate biosynthesis precursor	n/a		n/a
	algG	Alginate-c5-mannuronan-epimerase		-0.12	n/a
	algX	Alginate biosynthesis precursor		0.14	n/a
	algC	Phosphomannomutase	n/a		n/a

Table 5-8 Cyanogenesis of exopolysaccharide-related mutants. Genes are organised by operon.

Alginate genes/mucoid switch	*algD*	Glucose 6-dehydrogenase	**0.26**		n/a
	alg8	Glycosyltransferase	n/a		n/a
	algF	Alginate o-acetyltransferase		0.13	n/a
	algI	Alginate o-acetyltransferase		-0.66	n/a
	algJ	Alginate o-acetyltransferase	0.06		n/a
	algW	Cleaves MucA, regulated by MucB binding to MucA	**0.43**		n/a
	algU	Sigma factor, negatively regulates flagellar cell motility, positively regulates Alginate production		**1**	n/a
	mucA	Anti-sigma factor to AlgU, role in osmotic stress tolerance		n/a	n/a
	mucB	Negative regulator of AlgU		**1.45**	**0.87**
	mucC	Positive regulator of Alginate synthesis		n/a	n/a
	mucD	Activates mucA degradation via mucP	**0.75**		n/a
	mucP	Negative regulator of mucA via proteolysis		-0.03	n/a

Table 5-8 (continued) Cyanogenesis of exopolysaccharide-related mutants. Genes are organised by operon.

The two-component sensor and phosphatase KinB has been put forward as a mediator of the switch from acute to chronic virulence. KinB is essential for full *P. aeruginosa* virulence in zebra fish embryo and murine acute pneumonia infection models (Clatworthy *et al.*, 2009; Damron *et al.*, 2012). The way in which KinB is hypothesised to regulate virulence is to act as phosphatase that dephosphorylates AlgB and relieves phosphorylated AlgB's repression of acute virulence (Figure 5-24). Concordantly, in our study the *kinB* mutant was associated with a severe cyanogenesis defect of -2.11 log2 FC in the first screen, and -1.64 log2 FC in the re-screen. In addition, in accordance with previous data from Chand *et al.* (2012), in our screen an *algB* mutant did not appear to be impaired in virulence, and instead exhibited normal levels of cyanogenesis relative to the plate median.

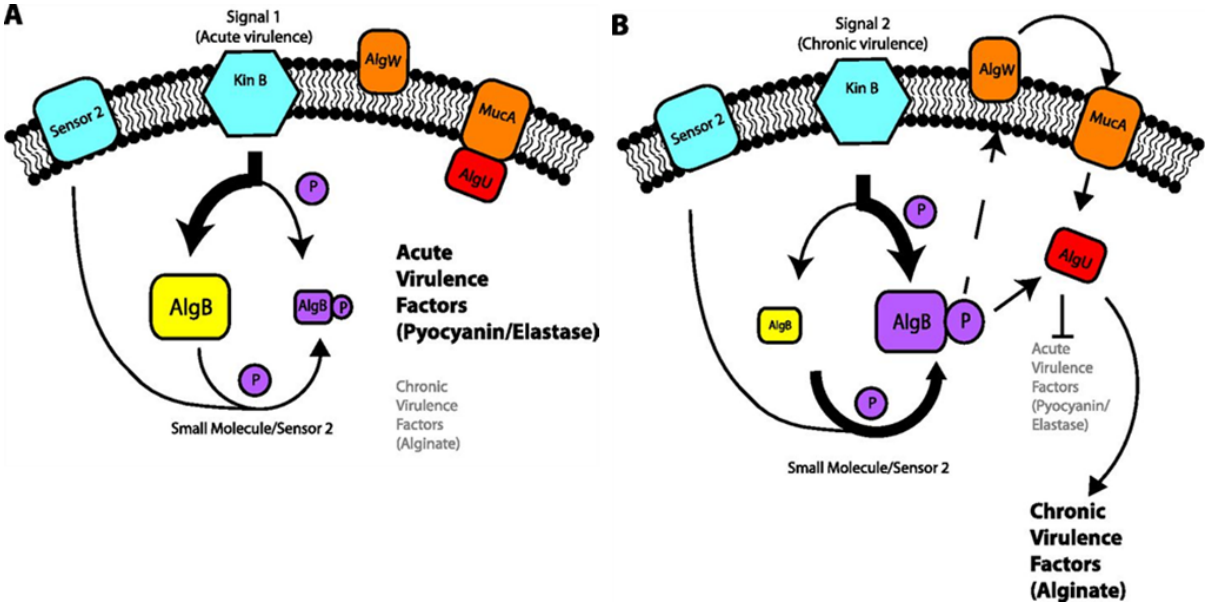


Figure 5-24 Model of KinB's role in the regulation of virulence (Chand *et al.*, 2012). KinB is a phosphatase and its activation of acute virulence relies on its phosphatase activity. Phosphorylated AlgB is a repressor of acute virulence, and KinB's main role in promoting acute virulence is to dephosphorylate AlgB.

5.4.10 Cyanogenesis of c-di-GMP regulators

c-di-GMP is an intracellular signalling molecule broadly conserved across many bacterial species (Lory *et al.*, 2009). Levels of c-di-GMP are regulated by diguanylate cyclases, which synthesise c-di-GMP from guanosine triphosphate (GTP), and phosphodiesterases, which degrade c-di-GMP. These enzymes possess domains that can sense diverse environmental signals including light, oxygen and nutrients, and are thought to modulate intracellular c-di-GMP concentrations accordingly. Over thirty genes encode diguanylate cyclases and phosphodiesterases in the *P. aeruginosa* genome. There has been speculation that sequestered local pools of c-di-GMP may be regulated by distinct diguanylate cyclases and phosphodiesterases (Giraud & de Bentzmann, 2012) .

The current paradigm is that c-di-GMP acts to stimulate various biofilm-related functions (Hengge, 2009). For example elevated levels of c-di-GMP were generally observed to promote biofilm formation, by upregulating the production of exopolysaccharides, and inhibit motility, by repressing flagellar biosynthesis (Hickman & Harwood, 2008; Baraquet *et al.*, 2012) Irie *et al.*, (2012) showed that two *P. aeruginosa* diaguanylate cyclases, SadC and SiaD, detect and are activated by the presence of the self-produced exopolysaccharide, Psl. Since elevated c-di-GMP promotes the production of

exopolysaccharide, including Psl, this regulatory circuit can be considered a feed-forward loop that, following biofilm formation initiation, favours the commitment of *P. aeruginosa* to a sessile lifestyle.

Figure 5-25 and Table 5-10 present cyanide screen data of *P. aeruginosa* c-di-GMP modulators which may be involved in regulating this switch. Interestingly, mutants in the diguanylate cyclase genes *mucR, roeA, sadC* and *siaD*, which are expected to possess reduced local pools of c-di-GMP, exhibited cyanogenesis impairments, of -0.47 log2 FC, -0.83 log2 FC, -0.81 log2 FC and -0.26 log2 FC, respectively.

TpbA is a tyrosine phosphatase which negatively regulates the diguanylate cyclase TpbB, and the local pool of c-di-GMP produced by TpbB is therefore expected to be elevated in the tpbA mutant. Ueda & Wood, (2010) reported that a *tpbA* mutant exhibited 150-fold increase in biofilm formation *via* increased production of c-di-GMP. In our screen, *tpbA* was impaired in cyanogenesis (-0.45 log2 FC).This is in contrast to the trend observed with *mucR, roeA, sadC* and *siaD*. Here, impaired cyanogenesis was associated with an increase rather than decrease in local c-di-GMP.

Altered cyanogenesis was also observed in mutants of the Wsp chemosensory pathway. *wspF* and *wspA* exhibited enhanced cyanogenesis: 0.9 and 0.31 log2 FC relative to the plate median, respectively. In contrast, *wspE* and *wspB* were impaired in cyanogenesis, with values of -0.4 and -0.23 log2 FC. This is surprising, since *wspA*, *wspB* and *wspE* would be expected to have similar phenotypes due to their roles in wspR activation. The cyanogenic phenotype of *wspR* was not consistent between the first screen, where it was a severe underproducer, -1.4 log2 FC, and the rescreen, where it was a sever overproducer, 0.65 log2 FC relative to wildtype. This inconsistency was also observed with the response regulator and phosphodiesterase *rocR*. Both *rocR* and *rocS1* exhibited impaired cyanogenesis of -1.31 and -0.41 log2 FC in the first screen. However, in the rescreen, *rocR* was a strong cyanide overproducer, exhibiting 0.71 log2 FC relative to the wildtype.

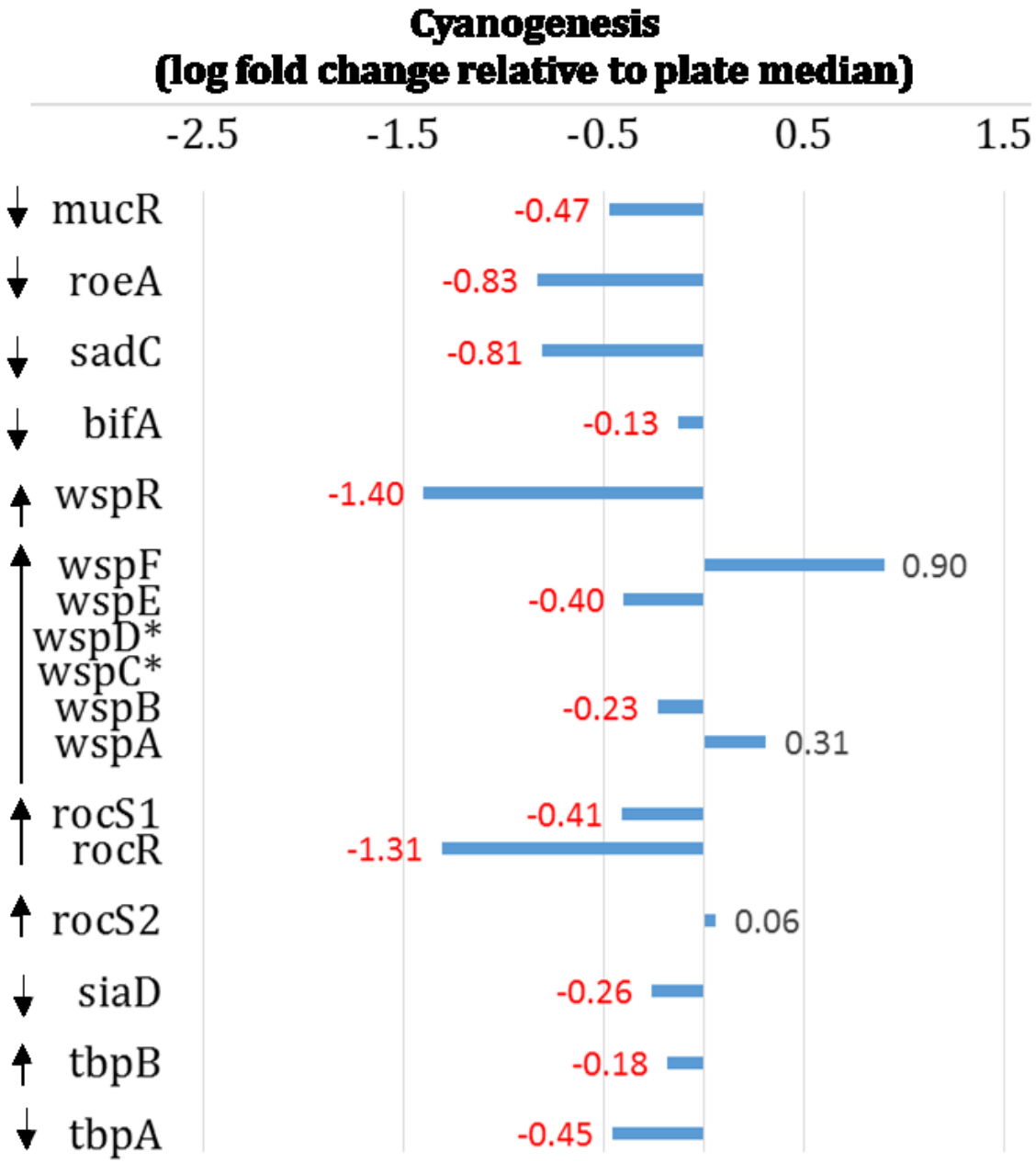


Figure 5-25 Cyanogenesis of c-di-GMP related mutants. Bar plot of cyanogenesis from whole library screen (log2 transformed fold-change relative to plate median). Mutants are organised by operon. * = mutant not in library. Dashed red line = 95% confidence interval.

	Gene	Description	Cyanogenesis (log fc)		
			Screen 1		Screen2
c-di-GMP modulators	*mucR*	c-di-GMP-synthesizing, membrane-associated negative regulator of *fliC*		-0.47	n/a
	roeA	c-di-GMP-synthesizing, present throughout the cell		-0.82	n/a
	sadC	c-di-GMP-synthesizing, localised to cell periphery		-0.8	n/a
	bifA	c-di-GMP degrading, inner membrane		-0.13	n/a
	wspR	c-di-GMP synthesizing when phosphorylated	-1.40		**0.65**
	wspF	Methyltransferase, regulates WspA methylation, negative regulator or WspR	**0.9**		n/a
	wspE	Kinase, phosphorylates WspR	-0.4		n/a
	wspD	Scaffolding protein, connects WspA to WspE		n/a	n/a
	wspC	Methyltransferase, regulates WspA methylation, positive regulator of WspR		n/a	n/a
	wspB	Scaffolding protein, connects WspA to WspE		-0.23	n/a
	wspA	Outer membrane sensor		**0.31**	n/a
	rocS1	Regulates cupC gene expression	-0.41		n/a
	rocR	c-di-GMP degrading, regulates cupC gene expression	-1.41		**0.71**
	rocS2	Regulates cupC gene expression		0.06	n/a
	siaD	c-di-GMP synthesizing, upregulates cupA fimbrae	-0.26		n/a
	tbpA	Tyrosine phosphatase, negatively regulates *tbpB*	-0.45		n/a
	tbpB	c-di-GMP synthesizing	-0.18		n/a

Table 5-9 Cyanogenesis of c-di-GMP related mutants. Genes are organised by operon.

5.4.11 Involvement of the RoxSR system in the regulation of cyanogenesis

Terminal oxidases are employed differentially by *P. aeruginosa* to respond to variations in environmental conditions, such as changes in oxygen availability. The redox responsive transcriptional regulators ANR and RoxSR control the timing of expression of terminal oxidases (Figure 1-8).

Interestingly, results of the cyanide screen, summarised in Figure 5-26 and Table 5-10 indicate that the *roxR* (-1.3 log2 FC) and *roxS* (-1.61 log2 FC) mutants are highly impaired in cyanogenesis. Anr, which is known to directly upregulate *hcnABC* genes, is also an underproducer (-0.6 log2 FC). Mutants in 2/3 Cbb3-1 genes (*ccoP1*, -1.17 log2 FC; *ccoQ1*, -0.73 log2 FC), and 2/3 Cbb3-2 genes (*ccoP2*, -0.32 log2 FC; *ccoQ2*, -0.73 log2 FC), were also found to be defective. Consistent with this, mutants in cytochrome BC, which provide electrons to the two cbb3 oxidases, were also severely affected (cytochrome C1, -2.59 log2 FC; cytochrome B, -1.31 log2 FC; cytochrome C, -1.3 log2 FC). In addition, 4/5 mutants in PA1551-7, which are putative cbb3 assembly factors located upstream of the Cbb3-1 genes, exhibited severely impaired cyanogenesis (PA1547, -1.74 log2 FC; PA1548, -1.23 log2 FC; PA1549, -0.67 log2 FC and PA1551, -0.91 log2 FC). In the case of the CIO, the *cioA* mutant was an underproducer, with cyanogenesis values -0.59 log2 FC, while the *cioB* mutant had a cyanogenesis value in the normal range, 0.15 log2 FC.

Considered together, these results suggest that disruption to parts of the RoxSR system results not only, as previously described, in altered CIO regulation, but also in altered cyanogenic output.

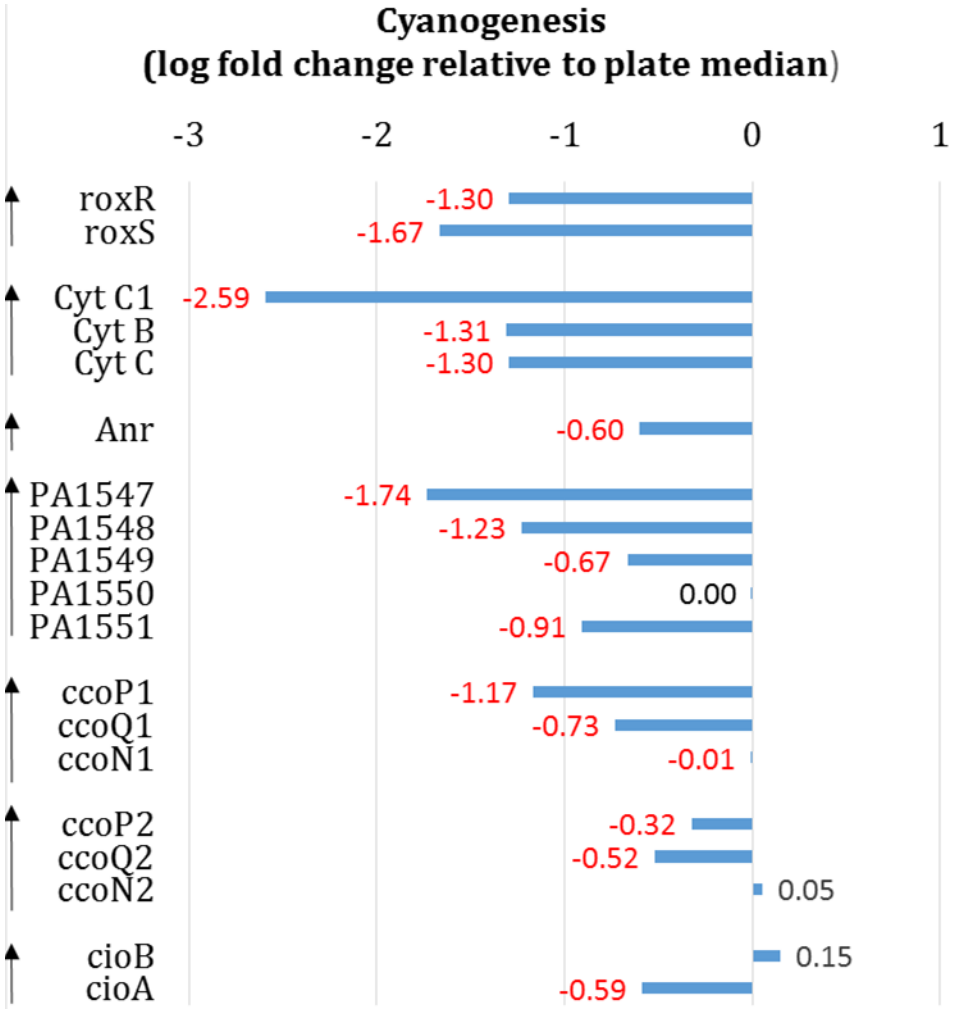


Figure 5-26 Cyanogenesis of mutants related to the RoxSR regulon. Bar plot of cyanogenesis from whole library screen (log2 transformed fold-change relative to plate median). Mutants are organised by operon. * = mutant not in library. Dashed red line = 95% confidence interval.

	Gene	Description	Cyanogenesis (log fc)	
			Screen 1	Screen2
RoxSR	*roxS*	Two-component sensor	-1.30	-4.1
	roxR	Two component response regulator	-1.67	-0.83
Cyt	*CytC1*	Cytochrome C1	-2.59	-1.75
	CytB	Cytochrome B	-1.31	n/a
	CytC	Cytochrome C	-1.30	-0.98
Anr	*Anr*	Anaerobic regulator	-0.6	n/a
Cbb3-1 assembly	*PA1547*	Unknown	-1.74	-0.69
	PA1548	ccoS homolog	-1.23	-0.48
	PA1549	ccoI homolog	-0.67	-0.53
	PA1550	ccoH homolog, ATPase	0.0	n/a
	PA1551	Ferredoxin, ccoS homolog	-0.91	n/a
Cbb3-1	*ccoP1*	Cbb3-1 subunit III	-1.17	-0.48
	ccoQ1	Cbb3-1 subunit II	-0.73	n/a
	ccoN1	Cbb3-1 subunit I	-0.01	n/a
Cbb3-2	*ccoP2*	Cbb3-2 subunit III	-0.32	n/a
	ccoQ2	Cbb3-2 subunit II	-0.52	n/a
	ccoN2	Cbb3-2 subunit I	-0.02	n/a
CIO	*cioB*	Cyanide-insensitive terminal oxidase subunit	0.15	n/a
	cioA	Cyanide-insensitive terminal oxidase subunit	-0.59	n/a

Table 5-10 Cyanogenesis of mutants related to the roxSR regulon. Genes are organised by operon.

5.4.12 Additional Regulators and Virulence Factors

Interestingly, although a link was not immediately apparent, upon further analysis several of the remaining outliers from the rescreen's top 250 underproducer/top 150 overproducer list could be related to the motile-sessile switch (Figure 5-27; Table 5-11).

For instance, PA3804 (-1.46 log2 FC) is a putative transcriptional regulator located upstream of the secretin pilotin pilF, involved in T4P biogenesis. Similarly, the severe underproducer tonB3 (-1.86 log2 FC) can be linked to T4P secretion or transport, as it was found to be required for pilus assembly and normal twitching motility (Huang *et al.*, 2004). Additionally, another cyanide underproducer, the FabF1 mutant, a putative acyl carrier, has previously been reported to be defective in all modes of motility (-1.18 log2 FC).

PA0633 (-1.06 log2 FC) was identified by Yeung *et al.*, (2009) as being required for swarming. The same study also reported complete loss of swarming motility in a mutant of the LysR family transcriptional regulator involved in d-arginine catabolism, gbuR (-1.58 log2 FC). Yeung *et al.* also reported an as yet unresolved link between C4-dicarboxylate transport and twitching motility. PA2571, a sensor kinase regulatating C4-dicarboxylate transport, was found to be defective in twitching. Interestingly, in our screen PA2571 (1.38 log2 FC) was a cyanide overproducer, while PA4616 (-1.24 log2 FC), a C4-dicarboxylate binding protein, was defective in cyanogenesis, suggesting that C4-dicarboxylate sensing can be linked to both motility and cyanogenesis.

One of the most striking cyanide overproducers, sagS (1.44 log2 FC), a probable sensor/response regulator hybrid, has been reported to modulate the timing of the motile-sessile switch *via* interactions with the GacA/sRNA/RsmA systems. In a previous study, a sagS mutant produced biofilms earlier than WT (Petrova & Sauer, 2011). However, these biofilms lacked complex architecture, leading the authors to suggest that sagS is also necessary for long-term attachment and for the maintenance of mature biofilms. In addition, inactivation of sagS resulted in a hypervirulent phenotype in A. thaliana. This is consistent with our finding that sagS is a cyanide overproducer. It is also in agreement with a previous study by Blom *et al.*, (2011) , which determined that cyanide was the major *P. aeruginosa* virulence factor responsible for volatile killing in the A. thaliana model.

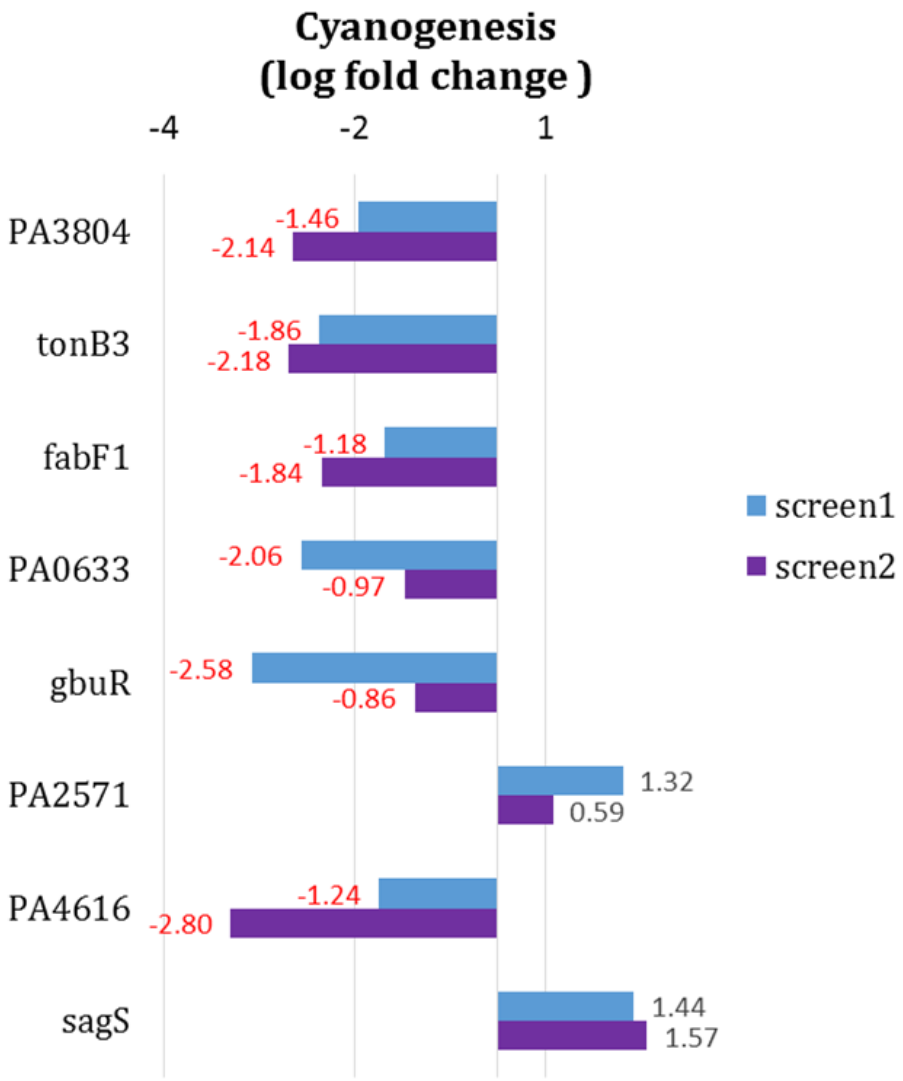


Figure 5-27 Cyanogenesis of additional mutants related to the motile-sessile switch. A number of the remaining outliers from the rescreen's top 250 underproducer/top 150 overproducer list also possessed links to the motile-sessile switch. Bar plot of cyanogenesis from whole library screen (blue, log2 transformed fold-change relative to plate median) and rescreen (purple, log2 transformed fold-change relative to plate WT).

Gene	Description	Phenotype	Reference	Cyanogenesis	
				Screen 1	Screen2
PA3804	Predicted transcriptional regulator, located next to *pilF*	Unknown	*Pseudomonas* database	-1.46	-2.14
tonB3	Transport protein, necessary for pilus assembly	Absence of surface pili	(Huang *et al.*, 2004)	-1.86	-2.18
fabF1	3-oxoacyl-[acyl-carrier-protein] synthase 2	Intact flagella, non-motile	(Zhang *et al.*, 2002)	-1.18	-1.84
PA0633	Hypothetical protein	No swarming	(Yeung *et al.*, 2009)	-2.06	-0.97
GbuR	LysR regulator	No swarming	(Yeung *et al.*, 2009)	-2.58	-0.86
PA2571	Sensor, C4-dicarboxylate transport	Moderate twitching defect	(Yeung *et al.*, 2009)	**1.38**	**0.59**
PA4616	C4-dicarboxylate binding protein	Upregulated by triclosan	(Chuanchuen & Schweizer, 2012)	-1.24	-2.8
SagS	Sensor/response regulator hybrid	Biofilm defect, hypervirulent	(Petrova & Sauer, 2011)	**1.44**	**1.57**

Table 5-11 Cyanogenesis of additional mutants related to the motile-sessile switch. A number of the remaining outliers from the rescreen's top 250 underproducer/top 150 overproducer list also possessed links to the motile-sessile switch.

Figure 5-28 present cyanogenesis data for other mutants of interest uncovered by both screens. These include the regulators EnvZ (1.45 log2 FC), an osmolarity sensor, Lon protease (-1.80 log2 FC), a negative regulator of type III secretion, DksA2 (-1.68 log2 FC), a transcription factor, PqsE (-1.44 log2 FC), a regulator which is thought to act independently of PqsR, and VqsR (-1.55 log2 FC), a global regulator of QS and virulence. In addition, other severe cyanogenesis outlier genes include the hibernation factor PA4463 (-1.34 log2 FC), the nucleotide biosynthetic genes, purN (-2.01 log2 FC) and pyrD (-2.47 log2 FC), and PA3958 (-1.33 log2 FC), which is directly regulated by RsmA. The two regulators indentified in the previous chapter, PA2196 (-1.77 log2 FC) and PA5339 (-1.72 log2 FC), were also amongst the most severe outliers recovered from the whole library screen and the rescreen.

A list of other genes of interest for which a cyanogenic defect was observed in both screens can be found in Appendices, where they have been ranked by severity.

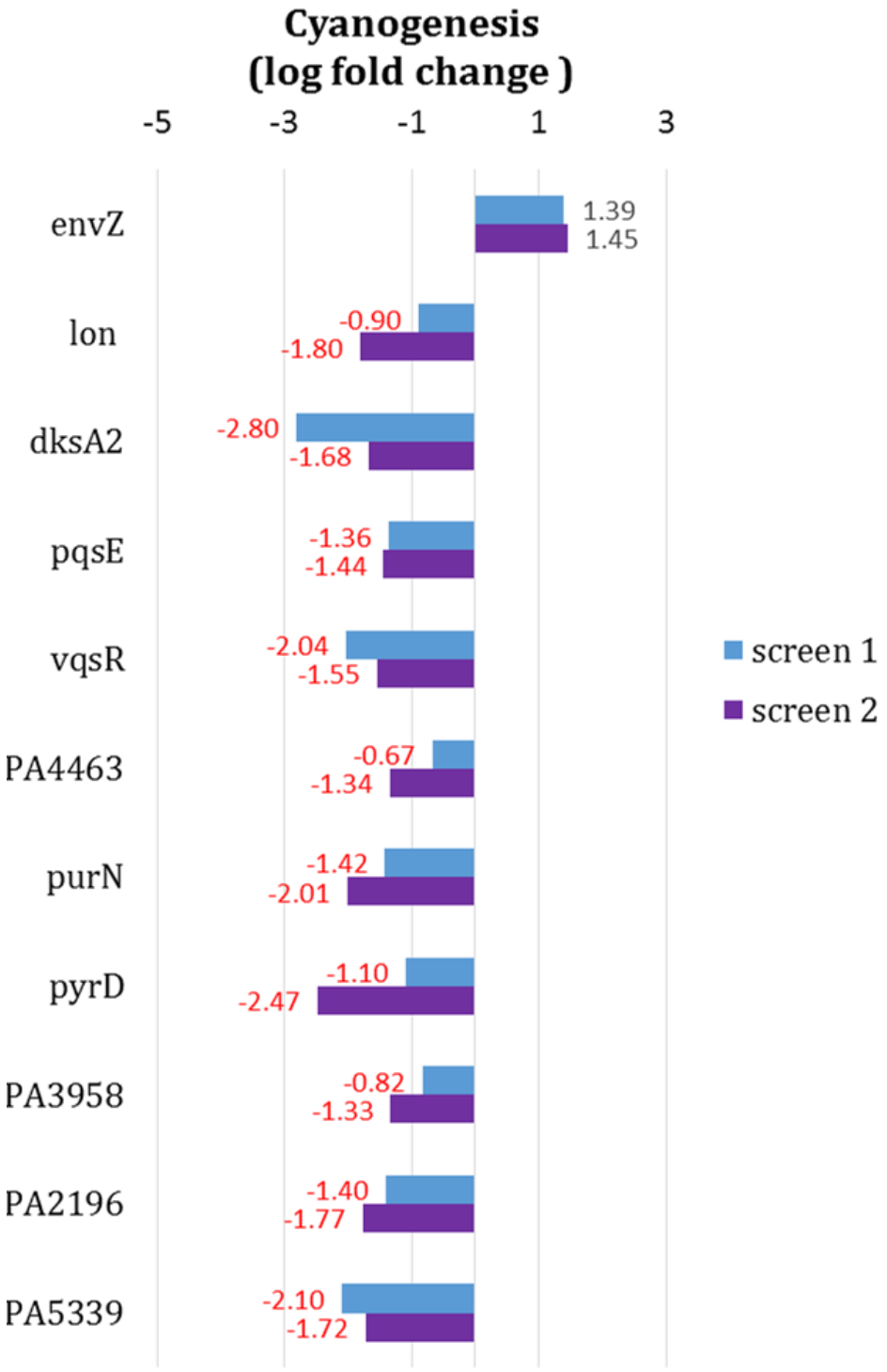


Figure 5-28 Cyanogenesis of additional severe outliers identified in both screens. Bar plot of cyanogenesis from whole library screen (blue, log2 transformed fold-change relative to plate median) and rescreen (purple, log2 transformed fold-change relative to plate WT).

Gene	Description	Phenotype	Reference	Cyanogenesis	
				Screen 1	Screen2
envZ	Osmolarity sensor/kinase	Abberant porin expression	(Chand & Hung, 2011)	**1.45**	**1.39**
lon protease	Negative regulator of type III secretion	Impaired biofilm formation	(Marr *et al.*, 2007)	-1.80	-0.89
dksA2	Zinc-independent transcriptional regulator, homolog of virulence regulator DksA	Unknown	(Furman *et al.*, 2013) .)	-1.68	-2.8
pqsE	Regulator of QS	No pyocyanin	(Farrow *et al.*, 2008)	-1.44	-1.36
vqsR	Global regulator of virulence	QS defect	(Juhas *et al.*, 2004)	-1.55	-2.03
PA4463	Hibernation factor, biofilm dormancy	mRNA at bottom of biofilm	(Williamson *et al.*, 2012)	-1.34	-0.66
purN	Nucleotide biosynthesis	Swarming defect	(Overhage *et al.*, 2007)	-2.01	-1.42
pyrD	Pyrimidine biosynthesis	Virulence defect, 40% less PYO	(Brichta *et al.*, 2004)	-2.47	-1.1
PA3958	Mutator gene, directly regulated by RsmA	Increased mutation rate	(Wiegand *et al.*, 2008)	-1.38	-0.8
PA2196	TetR regulator, located next to *hcnABC* biosynthetic genes	Unknown	Kim *et al.*, 2013	-1.77	-1.4
PA5339	Endoribonuclease, translational inhibitor	Unknown	Patell *et al.*, 2010	-1.72	-2.1

Table 5-12 Cyanogenesis of additional severe outliers identified in both screens.

5.4.13 Cyanogenesis of Core Biofilm Genes

Patell *et al.*, (2010) compared microarray data from three studies with the aim of identifying a set of core biofilm genes. Table 5-13 presents the cyanogenesis data for core biofilm genes identified in their microarray meta-analysis which also exhibited a cyanide defect in our screen. Among these, PA5339, previously identified in Chapter 4, was the most severe cyanide underproducer. Of particular interest, given the probable involvement of RoxRS, was the co-identification, in our analysis and theirs, of mutants related to the respiratory chain. In particular, the involvement of the orphan CcoN-like gene, PA4133, in cyanogenesis under biofilm conditions, may constitute a promising lead to investigate in future.

Gene	Description	Mikkelsen *et al.* (2009)	Waite *et al.* (2005)	Hentzer *et al.* (2005)	Cyanide Screen
PA5339	Putative endoribonuclease adjacent to spoT	1.5	2.5	1.6	-1.72
BkdA1	Valine catabolism	−2	−3.7	−2.1	-0.80
BkdA2	Valine catabolism	−2.4	−3.2	−2.1	-1.14
PA5148	Iron trafficking, oxidative stress-related	2	1.7	2.3	-0.52
PA0107	Assembly protein. Insertion of copper into subunit I of Aa3	−14.4	−1.8	−2.6	-0.96
PA4133	Orphan ccoN-like gene, similar to catalytic subunit of cbb 3 oxidases	4	2.3	3.2	-0.50
PA0110	Probable cytochrome c oxidase assembly factor	−6.3	−1.6	−2.5	-0.31
PA4131	Putative respiratory complex assembly protein, upregulate 10-fold under low oxygen conditions	3.6	2.3	1.7	0.59
PA0179	Probable chemotaxis response regulator, implicated in flagella-mediated chemotaxis	−5.1	−1.6	−1.4	-0.40
PA0409	PilH, pilus-mediated chemotaxis. Can produce pili and twitch, but displays altered motility pattern.	2.9	2.1	2.5	-0.34
PA0084	Type VI secretion machinery	2.1	1.6	2	0.32

Table 5-13 Core biofilm genes that exhibit a cyanogenesis defect. Genes were previously identified in 3 biofilm microarrays studies performed by Mikkelsen *et al.*, 2009, Waite *et al.*, 2005 and Hentzer *et al.*, 2005.

5.5 Discussion

This chapter aimed to explore the hypothesis that improvements to the screening methodology described in Chapter 4 would lead to the discovery of many additional determinants of cyanogenesis. This was the case. Improvements to the spot quality generated by the assay and the development of a purpose-built script, CyQuant, vastly increased screen coverage, from <50% to 93%.

Importantly, as CyQuant produces numerical values to represent the cyanogenesis of each mutant, this meant that mutants could be quantitatively demonstrated to be outliers, through comparison with each other, with a WT, or using means clustering. The means clustering method identified 3654 putative outliers, which suggests that cyanogenesis is interlinked with a high number of processes and that the WT cyanogenesis state can be easily perturbed.

Genomic mapping of the most severe outliers revealed interesting sub-groupings which lend themselves to testable hypotheses. For example, the over representation of genes among severe outliers related to the motile-sessile switch and to the RoxRS system, implicates a strong role for these processes in cyanogenesis. In addition, the identification of several genes and regulators, for which a previous role in cyanogenesis had not been assigned, puts these forward as candidates for future investigations.

5.5.1 Limitations of the Quantitative Screen

A limitation of the methodology used in this chapter is that while the cyanogenesis values generated by CyQuant provide a quantitative manner of ranking mutants against each other, these values have not been calibrated to correspond [CN-] in μM amounts. This could be achieved by spiking assay wells with known μM amounts of KCN, followed by acidification under safe conditions in order to volatilize HCN and to ensure that all added CN- reacts with the detection paper. CyQuant cyanogenesis values for the spots obtained could then be plotted against known spiked concentrations in order to obtain a calibration curve. This calibration curve could then be used to estimate the amount of volatile cyanide given off by mutants during the screen.

In addition to volatile cyanide, ISE measurements on the supernatants could provide information about [CN-] in solution. Volatile and dissolved [CN-] could then be considered together to provide a ‘total cyanogenesis’ measure for each mutant.

Another limitation of the method is that the assay in its current format produces one spot per mutant, which represents a cumulative measure of cyanogenesis up until a single time point (20 hours). For this reason, it may not be possible to discriminate between different kinetics of cyanogenesis dysregulation. An easily implementable solution would be to obtain four time points per mutant, by removing the cyanide detection papers, and replacing them with new papers, after 10 h, 20 h, 36 h and 48 h (Figure 4-29).

Using this modified methodology, means clustering should allow us to divide the mutants into a greater number of groups. In particular, it could help to distinguish between those mutants that produce no cyanide at all ('mutant G'), those that produce low cyanide ('mutant C'), and those that exhibit low sustained cyanogenesis ('mutant F').

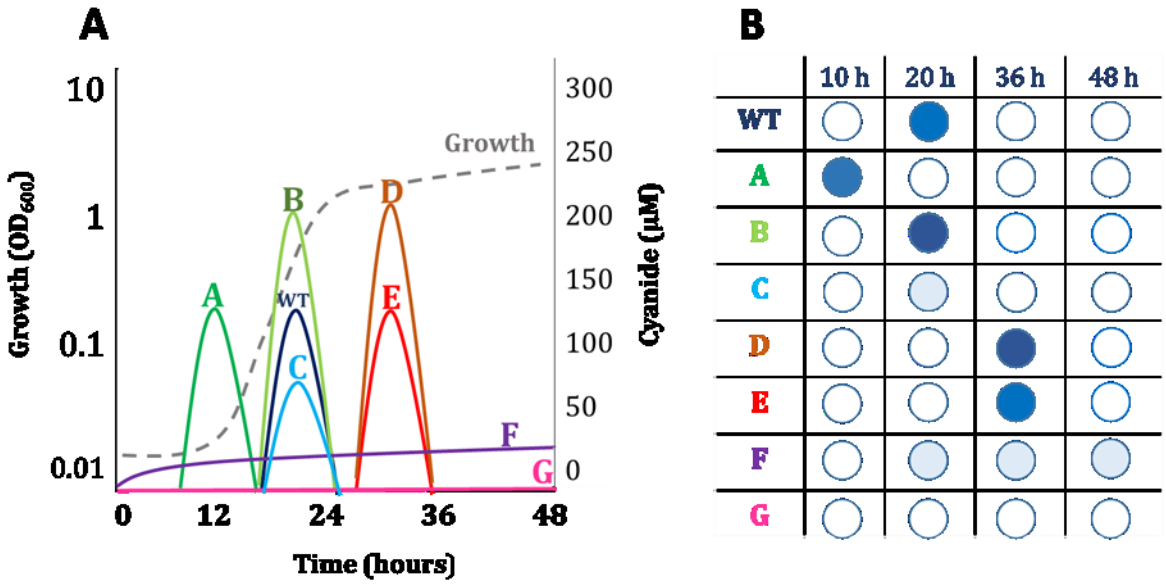


Figure 5-29 Proposed changes to the screen methodology in order to better classify cyanogenesis mutants. A. Illustration of hypothetical cyanogenesis kinetics that could be exerted by different mutants. Dashed line = growth. Solid lines = cyanogenesis. B. Predicted assay output for each hypothetical mutant if cyanide detection papers are removed and replaced with new papers after 10 h, 20 h, 36 h and 48 h. The additional time points allow mutants that produce WT amounts of cyanide early ('A') or late ('E') to be distinguished from overproducers ('B', normal overproducer, 'D', late overproducer) and severe underproducers ('C', low cyanogenesis, 'G', no cyanide; 'F', sustained low cyanogenesis).

5.5.2 Distinguishing Between 'No Cyanide' and 'Sustained Low Cyanogenesis'

One of the ways WT *P. aeruginosa* is thought to employ to tightly regulate cyanogenesis is by switching cyanide production 'on' during entry into stationary phase, *via* QS, and 'off' thereafter. As previously described, an intriguing finding by Ryall *et al.* (2014) was that mucA mutants not only produced lower levels than WT during early stationary phase, with hcnABC expression ~ 10-fold lower than WT, but that these mutants also maintain low levels of cyanogenesis in late stationary phase. These results suggested that during the time frame observed, cyanide production in the mucA mutant was 'leakier' than in the WT. If this low level leakiness were to occur in the long term, this could help to explain the accumulation of cyanide observed in the lungs of CF patients chronically infected with mucoid strains of *P. aeruginosa* (Ryall *et al.*, 2008).

The 'sustained low cyanide' phenotype, which may be typical of mucA mutants, is illustrated by the hypothetical mutant 'F' in Figure 5-29. The screen in its current format, with a single time point at 20 h, may be unable to distinguish between no/low cyanogenesis ('C'/'G') and 'sustained low cyanogenesis' ('F').

Interestingly, preliminary follow up data on the flagella-related mutants carried out by two undergraduate students, using PA14NR strains and flagellar mutants in other *P. aeruginosa* backgrounds, confirmed a cyanogenesis defect. Their data also seemed to suggest that the loss of flagella function resulted in a 'sustained low cyanide' phenotype, rather than no cyanide at all (data not shown).

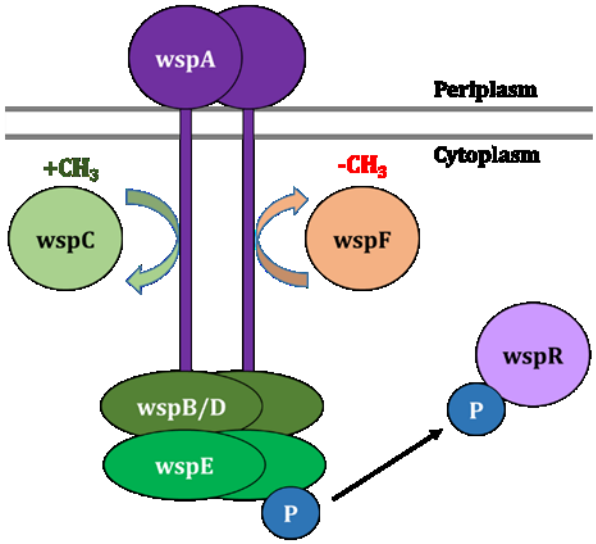
This warrants further investigation into the cyanogenesis kinetics of other candidate outliers uncovered by the screen, for instance by acquiring later time points which may be more reflective of a chronic context.

5.5.3 Screening Inconsistencies

A caveat of the screening methodology is that the 96-well format in which the library is stored, and in which the assay is performed, is prone to inter-well contamination. In addition, the library creators Liberati *et al.*, 2006 expect 2.8% of the library mutants to be mislabelled. It is therefore likely that some of the wells from which data was analysed in this chapter did not contain the intended mutant. This could, in part, help to explain the observation of opposing phenotypes for the same mutant in the whole

library screen compared to the rescreen (wspR, rocR; Table 5-9), as well as inconsistent trends observed for genes within the same regulon.

For instance, in Figure 5 26, if the behaviour of the putative wspA mutant is discounted, other related genes wspR (-1.40 log2 FC), wspF (0.9 log2 FC), wspE (-0.4 log2 FC) and wspB (-0.23 log2 FC) tell a consistent story (Figure 5-30): predicted repression of WspR activity (wspR, wspE, wspB) impairs cyanogenesis while predicted consitutive promotion of WspR activity (wspF) results in cyanide overproduction. As WspR is a diguanylate cyclase, constitutive WspR expression is expected to result in elevate local c-di-GMP and increased biofilm formation. Therefore, if wspA is removed from the analysis, the results suggest that elevated intracellular c-di-GMP in the local WspR-mediated pool results in increased cyanide production.



Mutation	Prediction	CN-
wspR	n/a	-1.4
*wspA**	Similar to *wspR*	0.31
wspF	Consitutive wspR expression, opposite of *wspR*	0.9
wspE	Similar to *wspR*	-0.4
wspB	Similar to *wspR*	-0.23

Figure 5-30 Interconsistency of wspR, wspF, wspE and wspB cyanogenesis phenotypes. Mutation of WspF is expected to result in constitutive expression of WspR. Thus, a wspF mutant is expect to exhibit an opposing phenotype to a wspR mutant. In contrast, WspB and WspE contribute to WspR activation, and wspB and wspE mutant are therefore expected to behave similarly to the wspR mutant. * WspA provides the signal required to activate WspR. It is therefore expected that wspA should behave similarly to wspR. This was not the case, suggesting an issue with the identity of the wspA mutant used in the screen.

Mutant identity issues such as the one described above highlight the utility of the screen as a tool that can be used to draw attention to putative candidates, in particular to groups of genes, rather than as a definitive list of accurate cyanogenic values for individual mutants. For this reason, all mutants identified by the screen should be re-tested to confirm their identities. Moreover, complementation of

clean deletion mutants or of mutants in other backgrounds should be used to conclusively confirm potential cyanogenesis defects.

5.5.4 Cyanogenesis of *P. aeruginosa* Appendage-Related Mutants

Appendages involved in different stages of attachment include the flagellum, T4P and Cup pili (Figure 5-31) (Nicastro *et al.*, 2009; Wang *et al.*, 2014; Burrows, 2012; Tomich *et al.*, 2007; Ruer *et al.*, 2007; Taguchi *et al.*, 2014).

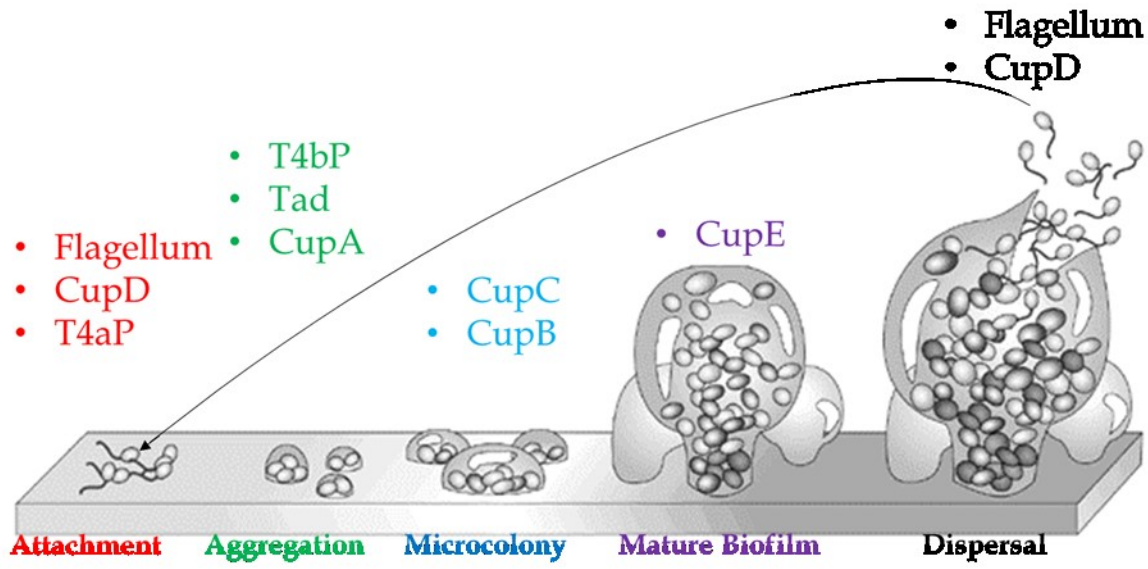


Figure 5-31 *P. aeruginosa* appendages are employed at different stages of biofilm formation. The process of biofilm formation observed in vitro can be divided into 5 stages. Attachment: Reversible attachment; Aggregation: Irreversible attachment; Microcolony formation: Bacteria spread by colony replication and twitching motility; Maturation: Bacteria employ T4P to climb to the top of the biofilm structure and form a 'cap'. Within this exopolysaccharide encased mushroom structure, aqueous channels facilitate the transport of nutrients and the excretion of waste. Dispersal: Unfavourable conditions trigger the release of free-living cells. These can attach to a new surface to form another biofilm.

P. aeruginosa employs its flagellum and pili to find suitable points of attachment. The single unipolar flagellum shares its basic structure with other bacterial species, comprising three main components: a basal body, which contains the rotary motor and is involved in export, a rigid helical filament, which acts as a propeller, and a flexible hook, which acts as a joint (Erhardt *et al.*, 2010)(Figure 5-32).

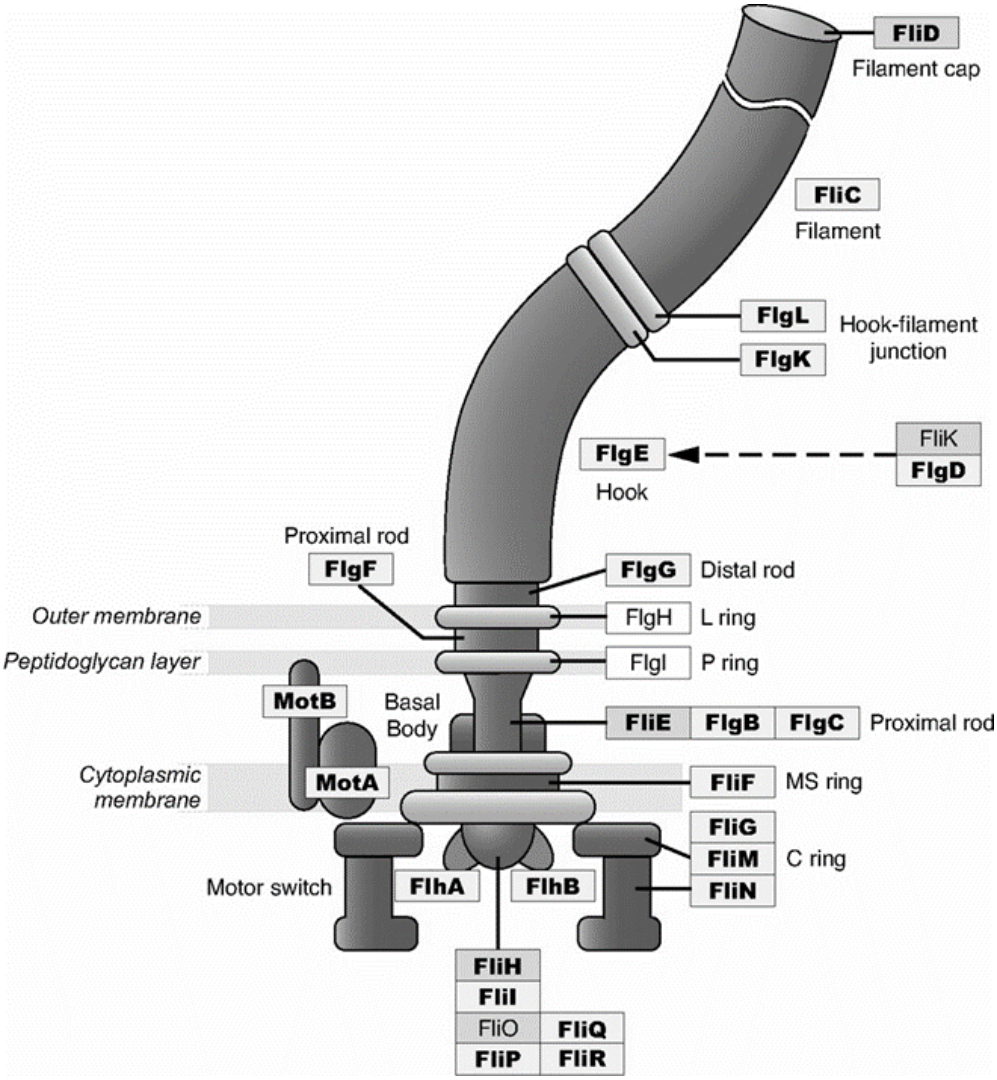


Figure 5-32 Components of the bacterial flagellum (adapted from Liu & Ochman, 2007). The flagellum consists of a rigid filament, made up of polymerised FliC subunits, a flexible hook and a basal body, containing the rotary motor. Rotation of the flagellum is powered by the proton motive force. Proteins encoded by the core genes, which have homologs in all flagellated bacteria, are designated in bold.

The flagellum is used to swim in liquid environments and additionally to swarm on slippery surfaces (Köhler *et al.*, 2000). It also helps bacteria anchor themselves to non-flat surfaces (Conrad *et al.*, 2011; Friedlander *et al.*, 2013). In our screen, mutants defective in any aspect of flagellar gene expression, structure or function were severely impaired in cyanogenesis. Since flagella-related mutants are known to be impaired in their ability to aggregate or adhere to surfaces, the results could be interpreted to mean that the initial reversible attachment step in biofilm formation, leading to aggregation, represents a turning point in the regulation of cyanogenesis. This is consistent with our previous understanding of cyanogenesis activation requiring high population density, for instance *via* the QS networks. Loss of

flagella may prevent *P. aeruginosa* cells from aggregating in sufficient densities to activate the QS networks. Alternatively, the flagellum may play a more direct role in the regulation of cyanogenesis.

In addition to the flagellum, *P. aeruginosa* possesses long helical protein fibres, T4P, which play a role in flagellum-independent twitching motility, adhesion, microcolony formation, and the uptake of DNA (Ottow, 1975; Mattick, 2002; Aas *et al.*, 2002). Twitching motility on a solid surface occurs by pilus retraction: Attached pili become shortened and taut, thus translocating the cell body (Skerker & Berg, 2001). At present, *P. aeruginosa* is the only species which has been found to harbour all three kinds of T4P in the same strain: T4aP, T4bP and Tad (Figure 5-33).

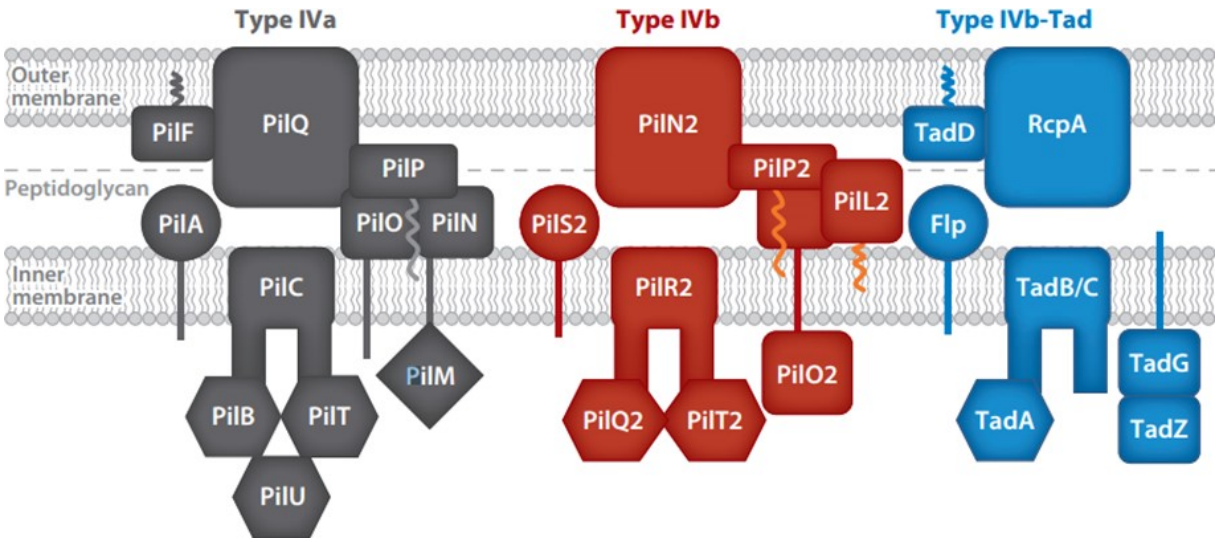


Figure 5-33 Components of Type IV Pili (Burrows, 2012). PilA, PilS2, and Flp are the major pilin subunits. These are the major building blocks of pili; PilQ, PilN2, and RcpA are secretins. Secretins form the channel through which the pilus is assembled; PilF and TadD are putative pilotins. Pilotins are required for correct oligomerisation and localisation of the secretins in the outer membrane; PilC, PilR2, TadB, and TadC are putative platform proteins; PilB, PilQ2, and TadA are pilin polymerases, while PilT, PilU, and PilT2 are pilin depolymerases. These motor proteins provide the energy for pilus assembly and retraction.

T4aP are associated with surface motility, T4bP are linked to aggregation and Tad pili may play a role in tight, irreversible adhesion. T4aP pili are present in all *P. aeruginosa* strains, while T4bP and Tad are found in strains encoding the *P. aeruginosa* pathogenecity island 1 (PAPI-1).

In our screen, a pilZ mutant, which is defective in T4P and is a poor biofilm former, was found to be severely impaired in cyanogenesis (-0.95 logFC) (Merighi *et al.*, 2007) . The results were less clear with individual T4aP and T4bP genes. Due to these inconsistencies, further studies with clean deletion

mutants, generating supplementary phenotypic data, such as the impact of individual mutations on motility, biofilm formation and intracellular c-di-GMP levels, should be investigated.

Interestingly, in the case of Tad pili, which are required during the irreversible attachment stage of biofilm formation, mutants were found to exhibit strong cyanide overproducer phenotypes. This suggests that, in wildtype strains, the timing of Tad pilus function, that is, tight adhesion, may coincide with a downregulation of cyanide production. This is consistent with the idea that the transition to sessility in *P. aeruginosa* is accompanied with altered virulence.

Cup pili are another type of *P. aeruginosa* pilus. While their biological functions have yet to be resolved, current evidence suggests they are required at various stages in biofilm formation (Mikkelsen *et al.*, 2009). The main components of Cup pilus assembly are pilin subunits, an outer membrane usher pore and periplasmic chaperones. Pilin subunits are transported across the inner membrane, and are then folded and stabilised by periplasmic chaperones. Next, the chaperones target the subunits to the outer membrane usher, which forms a platform for pilus assembly.

CupD pili may play a role in decreasing swimming motility and promoting attachment (Mikkelsen *et al.*, 2009). CupA pili may be required for stable attachment to abiotic surfaces. Disruption of cupA2 and cupA3 causes a 70% decrease in biofilm formation compared mutation of pilA alone (Vallet *et al.*, 2001). Constrastedly, CupB and CupC pili have been hypothesised to work together to improve cell-to-cell interactions necessary at the microcolony stage. Overexpression of the cupB operon increased pellicle formation, while a cupB3 mutant formed sparser biofilms than wildtype (Kulasekara *et al.*, 2005; Ruer *et al.*, 2007). CupE pili seem to be involved in the maturation stage of biofilms, promoting cells to cluster into more complex configurations, such as a ‘mushroom’ shape, which is a hallmark of mature *P. aeruginosa* biofilms in vitro.

Our screen data for the Cup fimbriae did not reveal consistent trends within each operon. Therefore, future studies on the role of individual fimbrial genes in biofilms would help towards elucidating their involvement in cyanogenesis.

5.5.5 Concomitant Loss of Flagellum and Loss of Cyanogenesis

One of the clearest observations in this chapter was that mutants defective in any aspect of flagellar gene expression, biosynthesis, mechanical rotation or chemotaxis were also defective in acute cyanogenesis. A possible hypothesis to explain the benefit of concomitant loss of both these functions is that they are required at the same time during an aspect of *P. aeruginosa*'s colonisation strategy.

A current paradigm is that loss of flagellar expression occurs during the motile-sessile switch. Unknown environmental cues, associated with surface sensing, promote the production of c-di-GMP, which competitively inhibits the master regulator of flagellar synthesis, FleQ (Hickman & Harwood, 2008). It is possible that *P. aeruginosa* may have evolved mechanisms to couple the loss of flagella with the switching off of, or more likely, the dampening of, cyanide production, because swimming motility and acute cyanogenesis are advantageous during the early stages of colonisation, but not after attachment has occurred.

In the context of CF lung infections, this could be consistent with the hypothesis made in Chapter 3, that cilio-inhibition by acute cyanogenesis plays a role early on during colonisation, contributing to *P. aeruginosa*'s ability to gain a foothold. Following successful inhibition of muco-ciliary defences, it is possible that a switch from acute to low, but sustained cyanogenesis may be favourable for subsequent chronic establishment (Figure 5-34). This is consistent with the high occurrence of mucA mutants recovered from chronically infected CF patients, which, as previously discussed, were shown to be defective in acute cyanogenesis, but were able to maintain low levels of cyanide production in late stationary phase (Ryall *et al.*, 2014). If a mechanism by which the timing of flagellar function loss and cyanogenesis deregulation is coordinated exists, it remains to be elucidated.

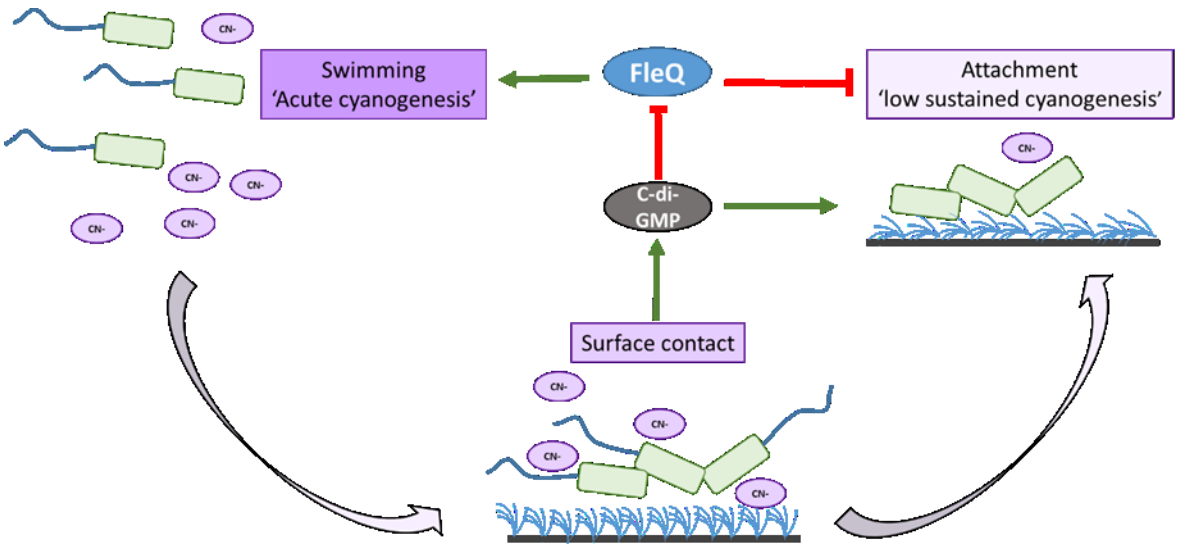


Figure 5-34 Model: Concomitant loss of flagella and downregulation of cyanogenesis may play a role in lung infections.

Mutants suffering from flagella-related defects were found to be highly defective in cyanogenesis. A possible explanation for this association is that coupling the loss of these features could be advantageous. In the context of lung infections, a possible hypothesis is that acute cyanogenesis, like swimming, is beneficial during the early stages of infection. In particular, acute cyanogenesis could contribute to cilioinhibition during invasion and may help *P. aeruginosa* gain a foothold in the lung. Upon surface contact and initiation of attachment, however, it is possible that flagellar loss and a dampening of cyanogenesis, as is commonly seen in clinical isolates, may constitute a more successful strategy.

Simultaneous loss of flagella and cyanogenesis could have different ramifications for *P. aeruginosa*'s survival strategy in other habitats. For example, acute cyanogenesis of motile environmental strains may aid *P. aeruginosa* compete for resources against cyanide-sensitive species. Once *P. aeruginosa* has successfully colonised a surface, it may no longer require flagella or acute chemical warfare. Additionally, as cyanide is volatile and diffusible, one may speculate that once *P. aeruginosa* exists as dense communities, low level cyanogenesis by individual cells could constitute a 'common good', with the energetic costs of production spread out across the entire biofilm (Chuang *et al.*, 2009). Alternatively, a switch in cyanogenesis and motility may play a role in either combatting or evading predation by environmental eukaryotic phagocytes, such as the amoeba D. discoideum.

5.5.6 Hypothesis: Cyanogenesis Plays a Role in Immune Evasion

Returning to the context of clinical infections, it is possible that concomitant loss of flagellar and acute cyanogenic function may contribute to immune evasion. It is widely understood that loss of flagella consitutes a mechanism by which bacteria evade the flagellin-mediated Toll-like receptors of phagocytes. Interestingly, Amiel *et al.*, (2010) found that the evasion of phagocytosis by *P. aeruginosa* was independent of flagellum expression, as mutants defective in flagellar function, but retaining an intact flagellum, were as resistant to phagocytosis as flagellum-deficient mutants. This led the authors to conclude that loss of swimming motility, rather than loss of flagella per se, was the phenotype which confered an advantage in immune invasion.

However, the data presented in this chapter suggests that a possible additional feature of mutants with intact flagella, but defective in flagellar function, is concomitant loss of cyanogenic ability. Is it therefore possible that reduced cyanogenesis in these mutants could also have played a role in the enhanced evasion observed by the authors?

In a screen of a library of 48 *P. aeruginosa* two-component regulators to uncover factors influencing the ability to induce polymorphonuclear leukocytes (PMN) migration, Hurley *et al.*, (2010) identified only 5 mutants: ΔfleR, ΔwspR, ΔpilR, ΔalgR and ΔroxR. Strikingly, 3/5 these mutants were identified as severe cyanide underproducers in our screen.

Additionally, the fact that we did not find algR to be an underproducer in our screen could be explained by the fact that PA14, unlike most *P. aeruginosa* strains, lacks an AlgR binding site upstream of the hcnABC genes (Okkotsu *et al.*, 2014). In PAO1, which was used by Hurley *et al.*, the ΔalgR mutant retains the binding site and is therefore expected to be cyanide-deficient. Therefore, unbeknown to the authors, a common point between 4/5 mutants identified in their screen may have been a loss of cyanogenic ability.

Moreover, while the a pilR mutant in our screen did not give an outlier phenotype, pilS and several other T4P-related genes were impaired in cyanogenesis. It would therefore be of interest to verify the identity of the PA14NR library pilR mutant and, additionally, to investigate cyanogenesis of pilR mutants in other *P. aeruginosa* backgrounds. We hypothesise that clean deletion pilR mutants may be impaired in both their ability to induce PMN transmigration and cyanogenesis.

Hurley *et al.* went on to show that the inability of ΔroxR to induce PMN transmigration was independent of cioAB, as ΔcioAB did not exhibit a defect. This is consistent with our finding that the roxSR mutants (roxS, -1.3 log2 FC; roxR, -1.67 log2 FC) were much more severely impaired in cyanogenesis than the cioAB mutants (cioA, -0.59 log2 FC; cioB, 0.15 log2 FC). Previous data on cioAB mutants suggests that these mutants produce wildtype levels of cyanide (Zlosnik *et al.*, 2006). We therefore hypothesise that cyanide could be a diffusible signal that promotes PMN transmigration, and that mutants severely defective in cyanogenesis may be better able to evade PMN clearance. Further experiments specifically investigating the effect of cyanogenesis on PMN migration will be required to test this.

5.5.7 Hypothesis: The RoxSR System Regulates Cyanogenesis

Comolli & Donohue, (2002) first characterized the RoxSR system as a regulator of CIO production, with roxR and roxS mutants exhibiting 64-90% reduction in cioAB expression. In addition, the authors observed a 10-fold increase in sensitivity to CN- exposure in the absence of RoxSR. As inactivation of cioAB had a lesser effect on cyanide sensitivity, this suggested that *P. aeruginosa* possesses RoxSR-

dependent cyanide detoxification mechanisms independent of the CIO. The results of our screen indicate that mutation of RoxS or RoxR not only results in increased cyanide sensitivity, as observed by Comolli and Donohue, but also in severely impaired cyanogenesis.

This leads us to hypothesise that RoxSR may play an additional protective role beyond upregulating the CIO and an unknown cyanide detoxification mechanism: RoxSR may also be responsible for preventing cyanogenesis in the absence of protective mechanisms (Figure 5-35). If cyanogenesis were to be halted in the absence of the right signal from RoxSR, this would explain why roxR and roxS mutants, which are hypothesised to lack the unknown cyanide detoxification mechanism, are nevertheless able to exhibit normal growth into stationary phase. In addition, RoxSR upregulation of the CIO is increased in the presence of cyanide. It is therefore possible that this system, which appears to prepare *P. aeruginosa* against potential negative consequences of cyanogenesis, may sense, and be regulated by, the presence of cyanide itself.

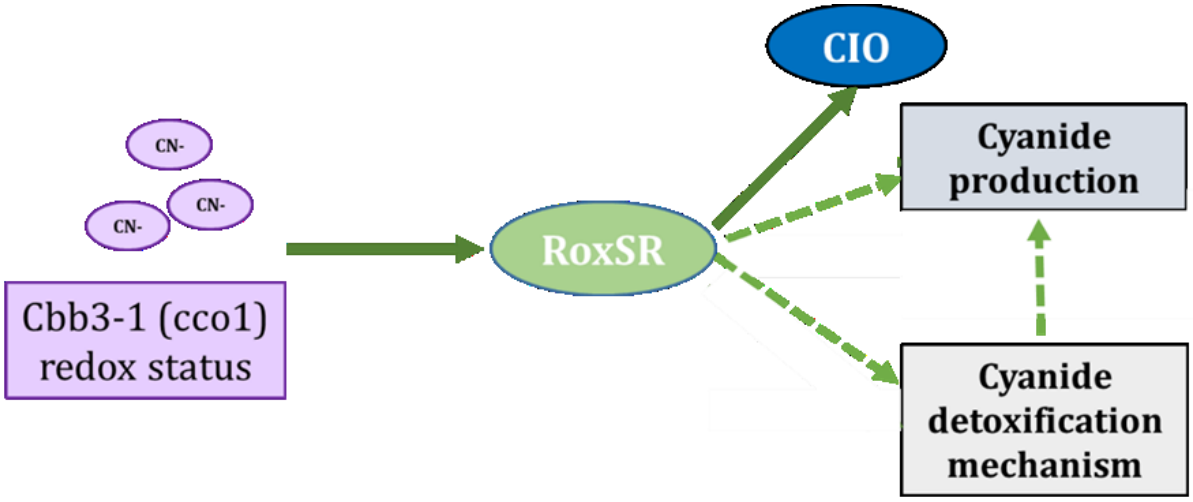


Figure 5-35 Model: The role of the RoxSR system may be to ensure that cyanogenesis only occurs when *P. aeruginosa* is able to protect itself from potential deleterious effects. We hypothesise that cyanide, perhaps in conjunction with alterations to the redox status of Cbb3-1, may constitute the signal which is sensed by the RoxSR system. Once activated, RoxSR is known to upregulate the CIO, and is hypothesised to also promote both a CIO-independent detoxification mechanism and cyanogenesis itself.

What is the nature of the signal recognised by RoxS? Electron flow through cytochrome Cbb3-1 CcoN subunit has been proposed as a signal (Elsen *et al.*, 2004). RoxSR is closely related to the better characterised PrrBA system, which in Rhodobacter sphaeroides, is one of the main regulators of gene expression in response to changes in oxygen levels (Oh *et al.*, 2004). In the PrrBA system, Cbb3

oxidase, with its high O2 affinity, acts as redox sensor. The strength of inhibition of PrrBA by Cbb3 oxidase is proportional to the extent of electron flow, which is itself determined by oxygen tension. The higher the oxygen concentration the greater the electron flow through Cbb3 oxidase, which in turn creates a stronger inhibitory signal. The as yet uncharacterized inhibitory signal is then hypothesised to shift the equilibrium of the PrrB histidine kinase activity from kinase mode to phosphatase mode. The case for direct interaction between PrrB and Cbb3 oxidase was strengthened by the finding that replacing a histidine residue (H303) of the CcoN subunit of Cbb3 oxidase with alanine resulted in normal Cytochrome C oxidase activity but abrogated repression of PrrB activity in the presence of at high oxygen tension (Kim *et al.*, 2007).

As cyanide is a potent inhibitor of haem-copper oxidases, inhibition of Cbb3-1 leading to decreased electron flow through its CcoN subunit may be a possible mechanism through which cyanide relieves the inhibition of the RoxSR system, thus allowing RoxS to transition to kinase mode. Its active cognate response regulator RoxR is then able to upregulate the CIO, additional cyanide tolerance mechanisms, and perhaps cyanogenesis as well.

Transcriptome analysis of a double ΔroxSR mutant, albeit under aerobic conditions, uncovered 11 and 43 genes that were differentially expressed compared to the WT during exponential and early stationary phase, respectively (Kawakami *et al.*, 2010). Of these, the PQS synthase genes (PA0699, 0998-1000), which were downregulated in ΔroxSR during entry into stationary phase, could be responsible for activating cyanogenesis. PA0699 was not in the PA14NR library. However, the other PQS synthase genes were, and all of these, with the exception of pqsC, were found to be impaired in cyanogenesis (Figure 5-36). pqsH, an FAD-dependent monooxygenase which is responsible for the final step in PQS synthesis, appears to be severely and reproducibly affected. Interestingly, pqsE, which is thought to act independently of other PQS genes, exhibited marked cyanide underproducer phenotypes in both the whole library screen and the rescreen.

Gene	Description	Cyanogenesis (log fc)	
		Screen 1	Screen2
pqsA	*Pseudomonas* quinolone signal biosynthesis, anthranilate-coenzyme A ligase	-0.45	n/a
pqsB	*Pseudomonas* quinolone signal biosynthesis, B-Ketoacyl-acyl protein synthase	-0.43	n/a
pqsC	*Pseudomonas* quinolone signal biosynthesis, B-Ketoacyl-acyl protein synthase	**0.70**	n/a
pqsD	*Pseudomonas* quinolone signal biosynthesis, B-Ketoacyl-acyl protein synthase	-0.36	n/a
pqsE	synthesis of 4-quinolone compounds, independent regulator	-1.44	-1.35
pqsH	putative FAD-dependent monooxygenase, may be involved in addition of hydroxyl group to PQS	-1.50	-2.23

Figure 5-36 PQS genes, which are upregulated by RoxSR during entry into stationary phase, may play a positive regulatory role in cyanogenesis.

We compared the RoxSR microarray data (log FC expression rel. to WT) from the Kawakami *et al.* (2010) paper with the cyanogenesis values obtained from our screen. Of the 56 gene identified in the RoxSR microarray, 18 were cyanide underproducers (Figure 5-37) and 12 were overproducers (Figure 5-38).

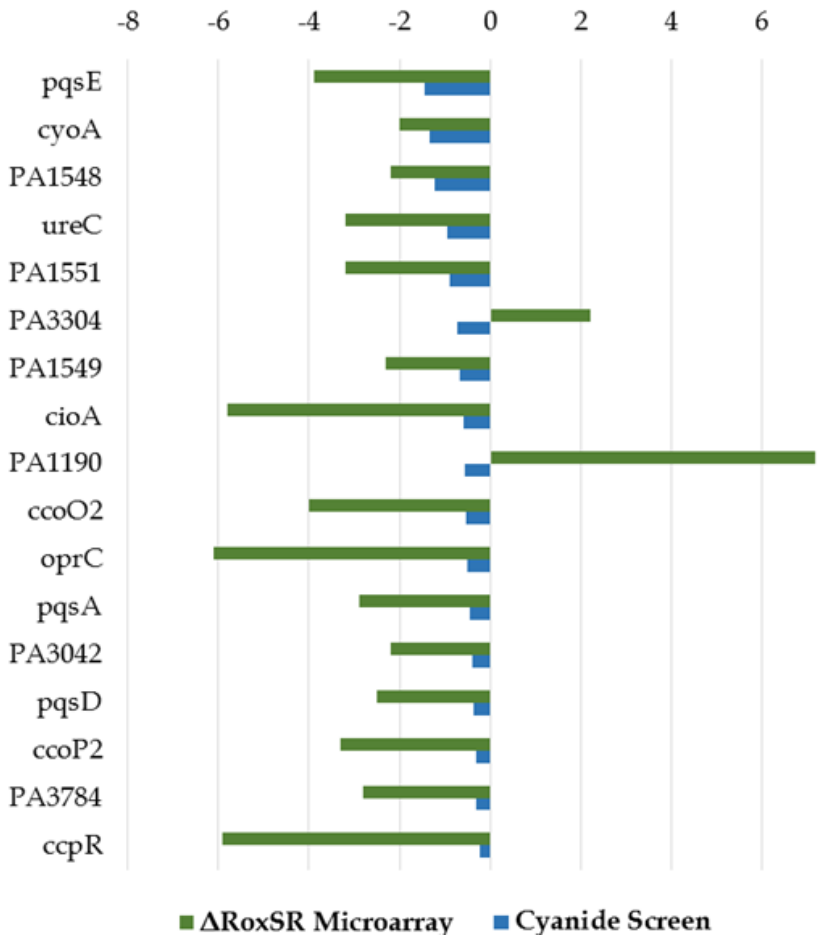


Figure 5-37 Cyanogenesis underproducers also identified by Kawakami *et al.* (2010)

Gene	Annotation	ΔRoxSR Microarray	Cyanide Screen
pqsE	quinolone signal response protein	-3.9	-1.44
cyoA	cytochrome o ubiquinol oxidase subunit II	-2	-1.34
PA1548	conserved hypothetical protein	-2.2	-1.23
ureC	urease alpha subunit	-3.2	-0.94
PA1551	probable ferredoxin	-3.2	-0.91
PA3304	conserved hypothetical protein	2.2	-0.73
PA1549	probable cation-transporting P-type ATPase	-2.3	-0.67
cioA	cyanide insensitive terminal oxidase	-5.8	-0.59
PA1190	conserved hypothetical protein	7.18	-0.55
ccoO2	probable cytochrome c oxidase subunit	-4	-0.52
oprC	OprC precursor	-6.1	-0.49
pqsA	probable coenzyme A ligase	-2.9	-0.45
PA3042	hypothetical protein	-2.2	-0.40
pqsD	3-oxoacyl-[acyl-carrier-protein] synthase III	-2.5	-0.36
ccoP2	probable cytochrome c	-3.3	-0.32
PA3784	hypothetical protein	-2.8	-0.32
ccpR	cytochrome c551 peroxidase precursor	-5.9	-0.22

Table 5-14 Cyanogenesis underproducers also identified by Kawakami *et al.* (2010)

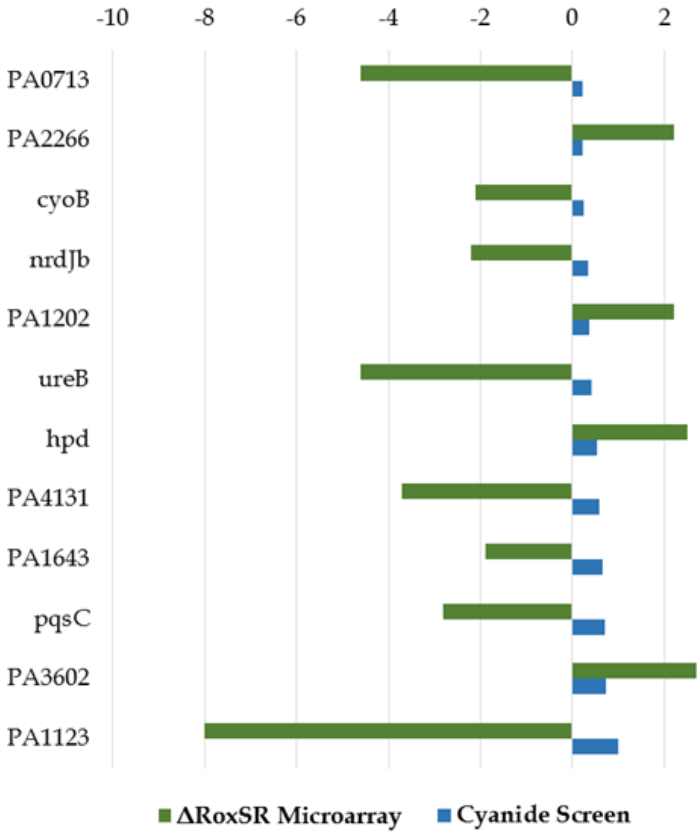


Figure 5-38 Cyanogenesis overproducers also identified by Kawakami *et al.* (2010)

Gene	Annotation	ΔRoxSR Microarray	Cyanide Screen
PA0713	hypothetical protein	-4.6	0.21
PA2266	probable cytochrome c precursor	2.2	0.21
cyoB	cytochrome o ubiquinol oxidase subunit I	-2.1	0.24
nrdJb	class II (cobalamin-dependent) ribonucleotide-diphosphate reductase subunit	-2.2	0.35
PA1202	probable hydrolase	2.2	0.37
ureB	urease beta subunit	-4.6	0.41
Hpd	4-hydroxyphenylpyruvate dioxygenase	2.5	0.53
PA4131	probable iron-sulfur protein	-3.7	0.59
PA1643	tRNA 2-selenouridine synthase	-1.9	0.66
pqsC	homologous to beta-keto-acyl-acyl-carrier protein synthase	-2.8	0.70
PA3602	conserved hypothetical protein	2.7	0.73
PA1123	hypothetical protein	-8	1.00

Table 5-15 Cyanogenesis of genes identified by Kawakami *et al.* (cyanide overproducers).

Additional Δ*roxSR* transcriptome analyses under microaerobic conditions, or, alternatively, further investigation into the cyanide sensitivity of mutants co-identified in our screen and by Kawakami *et al.* (2010), could help to uncover the nature of the putative RoxSR-regulated, CIO-independent, cyanide detoxification mechanism.

5.6 Future Work

Improvements to the screening methodology allowed us to obtain numerical values for 93% of the PA14NR mutants. Due to mutants missing from the library, screening inconsistencies and other caveats, this chapter's results represent only a preliminary step in confirming the identity of novel cyanogenesis determinants. Complementation studies, as seen in Chapter 2, will be required to provide more definite results. A strength of the approach utilised here has been its breadth. It has allowed us to identify trends and has provided the basis for hypothesis generation. Notably, we identified genes involved in the motile-sessile switch, the RoxSR system and several additional novel genes as promising starting points for future studies into the regulation of cyanogenesis in *P. aeruginosa*.

The screening methodology could be further improved. For example, a calibration curve could be plotted to estimate cyanide concentrations, in µM. Obtaining more time points per mutant would also help distinguish between different kinetics of cyanide production. Additionally, the screen would better mimic *in vivo* conditions found in the CF lung if it were adapted to a 96-well agar format, utilizing LB-agar or Artificial Sputum Medium (ASM). In order to confirm putative defects identified through screening, cyanogenesis of mutants constructed in different backgrounds should be tested, and complementation studies should be carried out, preferably with clean deletions of the genes of interest. Cyanogenesis of these mutants could be measured directly, using an ISE. Additionally, MIC measurements with varying [KCN] could be used to test whether mutants of interest are involved in cyanide tolerance.

In order to explore the hypothesis that the regulation of cyanogenesis is linked to the motile-sessile switch, motility-related and c-di-GMP regulated mutants in different backgrounds should be subjected to a battery of phenotypic assays, including swimming, swarming, micro-colony formation, biofilm maturation, c-di-GMP, QS, PYO and cyanide. In order to test the hypothesis that cyanogenesis plays a role in *P.aeruginosa* interactions with immune cells, a first step could be to carry out PMN migration assays using WT, Δ*hcnABC*, and other cyanide-deficient strains. In order to test the hypothesis that the RoxSR system regulates cyanogenesis, RNA seq or other transcriptome analyses could be performed on RNA extracted from Δ*RoxSR* mutants and WT grown under microaerophilic conditions at different time points, including stationary phase. Additionally, cyanide measurements and MIC measurements with varying [KCN] could be carried out on the RoxSR regulon to identify the hypothesised CIO-independent detoxification mechanism.

Chapter 6
GENERAL DISCUSSION

6.1 Summary of the Findings Presented in this Thesis

This thesis set out firstly to explore the implications of the presence of cyanide in sputum, and secondly to uncover novel determinants of cyanogenesis. With regards to the first aim, the work presented in Chapter 3 demonstrates that cyanide levels found in infected CF sputum inhibit airway ciliary function *in vitro*, and may therefore support further investigation of *P. aeruginosa* cyanogenesis from a clinical stand point. With regards to the second aim, the screening approach developed in Chapter 4 and refined in Chapter 5 has been successful in identifying novel candidates, including a novel regulator located downstream of the hydrogen cyanide biosynthetic operon. The improved screening methodology also uncovered a number of gene clusters and operons affected in cyanogenesis, and has led to the generation of novel hypotheses.

The main conclusions of this work are summarised below.

- Cyanide concentrations detectable in CF sputum are sufficient to impair CBF, an important component of the lung's innate immune system, in two *in vitro* models of the airway. The cilio-inhibitory mechanism observed is transient, and, unlike CBF slowing by PYO, is not associated with a fall in ATP. In the ALI model, cyanide appears to be the major component of *P. aeruginosa* supernatant responsible for the cilio-inhibitory effects observed.

- PA2196, a putative TetR repressor, and PA5339, a putative translational inhibitor of the Yjgf family, are two uncharacterised regulators identified through cyanide screening, for which a role in cyanogenesis was confirmed by complementation studies. PA2196 is of particular interest for future investigation due to its location downstream of the hydrogen cyanide biosynthetic operon.

- Based on the results of the quantitative screen, the following testable hypotheses could benefit from further investigation:

a) *P. aeruginosa* cyanogenesis is co-regulated with the flagellar operon

b) *P. aeruginosa* cyanogenesis affects PMN migration

c) *P. aeruginosa* cyanogenesis is regulated by the redox-responsive transcriptional regulator RoxSR, *via* the PQS system.

6.2 Relevance of Cyanogenesis to Human Infection and Disease

Among bacteria, *P. aeruginosa* is unusual in its ability to produce cyanide. However, it shares this trait with the other major pathogen of chronic CF lung infections, *Bcc* (Ryall *et al.*, 2008). Despite the prominent role that *P. aeruginosa* and *Bcc* play in chronic CF airway disease, there has been a relative lack of investigation into cyanogenesis from a clinical perspective. The main finding of Chapter 3, that cyanide levels detectable in sputum inhibit ciliary function *in vitro*, may support a role for cyanogenesis in human virulence.

Why might cyanogenic pathogens dominate the CF lung? Filkins *et al.*, (2012) found that increased poly-microbial diversity in the CF lung was associated with patient stability. If cyanide is confirmed to be an important factor contributing to *P. aeruginosa* dominance of the CF lung, inhibition of cyanogenesis or direct detoxification of cyanide, for example through complex formation with hydroxycobalamin, has therapeutic potential.

We hypothesise that the advantage conferred by cyanogenesis to these pathogens over others, that can neither produce nor tolerate cyanide, is multifaceted. Fothergill *et al.*, (2014) report that the upper airways, including the paranasal sinuses and the nasopharynx, act as important reservoirs that are key in the later establishment of chronic lung infection. Early on in infection, we hypothesise that the cilio-inhibitory effect of cyanide may contribute to indiscriminate bacterial colonisation of the upper and lower respiratory tracts. Next, once muco-ciliary defenses have been overcome, and as *P. aeruginosa* switches from a motile to sessile lifestyle, we hypothesise that loss of flagella could coincide with impaired cyanide production. This loss of cyanogenic ability may enhance *P. aeruginosa*'s ability to modulate PMN activity. Later on, as *P. aeruginosa* forms biofilms in the thick mucus, low O_2 tensions activate ANR, which is known to enhance cyanogenesis. Cyanide inhibition of Cbb3-1 oxidase is then hypothesised to upregulate the RoxSR system, which is known to upregulate the CIO and, based on our results, may also upregulate cyanide production, *via* PQS, and detoxification, *via* an unknown mechanism. We hypothesise that subsequent cyanide accumulation in viscous CF mucus impacts lung microbial ecology, favouring the persistence of strains that can withstand the effects of cyanide, such as *Bcc*. This hypothetical model is presented in Figure 6-1.

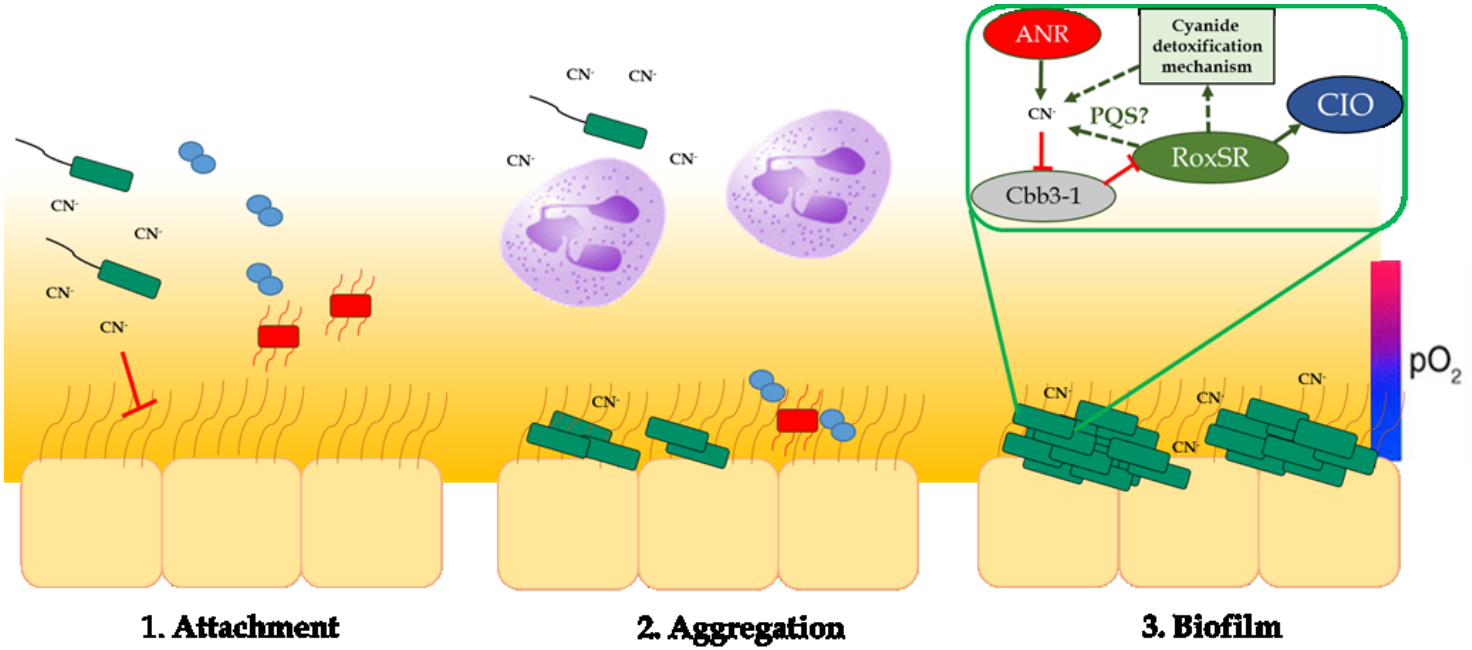


Figure 6-1 Hypothetical model of the role of cyanogenesis in *P. aeruginosa* chronic lung infections.

(1) Cyanogenic cilio-inhibitory activity facilitates poly-microbial colonisation of human respiratory epithelia by *P. aeruginosa* (green bacilli) and other hypothetical pathogens (blue cocci and red bacilli).

(2) The *P. aeruginosa* motile-sessile switch coincides with down-regulation of cyanogenesis and may modulate interactions with PMN (purple cells).

(3) Low O_2 tensions in hypoxic mucus zones activate ANR. ANR promotes cyanogenesis to the detriment of other microbes. Hypothesis: Cyanide inhibition of Cbb3-1 activates RoxSR, which promotes expression of the CIO, cyanogenesis *via* PQS, and an unknown cyanide tolerance or detoxification mechanism.

REFERENCES

Aas, F.E., Løvold, C. and Koomey, M. 2002. An inhibitor of DNA binding and uptake events dictates the proficiency of genetic transformation in *Neisseria gonorrhoeae*: mechanism of action and links to Type IV pilus expression. *Molecular microbiology*. 46, 5 (Dec. 2002), 1441–50.

Abd, H., Wretlind, B., Saeed, A., Idsund, E., Hultenby, K. and Sandström, G. 2008. *Pseudomonas aeruginosa* utilises its type III secretion system to kill the free-living amoeba Acanthamoeba castellanii. *The Journal of eukaryotic microbiology*. 55, 3 (Jan. 2008), 235–43.

Adam, E.C., Mitchell, B.S., Schumacher, D.U., Grant, G. and Schumacher, U. 1997. *Pseudomonas aeruginosa* II lectin stops human ciliary beating: therapeutic implications of fucose. *American journal of respiratory and critical care medicine*. 155, 6 (Jun. 1997), 2102–4.

Alvarez-Ortega, C. and Harwood, C.S. 2007. Responses of *Pseudomonas aeruginosa* to low oxygen indicate that growth in the cystic fibrosis lung is by aerobic respiration. *Molecular microbiology*. 65, 1 (Jul. 2007), 153–65.

Amiel, E., Lovewell, R.R., O'Toole, G.A., Hogan, D.A. and Berwin, B. 2010. *Pseudomonas aeruginosa* evasion of phagocytosis is mediated by loss of swimming motility and is independent of flagellum expression. *Infection and immunity*. 78, 7 (Jul. 2010), 2937–45.

Anderson, R.D., Roddam, L.F., Bettiol, S., Sanderson, K. and Reid, D.W. 2010. Biosignificance of bacterial cyanogenesis in the CF lung. *Journal of cystic fibrosis : official journal of the European Cystic Fibrosis Society*. 9, 3 (May 2010), 158–64.

Andrade, F.H., McMullen, C.A. and Rumbaut, R.E. 2005. Mitochondria are fast Ca2+ sinks in rat extraocular muscles: a novel regulatory influence on contractile function and metabolism. *Investigative ophthalmology & visual science*. 46, 12 (Dec. 2005), 4541–7.

Antigny, F., Girardin, N., Raveau, D., Frieden, M., Becq, F. and Vandebrouck, C. 2009. Dysfunction of mitochondria Ca2+ uptake in cystic fibrosis airway epithelial cells. *Mitochondrion*. 9, 4 (Jul. 2009), 232–41.

Arai, H. 2011. Regulation and Function of Versatile Aerobic and Anaerobic Respiratory Metabolism in *Pseudomonas aeruginosa*. *Frontiers in microbiology*. 2, (Jan. 2011), 103.

Balasubramanian, D., Schneper, L., Merighi, M., Smith, R., Narasimhan, G., Lory, S. and Mathee, K. 2012. The regulatory repertoire of *Pseudomonas aeruginosa* AmpC ß-lactamase regulator AmpR includes virulence genes. *PloS one*. 7, 3 (Jan. 2012), e34067.

Baldini, R.L., Starkey, M. and Rahme, L.G. 2014. Assessing *Pseudomonas* virulence with the nonmammalian host model: Arabidopsis thaliana. *Methods in molecular biology (Clifton, N.J.)*. 1149, (Jan. 2014), 689–97.

Baraquet, C., Murakami, K., Parsek, M.R. and Harwood, C.S. 2012. The FleQ protein from *Pseudomonas aeruginosa* functions as both a repressor and an activator to control gene expression from the pel operon promoter in response to c-di-GMP. *Nucleic acids research*. 40, 15 (Aug. 2012), 7207–18.

Bear, C.E., Li, C.H., Kartner, N., Bridges, R.J., Jensen, T.J., Ramjeesingh, M. and Riordan, J.R. 1992. Purification and functional reconstitution of the cystic fibrosis transmembrane conductance regulator (CFTR). *Cell*. 68, 4 (Feb. 1992), 809–18.

Behrends, V., Ryall, B., Wang, X., Bundy, J.G. and Williams, H.D. 2010. Metabolic profiling of *Pseudomonas aeruginosa* demonstrates that the anti-sigma factor MucA modulates osmotic stress tolerance. *Molecular bioSystems*. 6, 3 (Mar. 2010), 562–9.

Berkebile, A.R. and McCray, P.B. 2014. Effects of airway surface liquid pH on host defense in cystic fibrosis. *The international journal of biochemistry & cell biology*. 52, (Jul. 2014), 124–9.

Bhattacharya, R. and Vijayaraghavan, R. 2002. Promising role of alpha-ketoglutarate in protecting against the lethal effects of cyanide. *Human & experimental toxicology*. 21, 6 (Jun. 2002), 297–303.

Bianchi, S.M., Prince, L.R., McPhillips, K., Allen, L., Marriott, H.M., Taylor, G.W., Hellewell, P.G., Sabroe, I., Dockrell, D.H., Henson, P.W. and Whyte, M.K. 2008. Impairment of apoptotic cell engulfment by pyocyanin, a toxic metabolite of *Pseudomonas aeruginosa*. *American journal of respiratory and critical care medicine*. 177, 1 (Jan. 2008), 35–43.

Bitsori, M., Maraki, S., Koukouraki, S. and Galanakis, E. 2012. *Pseudomonas aeruginosa* urinary tract infection in children: risk factors and outcomes. *The Journal of urology*. 187, 1 (Jan. 2012), 260–4.

Blom, D., Fabbri, C., Eberl, L. and Weisskopf, L. 2011. Volatile-mediated killing of Arabidopsis thaliana by bacteria is mainly due to hydrogen cyanide. *Applied and environmental microbiology*. 77, 3 (Feb. 2011), 1000–8.

Blumer, C. and Haas, D. 2000. Mechanism, regulation, and ecological role of bacterial cyanide biosynthesis. *Archives of microbiology*. 173, 3 (Mar. 2000), 170–7.

Bobadilla, J.L., Macek, M., Fine, J.P. and Farrell, P.M. 2002. Cystic fibrosis: a worldwide analysis of CFTR mutations--correlation with incidence data and application to screening. *Human mutation*. 19, 6 (Jun. 2002), 575–606.

Bordi, C., Lamy, M.-C.C., Ventre, I., Termine, E., Hachani, A., Fillet, S., Roche, B., Bleves, S., Méjean, V., Lazdunski, A. and Filloux, A. 2010. Regulatory RNAs and the HptB/RetS signalling pathways fine-tune *Pseudomonas aeruginosa* pathogenesis. *Molecular microbiology*. 76, 6 (Jun. 2010), 1427–43.

Boyle, M.P. and De Boeck, K. 2013. A new era in the treatment of cystic fibrosis: correction of the underlying CFTR defect. *The Lancet. Respiratory medicine*. 1, 2 (Apr. 2013), 158–63.

Brichta, D.M., Azad, K.N., Ralli, P. and O'Donovan, G.A. 2004. *Pseudomonas aeruginosa* dihydroorotases: a tale of three pyrCs. *Archives of microbiology*. 182, 1 (Sep. 2004), 7–17.

Brint, J.M. and Ohman, D.E. 1995. Synthesis of multiple exoproducts in *Pseudomonas aeruginosa* is under the control of RhlR-RhlI, another set of regulators in strain PAO1 with homology to the autoinducer-responsive LuxR-LuxI family. *Journal of bacteriology*. 177, 24 (Dec. 1995), 7155–63

Britigan, B.E., Railsback, M.A. and Cox, C.D. 1999. The *Pseudomonas aeruginosa* secretory product pyocyanin inactivates alpha1 protease inhibitor: implications for the pathogenesis of cystic fibrosis lung disease. *Infection and immunity*. 67, 3 (Mar. 1999), 1207–12.

Broderick, K.E., Potluri, P., Zhuang, S., Scheffler, I.E., Sharma, V.S., Pilz, R.B. and Boss, G.R. 2006. Cyanide detoxification by the cobalamin precursor cobinamide. *Experimental biology and medicine (Maywood, N.J.)*. 231, 5 (May 2006), 641–9.

[11] Burman, J.D., Stevenson, C.E., Sawers, R.G. and Lawson, D.M. 2007. The crystal structure of Escherichia coli TdcF, a member of the highly conserved YjgF/YER057c/UK114 family. *BMC structural biology*. 7, (Jan. 2007), 30.

Burrows, L.L. 2012. *Pseudomonas aeruginosa* twitching motility: type IV pili in action. *Annual review of microbiology*. 66, (Jan. 2012), 493–520.

Campbell, S.C., Olson, G.J., Clark, T.R. and McFeters, G. 2001. Biogenic production of cyanide and its application to gold recovery. *Journal of industrial microbiology & biotechnology*. 26, 3 (Mar. 2001), 134–9.

Carterson, A.J., Morici, L.A., Jackson, D.W., Frisk, A., Lizewski, S.E., Jupiter, R., Simpson, K., Kunz, D.A., Davis, S.H., Schurr, J.R., Hassett, D.J. and Schurr, M.J. 2004. The transcriptional regulator AlgR controls cyanide production in *Pseudomonas aeruginosa*. *Journal of bacteriology*. 186, 20 (Oct. 2004), 6837–44.

Castric, P.A. 1975. Hydrogen cyanide, a secondary metabolite of *Pseudomonas aeruginosa*. *Canadian journal of microbiology*. 21, 5 (May 1975), 613–18.

Castric, P.A. 1983. Hydrogen cyanide production by *Pseudomonas aeruginosa* at reduced oxygen levels. *Canadian journal of microbiology*. 29, 10 (Oct. 1983), 1344–9.

Castric, K.F. and Castric, P.A. 1983. Method for rapid detection of cyanogenic bacteria. *Applied and environmental microbiology*. 45, 2 (Feb. 1983), 701–2.

Chand, N.S. and Hung, D.T. 2011. The two-component sensor kinase KinB acts as a non-canonical switch between acute and chronic infection. *Virulence*. 2, 6 (Jan. 2011), 553–8.

Chim, H., Tan, B.H. and Song, C. 2007. Five-year review of infections in a burn intensive care unit: High incidence of Acinetobacter baumannii in a tropical climate. *Burns : journal of the International Society for Burn Injuries*. 33, 8 (Dec. 2007), 1008–14.

Chuanchuen, R. and Schweizer, H.P. 2012. Global transcriptional responses to triclosan exposure in *Pseudomonas aeruginosa*. *International journal of antimicrobial agents*. 40, 2 (Aug. 2012), 114–22.

Chuang, J.S., Rivoire, O. and Leibler, S. 2009. Simpson's paradox in a synthetic microbial system. *Science (New York, N.Y.)*. 323, 5911 (Jan. 2009), 272–5.

Cipollone, R., Ascenzi, P., Tomao, P., Imperi, F. and Visca, P. 2008. Enzymatic detoxification of cyanide: clues from *Pseudomonas aeruginosa* Rhodanese. *Journal of molecular microbiology and biotechnology*. 15, 2-3 (Jan. 2008), 199–211.

Cipollone, R., Frangipani, E., Tiburzi, F., Imperi, F., Ascenzi, P. and Visca, P. 2007. Involvement of *Pseudomonas aeruginosa* rhodanese in protection from cyanide toxicity. *Applied and environmental microbiology*. 73, 2 (Jan. 2007), 390–8.

Coggan, K.A. and Wolfgang, M.C. 2012. Global regulatory pathways and cross-talk control *Pseudomonas aeruginosa* environmental lifestyle and virulence phenotype. *Current issues in molecular biology*. 14, 2 (Jan. 2012), 47–70.

Cohen, T.S. and Prince, A. 2012. Cystic fibrosis: a mucosal immunodeficiency syndrome. *Nature medicine*. 18, 4 (Apr. 2012), 509–19.

Cohen, T.S. and Prince, A.S. 2013. Bacterial pathogens activate a common inflammatory pathway through IFNλ regulation of PDCD4. *PLoS pathogens*. 9, 10 (Jan. 2013), e1003682.

Collins, F.S. 1992. Cystic fibrosis: molecular biology and therapeutic implications. *Science (New York, N.Y.)*. 256, 5058 (May 1992), 774–9.

Colvin, K.M., Gordon, V.D., Murakami, K., Borlee, B.R., Wozniak, D.J., Wong, G.C. and Parsek, M.R. 2011. The pel polysaccharide can serve a structural and protective role in the biofilm matrix of *Pseudomonas aeruginosa*. *PLoS pathogens*. 7, 1 (Jan. 2011), e1001264.

Colvin, K.M., Irie, Y., Tart, C.S., Urbano, R., Whitney, J.C., Ryder, C., Howell, P.L., Wozniak, D.J. and Parsek, M.R. 2012. The Pel and Psl polysaccharides provide *Pseudomonas aeruginosa* structural redundancy within the biofilm matrix. *Environmental microbiology*. 14, 8 (Aug. 2012), 1913–28.

Comolli, J.C. and Donohue, T.J. 2002. *Pseudomonas aeruginosa* RoxR, a response regulator related to *Rhodobacter sphaeroides* PrrA, activates expression of the cyanide-insensitive terminal oxidase. *Molecular microbiology*. 45, 3 (Aug. 2002), 755–68.

Comolli, J.C. and Donohue, T.J. 2004. Differences in two *Pseudomonas aeruginosa* cbb3 cytochrome oxidases. *Molecular microbiology*. 51, 4 (Feb. 2004), 1193–203.

Conrad, J.C., Gibiansky, M.L., Jin, F., Gordon, V.D., Motto, D.A., Mathewson, M.A., Stopka, W.G., Zelasko, D.C., Shrout, J.D. and Wong, G.C. 2011. Flagella and pili-mediated near-surface single-cell motility mechanisms in *P. aeruginosa*. *Biophysical journal*. 100, 7 (Apr. 2011), 1608–16.

Cottrell, J.E., Casthely, P., Brodie, J.D., Patel, K., Klein, A. and Turndorf, H. 1978. Prevention of nitroprusside-induced cyanide toxicity with hydroxocobalamin. *The New England journal of medicine*. 298, 15 (Apr. 1978), 809–11.

Davies, G., McShane, D., Davies, J.C. and Bush, A. 2003. Multiresistant *Pseudomonas aeruginosa* in a pediatric cystic fibrosis center: natural history and implications for segregation. *Pediatric pulmonology*. 35, 4 (Apr. 2003), 253–6.

Davies, J.C. and Bilton, D. 2009. Bugs, biofilms, and resistance in cystic fibrosis. *Respiratory care*. 54, 5 (May 2009), 628–40.

Dietrich, L.E., Teal, T.K., Price-Whelan, A. and Newman, D.K. 2008. Redox-active antibiotics control gene expression and community behavior in divergent bacteria. *Science (New York, N.Y.)*. 321, 5893 (Aug. 2008), 1203–6.

Diggle, S.P., Cornelis, P., Williams, P. and Cámara, M. 2006. 4-quinolone signalling in *Pseudomonas aeruginosa*: old molecules, new perspectives. *International journal of medical microbiology : IJMM*. 296, 2-3 (Apr. 2006), 83–91.

Diggle, S.P., Winzer, K., Lazdunski, A., Williams, P. and Cámara, M. 2002. Advancing the quorum in *Pseudomonas aeruginosa*: MvaT and the regulation of N-acylhomoserine lactone production and virulence gene expression. *Journal of bacteriology*. 184, 10 (May 2002), 2576–86.

Donaldson, S.H. and Boucher, R.C. 2003. Update on pathogenesis of cystic fibrosis lung disease. *Current opinion in pulmonary medicine*. 9, 6 (Nov. 2003), 486–91.

Donkó, A., Péterfi, Z., Sum, A., Leto, T. and Geiszt, M. 2005. Dual oxidases. *Philosophical transactions of the Royal Society of London. Series B, Biological sciences*. 360, 1464 (Dec. 2005), 2301–8.

Enderby, B., Smith, D., Carroll, W. and Lenney, W. 2009. Hydrogen cyanide as a biomarker for *Pseudomonas aeruginosa* in the breath of children with cystic fibrosis. *Pediatric pulmonology*. 44, 2 (Feb. 2009), 142–7.

Erhardt, M., Namba, K. and Hughes, K.T. 2010. Bacterial nanomachines: the flagellum and type III injectisome. *Cold Spring Harbor perspectives in biology*. 2, 11 (Nov. 2010), a000299.

Essar, D.W., Eberly, L., Hadero, A. and Crawford, I.P. 1990. Identification and characterization of genes for a second anthranilate synthase in *Pseudomonas aeruginosa*: interchangeability of the two anthranilate synthases and evolutionary implications. *Journal of bacteriology*. 172, 2 (Feb. 1990), 884–900.

Farrow, J.M., Sund, Z.M., Ellison, M.L., Wade, D.S., Coleman, J.P. and Pesci, E.C. 2008. PqsE functions independently of PqsR-*Pseudomonas* quinolone signal and enhances the rhl quorum-sensing system. *Journal of bacteriology*. 190, 21 (Nov. 2008), 7043–51.

Feigal, R.J. and Shapiro, B.L. 1986. Cystic fibrosis--a lethal exocrinopathy with altered mitochondrial calcium metabolism. *Annals of the New York Academy of Sciences*. 488, (Jan. 1986), 82–98.

Flynn, J.L. and Ohman, D.E. 1988. Cloning of genes from mucoid *Pseudomonas aeruginosa* which control spontaneous conversion to the alginate production phenotype. *Journal of bacteriology*. 170, 4 (Apr. 1988), 1452–60.

Fodor, A.A., Klem, E.R., Gilpin, D.F., Elborn, J.S., Boucher, R.C., Tunney, M.M. and Wolfgang, M.C. 2012. The adult cystic fibrosis airway microbiota is stable over time and infection type, and highly resilient to antibiotic treatment of exacerbations. *PloS one*. 7, 9 (Jan. 2012), e45001.

Friedlander, R.S., Vlamakis, H., Kim, P., Khan, M., Kolter, R. and Aizenberg, J. 2013. Bacterial flagella explore microscale hummocks and hollows to increase adhesion. *Proceedings of the National Academy of Sciences of the United States of America*. 110, 14 (Apr. 2013), 5624–9.

Fulcher, M.L., Gabriel, S., Burns, K.A., Yankaskas, J.R. and Randell, S.H. 2005. Well-differentiated human airway epithelial cell cultures. *Methods in molecular medicine*. 107, (Jan. 2005), 183–206.

Furman, R., Biswas, T., Danhart, E.M., Foster, M.P., Tsodikov, O.V. and Artsimovitch, I. 2013. DksA2, a zinc-independent structural analog of the transcription factor DksA. *FEBS letters*. 587, 6 (Mar. 2013), 614–9.

Garrett, E.S., Perlegas, D. and Wozniak, D.J. 1999. Negative control of flagellum synthesis in *Pseudomonas aeruginosa* is modulated by the alternative sigma factor AlgT (AlgU). *Journal of bacteriology*. 181, 23 (Dec. 1999), 7401–4.

Geiszt, M., Witta, J., Baffi, J., Lekstrom, K. and Leto, T.L. 2003. Dual oxidases represent novel hydrogen peroxide sources supporting mucosal surface host defense. *FASEB journal : official publication of the Federation of American Societies for Experimental Biology*. 17, 11 (Aug. 2003), 1502–4.

Gilchrist, F.J., Alcock, A., Belcher, J., Brady, M., Jones, A., Smith, D., Spaněl, P., Webb, K. and Lenney, W. 2011. Variation in hydrogen cyanide production between different strains of *Pseudomonas aeruginosa*. *The European respiratory journal*. 38, 2 (Aug. 2011), 409–14.

Giraud, C. and de Bentzmann, S. 2012. Inside the complex regulation of *Pseudomonas aeruginosa* chaperone usher systems. *Environmental microbiology*. 14, 8 (Aug. 2012), 1805–16.

Gustafsson, J.K., Ermund, A., Ambort, D., Johansson, M.E., Nilsson, H.E., Thorell, K., Hebert, H., Sjövall, H. and Hansson, G.C. 2012. Bicarbonate and functional CFTR channel are required for proper mucin secretion and link cystic fibrosis with its mucus phenotype. *The Journal of experimental medicine*. 209, 7 (Jul. 2012), 1263–72.

Hagins, J.M., Locy, R. and Silo-Suh, L. 2009. Isocitrate lyase supplies precursors for hydrogen cyanide production in a cystic fibrosis isolate of *Pseudomonas aeruginosa*. *Journal of bacteriology*. 191, 20 (Oct. 2009), 6335–9.

Hall, A.J., Fothergill, J.L., McNamara, P.S., Southern, K.W. and Winstanley, C. 2014. Turnover of strains and intraclonal variation amongst *Pseudomonas aeruginosa* isolates from paediatric CF patients. *Diagnostic microbiology and infectious disease*. (Sep. 2014).

Hamood, A.N., Griswold, J. and Colmer, J. 1996. Characterization of elastase-deficient clinical isolates of *Pseudomonas aeruginosa*. *Infection and immunity*. 64, 8 (Aug. 1996), 3154–60.

Hardalo, C. and Edberg, S.C. 1997. *Pseudomonas aeruginosa*: assessment of risk from drinking water. *Critical reviews in microbiology*. 23, 1 (Jan. 1997), 47–75.

Hart, C.A. and Winstanley, C. 2002. Persistent and aggressive bacteria in the lungs of cystic fibrosis children. *British medical bulletin*. 61, (Jan. 2002), 81–96.

Hayes, E., Pohl, K., McElvaney, N.G. and Reeves, E.P. 2011. The cystic fibrosis neutrophil: a specialized yet potentially defective cell. *Archivum immunologiae et therapiae experimentalis*. 59, 2 (Apr. 2011), 97–112.

He, J., Baldini, R.L., Déziel, E., Saucier, M., Zhang, Q., Liberati, N.T., Lee, D., Urbach, J., Goodman, H.M. and Rahme, L.G. 2004. The broad host range pathogen *Pseudomonas aeruginosa* strain PA14 carries two pathogenicity islands harboring plant and animal virulence genes. *Proceedings of the National Academy of Sciences of the United States of America*. 101, 8 (Feb. 2004), 2530–5.

Hengge, R. 2009. Principles of c-di-GMP signalling in bacteria. *Nature reviews. Microbiology*. 7, 4 (Apr. 2009), 263–73.

Hentzer, M. 2003. Attenuation of *Pseudomonas aeruginosa* virulence by quorum sensing inhibitors. *The EMBO journal*. 22, 15 (Aug. 2003), 3803–15.

Hickman, J.W. and Harwood, C.S. 2008. Identification of FleQ from *Pseudomonas aeruginosa* as a c-di-GMP-responsive transcription factor. *Molecular microbiology*. 69, 2 (Jul. 2008), 376–89.

Hingley, S.T., Hastie, A.T., Kueppers, F. and Higgins, M.L. 1986. Disruption of respiratory cilia by proteases including those of *Pseudomonas aeruginosa*. *Infection and immunity*. 54, 2 (Nov. 1986), 379–85.

Hogardt, M. and Heesemann, J. 2010. Adaptation of *Pseudomonas aeruginosa* during persistence in the cystic fibrosis lung. *International journal of medical microbiology : IJMM*. 300, 8 (Dec. 2010), 557–62.

Høiby, N., Ciofu, O., Johansen, H.K., Song, Z.J., Moser, C., Jensen, P.Ø., Molin, S., Givskov, M., Tolker-Nielsen, T. and Bjarnsholt, T. 2011. The clinical impact of bacterial biofilms. *International journal of oral science*. 3, 2 (Apr. 2011), 55–65.

Huang, B., Ru, K., Yuan, Z., Whitchurch, C.B. and Mattick, J.S. 2004. tonB3 is required for normal twitching motility and extracellular assembly of type IV pili. *Journal of bacteriology*. 186, 13 (Jul. 2004), 4387–9.

Hurley, B.P., Goodman, A.L., Mumy, K.L., Murphy, P., Lory, S. and McCormick, B.A. 2010. The two-component sensor response regulator RoxS/RoxR plays a role in *Pseudomonas aeruginosa* interactions with airway epithelial cells. *Microbes and infection / Institut Pasteur*. 12, 3 (Mar. 2010), 190–8.

Huse, H.K., Kwon, T., Zlosnik, J.E., Speert, D.P., Marcotte, E.M. and Whiteley, M. 2010. Parallel evolution in *Pseudomonas aeruginosa* over 39,000 generations in vivo. *mBio*. 1, 4 (Jan. 2010).

Irie, Y., Borlee, B.R., O'Connor, J.R., Hill, P.J., Harwood, C.S., Wozniak, D.J. and Parsek, M.R. 2012. Self-produced exopolysaccharide is a signal that stimulates biofilm formation in *Pseudomonas aeruginosa*. *Proceedings of the National Academy of Sciences of the United States of America*. 109, 50 (Dec. 2012), 20632–6.

Jain, S. and Ohman, D.E. 2005. Role of an alginate lyase for alginate transport in mucoid *Pseudomonas aeruginosa*. *Infection and immunity*. 73, 10 (Oct. 2005), 6429–36.

Jayaraman, S., Song, Y. and Verkman, A.S. 2001. Airway surface liquid pH in well-differentiated airway epithelial cell cultures and mouse trachea. *American journal of physiology. Cell physiology*. 281, 5 (Nov. 2001), C1504–11.

Jo, J., Price-Whelan, A. and Dietrich, L.E. 2014. An Aerobic Exercise: Defining the Roles of *Pseudomonas aeruginosa* Terminal Oxidases. *Journal of bacteriology*. (Sep. 2014).

Johnson, J.D., Conroy, W.G. and Isom, G.E. 1987. Alteration of cytosolic calcium levels in PC12 cells by potassium cyanide. *Toxicology and applied pharmacology*. 88, 2 (Apr. 1987), 217–24.

Juhas, M., Wiehlmann, L., Huber, B., Jordan, D., Lauber, J., Salunkhe, P., Limpert, A.S., von Götz, F., Steinmetz, I., Eberl, L. and Tümmler, B. 2004. Global regulation of quorum sensing and virulence by VqsR in *Pseudomonas aeruginosa*. *Microbiology (Reading, England)*. 150, Pt 4 (Apr. 2004), 831–41.

Juhas, M., Wiehlmann, L., Salunkhe, P., Lauber, J., Buer, J. and Tümmler, B. 2005. GeneChip expression analysis of the VqsR regulon of *Pseudomonas aeruginosa* TB. *FEMS microbiology letters*. 242, 2 (Jan. 2005), 287–95.

Kang, Y. and Choe, J. 2011. Crystal structure of *Pseudomonas aeruginosa PA2196*, a putative TetR family transcriptional repressor. *Biochemical and biophysical research communications*. 410, 1 (Jun. 2011), 52–6.

Kanthakumar, K., Taylor, G., Tsang, K.W., Cundell, D.R., Rutman, A., Smith, S., Jeffery, P.K., Cole, P.J. and Wilson, R. 1993. Mechanisms of action of *Pseudomonas aeruginosa* pyocyanin on human ciliary beat in vitro. *Infection and immunity*. 61, 7 (Jul. 1993), 2848–53.

Kartner, N., Augustinas, O., Jensen, T.J., Naismith, A.L. and Riordan, J.R. 1992. Mislocalization of delta F508 CFTR in cystic fibrosis sweat gland. *Nature genetics*. 1, 5 (Aug. 1992), 321–7.

Kawakami, T., Kuroki, M., Ishii, M., Igarashi, Y. and Arai, H. 2010. Differential expression of multiple terminal oxidases for aerobic respiration in *Pseudomonas aeruginosa*. *Environmental microbiology*. 12, 6 (Jun. 2010), 1399–412.

Kim, Y., Kang, Y. and Choe, J. 2013. Crystal structure of *Pseudomonas aeruginosa* transcriptional regulator *PA2196* bound to its operator DNA. *Biochemical and biophysical research communications*. 440, 2 (Oct. 2013), 317–21.

Kim, Y.-J.J., Ko, I.-J.J., Lee, J.-M.M., Kang, H.-Y.Y., Kim, Y.M., Kaplan, S. and Oh, J.-I.I. 2007. Dominant role of the cbb3 oxidase in regulation of photosynthesis gene expression through the PrrBA system in *Rhodobacter sphaeroides* 2.4.1. *Journal of bacteriology*. 189, 15 (Aug. 2007), 5617–25.

Knowles, C.J. and Bunch, A.W. 1986. Microbial cyanide metabolism. *Advances in microbial physiology*. 27, (Jan. 1986), 73–111.

Kotov, N.V., Bates, D.G., Gizatullina, A.N., Gilaziev, B., Khairullin, R.N., Chen, M.Z., Drozdov, I., Umezawa, Y., Hundhausen, C., Aleksandrov, A., Yan, X.G., Spurgeon, S.K., Smales, C.M. and Valeyev, N.V. 2011. Computational modelling elucidates the mechanism of ciliary regulation in health and disease. *BMC systems biology*. 5, (Jan. 2011), 143.

Kulasekara, H.D., Ventre, I., Kulasekara, B.R., Lazdunski, A., Filloux, A. and Lory, S. 2005. A novel two-component system controls the expression of *Pseudomonas aeruginosa* fimbrial cup genes. *Molecular microbiology*. 55, 2 (Jan. 2005), 368–80.

Köhler, T., Curty, L.K., Barja, F., van Delden, C. and Pechère, J.C. 2000. Swarming of *Pseudomonas aeruginosa* is dependent on cell-to-cell signaling and requires flagella and pili. *Journal of bacteriology*. 182, 21 (Nov. 2000), 5990–6.

Lansley, A.B. and Sanderson, M.J. 1999. Regulation of airway ciliary activity by Ca2+: simultaneous measurement of beat frequency and intracellular Ca2+. *Biophysical journal*. 77, 1 (Jul. 1999), 629–38.

Laville, J., Blumer, C., Von Schroetter, C., Gaia, V., Défago, G., Keel, C. and Haas, D. 1998. Characterization of the *hcnA*BC gene cluster encoding hydrogen cyanide synthase and anaerobic regulation by ANR in the strictly aerobic biocontrol agent *Pseudomonas* fluorescens CHA0. *Journal of bacteriology*. 180, 12 (Jun. 1998), 3187–96.

Lee, R.J. 2012. T2R38 taste receptor polymorphisms underlie susceptibility to upper respiratory infection. *The Journal of clinical investigation*. 122, 11 (Nov. 2012), 4145–59.

Lee, B., Schjerling, C.K., Kirkby, N., Hoffmann, N., Borup, R., Molin, S., Høiby, N. and Ciofu, O. 2011. Mucoid *Pseudomonas aeruginosa* isolates maintain the biofilm formation capacity and the gene expression profiles during the chronic lung infection of CF patients. *APMIS : acta pathologica, microbiologica, et immunologica Scandinavica*. 119, 4-5 (Apr. 2011), 263–74.

Lelong, E., Marchetti, A., Simon, M., Burns, J.L., van Delden, C., Köhler, T. and Cosson, P. 2011. Evolution of *Pseudomonas aeruginosa* virulence in infected patients revealed in a Dictyostelium discoideum host model. *Clinical microbiology and infection : the official publication of the European Society of Clinical Microbiology and Infectious Diseases*. 17, 9 (Sep. 2011), 1415–20.

Levin, R., Braiman, A. and Priel, Z. 1997. Protein kinase C induced calcium influx and sustained enhancement of ciliary beating by extracellular ATP. *Cell calcium*. 21, 2 (Feb. 1997), 103–13.

Liberati, N.T., Urbach, J.M., Miyata, S., Lee, D.G., Drenkard, E., Wu, G., Villanueva, J., Wei, T. and Ausubel, F.M. 2006. An ordered, nonredundant library of *Pseudomonas aeruginosa* strain PA14 transposon insertion mutants. *Proceedings of the National Academy of Sciences of the United States of America*. 103, 8 (Feb. 2006), 2833–8.

Liedtke, W.B. and Heller, S. 2007. TRP Ion Channel Function in Sensory Transduction and Cellular Signaling Cascades. *CRC Press*. (Jan. 2007).

Lima, W.C., Lelong, E. and Cosson, P. 2011. What can Dictyostelium bring to the study of *Pseudomonas* infections? *Seminars in cell & developmental biology*. 22, 1 (Feb. 2011), 77–81.

Liu, R. and Ochman, H. 2007. Stepwise formation of the bacterial flagellar system. *Proceedings of the National Academy of Sciences of the United States of America*. 104, 17 (Apr. 2007), 7116–21.

Lorentzen, D., Durairaj, L., Pezzulo, A.A., Nakano, Y., Launspach, J., Stoltz, D.A., Zamba, G., McCray, P.B., Zabner, J., Welsh, M.J., Nauseef, W.M. and Bánfi, B. 2011. Concentration of the antibacterial precursor thiocyanate in cystic fibrosis airway secretions. *Free radical biology & medicine*. 50, 9 (May 2011), 1144–50.

Lorenzo, I.M., Liedtke, W., Sanderson, M.J. and Valverde, M.A. 2008. TRPV4 channel participates in receptor-operated calcium entry and ciliary beat frequency regulation in mouse airway epithelial cells. *Proceedings of the National Academy of Sciences of the United States of America*. 105, 34 (Aug. 2008), 12611–6.

MacEachran, D.P., Stanton, B.A. and O'Toole, G.A. 2008. Cif is negatively regulated by the TetR family repressor CifR. *Infection and immunity*. 76, 7 (Jul. 2008), 3197–206.

Mahenthiralingam, E., Campbell, M.E. and Speert, D.P. 1994. Nonmotility and phagocytic resistance of *Pseudomonas aeruginosa* isolates from chronically colonized patients with cystic fibrosis. *Infection and immunity*. 62, 2 (Feb. 1994), 596–605.

Markussen, T., Marvig, R.L., Gómez-Lozano, M., Aanæs, K., Burleigh, A.E., Høiby, N., Johansen, H.K., Molin, S. and Jelsbak, L. 2014. Environmental heterogeneity drives within-host diversification and evolution of *Pseudomonas aeruginosa*. *mBio*. 5, 5 (Jan. 2014), e01592–14.

Marr, A.K., Overhage, J., Bains, M. and Hancock, R.E. 2007. The Lon protease of *Pseudomonas aeruginosa* is induced by aminoglycosides and is involved in biofilm formation and motility. *Microbiology (Reading, England)*. 153, Pt 2 (Feb. 2007), 474–82.

Martin, D.W., Schurr, M.J., Mudd, M.H., Govan, J.R., Holloway, B.W. and Deretic, V. 1993. Mechanism of conversion to mucoidy in *Pseudomonas aeruginosa* infecting cystic fibrosis patients. *Proceedings of the National Academy of Sciences of the United States of America*. 90, 18 (Sep. 1993), 8377–81.

Massier, S., Rincé, A., Maillot, O., Feuilloley, M.G., Orange, N. and Chevalier, S. 2012. Adaptation of *Pseudomonas aeruginosa* to a pulsed light-induced stress. *Journal of applied microbiology*. 112, 3 (Mar. 2012), 502–11.

Mathee, K., Ciofu, O., Sternberg, C., Lindum, P.W., Campbell, J.I., Jensen, P., Johnsen, A.H., Givskov, M., Ohman, D.E., Molin, S., Høiby, N. and Kharazmi, A. 1999. Mucoid conversion of *Pseudomonas aeruginosa* by hydrogen peroxide: a mechanism for virulence activation in the cystic fibrosis lung. *Microbiology (Reading, England)*. 145 (Pt 6), (Jun. 1999), 1349–57.

Mathee, K., McPherson, C.J. and Ohman, D.E. 1997. Posttranslational control of the algT (algU)-encoded sigma22 for expression of the alginate regulon in *Pseudomonas aeruginosa* and localization of its antagonist proteins MucA and MucB (AlgN). *Journal of bacteriology*. 179, 11 (Jun. 1997), 3711–20.

Mattick, J.S. 2002. Type IV pili and twitching motility. *Annual review of microbiology*. 56, (Jan. 2002), 289–314.

McShane, D., Davies, J.C., Davies, M.G., Bush, A., Geddes, D.M. and Alton, E.W.F.W. 2003. Airway surface pH in subjects with cystic fibrosis. *The European respiratory journal*. 21, 1 (Jan. 2003), 37–42.

McShane, D., Davies, J.C., Wodehouse, T., Bush, A., Geddes, D. and Alton, E.W.F.W. 2004. Normal nasal muco-ciliary clearance in CF children: evidence against a CFTR-related defect. *The European respiratory journal*. 24, 1 (Jul. 2004), 95–100.

Merighi, M., Lee, V.T., Hyodo, M., Hayakawa, Y. and Lory, S. 2007. The second messenger bis-(3'-5')-cyclic-GMP and its PilZ domain-containing receptor Alg44 are required for alginate biosynthesis in *Pseudomonas aeruginosa*. *Molecular microbiology*. 65, 4 (Aug. 2007), 876–95.

Mewe, M., Tielker, D., Schönberg, R., Schachner, M., Jaeger, K.-E.E. and Schumacher, U. 2005. *Pseudomonas aeruginosa* lectins I and II and their interaction with human airway cilia. *The Journal of laryngology and otology*. 119, 8 (Aug. 2005), 595–9.

Mikkelsen, H., Bond, N.J., Skindersoe, M.E., Givskov, M., Lilley, K.S. and Welch, M. 2009. Biofilms and type III secretion are not mutually exclusive in *Pseudomonas aeruginosa*. *Microbiology (Reading, England)*. 155, Pt 3 (Mar. 2009), 687–98.

Mikkelsen, H., Sivaneson, M. and Filloux, A. 2011. Key two-component regulatory systems that control biofilm formation in *Pseudomonas aeruginosa*. *Environmental microbiology*. 13, 7 (Jul. 2011), 1666–81.

Minarowski, Ł.• ., Sands, D., Minarowska, A., Karwowska, A., Sulewska, A., Gacko, M. and Chyczewska, E. 2008. Thiocyanate concentration in saliva of cystic fibrosis patients. *Folia histochemica et cytobiologica / Polish Academy of Sciences, Polish Histochemical and Cytochemical Society*. 46, 2 (Jan. 2008), 245–6.

Mowat, E., Paterson, S., Fothergill, J.L., Wright, E.A., Ledson, M.J., Walshaw, M.J., Brockhurst, M.A. and Winstanley, C. 2011. *Pseudomonas aeruginosa* population diversity and turnover in cystic fibrosis chronic infections. *American journal of respiratory and critical care medicine*. 183, 12 (Jun. 2011), 1674–9.

Nagahara, N. and Nishino, T. 1996. [Mercaptopyruvate sulfurtransferase is a rhodanese family]. *Seikagaku. The Journal of Japanese Biochemical Society*. 68, 3 (Mar. 1996), 197–201.

Nair, C.G., Ryall, B. and Williams, H.D. 2014. Cyanide measurements in bacterial culture and sputum. *Methods in molecular biology (Clifton, N.J.)*. 1149, (Jan. 2014), 325–36.

Nicastro, G.G., Boechat, A.L., Abe, C.M., Kaihami, G.H. and Baldini, R.L. 2009. *Pseudomonas aeruginosa* PA14 cupD transcription is activated by the RcsB response regulator, but repressed by its putative cognate sensor RcsC. *FEMS microbiology letters*. 301, 1 (Nov. 2009), 115–23.

Oh, J.-I.I., Ko, I.-J.J. and Kaplan, S. 2004. Reconstitution of the *Rhodobacter sphaeroides* cbb3-PrrBA signal transduction pathway in vitro. *Biochemistry*. 43, 24 (Jun. 2004), 7915–23.

Okkotsu, Y., Little, A.S. and Schurr, M.J. 2014. The *Pseudomonas aeruginosa* AlgZR two-component system coordinates multiple phenotypes. *Frontiers in cellular and infection microbiology*. 4, (Jan. 2014), 82.

Okkotsu, Y., Tieku, P., Fitzsimmons, L.F., Churchill, M.E. and Schurr, M.J. 2013. *Pseudomonas aeruginosa* AlgR phosphorylation modulates rhamnolipid production and motility. *Journal of bacteriology*. 195, 24 (Dec. 2013), 5499–515.

Ottow, J.C. 1975. Ecology, physiology, and genetics of fimbriae and pili. *Annual review of microbiology*. 29, (Jan. 1975), 79–108.

Patell, S., Gu, M., Davenport, P., Givskov, M., Waite, R.D. and Welch, M. 2010. Comparative microarray analysis reveals that the core biofilm-associated transcriptome of *Pseudomonas aeruginosa* comprises relatively few genes. *Environmental microbiology reports*. 2, 3 (Jun. 2010), 440–8.

Pessi, G. and Haas, D. 2001. Dual control of hydrogen cyanide biosynthesis by the global activator GacA in *Pseudomonas aeruginosa* PAO1. *FEMS microbiology letters*. 200, 1 (Jun. 2001), 73–8.

Pessi, G., Williams, F., Hindle, Z., Heurlier, K., Holden, M.T., Cámara, M., Haas, D. and Williams, P. 2001. The global posttranscriptional regulator RsmA modulates production of virulence determinants and N-acylhomoserine lactones in *Pseudomonas aeruginosa*. *Journal of bacteriology*. 183, 22 (Nov. 2001), 6676–83.

Petrova, O.E., Cherny, K.E. and Sauer, K. 2014. The diguanylate cyclase GcbA facilitates *Pseudomonas aeruginosa* biofilm dispersion by activating BdlA. *Journal of bacteriology*. (Oct. 2014).

Petrova, O.E. and Sauer, K. 2011. SagS contributes to the motile-sessile switch and acts in concert with BfiSR to enable *Pseudomonas aeruginosa* biofilm formation. *Journal of bacteriology*. 193, 23 (Dec. 2011), 6614–28.

Pettersen, J.C. and Cohen, S.D. 1993. The effects of cyanide on brain mitochondrial cytochrome oxidase and respiratory activities. *Journal of applied toxicology : JAT*. 13, 1 (Jan. 1993), 9–14.

Pezzulo, A.A. 2012. Reduced airway surface pH impairs bacterial killing in the porcine cystic fibrosis lung. *Nature*. 487, 7405 (Jul. 2012), 109–13.

Pilewski, J.M. and Frizzell, R.A. 1999. Role of CFTR in airway disease. *Physiological reviews*. 79, 1 Suppl (Jan. 1999), S215–55.

Pruitt, K.M. and Tenovuo, J. 1982. Kinetics of hypothiocyanite production during peroxidase-catalyzed oxidation of thiocyanate. *Biochimica et biophysica acta*. 704, 2 (Jun. 1982), 204–14.

Quinton, P.M. 2008. Cystic fibrosis: impaired bicarbonate secretion and mucoviscidosis. *Lancet*. 372, 9636 (Aug. 2008), 415–7.

Rahme, L.G., Stevens, E.J., Wolfort, S.F., Shao, J., Tompkins, R.G. and Ausubel, F.M. 1995. Common virulence factors for bacterial pathogenicity in plants and animals. *Science (New York, N.Y.)*. 268, 5219 (Jun. 1995), 1899–902.

Ramos, J.L., Martínez-Bueno, M., Molina-Henares, A.J., Terán, W., Watanabe, K., Zhang, X., Gallegos, M.T., Brennan, R. and Tobes, R. 2005. The TetR family of transcriptional repressors. *Microbiology and molecular biology reviews : MMBR*. 69, 2 (Jun. 2005), 326–56.

Rau, M.H., Hansen, S.K., Johansen, H.K., Thomsen, L.E., Workman, C.T., Nielsen, K.F., Jelsbak, L., Høiby, N., Yang, L. and Molin, S. 2010. Early adaptive developments of *Pseudomonas aeruginosa* after the transition from life in the environment to persistent colonization in the airways of human cystic fibrosis hosts. *Environmental microbiology*. 12, 6 (Jun. 2010), 1643–58.

Reddy, M.M. and Quinton, P.M. 2005. ENaC activity requires CFTR channel function independently of phosphorylation in sweat duct. *The Journal of membrane biology*. 207, 1 (Sep. 2005), 23–33.

Regnis, J.A., Robinson, M., Bailey, D.L., Cook, P., Hooper, P., Chan, H.K., Gonda, I., Bautovich, G. and Bye, P.T. 1994. Muco-ciliary clearance in patients with cystic fibrosis and in normal subjects. *American journal of respiratory and critical care medicine*. 150, 1 (Jul. 1994), 66–71.

Riordan, J.R., Rommens, J.M., Kerem, B., Alon, N., Rozmahel, R., Grzelczak, Z., Zielenski, J., Lok, S., Plavsic, N. and Chou, J.L. 1989. Identification of the cystic fibrosis gene: cloning and characterization of complementary DNA. *Science (New York, N.Y.)*. 245, 4922 (Sep. 1989), 1066–73.

Robinson, M. and Bye, P.T. 2002. Muco-ciliary clearance in cystic fibrosis. *Pediatric pulmonology*. 33, 4 (Apr. 2002), 293–306.

Rock, M.J., Makholm, L. and Eickhoff, J. 2014. A new method of sweat testing: the CF Quantum®sweat test. *Journal of cystic fibrosis : official journal of the European Cystic Fibrosis Society*. 13, 5 (Sep. 2014), 520–7.

Rodrigue, A., Quentin, Y., Lazdunski, A., Méjean, V. and Foglino, M. 2000. Two-component systems in *Pseudomonas aeruginosa*: why so many? *Trends in microbiology*. 8, 11 (Nov. 2000), 498–504.

Von Ruecker, A.A., Bertele, R. and Harms, H.K. 1984. Calcium metabolism and cystic fibrosis: mitochondrial abnormalities suggest a modification of the mitochondrial membrane. *Pediatric research*. 18, 7 (Jul. 1984), 594–9.

Ruer, S., Stender, S., Filloux, A. and de Bentzmann, S. 2007. Assembly of fimbrial structures in *Pseudomonas aeruginosa*: functionality and specificity of chaperone-usher machineries. *Journal of bacteriology*. 189, 9 (May 2007), 3547–55.

Rutland, J. and Cole, P.J. 1981. Nasal muco-ciliary clearance and ciliary beat frequency in cystic fibrosis compared with sinusitis and bronchiectasis. *Thorax*. 36, 9 (Sep. 1981), 654–8.

Rutland, J., Penketh, A., Griffin, W.M., Hodson, M.E., Batten, J.C. and Cole, P.J. 1983. Cystic fibrosis serum does not inhibit human ciliary beat frequency. *The American review of respiratory disease*. 128, 6 (Dec. 1983), 1030–4.

Ryall, B., Carrara, M., Zlosnik, J.E., Behrends, V., Lee, X., Wong, Z., Lougheed, K.E. and Williams, H.D. 2014. The mucoid switch in *Pseudomonas aeruginosa* represses quorum sensing systems and leads to complex changes to stationary phase virulence factor regulation. *PloS one*. 9, 5 (Jan. 2014), e96166.

Ryall, B., Davies, J.C., Wilson, R., Shoemark, A. and Williams, H.D. 2008. *Pseudomonas aeruginosa*, cyanide accumulation and lung function in CF and non-CF bronchiectasis patients. *The European respiratory journal*. 32, 3 (Sep. 2008), 740–7.

Ryall, B., Lee, X., Zlosnik, J.E., Hoshino, S. and Williams, H.D. 2008. Bacteria of the Burkholderia cepacia complex are cyanogenic under biofilm and colonial growth conditions. *BMC microbiology*. 8, (Jan. 2008), 108.

Ryall, B., Mitchell, H., Mossialos, D. and Williams, H.D. 2009. Cyanogenesis by the entomopathogenic bacterium *Pseudomonas* entomophila. *Letters in applied microbiology*. 49, 1 (Jul. 2009), 131–5.

Salathe, M. 2007. Regulation of mammalian ciliary beating. *Annual review of physiology*. 69, (Jan. 2007), 401–22.

Salathe, M. and Bookman, R.J. 1999. Mode of Ca2+ action on ciliary beat frequency in single ovine airway epithelial cells. *The Journal of physiology*. 520 Pt 3, (Nov. 1999), 851–65.

Sanderson, K., Wescombe, L., Kirov, S.M., Champion, A. and Reid, D.W. 2008. Bacterial cyanogenesis occurs in the cystic fibrosis lung. *The European respiratory journal*. 32, 2 (Aug. 2008), 329–33.

Schobert, M. and Tielen, P. 2010. Contribution of oxygen-limiting conditions to persistent infection of *Pseudomonas aeruginosa*. *Future microbiology*. 5, 4 (Apr. 2010), 603–21.Schurr, M.J. 2013. Which bacterial biofilm exopolysaccharide is preferred, Psl or alginate? *Journal of bacteriology*. 195, 8 (Apr. 2013), 1623–6.

Seybold, Z.V., Mariassy, A.T., Stroh, D., Kim, C.S., Gazeroglu, H. and Wanner, A. 1990. Muco-ciliary interaction in vitro: effects of physiological and inflammatory stimuli. *Journal of applied physiology (Bethesda, Md. : 1985)*. 68, 4 (Apr. 1990), 1421–6.

Shah, A.S., Ben-Shahar, Y., Moninger, T.O., Kline, J.N. and Welsh, M.J. 2009. Motile cilia of human airway epithelia are chemosensory. *Science (New York, N.Y.)*. 325, 5944 (Aug. 2009), 1131–4.

Skerker, J.M. and Berg, H.C. 2001. Direct observation of extension and retraction of type IV pili. *Proceedings of the National Academy of Sciences of the United States of America*. 98, 12 (Jun. 2001), 6901–4.

Stover, C.K. 2000. Complete genome sequence of *Pseudomonas aeruginosa* PAO1, an opportunistic pathogen. *Nature*. 406, 6799 (Aug. 2000), 959–64.

Stutz, M.D., Gangell, C.L., Berry, L.J., Garratt, L.W., Sheil, B. and Sly, P.D. 2011. Cyanide in bronchoalveolar lavage is not diagnostic for *Pseudomonas aeruginosa* in children with cystic fibrosis. *The European respiratory journal*. 37, 3 (Mar. 2011), 553–8.

Taguchi, F., Inoue, Y., Suzuki, T., Inagaki, Y., Yamamoto, M., Toyoda, K., Noutoshi, Y., Shiraishi, T. and Ichinose, Y. 2014. Characterization of quorum sensing-controlled transcriptional regulator MarR and Rieske (2Fe-2S) cluster-containing protein (Orf5), which are involved in resistance to environmental stresses in *Pseudomonas* syringae pv. tabaci 6605. *Molecular plant pathology*. (Aug. 2014).

Tate, S., MacGregor, G., Davis, M., Innes, J.A. and Greening, A.P. 2002. Airways in cystic fibrosis are acidified: detection by exhaled breath condensate. *Thorax*. 57, 11 (Nov. 2002), 926–9.

Tielen, P., Narten, M., Rosin, N., Biegler, I., Haddad, I., Hogardt, M., Neubauer, R., Schobert, M., Wiehlmann, L. and Jahn, D. 2011. Genotypic and phenotypic characterization of *Pseudomonas aeruginosa* isolates from urinary tract infections. *International journal of medical microbiology : IJMM*. 301, 4 (Apr. 2011), 282–92.

Tomich, M., Planet, P.J. and Figurski, D.H. 2007. The tad locus: postcards from the widespread colonization island. *Nature reviews. Microbiology*. 5, 5 (May 2007), 363–75.

Trejo-Hernández, A., Andrade-Domínguez, A., Hernández, M. and Encarnación, S. 2014. Interspecies competition triggers virulence and mutability in Candida albicans-*Pseudomonas aeruginosa* mixed biofilms. *The ISME journal*. 8, 10 (Oct. 2014), 1974–88.

Tümmler, B., Wiehlmann, L., Klockgether, J. and Cramer, N. 2014. Advances in understanding *Pseudomonas*. *F1000prime reports*. 6, (Jan. 2014), 9.

Udroiu, I., Domenici, F., Giliberti, C., Bedini, A., Palomba, R., Luongo, F., Pozzi, D., Bordi, F. and Castellano, A.C. 2014. Potential genotoxic effects of low-intensity ultrasound on fibroblasts, evaluated with the cytokinesis-block micronucleus assay. *Mutation research. Genetic toxicology and environmental mutagenesis*. 772, (Sep. 2014), 20–4.

Vallet, I., Diggle, S.P., Stacey, R.E., Cámara, M., Ventre, I., Lory, S., Lazdunski, A., Williams, P. and Filloux, A. 2004. Biofilm formation in *Pseudomonas aeruginosa*: fimbrial cup gene clusters are controlled by the transcriptional regulator MvaT. *Journal of bacteriology*. 186, 9 (May 2004), 2880–90.

Vallet, I., Olson, J.W., Lory, S., Lazdunski, A. and Filloux, A. 2001. The chaperone/usher pathways of *Pseudomonas aeruginosa*: identification of fimbrial gene clusters (cup) and their involvement in biofilm formation. *Proceedings of the National Academy of Sciences of the United States of America*. 98, 12 (Jun. 2001), 6911–6.

Waite, R.D., Papakonstantinopoulou, A., Littler, E. and Curtis, M.A. 2005. Transcriptome analysis of *Pseudomonas aeruginosa* growth: comparison of gene expression in planktonic cultures and developing and mature biofilms. *Journal of bacteriology*. 187, 18 (Sep. 2005), 6571–6.

Wang, Y., Haitjema, C.H. and Fuqua, C. 2014. The Ctp type IVb pilus locus of Agrobacterium tumefaciens directs formation of the common pili and contributes to reversible surface attachment. *Journal of bacteriology*. 196, 16 (Aug. 2014), 2979–88.

Way, J.L., Leung, P., Cannon, E., Morgan, R., Tamulinas, C., Leong-Way, J., Baxter, L., Nagi, A. and Chui, C. 1988. The mechanism of cyanide intoxication and its antagonism. *Ciba Foundation symposium*. 140, (Jan. 1988), 232–43.

Wiegand, I., Marr, A.K., Breidenstein, E.B., Schurek, K.N., Taylor, P. and Hancock, R.E. 2008. Mutator genes giving rise to decreased antibiotic susceptibility in *Pseudomonas aeruginosa*. *Antimicrobial agents and chemotherapy*. 52, 10 (Oct. 2008), 3810–3.

Williams, H.D. and Davies, J.C. 2012. Basic science for the chest physician: *Pseudomonas aeruginosa* and the cystic fibrosis airway. *Thorax*. 67, 5 (May 2012), 465–7.

Williams, H.D., Zlosnik, J.E. and Ryall, B. 2007. Oxygen, cyanide and energy generation in the cystic fibrosis pathogen *Pseudomonas aeruginosa*. *Advances in microbial physiology*. 52, (Jan. 2007), 1–71.

Williamson, K.S., Richards, L.A., Perez-Osorio, A.C., Pitts, B., McInnerney, K., Stewart, P.S. and Franklin, M.J. 2012. Heterogeneity in *Pseudomonas aeruginosa* biofilms includes expression of ribosome hibernation factors in the antibiotic-tolerant subpopulation and hypoxia-induced stress response in the metabolically active population. *Journal of bacteriology*. 194, 8 (Apr. 2012), 2062–73.

Wilson, R., Pitt, T., Taylor, G., Watson, D., MacDermot, J., Sykes, D., Roberts, D. and Cole, P. 1987. Pyocyanin and 1-hydroxyphenazine produced by *Pseudomonas aeruginosa* inhibit the beating of human respiratory cilia in vitro. *The Journal of clinical investigation*. 79, 1 (Jan. 1987), 221–9.

Wilson, R., Sykes, D.A., Watson, D., Rutman, A., Taylor, G.W. and Cole, P.J. 1988. Measurement of *Pseudomonas aeruginosa* phenazine pigments in sputum and assessment of their contribution to sputum sol toxicity for respiratory epithelium. *Infection and immunity*. 56, 9 (Sep. 1988), 2515–7.

Wine, J.J. 2001. Cystic fibrosis: the “bicarbonate before chloride” hypothesis. *Current biology : CB*. 11, 12 (Jun. 2001), R463–6.

Winsor, G.L., Lam, D.K., Fleming, L., Lo, R., Whiteside, M.D., Yu, N.Y., Hancock, R.E. and Brinkman, F.S. 2011. *Pseudomonas* Genome Database: improved comparative analysis and population genomics capability for *Pseudomonas* genomes. *Nucleic acids research*. 39, Database issue (Jan. 2011), D596–600.

Wissing, F. 1975. Cyanide production from glycine by a homogenate from a *Pseudomonas* species. *Journal of bacteriology*. 121, 2 (Feb. 1975), 695–9.

Wood, L.F. and Ohman, D.E. 2012. Identification of genes in the σ^{22} regulon of *Pseudomonas aeruginosa* required for cell envelope homeostasis in either the planktonic or the sessile mode of growth. *mBio*. 3, 3 (Jan. 2012).

Worlitzsch, D. 2002. Effects of reduced mucus oxygen concentration in airway *Pseudomonas* infections of cystic fibrosis patients. *The Journal of clinical investigation*. 109, 3 (Feb. 2002), 317–25.

Yan, P., Liu, W., Kong, J., Wu, H. and Chen, Y. 2014. Prevention of catheter-related *Pseudomonas aeruginosa* infection by levofloxacin-impregnated catheters in vitro and in vivo. *Chinese medical journal*. 127, 1 (Jan. 2014), 54–8.

Yeung, A.T., Torfs, E.C., Jamshidi, F., Bains, M., Wiegand, I., Hancock, R.E. and Overhage, J. 2009. Swarming of *Pseudomonas aeruginosa* is controlled by a broad spectrum of transcriptional regulators, including MetR. *Journal of bacteriology*. 191, 18 (Sep. 2009), 5592–602.

Yu, Z., Reichheld, S.E., Savchenko, A., Parkinson, J. and Davidson, A.R. 2010. A comprehensive analysis of structural and sequence conservation in the TetR family transcriptional regulators. *Journal of molecular biology*. 400, 4 (Jul. 2010), 847–64.

Zhang, Y.-M.M., Marrakchi, H. and Rock, C.O. 2002. The FabR (YijC) transcription factor regulates unsaturated fatty acid biosynthesis in Escherichia coli. *The Journal of biological chemistry*. 277, 18 (May 2002), 15558–65.

Zhou, Z., Duerr, J., Johannesson, B., Schubert, S.C., Treis, D., Harm, M., Graeber, S.Y., Dalpke, A., Schultz, C. and Mall, M.A. 2011. The ENaC-overexpressing mouse as a model of cystic fibrosis lung disease. *Journal of cystic fibrosis : official journal of the European Cystic Fibrosis Society*. 10 Suppl 2, (Jun. 2011), S172–82.

Zlosnik, J.E., Mori, P.Y., To, D., Leung, J., Hird, T.J. and Speert, D.P. 2014. Swimming Motility in a Longitudinal Collection of Clinical Isolates of Burkholderia cepacia Complex Bacteria from People with Cystic Fibrosis. *PloS one*. 9, 9 (Jan. 2014), e106428.

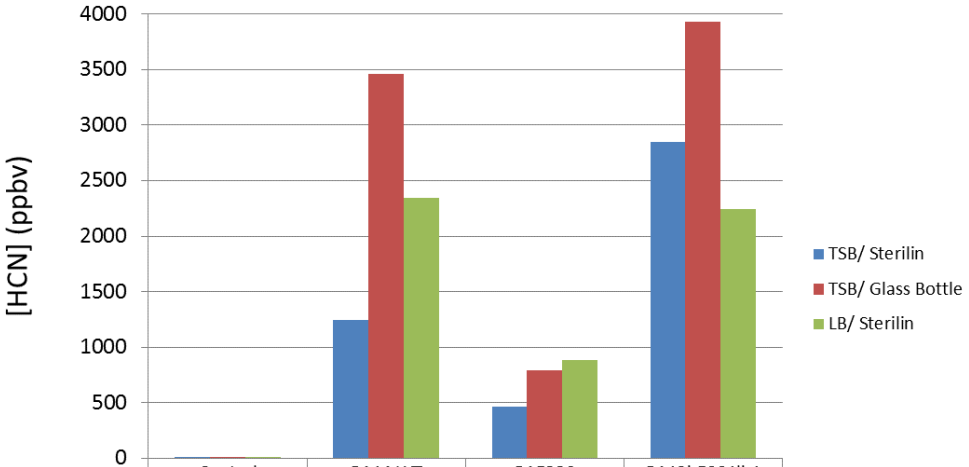
Zlosnik, J.E., Tavankar, G.R., Bundy, J.G., Mossialos, D., O'Toole, R. and Williams, H.D. 2006. Investigation of the physiological relationship between the cyanide-insensitive oxidase and cyanide production in *Pseudomonas aeruginosa*. *Microbiology (Reading, England)*. 152, Pt 5 (May 2006), 1407–15.

Zlosnik, J.E. and Williams, H.D. 2004. Methods for assaying cyanide in bacterial culture supernatant. *Letters in applied microbiology*. 38, 5 (Jan. 2004), 360–5.

APPENDICES

SIFT-MS Measurements on PA5339

The potential of volatile compounds emitted by *P. aeruginosa* as surrogate markers for infection is currently being investigated. In parallel to the ion-selective cyanide measurements, a cyanogenesis defect in *PA5339* was also confirmed by a colleague, Dr Rishi Parbary, through direct CN^- measurement using selected-ion flow-tube mass spectrometry (SIFT-MS) at St Mary's Hospital London. HCN gas is detected and quantified in parts-per-billion by volume (ppbv). Preliminary SIFT-MS measurements carried out on the mutant *PA5339* confirm a cyanogenesis defect.



	Control	PA14 WT	PA5339	PA12b5001lb1
TSB/ Sterilin	10.25	1242.65	467.8	2845.7
TSB/ Glass Bottle	9.8	3458.5	793.5	3927.9
LB/ Sterilin	6.05	2343.1	884.6	2240.75

SIFT-MS measurements confirm *PA5339* cyanogenesis defect (n=2). Measurements were carried out on PA14, *PA5339* and a clinical isolate, PA12b5001lb1. Strains were grown overnight at 37 ˚C in either Tryptone Soy Broth (TSB) or Luria Broth (LB) (5mL cultures), and in either glass bottles or 30 mL universal tubes (Sterilin, UK).

Rescreened Mutant List

Re-screened mutants were ranked by severity of cyanogenesis defect based on log2 FC relative to WT. The top 150 underproducers and top 50 overproducers are presented below.

Cyanogenesis of rescreened PA14NR mutants ranked by severity

Gene	LogFC (rel. to WT)	Annotation
roxS	-4.14	A two-component sensor known to regulate CIO expression Interestingly, mutants are more sensitive to HCN (unlike *cio* mutants) RoxR is also cyanide-deficient
rhlR	-3.07	Transcriptional regulator, QS response
hcnA	-3.02	Hydrogen Cyanide synthase subunit Glycine dehydrogenase
fliA	-3.01	Also known as rpoF Alternative sigma factor required for flagellin synthesis
atpG	-2.89	ATPase synthase gamma chain
dksA2	-2.80	A zinc-independent structural analog of the transcription factor/suppressor DksA, functions similarly
PA4616	-2.80	Transport of small molecules Probable C4 dicarboxylate-binding protein Upregulated 9 8 fold in response to triclosan
fliQ	-2.79	Flagellar biosynthesis gene
flgF	-2.56	Flagellar basal body rod
flgG	-2.24	Flagellar basal body rod
gacS	-2.24	Sensor kinase of a two-component global regulatory system
pqsH	-2.23	Catalyses terminal step in biosynthesis of PQS signal
tonB3	-2.18	tonB-like gene whose product is required for pili assembly and normal twitching motility
PA3804	-2.14	Located next to pilF, predicted transcriptional regulator
norB	-2.13	Nitric oxide reductase cytochrome b subunit

fliD	-2.10	Flagellar cap protein responsible for mucin adhesion Regulated by fleQ
PA5339	-2.10	Putative translational repressor Part of core biofilm transcriptome and upregulated in response to benzalkonium chloride and pulsed-light stress
fleS	-2.08	Transciptional regulator of motility
PA14_ 45710	-2.05	Unknown function Located near flagella genes
vqsR	-2.04	Lux transcriptional regulator, global regulation of virulence
flgJ	-2.02	Flagellar rod formation
flgH	-1.98	Flagellar L-ring precursor
fliF	-1.95	Flagellar ring complex subunit
flgE	-1.93	Flagellar hook protein
fliG	-1.92	Flagellar motor switch (c ring, determines direction and interacts with cheY and cheZ)
fabF1	-1.84	Beta-ketoacyl-acyl carrier protein synthase II Defective in all three kinds of motility
gacA	-1.82	Two-component global regulatory system
fliG	-1.81	Flagellar motor switch (c ring, determines direction and interacts with cheY and cheZ)
pilW	-1.76	Pilus biogenesis
PA4429	-1.75	Similar to cytochrome c1 precursor, might be involved in resistance to aminoglycosides or in swarming motility
fliQ	-1.74	Flagella biosynthesis
hcnC	-1.72	Hydrogen Cyanide synthase subunit Oxidoreductase
dadA	-1.72	D-amino acid dehydrogenase Glycine metabolism, known effect on cyanide-production
pilW	-1.68	Pilus biogenesis

pepA	-1.67	PepA, a secreted protein of *Pseudomonas aeruginosa*, is necessary for cytotoxicity and virulence
fliP	-1.67	Flagellar biosynthesis gene
kinB	-1.64	A two component sensor located next to algB Negatively regulates Alginate production
cyoA	-1.64	Cytochrome o ubiquinol oxidase subunit II
uvrC	-1.63	Located next to gacA Required for the excision of damaged DNA
fliQ	-1.60	Flagellar biosynthesis gene
flgC	-1.59	Flagellar basal body rod
argG	-1.57	Arginine biosynthesis
flgH	-1.57	Flagellar biosynthesis gene, L-ring
flgJ	-1.55	Flagellar rod formation
PA2057	-1.50	Predicted tonB-dependent receptor involved in metal uptake
flgJ	-1.50	Flagellar rod formation
flhB	-1.50	Flagellar biosynthesis gene
fliK	-1.49	Flagellar hook length control
fimV	-1.49	Promotes assembly of pili Required for twitching motility
fliM	-1.46	Flagellar motor switch (c ring, determines direction and interacts with cheY and cheZ)
flgJ	-1.45	Flagellar rod formation
purN	-1.42	Phosphoribosylaminoimidazole synthetase Nucleotide biosynthesis Defect in swarming
folX	-1.42	Biosynthesis of cofactors, prosthetic groups and carriers
PA2196	-1.40	Probable TetR regulator involved in transcriptional repression Known crystal structure
fliJ	-1.40	Flagellar biosynthesis chaperone
motB	-1.37	Flagellar torque generator

aroB	-1.37	3-dehydroquinate synthase Amino acide biosynthesis and metabolism
PA0318	-1.36	Catechol pathway Secondary metabolites biosynthesis
pqsE	-1.36	Activates PQS-regulated genes independently of pqsR Required RhlR
fliH	-1.34	Flagellar assembly protein
fliL	-1.33	Flagellar biosynthesis protein
Sth	-1.30	Soluble pyridine nucleotide transhydrogenase Unknown function
gacS	-1.30	Two-component global regulatory system
PA0421	-1.29	Putative enzyme involved in glycine/amino acid biosynthesis and metabolism
sucD	-1.28	Aromatic catabolic pathway
fliN	-1.28	Flagellar rotor protein
fliF	-1.27	Flagellar assembly protein
ilvC	-1.25	Amino acid biosynthesis and metabolism
fliF	-1.25	Flagellar assembly protein
PA1348	-1.24	Unknown
PA2423	-1.20	Unknown function Regulated by QS
PA2068	-1.18	Probable MFS transporter, 3-phenylpropionic acid transport Controlled by QS
PA3851	-1.18	Hypothetical protein Possibly regulated by rsmA directly
argH	-1.15	Arginine metabolism
flhF	-1.14	Flagellar biosynthesis gene
pdxB	-1.14	Vitamin B6 biosynthesis Erythronate-4-phosphate dehydrogenase
motY	-1.13	Flagellar motor Part of algR regulon, OmpA family membrane protein precursor
cheZ	-1.12	Chemotaxis phosphatase
pilF	-1.10	Multimerization and localisation of pili

pyrD	-1.10	Pyrimidine biosynthesis (known impaired virulence in PhD thesis of Ralli, 2005 University of Texas)
flgB	-1.10	Flagellar basal body
PA1237	-1.08	Transport of small molecules Probable multidrug efflux pump
flgL	-1.06	Flagellar structural gene
PA14_ 51860	-1.05	Putative diadenosine tetraphosphate involved in nucleotide transport
tatC	-1.05	sec-independent protein translocase Transports proteins containing twin-arginine motif
rpoC	-1.03	RNA polymerase subunit
PA3749	-1.02	Transport of small molecules Hydrogen symporter Probable MFS transporter
PA4431	-0.99	Probable cytochrome b
flhF	-0.98	G-protein Polar flagellar placement, required for swimming and swarming
PA0633	-0.97	Required for swarming motility
flgK	-0.96	Mutants lack the hook-associated proteins but constitutively express unpolymerized monomeric flagellin
fliI	-0.91	Flagellar basal body associated protein
Lon	-0.90	Protease involved in biofilm formation
PA4430	-0.87	Energy metabolism
gbuR	-0.86	Arginine metabolism pathway Mutant unable to swarm
PA1123	-0.85	Unknown, induced in microaerophilic conditions
metH	-0.84	Methionine biosynthesis
fliQ	-0.83	Flagellar biosynthetic gene
roxR	-0.83	roxR, regulation of CIO genes
PA3958	-0.82	Putative metal-dependent hydrolase
fumarase	-0.74	Energy metabolism

motB	-0.74	Flagellar motor
Map	-0.73	Probable methionine aminopeptidase
PA1547	-0.70	Controlled by PaQa Type2 Secretion
YidC	-0.70	Protein insertion into membrane
fliI	-0.70	Flagellar basal body associated protein
nadA	-0.70	L-aspartate oxidase Amino acid biosynthesis and metabolism
fha2	-0.69	PA1665 Type 6 secretion
PA14_ 39480	-0.68	Unknown No ortholog in PAO1
PA3714	-0.68	Probably two component regulator involved in the regulation of nitrogen utilization
fliH	-0.68	Flagellar assembly protein
PA3349	-0.67	Chemotaxis signal transduction protein related to nitrogen utilization
PA4463	-0.67	Translation regulator activity Ribosomal hibernation
flgA	-0.66	Flagellar p-ring formation
flhA	-0.66	Flagellum assembly
PA0902	-0.65	Threonine aldolase
PA2529	-0.64	Predicted Zn-dependent proteases
PA1254	-0.61	Lysine biosynthesis
PA4830	-0.60	HGG motif-containing thioesterase Possibly involved in aromatic compounds catabolism
PA0192	-0.57	Probable tonB dependent receptor
tpiA	-0.57	Glycolysis Triosephosphate isomerase
PA14_ 24190	-0.56	Not in PAO1 1-aminocyclopropane-1-carboxylate deaminase
PA1548	-0.53	Energy metabolism Respiratory chain complex IV assembly
pelB	-0.52	pelB mutants are defective in biofilm formation
PA14_ 00980	-0.52	Not in PAO1 Unkown function
PA4697	-0.51	Unkown

ccoP1	-0.48	Cytochrome c oxidase, cbb3-type subunit III
PA3341	-0.48	MarR transcriptional regulator
lysC	-0.48	Aspartate metabolism
pdxA	-0.48	Amino acid biosynthesis and metabolism
dppD	-0.46	Dipeptide transport
pilU	-0.46	Hyperpiliation, impaired twitching motility
Oxidoreductase	-0.45	Oxidoreductase
pstB	-0.45	Phosphate ion transport
PA2307	-0.45	ABC permease transporter
PA1504	-0.45	TetR regulator
flgA	-0.44	Flagellar p-ring formation
fpvA	-0.44	Pyoverdine biosynthesis
fimV	-0.40	Twitching motility
pilF	0.52	Multimerization and localisation of pili
PA4887	0.53	MFS transporter of arabinose or xenobiotics
PA14_ 46320	0.54	Pyruvate carboxylase involved in gluconeogenesis
Rho	0.54	GTPase
minD	0.54	Cell division inhibitor
PA1832	0.55	Periplasmic serine protease
PA1025	0.55	Porin, transport of small molecules
rcpA	0.55	Flp pilus assembly protein
aphA	0.56	Acetylpolyamine aminohydrolase
wspR	0.57	Response regulator involved in cell attachment
pilF	0.58	Multimerization and localisation of pili
PA2571	0.59	Signal transduction histidine kinase regulating C4-dicarboxylate transport system Known defect in twitching

TadD	0.60	Pilus assembly protein
PA14_ 05820	0.61	Predicted acyl-CoA transferases or carnitine dehydratase
PA5314	0.62	Predicted enzyme of the cupin superfamily
flgK	0.62	Wrong protein in library, acknowledged by Liberati et al
PA2125	0.63	Aldehyde dehydrogenase
PA5145	0.64	Glycerol-3-phosphate dehydrogenase complex
wspR	0.65	Two-component response regulator involved in cell attachment
pchB	0.65	Salicylate biosynthesis
trmE	0.66	tRNA modification GTPase
PA3468	0.66	Small-conductance mechanosensitive channel
PA4606	0.70	Involved in carbon starvation
PA14_ 16480	0.71	Biosynthesis of cofactors, prosthetic groups and carriers
PA0749	0.71	Uncharacterised, might be related to vancomycin resistance
thiD	0.71	Pyrimidine kinase, synthesis of co-factors
rocR	0.72	c-di-GMP phosphodiesterase class I
polA	0.79	DNA polymerase I
bglX	0.79	Beta-glucosidase, carbohydrate metabolism
triB	0.79	Antibiotic resistance
fppA	0.82	Type III secretion type 4b pilus assembly
CheW	0.82	Probable purine-binding chemotaxis protein
gltX	0.84	Glutamyl-tRNA synthetase post-translational modification
PA5245	0.86	Putative isoprenoid biosynthesis protein with amidotransferase-like domain
mucB	0.88	Negative regulator of Alginate biosynthesis
hemF	0.93	Coproporphyrinogen III oxidase
PA2882	1.18	Phosphate ion transport

PA0529	1.20	Unknown
PA2072	1.22	Sensory box protein with cyclase activity Possible link to c-di-GMP and biofilms/virulence
envZ	1.39	Osmolarity sensor, controls virulence in *Shigella*
rsmA	1.46	Negative regulator of virulence
sagS	1.57	Sensor/response regulator hybrid regulating motile-sessile switch Mutants exhibit hyperattachment, an HptB-dependent increase in rsmYZ, increased Psl polysaccharide production, and increased virulence